Measuring Ocean Waves: Proceedings of a Symposium and Workshop on Wave Measurement Technology (1982)

Pages
259

Size
8.5 x 10

ISBN
0309328160

Committee on Wave-Measurement Technology; Marine Board; Commission on Engineering and Technical Systems; National Research Council

Ocean Instrumentation to Serve Science and Engineering

MEASURING OCEAN WAVES

Proceedings of a Symposium and Workshop on Wave-Measurement Technology April 22-24, 1981 Washington, D.C.

Convened by the

Committee on Wave-Measurement Technology
Marine Board
Commission on Engineering and Technical Systems
National Research Council

NATIONAL ACADEMY PRESS
Washington, D.C. 1982

NOTICE: The project that is the subject of this report was approved by the Governing Board of the National Research Council, whose members are drawn from the councils of the National Academy of Sciences, the National Academy of Engineering, and the Institute of Medicine. The members of the panel responsible for the report were chosen for their special competences and with regard for appropriate balance. This report has been reviewed by a group other than the authors according to procedures approved by a Report Review Committee consisting of members of the National Academy of Sciences, the National Academy of Engineering, and the Institute of Medicine.

The National Research Council was established by the National Academy of Sciences in 1916 to associate the broad community of science and technology with the Academy's purposes of furthering knowledge and of advising the federal government. The Council operates in accordance with general policies determined by the Academy under the authority of its congressional charter of 1863, which establishes the Academy as a private, nonprofit, self-governing membership corporation. The Council has become the principal operating agency of both the National Academy of Sciences and the National Academy of Engineering in the conduct of their services to the government, the public, and the scientific and engineering communities. It is administered jointly by both Academies and the Institute of Medicine. The National Academy of Engineering and the Institute of Medicine were established in 1964 and 1970, respectively, under the charter of the National Academy of Sciences.

This report represents work supported by Grant Number N00014-82-G-0032 between the Office of Naval Research and the National Academy of Sciences.

Copies available in limited quantity from:

Marine Board
Commission on Engineering and Technical Systems
National Research Council
2101 Constitution Avenue, N.W.
Washington, D.C. 20418

Printed in the United States of America

COMMITTEE ON WAVE-MEASUREMENT TECHNOLOGY

Robert G. Dean, Chairman
University of Florida
Gainesville, Florida

Frank Hsu
Amoco International
Houston, Texas

Foster H. Middleton
University of Rhode Island
Kingston, Rhode Island

Denzil Pauli
Marine Planning Consultant
Silver Spring, Maryland

Richard J. Seymour
Scripps Institution of Oceanography
La Jolla, California

LIAISON WITH FEDERAL AGENCIES

A. W. Green
Naval Ocean Research and Development Activity
Bay St. Louis, Mississippi

Norden E. Huang
NASA Wallops Flight Center
Wallops Island, Virginia

Y. Phil Hsueh
National Science Foundation
Washington, D.C.

William Iseley
National Oceanic and Atmospheric Administration
Rockville, Maryland

Charles D. Kearse
National Oceanic and Atmospheric Administration
Rockville, Maryland

Sheldon Lazanoff
Fleet Numerical Oceanographic Center
U.S. Navy
Monterey, California

Paul Teleki
U.S. Geological Survey
Reston, Virginia

Edward Thompson
Coastal Engineering Research Center
U.S. Army Corps of Engineers
Fort Belvoir, Virginia

CONTENTS

PREFACE

John E. Flipse
Chairman
Marine Board

An issue of highest priority to the Marine Board is the development and promulgation of technology to serve the ocean science and engineering professions. The measurement of ocean waves has long been of particular interest, as wave data and an understanding of wave phenomena are essential to ocean engineering and to many marine operations. Wave data and the calculations made using these measurements are needed to validate scientific theories and concepts; to determine design loads for efficient offshore structures; and to forecast the response of marine vehicles to this complex excitation medium.

These needs create diverse and challenging demands: for synoptic worldwide measurement and for intensive site-specific studies; for detailed analyses of various wave spectra and for simple--but reliable and timely--forecasts; for a general picture of an area's waves and for exclusive focus on the rare extremes.

The differences in requirements have led to diverse approaches to the development of wave-measurement technology by increasingly separated communities. In the interest of establishing a central wave-measurement program to serve many needs, the Engineering Development Office of the National Oceanic and Atmospheric Administration asked the Marine Board to prepare a summary of the present state of the art in wave-measurement technologies, to promote exchange of methods and results among experts conducting research with different wave-measuring systems, and to identify the most significant problems remaining for research and development in wave measurement. The Marine Board agreed to this request, and in 1981, the National Research Council appointed a committee under the direction of the board to review the status of the leading wave-measurement technologies, and to define present and future needs.

The Committee on Wave-Measurement Technology convened a meeting of about 80 experts who met for three days in April 1981 to deliver and hear formal presentations detailing the technologies, and to develop in a structured workshop a list of problems in wave measurement most urgently needing attention.

The meeting that is the subject of these proceedings was also planned to complement and enhance two meetings on closely related topics planned for the same year: a Symposium on Wave Dynamics and Radio Probing of the Ocean Surface* held in May, followed in

---

*The proceedings (in preparation) will be published by Plenum Press.

SUMMARY

Robert G. Dean
Chairman

Symposium and Workshop on Wave-Measurement Technology

The technology of wave measurements has developed rapidly in the past two decades. Remote sensing of ocean waves has advanced from concepts to operational systems--to systems that demonstrate considerable potential for wide use in the near future. The development of *in situ* systems in the same period, although proceeding at a slower pace, has achieved significant improvements in reliability, in reduction of costs, and in ability to measure directional characteristics.

The technological responses to wave-measurement problems have addressed a variety of diverse and urgent needs. At the time this symposium was convened, many *in situ* and remote sensing systems were known to be available, but general uncertainty surrounded the quality of their data.

In the interest of meeting these needs, members of the technical community met for a three-day symposium and structured workshop to review the status and prospects of wave-measurement technologies, identify the most pressing or important problems remaining to be solved, and attempt a preliminary description of research and development directed to solution of these problems.

Formal presentations addressing the needs of users for ocean wave data initiated the symposium, and technical papers were offered in response detailing the principal wave-measuring systems and their results, as well as one speculating about wave-measuring systems of the future. In the workshop sessions, each participant developed statements of the outstanding problems remaining to be solved. These were then displayed (similar statements were grouped together), and each participant assigned a weighted vote to the ten he or she considered most important or urgent (or both). The formal presentations and results of the workshop are briefly recapitulated in this summary.

Needs for Wave Measurements

L. Baer ("Operational Needs for Wave Data") describes the variety of users for wave data, and the economic justification for gathering data. The results of one survey indicate that the annual cost savings to engineering construction alone from good-quality wave information would be $100 million to $1 billion per year. In addition, the safety of recreational and commercial vessels and the integrity of offshore structures could be enhanced by improved wave data. Baer shows that

fairly short unbiased records can nevertheless result in substantial bias in the extrapolated values; thus, a meaningful wave-measurement program should be committed to establishing a fairly long record to reduce this bias to acceptable limits. With the possible exception of the offshore petroleum industry, most commercial users are unlikely to collect long-term data. In addition, events such as hurricanes, giving rise to unique data, cannot be predicted sufficiently before their occurrence to plan and carry out experiments for the event. Thus, a governmental agency needs to take responsibility for collecting, reducing, disseminating, and storing long-term wave data. Rapid advances in less expensive, more reliable instrumentation should allow a cost-effective program to be instituted in the very near future.

The types and quality of wave measurements required for research or statistical treatment are discussed by L. E. Borgman ("Research Needs for Wave Data"). These requirements differ with application: spectral representation, for example, may range from low-frequency tides to high-frequency capillary waves. Probability description needs include those for daily operational purposes and may extend to return periods of 1×10^6 years (required, for example, in nuclear power plant design), and the environment of interest may vary from the relative homogeneity of deep water to the strong spatial gradients of the nearshore. Four major research problems are, first, the properties of successions of individual waves, including the effects of "groupiness" and the associated first- and second-order kinematics. There is considerable uncertainty about the relative role of nonlinearities in the character of wave groups. Improved understanding will require more definitive field measurements of the two-dimensional sea-surface character and theoretical developments.

Second, knowledge of the interaction of waves with currents, bottom bathymetry, winds, and other forces or features of the physical environment--while much needed for coastal design and engineering, as well as understanding and predicting hurricane damage--is lacking. Several coastal sites could be selected for long-term and fairly complete instrumentation.

Third, understanding rare, extreme events requires better definition of the long-term statistics of an area, and of the effects of such events on vessels, fixed structures, and the nearshore environment. Long-term wave measurements would be required in areas prone to extreme events (such as hurricanes), as would be well-organized plans to investigate and document effects of the event immediately after occurrence.

The fourth problem is that of wave directionality. Both in situ and remote sensing instrumentation is under development that should allow the routine, reliable, and continuous measurement of directional spectra. For example, reviewing the directional measurements that can be made today, Borgman indicates that the directional spread of waves sensed by heave-pitch-roll buoys may be fairly broad, but the principal direction can be obtained within approximately 4^o-5^o.

Borgman makes an appeal for maintaining data quality through pre- and post-measurement calibrations and through careful documentation of the data characteristics for future users.

Remote Sensing of Waves

A number of different approaches can be used for remote sensing of water waves. Several are still being developed; thus, their long-term potential, reliability for routine measurements, and costs are not available. Among the attractive features of remote sensing systems are their ability to obtain wave data over a large area; freedom from fixed in situ supports or bottom-mounting with umbilical cords or data links to shore; (in some cases) ability to sample in extreme conditions; and (for some systems) relatively low cost.

N. E. Huang ("Survey of Remote Sensing Techniques for Wave Measurement") gives a detailed, comprehensive review of the various principles used in remote sensing, and of the systems in operation or development, and describes recent results. A helpful tabular summary developed by Huang sets out characteristics for nine remote sensing systems, such as status (operational or developmental), accuracy of wave parameters measured, spatial coverage, platform, data acquisition time, data processing requirements, restrictions on operational environmental conditions, initial system cost, and data reduction cost, some of which is used here to compare various systems (see Table 1).

E. J. Walsh ("Remote Sensing of Ocean Waves by Surface Contour Radar") describes an airborne surface contour radar (SCR) that produces a near real-time topographical map of the sea surface. A 0.085° x 1.2° radar pencil beam is oscillated laterally to measure the sea surface within a swath approximately half the aircraft's altitude in width. The length of each swath is approximately 5 km. At each of the 51 points measured in one oscillation, the measured range distance is corrected for the off-vertical angle of the beam to yield the true vertical distance between the aircraft and the sea surface. The contamination owing to vertical aircraft motion is minimized by removing the double integration of aircraft motion sensed by a vertical accelerometer. An onboard computer with color-coded display portrays the sea-surface topography, and can also analyze the data with a two-dimensional fast Fourier transform to produce wavenumber spectra.

One feature of the analyzed data requiring interpretation is that initially a 180° directional ambiguity appears in the directional spectrum. This ambiguity is eliminated through spectra obtained from two flight lines, each of which produces a different "encounter spectrum." The information available from the two flight lines is adequate to identify the image spectrum and to correct the actual spectrum for any drift of the aircraft due to crosswinds.

Additional notable features of the SCR are that it does not require calibration against sea-truth data, it yields quantitative results, and it can see through clouds. Although the SCR is not available commercially, the quality and type of results it yields

Table 1 Summary of Remote Sensing Systems for Measuring Ocean Waves*

Sensors		SCR (Surface Contour Radar)	SAR (Synthetic Aperture Radar)	ΔK-radar and short-pulse microwave spectrometer	Laser profilometer
Status		Operational	Quasi-operational	Developmental	Operational
Height	Wave Parameters	± 5 cm or ± 5%, whichever is larger	> 1 m possible through model	± 20 cm	± 15 cm
Length/Period	Wave Parameters	± 1 m in wavelength	L > 50 m (satellite) ± 3% L > 20 m (aircraft)	5 m-400 m	5 m and longer
Direction	Wave Parameters	± 2°	± 2°	± 5° mean direction	Not directly, but directions of the energy containing components can be derived within ± 15°
Spectrum	Wave Parameters	Up to 9 Fourier coefficients in direction	Directional wavenumber spectrum with relative energy density scale	2-D wavenumber spectrum with angular resolution 15°	One-dimensional wavenumber
Spatial Coverage/ Cell Size		Basic swath width = ½ altitude (0.1-0.4 km) length for FFTs is 5 km	100 km swath (satellite); 1 km (aircraft) with spatial resolutions: 25 m (satellite); 3 m (aircraft)	5 x 12 km aircraft 130 km x 130 km satellite	Typical section 20 km
Platform		Aircraft	Aircraft or satellite	Aircraft and satellite	Aircraft and tower (from stationary platform, results in frequency spectrum)
Data Acquisition Time		50 sec for a single FFT run	2 sec (satellite); 10 sec (aircraft)	20 sec (satellite) 2 min (aircraft)	5 min/FFT
Data Processing Requirements		2-D FFT on minicomputer ~ 1.5 hr/FFT	Large computer for digital image formation and FFT; optical Fourier transform possible	Onboard real time by microcomputer	Minicomputer
Operational/Environmental Conditions/Restrictions		All weather: no restrictions	Wind speed > 3 m/sec, $H_{1/3}$ > 1 m	Aircraft altitude ≥ 10 km all weather: no restrictions	Clear atmosphere required to permit laser transmission
Cost of System		$0.5 million	Very expensive	Satellite system $5-10 million	~ $100,000
Cost of Measurement per Typical Data Set		Aircraft flight time ≃ $2000/hr	$1000 per 5 km x 5 km patch	$500; major cost aircraft flight time	Major cost is aircraft flight time
Comments and Remarks		Once on site, 15 min is sufficient for data acquisition	15° wave direction compared to pitch and roll buoys; 15% wavelength compared to pitch and roll buoys	NASA-GSFC short-pulse spectrometer will have onboard processing capability by 1983	

Table 1 (continued)

Sensors		HF radar	Coastal Wave Imaging Radar (Marine Navigation Radar)	Altimeter	Stereophotography
Status		Quasi-operational	Operational	Operational	Operational
Height	Wave Parameters	Not direct, but possible through model ± 1% relative, ± 20% absolute	No	$H_{1/3}$ 0-20 m (± 10% or 50 cm)	Not direct, possible through model
Length/Period		Wavelength ± 5%	Length > 20 m, ± 10%	Not direct, possible through model	± 5%
Direction		± 10°	± 3°	No	± 5°
Spectrum		1-D wavenumber spectrum/scan to produce 2-D spectrum	Directional slope spectrum on analogy data	1-D frequency spectrum through model	2-D slope spectrum in wavenumber
Spatial Coverage/ Cell Size		Surface wave 200 km x 200 km area with cell 7 km x 7 km, skywave up to 1000 km x 1000 km	2.5 km x 2.5 km/data cell size 20 m x 20 m	3 km x 20 km	40° viewing angle area depends on height
Platform		Ground based	Fixed tower	Satellite or airplane	Aircraft or tower
Data Acquisition Time		1 hr	1.8 sec	3 sec	1/100 sec
Data Processing Requirements		Minicomputer	Digital processing on minicomputer; optical Fourier transform possible	Waveform fitting on minicomputer	Laser optical Fourier transform and minicomputer
Operational/Environmental Conditions/Restrictions		Clear of noise from thunderstorms, ionospheric variation, and man-made noises	Wind speed > 3 m/sec, wavelength > 20 m, not under heavy rain	All weather. Footprint of radar has to be all on water surface.	Fair weather with overcast the best. Day only.
Cost of System		~$100,000	$50,000		$100,000
Cost of Measurement per Typical Data Set		Low	$100		Less than $1000
Comments and Remarks		In surface-wave mode, synthetic aperture technique can be used	Automatic data processing capability under development	Other statistical properties of the wave field such as skewness can also be derived from the data	

*Source: N. E. Huang.

should be widely applicable to a number of practical projects and scientific studies. The comparisons of significant wave-height results from an SCR flight and buoy data (collected in the course of the Atlantic Remote Sensing Land-Ocean Experiment, or ARSLOE), and sea-surface topography data from a different type of airborne elevation sensor are generally good. Huang assesses the system as "quasi-operational," the initial cost as $0.5 million, and the accuracies of measurement of wave parameters as follows: significant wave height, $H_s \pm 5$ cm, or $\pm 5\%$; wavelength, $L \pm 5$ m; principal wave direction, $\theta_o \pm 2^o$.

R. A. Shuchman ("The Use of Synthetic Aperture Radar (SAR) to Measure Ocean Gravity Waves") gives an account of measuring ocean gravity waves using synthetic aperture radar (SAR). SAR is an airborne or spacecraft-borne system that synthesizes a very narrow beam by the motion of a fairly broad physical antenna beam. It is of interest that there is no consensus about the actual imaging mechanism of SAR. The most widely accepted view is that the radar resonantly interacts with the shorter waves (on the order of centimeters) that tend to be accentuated on the crests of longer waves. SAR data consist of the "phase history" of the scattering points, which, through analysis by optical or digital transforms, yields the wavenumber spectrum. There is as yet no method for scaling these spectra to determine absolute energy, but researchers are confident this will be possible in the future.

Three airborne SAR systems routinely collect water-wave information. In addition, a SAR system was mounted on Seasat (launched in June 1978). Since the measured signal return requires the presence of short waves, SAR can only operate if winds are in excess of approximately 3 m/s, significant wave heights are greater than 1 m, and the longer wavelengths exceed 25 m. Huang lists the cost of a SAR system as greater than $10 million, and the following accuracies in wave parameters: $L \pm 3\%$, $\theta_o \pm 2^o$.* SAR has been applied with favorable results to the comparison of measured and calculated wave refraction patterns off Cape Hatteras. Additionally, there is evidence that SAR is capable of detecting internal gravity waves and surf beat (long second-order surface waves).

D. E. Barrick reviews the status of high-frequency (HF) radars for the measurement of sea-surface characteristics ("Status of HF Radars for Wave-Height Directional Spectral Measurements"). These systems use polarized electromagnetic waves that are reflected back to the radar owing to the Bragg effect. The directional spectra are extracted from a portion of the returned signal produced by the interaction of all pairs of wave trains in the wave spectrum. In addition to wave-height information, ocean currents cause a Doppler

*A new lightweight, airborne X-band SAR being developed by Environmental Research Institute of Michigan for the petroleum industry will cost approximately $2.5 million, exclusive of the aircraft. [Note added in proof by R. A. Shuchman.]

shift in the signal from which the strength and direction of the current can be extracted. Two applications have been made of HF radar to measure ocean waves: sky wave and surface or ground wave. Sky-wave systems, through reflectance of the transmitted signal from the ionosphere, allow sea-surface characteristics to be monitored to a distance some 3000 km from the source/receiver. The short-term temporal characteristics of the ionosphere contaminate the returned signal and must be accounted for in the analysis.

Huang reports the following accuracies: $H_s \pm 8\%$, for $H_s > 1$ m; period, $T \pm 1$ s; $\theta_o \pm 7^o$, for unimodal waves. Huang also notes that it is possible to obtain the one-dimensional spectrum only for certain data sets.

Surface-wave or ground-wave radars can be very compact and appear ideally suited for the measurement of nearshore directional spectra and currents. The spatial resolution of the patch of illuminated sea surface varies from kilometers to tens of kilometers, and through diffraction of the transmitted signal beyond the horizon, ranges up to 50 km are possible. Surface-wave or ground-wave radars are categorized according to whether the transmitted signal is narrow- or broad-beam. The narrow-beam radar requires the physical size of the antenna to be hundreds of meters. Most initial efforts were directed to narrow-beam systems, since the interpretation of the returned signal is more straightforward. Analysis techniques are much simpler for the longer wave periods (> 10 s), but methodologies have been developed for wave periods as low as 3 s. Analysis of data from three narrow-beam radars and comparison to data from heave-pitch-roll buoys in study areas indicate the following accuracies: $H_s \pm 5\%$, $T \pm 0.5$ s, $\theta_o \pm 7^o$.

Broad-beam surface-wave radars have the very attractive feature of small antennas. The height of the antenna is of the order of 2 m and can be placed directly on the beach on a portable support. In addition to currents, this system yields the same directional information as a heave-pitch-roll buoy. Some development is still under way for extraction of the directional spectrum for wave periods less than 9 s. Huang assesses the system as "operational" with the following accuracies: $H_s \pm 5\%$, for $H_s > 1$ m; $T \pm 0.5$ s; direction $\pm 4^o$, for unimodal waves. The system scans a patch size of 0.5 km up to a distance of 50 km offshore. The cost of the system is approximately $100,000.

F. C. Jackson ("Aircraft and Satellite Measurement of Ocean Wave Directional Spectra Using Scanning-Beam Microwave Radars") describes wave measurement by pulsed microwave radar operating in a conical scan near vertical incidence. The radar "illumination pattern" is broad compared to the scale of the waves, and the signal is averaged laterally. Thus, only those waves oriented to the incoming radar signal survive this spatial averaging. Jackson has developed an elegant theory to interpret the radar return signal to yield quantitative directional wavenumber spectra.

A number of interesting comparisons of the radar's data to sea truth have been carried out, including eight overflights of areas near Waverider buoys or pitch-and-roll buoys. The significant wave heights range from 1.3 m to 9.4 m, and the radar-determined values are within 0.4 m of those determined by the buoys. Comparisons of the directional spectra with those obtained from a heave-pitch-roll buoy are encouraging: generally good agreement obtains for one-dimensional energy spectra, and the differences appear qualitatively to be of the same order as the limits of the 90% confidence interval. The cost of the system as estimated by Huang is $5-10 million. The system is assessed as "developmental," and as offering the following accuracies for wave parameters: $H_s \pm 20$ cm, $\theta_o \pm 5^o$.

In Situ Systems

R. J. Seymour ("Review of Wave Measurement Using In Situ Systems") surveys in situ instrumentation used for wave measurements, recognizing the following types: wave-measuring buoys, shipboard records, bottom-mounted height sensors, surface-piercing wave staffs, and fixed-orientation directional systems. Many (but not all) of these systems are best suited for shallow-water applications where a cable can be extended from shore, or when the wave-induced water pressure can be sensed (or both).

For some applications, such as computation of longshore sediment transport at a particular locality, it appears that nearshore measurements are most effective, owing to the inhomogeneity of the wave field resulting from shoaling, refraction, reflection, and diffraction of waves during propagation across the continental shelf. Measurements conducted in deep water can be extended computationally onto a fairly long segment of coastline if the transformation processes can be adequately represented.

The most significant recent advances enable routine measurement of the directional characteristics of water waves, among them additional development of the heave-pitch-roll buoy introduced by Longuet-Higgins et al. (1963), and the "slope array" developed by Seymour and Higgins (1978), which consists of four pressure sensors on the corners of a steel frame 6 m square.

A. G. Parker ("Wave Measurements Using Surface-Mounted Instruments") reviews the characteristics and requirements of surface-mounted sensors, such as those affixed to piers or to offshore platforms. These were among the earliest in situ systems, and have the advantages of ruggedness and relative ease of recovery and servicing. Parker emphasizes planning in making the proper selection of a measurement system. The measurement period, quality of results, method of analysis, and uniqueness of data are factors guiding selection of the optimum sensor system. If the primary requirement is to measure severe storm waves, for example, ruggedness of the instrument should be emphasized. Parker characterizes surface-mounted sensors as visual, electrical, acoustic, float, optical, radar, and other types. He notes

the value of the frequently dismissed data set from shipboard observations.

For cases in which a one-dimensional spectrum is adequate, many of the needed data are collected by a wave-guide system (e.g., Baylor Wave Staff) in which the roundtrip travel time from the above-water emitter to the water surface is measured. An advantage of wave-guide sensors is that they are affected less by corrosion and biofouling than resistance or capacitance wave gauges.

The acoustic gauge has no physical link to the water surface; rather, it beams a signal downward, and the time required for the roundtrip of the signal serves to locate the water surface. The analysis must include calibration for the variation of the speed of sound in air as a function of temperature. The primary limitation is the relatively high attenuation of the signal: for fairly high frequencies (≃40 kHz), which are desired to produce a narrow beam, distances are limited to approximately 10 m for a relatively low-power system.

Recently developed downward-directed lasers, using both continuous waves and pulsed waves, have many inherent advantages, including location above the water surface, independence from environmental factors, and ease of installation. The advantages of downward-directed radar systems are similar to those of laser systems, with the additional feature of being less susceptible to contamination than the optical lens of a laser. For cases in which the measurement of wave direction is required, several sensors can be installed in an array. The horizontally scanning Doppler microwave radar can be used to yield principal wave directions over a wide area.

L. R. LeBlanc ("Pitch-Roll Buoy Wave Directional Spectra Analysis") presents methods of analysis for extracting directional spectra from heave-pitch-roll buoys. The data discussed are from an ENDECO "orbital-following" buoy deployed during the 1980 ARSLOE program.* The "slopes" sensed by the orbital-following buoy result from the gradient in the vertical direction of the horizontal component of water-particle velocity. A "drogue-like" element suspended below the buoy tracks, approximately, the horizontal motion at the (below-surface) elevation of this element, whereas the buoy at the surface tends to follow the motion of the water particle at the surface. Since the measured slope would appear to depend nonlinearly on the wave properties, the theoretical approach to establishing the associated transfer function is not clear. LeBlanc states that the transfer function is established from the data, and presumably this is based on the known relationship between total energy densities in the sea-surface displacement and gradient of the horizontal velocity component.** Derived directional spectra are presented for a

---

*Atlantic Remote Sensing Land-Ocean Experiment, October 6 to November 30, 1980, off Duck, North Carolina.

**A signed square-root nonlinear correction factor is applied to the pitch-roll data prior to Fourier analysis; however (as observed in the ARSLOE data set), this factor seems to have minimal influence on the data, presumably because the heave sensor responds linearly to wave motion, and the directional spectra calculations are based on cross-spectral correlation of the heave sensor with the pitch-roll sensors. In the correlation process, the nonlinear components average out. [Note added in proof by L. R. LeBlanc.]

substantial storm that occurred during the ARSLOE program: significant wave heights of the spectra range from less than 2 m to approximately 5 m, with associated wind speeds of 7.5 m/s to 16.2 m/s.

G. Z. Forristall ("Subsurface Wave-Measuring Systems") addresses the capabilities and limitations of subsurface measuring systems, with special emphasis on pressure and velocity sensors. A review of previous investigations employing subsurface pressure measurements reveals a number of attempts to evaluate the linear pressure-transfer coefficient in wave-by-wave analyses. In general, these attempts have lead to the conclusion that the ratio, n, of measured to predicted pressure-response function is higher and lower than unity at low and high frequencies, respectively. Forristall argues that this conclusion is merely an artifact of analyzing individual waves composed of many frequency components on the basis of a single frequency component. Convincing results of a simulation are presented to support this view. However, careful measurements and Fourier analyses carried out by Cavaleri et al. (1978) support the behavior found by previous investigators.

Forristall describes his experiments to investigate this matter further. A sensitive pressure transducer was located 12 ft above the seafloor of the Gulf of Mexico (in water 68 ft deep), beneath a Baylor inductance wave staff. The results are presented in the form of the spectra of pressure and water surface, coherence, and the response function ratio, n, versus frequency. In general, coherence is near unity over frequency ranges in which the sea-surface spectrum is large. For the more energetic spectra, the value of n is near unity over the frequency range of high spectral energy. For the lower and higher frequency ranges, the values of n are higher and lower than unity, respectively, a result generally consistent with those obtained by other investigators employing the wave-by-wave analysis. For one spectrum of reasonably low energy and with the peak energy at higher frequencies (5-6 s), the coherence is again high, yet the value of n is approximately 1.2. Forristall states that "the reason for this behavior is not known, but we suspect that it may be due to poor response of our recording scheme at low signal levels." Forristall concludes that it should be possible, using high-quality pressure sensors, as well as Fourier analysis and linear wave theory, to reconstruct the sea-surface displacement (or its spectrum) for wavelengths greater than twice the submergence depth of the pressure sensor.

Forristall reviews three programs in which electromagnetic current meters were used to describe the directional wave spectrum. The Ocean Test Structure, for example, was fitted with 5 wave staffs and 11 biaxial electromagnetic current meters mounted on a platform 20 ft x 40 ft (in plan view), installed in 66 ft of water in the Gulf of Mexico. A thorough analysis by Borgman and Yfantis (1979) indicates marginal advantages from the availability of a large number of sensors. Additionally, the analysts were unable to identify any cases of bimodality in the directional spread during storm events.

Future Measurement Systems

A. W. Green ("Wave-Measurement Technology in the 1980s") briefly recapitulates the evolution of wave-measurement systems and projects their future course of development. Advances in instrumentation and microprocessors will certainly dominate as the slow evolution of wave sensors and more rapid development of electronics and procedures of analysis continue into the future.

Green considers several wave-measurement systems; for example, a pitch-roll buoy system in which rotational motions would be detected by the Sagnac effect in a fiber ring interferometer. This effect occurs with rotation of the interferometer about a normal axis; thus, the interferometer functions as a solid-state gyroscope with no moving parts. It is capable of detecting rates of rotation as slow as 10^{-3} degree per hour.

In a second system, the use of arrays of upward-looking sonar transducers to define the directional wave spectrum should become less expensive and more reliable with further development of the electronics. These sensors have the inherent advantage of linearity over near-bottom-mounted pressure sensors. Arrays of platform-mounted downward-looking radars or lasers could also be employed to define the directional spectrum. As noted by Parker, the above-water location of the active elements of this system would simplify installation and maintenance, as well as the geometric characteristics of the array. Green describes a futuristic air-deployable heave-pitch-roll buoy fitted with instruments to sense meteorological parameters and a telemetry link through a satellite to a ground station.

Results of the Workshop

The workshop was structured to elicit from all participants statements of problems and needed development in wave-measurement technology, and by progressive steps of distillation, redefinition, grouping, refinement, and ranking, the meeting's sense of the ten most significant problems demanding attention, in order of importance. The participants developed a detailed description and suggested program for the resolution of each problem (see "Results of the Workshop").

As defined and ranked by the participants in the meeting, the ten most urgent problems for research and development in wave-measurement technology are:

Priority 1: <u>Technology for Measurement, Analysis, and Reporting of Directional Wave Spectra</u>

Systems need to be developed that will function in shallow and deep water, and in high seas. These systems should operate reliably for extended periods, be inexpensive enough to be used routinely, and provide directional data verifiable by calibration and intercomparison.

Priority 2: **Assurance of Data Quality and Improvement of Data and Display Techniques**

Procedures should be developed to ensure the calibration of wave-measuring systems, and to better document the characteristics of any software employed. Where helpful, standardized methods and units should be used.

Priority 3: **Program for Intercomparing Various Measurement Systems to Determine Differences in Resulting Data Sets**

A field program should be planned for intercomparison of many in situ and remote sensors, and sustained until a sufficiently wide range of environmental conditions has occurred. The program might be seen as an extension of ARSLOE, which allowed several very useful intercomparisons to be made. Large-scale wave basins are being constructed in which realistic directional spectra can be generated: these basins may form a controlled but size-limited element of the intercomparison program.

Priority 4: **Nearshore Wave Fields and Related Processes**

Wave-measurement and analysis technologies need to be improved to allow better definition of the directional wave field in nearshore areas, where strong spatial gradients exist.

Priority 5: **Nonlinear Phenomena**

An understanding must be gained of nonlinear phenomena and their effects on the measurement and interpretation of wave characteristics. In addition, measurement procedures should be developed to identify or isolate nonlinear effects, such as the enhancement of shorter waves on the crests of longer waves, and the forms of breaking waves over a wide range of relative water depths.

Priority 6: **Development of Remote Sensors**

Available microwave sensors should be optimized for accuracy, resolution, and calibration in coastal, tower, ship, aircraft, and satellite operation. There is a particular need to deploy, on an operational basis, some of the sensors that are now available only in breadboard form.

Priority 7: **Global Wave-Measurement Systems**

Development should be pursued of a global wave-measurement system consisting of remote sensors and a central data bank for reporting and distributing results.

Priority 8: Buoy Development

Buoys offer significant near-term potential for the routine measurement of deep-water directional spectra. Areas requiring special attention are buoy transfer functions, robust solid-state sensors, onboard signal processors, survivability in extreme sea states, and development of expendable buoys with several months' reporting life.

Priority 9: New Sensors and Processing Techniques for Integration into Wave-Measurement Systems

Deficiencies that could be remedied by new sensors and processing techniques include measurement of: capillary waves; ocean surface curvature and higher-order descriptors; wave-induced, large-amplitude water-particle motions; momentum of breaking waves; and concurrent measurement of surface-wave and bottom topographic parameters. Techniques need to be developed for the processing, storage, and presentation of the multidimensional parameters of surface waves.

Priority 10: Wave-Measurement Resolution and Accuracy Needed and Attainable; Development of Procedures and Instruments to Improve Resolution

The users of wave data should be identified and grouped, and the resolution needed by each group quantified. Analytic procedures and new sensors could then be developed to make measurements where information of the desired quality is now lacking. In the meantime, available information may be usefully applied to enhancing the resolution of instrument data.

References

Borgman, L. E. and E. Yfantis (1979), "Three-Dimensional Character of Waves and Forces," Proceedings: Conference on Civil Engineering in the Oceans, IV (New York: American Society of Civil Engineers), pp. 781-804.

Cavaleri, L., J. A. Ewing, and N. D. Smith (1978), "Measurement of the Pressure and Velocity Field Below Surface Waves," Turbulent Fluxes Through the Sea Surface, Wave Dynamics and Prediction, A. Favre and K. Hasselmann, eds. (New York: Plenum Press).

Longuet-Higgins, M. S., D. E. Cartwright, and W. D. Smith (1963), "Observations of the Directional Spectrum of Sea Waves Using the Motions of a Floating Buoy," Ocean Wave Spectra (Englewood Cliffs, N.J.: Prentice-Hall), pp. 111-136.

Seymour, R. J. and A. L. Higgins (1978), "Continuous Estimation of Longshore Sand Transport," Proceedings: Coastal Zone '78 (New York: American Society of Civil Engineers), pp. 2308-2318.

OPERATIONAL NEEDS FOR WAVE DATA

Ledolph Baer[1]

Introduction

Information about ocean waves is needed to improve our understanding of the ocean's dynamics and its interactions, and to design and operate ships and offshore platforms, to plan shipping routes, and to design engineering works--ports and harbors for example, or beach protective systems--to understand coastal processes, and for commercial and recreational fishing.

While ocean waves have been studied and measured for these and other purposes, demands have increased in recent years for more and better wave data. Besides the range of needs for wave data entailed by ocean science and engineering, those responsible for planning the use of coastal lands or for emergency preparedness need accurate knowledge of wave conditions in advance of their occurrence, the effects of the waves, and the nature and probability of particularly destructive waves.

Assessment of Needs

The National Oceanic and Atmospheric Administration has investigated these demands in the course of planning how they might be met. The results of a preliminary survey of users of wave data in three categories--federal agencies, state and local governments, and other public entities and private industry--and of their needs are arrayed in Figure 1. While these results cannot be regarded as complete, they indicate that a large number and variety of users need wave data, and that the applications for which the data are required group naturally into six categories: ocean and coastal engineering, coastal and offshore operations, coastal erosion projects and evaluations, evaluation and mitigation of coastal hazards, environmental quality assessments, and wave energy.

Table 1 offers a brief summary of a national study carried out in 1977 that concluded the savings to engineering construction alone from good wave information would be from $80 to $100 million a year. A working group at the Ocean Wave Climate Symposium later that year estimated annual savings of about $1 billion from better wave data. Savings to shipping from better forecasts would probably be even

---

[1]Coastal Waves Program, National Oceanic and Atmospheric Administration

FIGURE 1 Users and Uses of Wave Information

	Ocean and Coastal Engineering	Coastal and Offshore Operations	Coastal Erosion	Coastal Hazards	Environmental Assessments	Wave Energy
FEDERAL USERS						
National Oceanic and Atmospheric Administration	U	U		U	U	
U.S. Corps of Engineers	U	U	U	U	U	
U.S. Coast Guard		U			U	
U.S. Navy	U	U				
U.S. Geological Survey	U					
Bureau of Land Management					U	
Nuclear Regulatory Commission	U			U		
Department of Energy	U					U
Maritime Administration	U					
Federal Emergency Management Administration				U		
TYPICAL STATE AND LOCAL GOVERNMENT USERS						
Port Authorities	U	U		U	U	
Coastal Planning Organizations			U	U	U	
Recreational Organizations	U	U	U	U		
Civil Defense Directors				U		
Public Works Department	U	U	U	U		
PRIVATE INDUSTRY AND OTHER PUBLIC USERS						
Ship Design	U	U				
Coastal and Offshore Design	U			U		U
Fishing		U				
Recreational Boating		U				
Offshore Oil and Gas Production	U	U			U	
Dredging		U	U	U		
Salvage		U	U			
Shore Protection	U	U	U	U		
Shipping	U	U				

Table 1 Annual savings to engineering construction from improved wave data (1977 survey)

Structure or Activity	Savings (in millions of dollars)
Marine Operations	10
Breakwaters	10-20
Prevention of Coastal Erosion	20
Submarine Pipelines	20
Offshore Structures	20-30
TOTAL	80-100

larger--and contribute to maritime safety. Someday, the nation should decide to spend a few million dollars in the interest of saving 50-100 times as much.

The wave-data users as shown in Table 2 need wave data for three basic types of activities. These activities are developing engineering design criteria, preoperational planning, and operational decision making.

Engineering design criteria are applied to ensure that offshore structures, coastal works, buoys, and ships will function as intended, and meet agreed-upon standards of safety, efficiency, and economy. Long-term probabilistic descriptions of the physical environment are vital to establishing adequate criteria. The development of these criteria requires relatively sophisticated wave information such as directional spectra, extreme value statistics, and such nonlinear properties as wave shape and groupiness.

Operational decisions, on the other hand, are often taken quickly, in response to prevailing or ensuing conditions. Ship captains, for example, need timely short-term forecasts of such relatively simple parameters as significant wave height, direction, and period. If these two very different needs could be met, the needs for wave data for pre-operational planning (scheduling, routing, and cost analysis) would also very likely be met.

Table 3 is abstracted from a recent internal NOAA assessment of over-all needs for marine environmental information in the waters of the United States. The decisions that must be made by a representative group of six major users of marine environmental information (offshore oil and gas operators, transportation industries, commercial fisheries, marine recreation, construction, and local communities) were analyzed in some detail. The wave data needed for these decisions were then, upon consolidation, assumed to represent the needs of all users: these are set out in Table 3. Generally, wave-height data are needed with accuracy of the order of 0.3 m at the 3-sigma level in a range of spatial resolutions from 1 to 1000 km^2, and temporal intervals from 2 to 6 hours. The consolidation process tends to raise the resolution requirements, quicken the required response times, and elevate the higher priorities. I should note that assignment of highest priority (number 1) was restricted to cases of nearly real-time safety. Thus, for example, climatological information that is considered absolutely

Table 2 Wave-data needs by major activities and purposes

Major Activities	Purposes for Which Data Needed	Data Required
Engineering design criteria	Offshore structures, coastal works, ports, submarine pipelines, naval architecture,...	Wave directional spectra, statistical analyses of extreme waves, nonlinear properties
Preoperational planning	Scheduling, routing, estimating and analyzing costs	Near-term and long-range forecasts, geographical statistics
Operational decisions	Safety, efficiency	Forecasts of significant wave height, direction, and period

necessary but not urgent for immediate safety decisions, rates priority-2 designation. I should also point out that scientific research needs for data were not considered.

NOAA's Plans to Meet Needs

The set of users' requirements set out in Table 3 can only be met by a combination of forecast and statistical products based on measurements, analysis, and theory. The wave measurements that were generally thought to be the necessary foundation for analyses and forecasts are given in Table 4. These are the requirements that it may be possible to meet in the reasonably near future: needs that exceed the probable state of the art are not shown. A preliminary plan to make the needed observations is sketched in Figure 2: basically, a line of widely spaced but sophisticated wave-measuring systems around the United States, and near the edge of the continental shelf, augmented by special measurements inshore of the network and a minimum suite of measurements covering the high seas. Wind fields and other such necessary information would, of course, be provided on a global basis.

A limited federal budget cannot provide all needed data with today's state-of-the-art wave-measurement systems. We must plan for relatively few direct observations and interpolation by some scientifically credible means to estimate the waves in other places. The preliminary plan of measurements for the NOAA Coastal Waves Program pictured in Figure 2 calls for about 20 wave-measurement

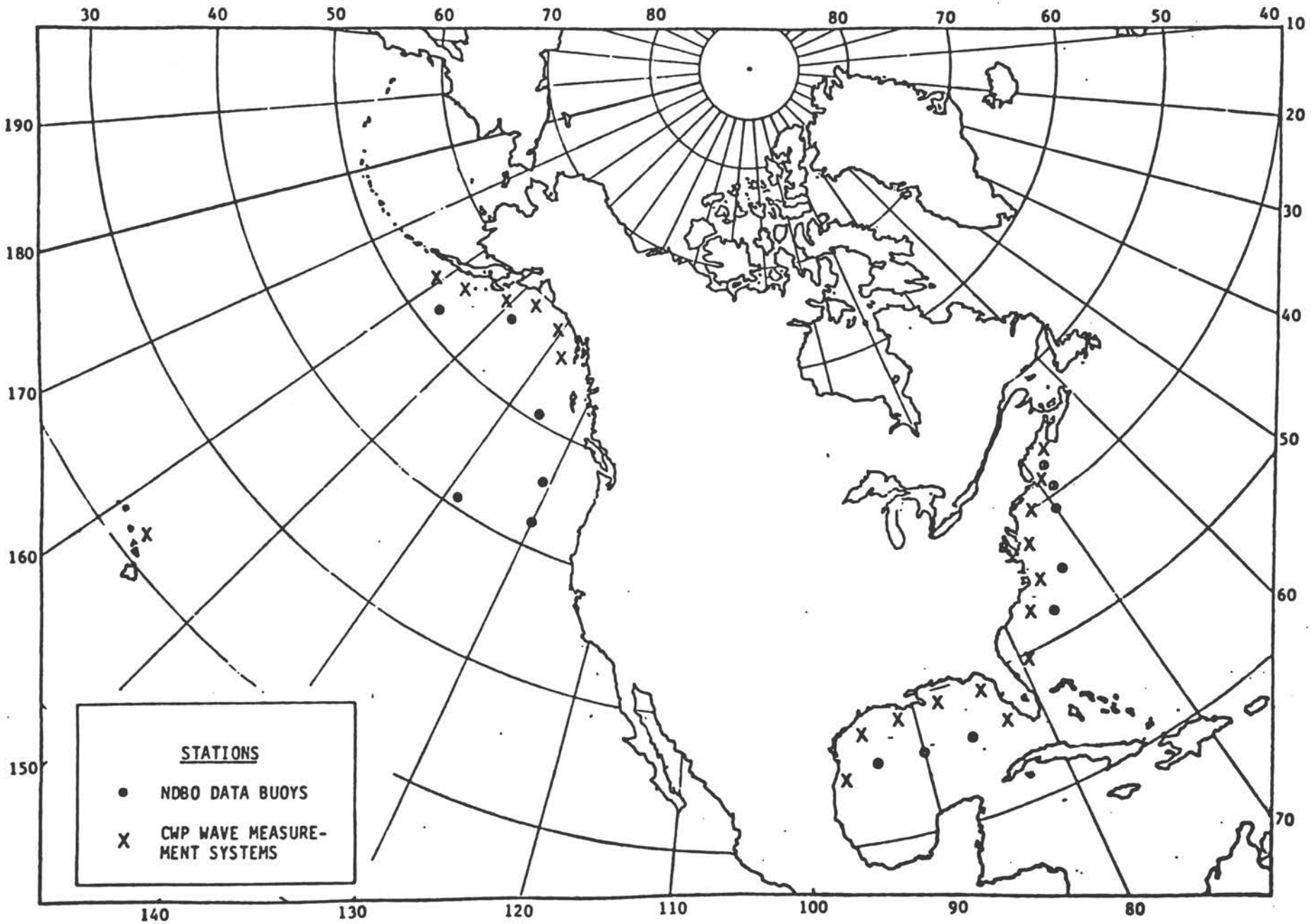

Figure 2 Hypothetical Long-Term Wave-Measurement System

TABLE 3 Consolidated Requirements of Wave Data

Parameter or Phenomenon	Priority	Units	Accuracy (3 σ)	Resolution Space (km^2)	Resolution Time (hrs)	Zone	Forecast Length (Days)	Update Interval (Time/Day)	Significant Thresholds	Notes
Surf Height	1	m	0.6	100	3	S&B	3	2		
Surf Height	1	m	0.4	1	3		1+	2		
Wave Direction	2	deg	15	10	3	S, C&O	1	2-4		
Wave Height	1	m	0.3	10	3	S, C&O	1	2-4	2-5	
Wave Height	1	m	0.3	1	2	S&C	1	3	0.6	
Wave Height	1	m	0.5	1 K	6	C&O	3	2	0.6	
Wave Period	2	sec	20%	100	6	C&O	1-3	2		
Wave Period	2	sec	2	10	3	S, C&O	1	2-4		
Wave Directional Spectra	2	m^2/sec/deg	Note	10	1/2	S, C&O			2m	Accuracy equiv. to 10°, 0.3m, 1 sec. Accuracy equiv. to 0.3m, 1 sec.
Wave Bispectrum	3	m^2/sec	Note	10	1/2	S, C&O	0			

PRIORITIES

1 - Critical to Safety
2 - Important
3 - Desirable
4 - Useful

ZONES

B - Beaches (Inland)
C - Coastal (0-30 km)
O - Offshore (30-500 km)
P - Ports
S - Shallow Areas
Z - Specific Sites

TABLE 4 Summary of Required Observations

Parameter	Priority	Accuracy 1%	Range	Sampling Space (km)	Interval Time (Day)	Region	Resolution Space (km2)	Resolution Time (hrs)	Accept Delay (hrs)	Notes
66. Waves-Directional Spectra	2	Eq. to 0.5m Sig. ht. 10°	True	400 line	4+	Line along shelf edge	10	1/2	2	66. Total 25 locations. Need observations at highest conditions even if not at standard observation time. If directional spectra are not available, measure frequency spectra only.
67. Waves-Frequency Spectra	3	Eq. to 0.5m Sig. ht.	True	Variable	4+	Inshore from shelf line	1	1/2	2	67. Total 25 locations which are shifted frequently.
68. Waves Frequency Spectra	4	Eq. to 0.5m Sig. ht.	True	Note	4	"	"	"	"	68. Network totaling about 100 permanent locations (potentially coop. with local agencies).
69. Waves-Directional Spectra	3	Eq. to 0.5m 10°	True	Note	4	Open Ocean	L	L	3	69. Min. 10 locations. If directional spectra not available, measure frequency spectra only.
70. Significant Height	3	0.5m	True	150	2	Global	"	"	"	70. Prefer spectra if feasible.
78. Local Conditions (for toxic spill movement)										
Wave Direction	3	Eq. to 1m Sig. ht.	0-360	10	24	Near Spill	S	S	1	78. Special network of up to 5 sites.
Wave Spectra	3	Eq. to 10m	"	"	"	"	"	"	"	

L = Large Scale; 100 km^2 and 3-6 hr resolution
S = Small Scale; 100 km^2 and 0.5-1 hr resolution

PRIORITIES:
1 - Critical to Safety
2 - Important
3 - Desirable
4 - Useful

locations on the continental shelf. None is shown for the California, Washington, and Oregon coasts, where wave-measurement programs are being planned or carried out by the U.S. Army Corps of Engineers. The dots farther offshore designate data buoys operated by the NOAA Data Buoy Office, most of which also measure waves.

Objectives for Accuracy

Table 5 shows the preliminary objectives for accuracy established for the NOAA Coastal Waves Program. Those set for actual measurements are considered achievable and reasonable; those set for hindcasts and other analyses are derived. These values should meet the needs of many different users; however, some users have already suggested that higher objectives of accuracy should be set for wave period.

Table 5 Preliminary CWP accuracy objectives (3σ)*

o Parameters Derived from Measurements (Not Including Statistical Confidence)	
Individual Height	±5%
Significant Height	±2%
Period of Maximum Variance	±0.5 s
Mean Direction	±5°
Spectral Energy Density	±10%
Resolution of Wave Energy Directional Spectra	±15°
o Parameters Derived from Hindcasts of Directional Spectra	
Significant Height	±10%
Period of Maximum Variance	±0.5 s
Directional Resolution	±15°
o Output Products (Including Statistical Confidence and Representativeness)	
Nonextreme Height Statistics	±10%
Nonextreme Spectral Density Statistics	±15%
Extreme Height for 100-Year Return Period	±15%

*Based on heights of 3 m or more.

Problems to be Resolved

Error Some exciting new results highlight issues of accuracy. The top set of curves in Figure 3 shows the bias in estimating the 100-year maximum significant wave height from records of various length and random errors in the measurements. Bias results from the ordering process used in the analysis. Such a bias can be removed if the underlying system accuracy is known. The errors shown are for 90 percent confidence and are total-system errors: sensor error +

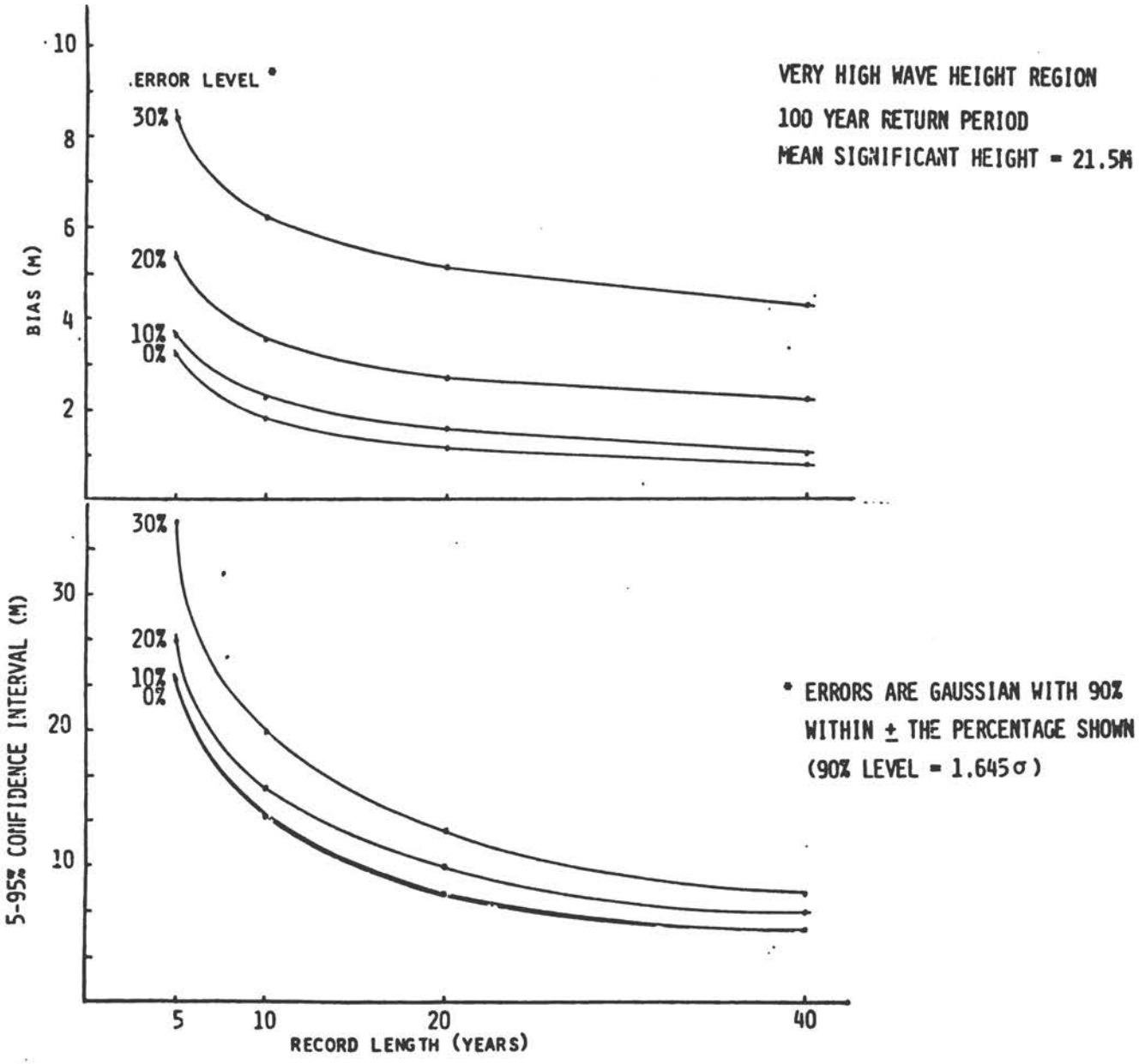

Figure 3 Bias in estimations of 100-year maximum significant wave height from various records (top); effects of errors in the records on confidence intervals (bottom)

sampling variability + nonstationarity effects + analysis errors. Since sampling variability alone is 10-15 percent at 90 percent confidence for typical 17-minute records, there must be errors of significant size in the records.

The set of curves at the bottom of Figure 3 shows the effects of errors in the records on the confidence intervals for the 100-year maximum significant wave height. A complete risk analysis to establish optimum design criteria must consider the width of these confidence intervals. The curves also show that we can never achieve high accuracy with hindcasts alone because the larger errors do not completely cancel. These values are significant. Biases might typically be 3-6 m; confidence intervals are typically 10-15 m.

Calibration The measurement system may pose problems in meeting objectives of accuracy as well. Figure 4 shows calibration plots of the most commonly used wave-measuring instrumented buoy. The top curve gives the calibration corrections specified by the manufacturer. The bottom curve is the calibration curve that NOAA's Engineering Support Office measured on a rotating arm. The amplitude differences between the manufacturer's specification and the measurements are sometimes as great as 8 percent, and almost all have indicated that wave measurements will be too low.* We hope to carry out an intercalibration program between facilities conducting similar tests to gain more knowledge of inaccuracies of this type.

Among the questions to be answered is whether significant changes occur in heave response as a function of current speed and mooring configuration. What accuracy do we really have? Nonlinear effects need to be evaluated. Known frequency-dependent phase relationships could have significant implications for the phase relationships of the different spectral components that make up individual wave heights. A further implication, depending on the results, could be that zero-crossing analyses, groupiness studies, and many other techniques of analysis and research cannot be effectively applied to the data collected by these instrument systems.

Data Communications We have found that the reliability of communications systems on standard instrumented buoys declines with distance. As a pilot test, NOAA operated three such instrumented buoys in the Atlantic about 25 km off Ocean City, Cape Henry, and Cape May. Many phase-lock losses were discovered in the telecommunications to the shore. Only 47 percent of our records were found to have good communications. The Institute of Oceanographic Sciences also reported interference problems off the coasts of England in its 1979 Annual Report. NOAA has since substituted a narrow-band filter and a more

*The manufacturer of this instrument has made a design change that appears to correct the problem.

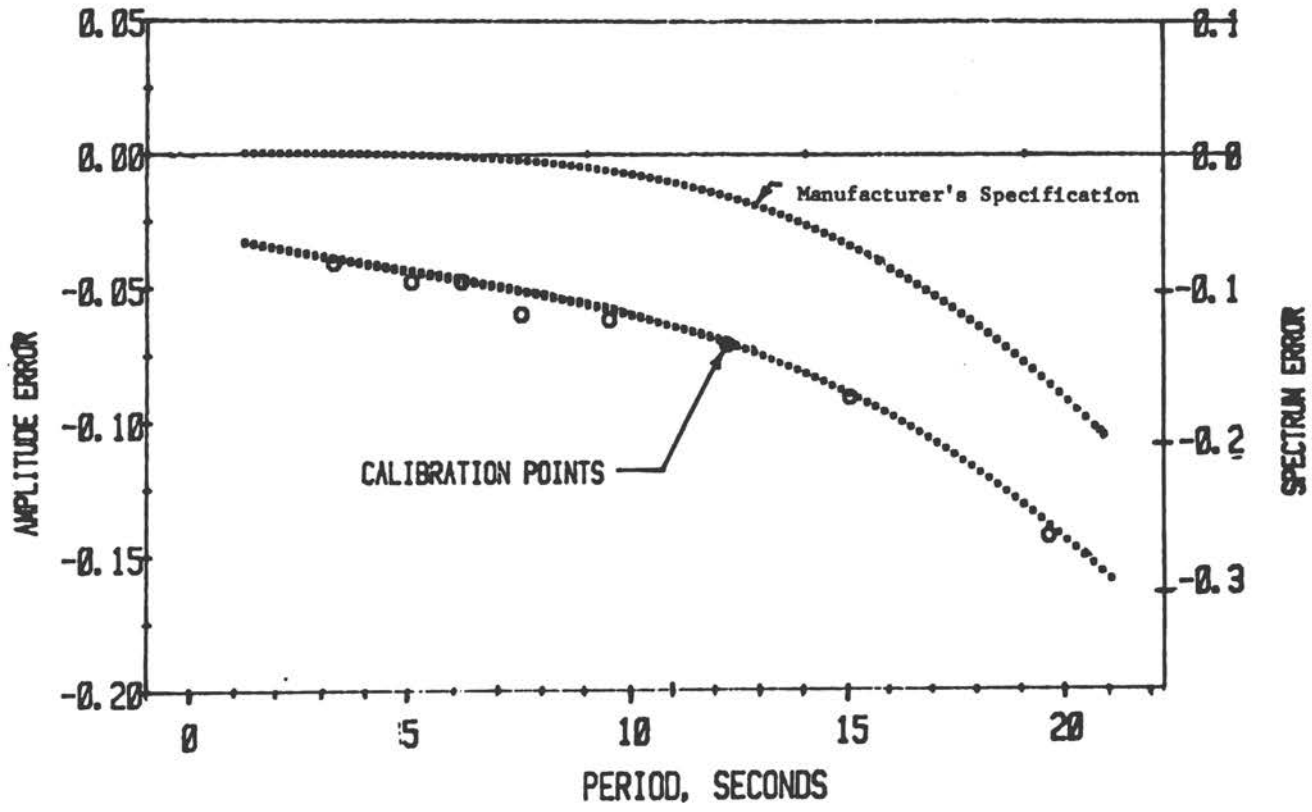

Figure 4 Typical buoy pre-deployment calibration*

*SOURCE: Engineering Support Office, National Oceanic and Atmospheric Administration

directional antenna on these buoys, and achieved much higher reliability. We now have buoys on order modified to communicate via GOES satellite for deployment farther offshore--and it is hoped, with improved reliability. These satellite communication systems offer "thresholding," or the capability of taking more data when the waves are high or otherwise interesting. The problem, of course, is that satellite communication systems are much more expensive and have significant power limitations.

Directional Resolution Figure 5 illustrates a problem in acquiring directional wave measurements with the available instrumented buoy systems. Pitch-roll buoys and equivalent systems provide only five Fourier coefficients to discriminate directions. The plot shows that use of the standard analysis (as proposed by Longuet-Higgins and others) for the coefficients supplied by such a system yields resolution of about 130°. This means that two individual spectral components of the same frequency that are 90° apart could not be resolved: the resulting directional plot would look like the dashed curve. If, on the other hand, all the energy were in a single spike, the directional distribution would look like the solid line. Even for this spike spectrum, the computed directional distribution is much broader than that found in the Stereo Wave Observation Project (SWOP).

Perhaps the only useful directional information from such systems is the mean direction for each frequency, which can be extracted with reasonably high resolution. Hindcast models based on wind fields can then be used to define a more precise directional spectrum for measurement. Several new methods of analysis are being developed that might improve the resolution. Some method is obviously needed for computing directional spectral components with much higher resolution than is now available.

Summary

Table 6 gives a brief summary of the principal wave-measurement problems I feel most urgently need attention to meet the needs of users.

Table 6 Wave-measurement problems needing attention

Data Quality: Evaluations and Standards
- Over-all accuracy--influence of mooring, calibration specifications, variability with environmental conditions, standards for analysis
- Reliability--phase-lock losses
- Phase-shift effects on true wave heights

Operational Limitations
- Range/depth
- Power-supply limitations on operating time
- Message-length limitations of satellites
- Reliability in all weather conditions
- Directional resolution

System Cost

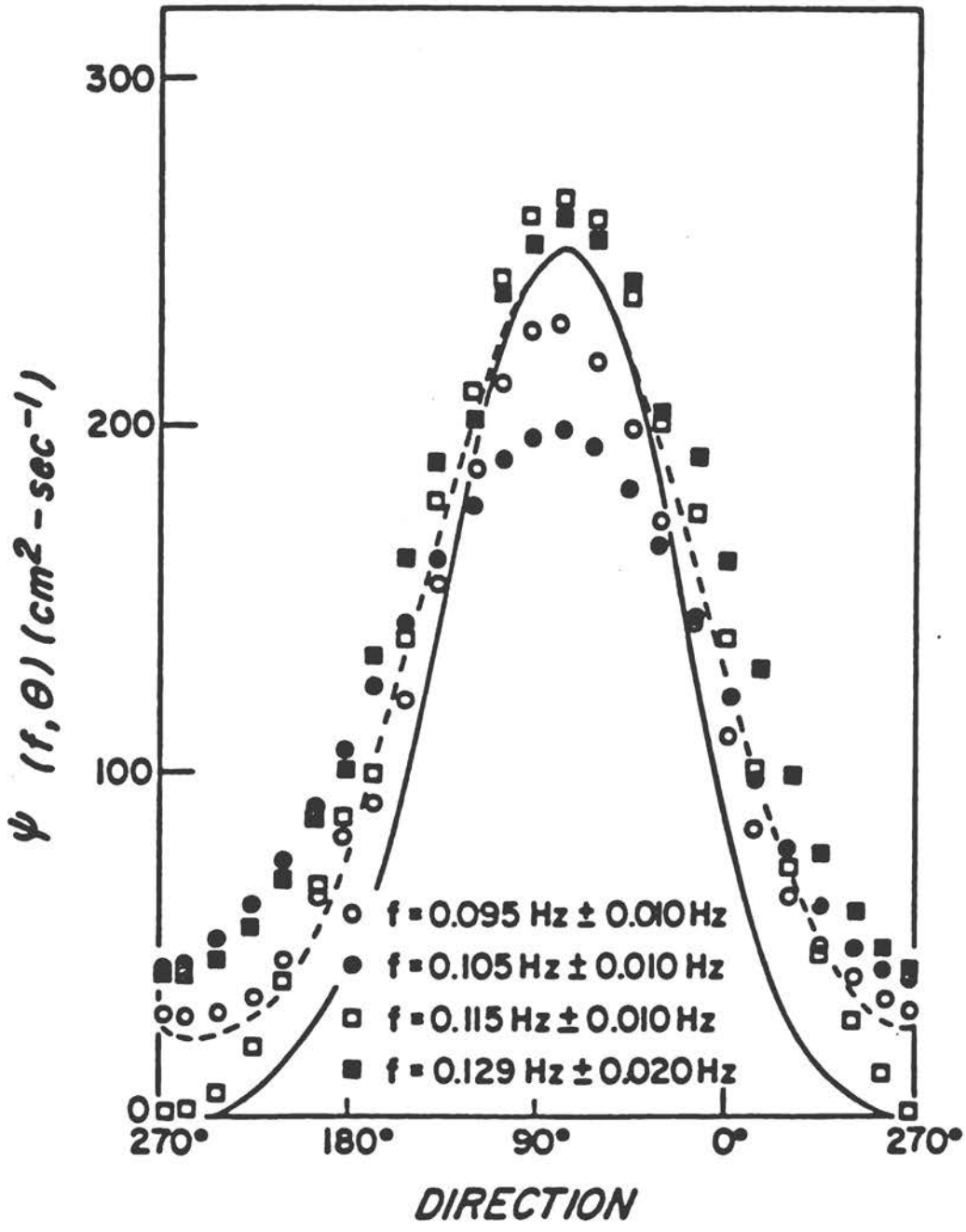

o, •, □, ■ Directional spectra from first 5 Fourier coefficients, calculated from 3 components of wave orbital velocity

——————— Directional spectrum from same method if all energy traveling in mean direction

---------- Directional spectrum from same method if energy split between 45° and 135°

(Amplitude of —— and ---- adjusted so that peaks coincide.)

Figure 5 Broadening of spectra owing to methods of analysis*

*SOURCE: M. D. Earle, personal communication.

Evaluating the quality of the data and establishing standards are basic. We need to know the accuracy of measurement methods even if the objectives we set cannot be met. We need improved analytical methods or better measurement systems (or both) to achieve greater accuracy and to account for nonlinear effects. Many problems also remain to be solved in providing the data needed for ocean science.

Problems affecting the reliability of communications, such as the phase-lock losses mentioned in a preceding section, must be overcome. There are many serious operational limitations in available systems; among them, a special problem with directional resolution.

Practical considerations also need attention. We lose too many expensive instrumented buoys, especially in high wave conditions, when we need the data most. Operational needs require long-term measurements, especially when the waves are high. Finally, we need to lower the cost of wave-measuring systems.

RESEARCH NEEDS FOR WAVE DATA

Leon E. Borgman[1]

Abstract

Research in ocean wave phenomena may be classified in different ways: 1) by wave frequency or period, 2) by probabilistic frequency or return period, 3) by environment of occurrence, 4) by area of application, 5) by potential for new results, and 6) by degree of innovation. The problems that appear important to individual researchers are conditioned by their experience within these various classifications. Four significant problem areas are selected in this paper for detailed examination and discussion of needed data. These are 1) probabilistic properties of sequences of waves, 2) the statistics of wave interaction with current and bathymetry, 3) probabilities for extremes of coastal flooding and wind-wave effects, and 4) measurement systems for wave directionality. Finally, the suggestion is made that 5-10 percent of each project budget be set aside to fund subsequent analysis of the data by another agency or university to extract information of a more general nature than that for which the project was planned.

A Research Parable

"Three mountain climbers separately studied a mountain to determine how it could be climbed. One, finding snow and ice, decided to prepare himself by learning ice techniques. Another encountered a rocky overhang, and spent years learning technical rock-climbing methods using pitons and ropes under tension. The third climber was confronted with large inclined rock slabs that could be traversed by friction--carefully balancing vertically over the rocks with rope-soled shoes--so he perfected that technique. When they returned to climb the mountain, each failed because he encountered problems for which he had not prepared. They met in the village below the mountain, and decided to pool their efforts and try again. This time, with the expert for that particular terrain leading the rope whenever difficulties were encountered, they reached the top after a great deal of effort...."

The obvious point of this story is that a variety of skills is required to solve most problems. Researchers rely on each other. But

---

[1]University of Wyoming

there are other analogies to the real world of research: it is not always clear which mountain needs to be climbed. Of course, for truly "pure" science, the problem is attacked just because it is "interesting." More commonly, there is some audience urging the effort. Most ocean engineering is "applied," although the connection is sometimes indirect. In reviewing the needs for ocean wave data by scientists and engineers, a good starting point is to examine what "mountains" need to be climbed, who constitutes the "audience," and what array of "climbing" techniques may be needed.

A Multivariate Overview

Each participant in a meeting such as this one needs to re-examine his area of expertise to see how it may effectively interrelate with the various aspects of the field. There are many ways to subdivide ocean wave research. The field may be viewed as multivariate, with each coordinate axis providing another way to classify the various aspects of wave phenomena as they interact with the geographic features of the earth.

Some of the coordinate axes in the multivariate space are as follows. Waves may be classified by frequency, as shown in Figure 1. This dimension extends from very low-frequency waves, such as tides and tsunamis, through storm waves and very high-frequency wavelets and "cat's paw" ripples. Probabilistic frequency is another classification of waves. The return period for wave intensity provides a measurement basis for this axis, as given in Figure 2. Another dimension for wave classification is by environment of occurrence, which lends itself to subdivision according to distance from land, as shown in Figure 3. Coastal flooding is at one extreme and deep-ocean phenomena at the other. The area of application for various aspects of wave research is really a multivariate subspace, but for purposes of discussion, a loose subdivision can be made (such as that shown in Figure 4) by concerns related to real estate (coastal flooding, beaches), energy and minerals (offshore oil, seafloor mining), commerce (harbors, ship routing), food (fisheries, oyster beds), and defense (storm forecasting for military logistics).

Two additional, somewhat more abstract dimensions that are nevertheless significant in organizing wave research are the scale of examination and the potential for significant new results. Wave features may be studied individually, regionally, or on an oceanwide scale, as indicated by Figure 5. New concepts or equipment may make certain areas of wave research particularly ripe for significant discoveries (see Figure 6). In particular, the statistical examination of previous deterministic problems has often led to new insights and interpretations of old problems.

The six dimensions mentioned do not, of course, provide an exhaustive description of the multivariate space. There are other dimensions. Three come immediately to mind: political pressure for solutions to problems, historical thrust or direction (mainstream

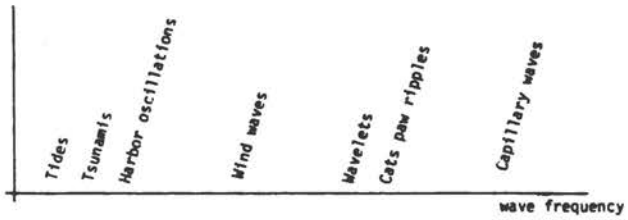

Figure 1 Classification by wave frequency (hertz)

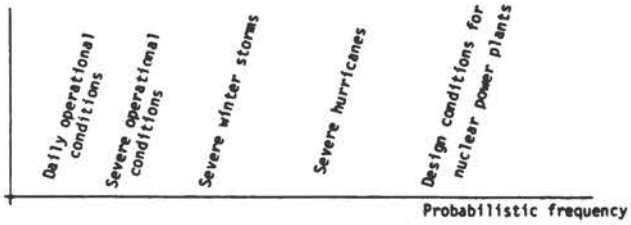

Figure 2 Classification by probabilistic frequency (return period)

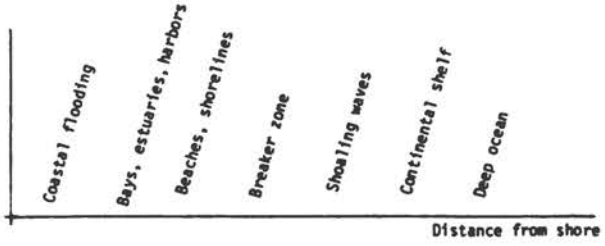

Figure 3 Classification by environment of occurrence

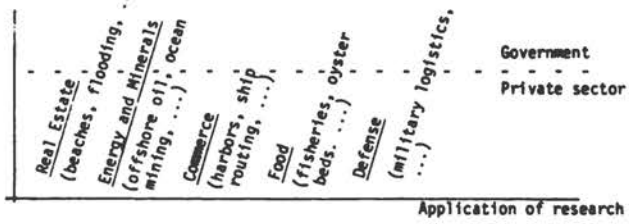

Figure 4 Classification by application

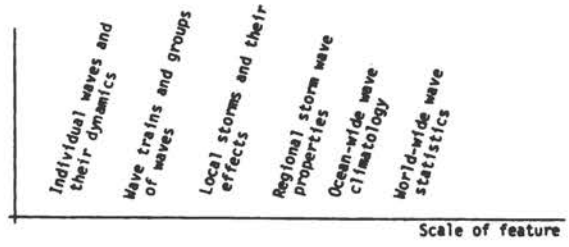

Figure 5 Classification by scale of feature of interest

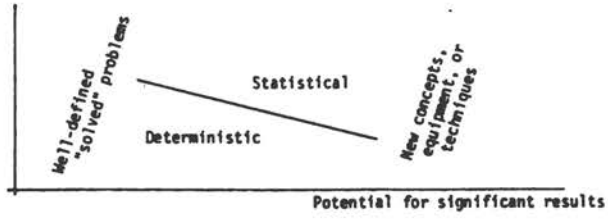

Figure 6 Classification by research potential

topics versus unusual research fields), and degree of innovation. Other, perhaps more significant, dimensions may occur to the participants attending this meeting.

An important implication of this analysis is that each investigator of wave problems occupies a region within the multivariate space of wave research. By virtue of education, research history, and intellectual interest, each has valuable, intimate knowledge of some part of this space. Conversely, that part is not the whole space, and some degree of tolerance is needed for the knowledge and viewpoints of other researchers.

The author's subspace and viewpoint have been influenced by a statistical, geological, and civil engineering education, an interest in extreme statistics, spatial geostatistics, the statistical theory of waves, and related measurement systems, a long history of projects related to the U.S. Army Corps of Engineers and the oil industry in coastal and continental shelf waters, and of course, an academic perspective. Certainly, the recommendations for ocean wave data presented in this paper should be judged as representative of this particular combination of history and interest.

Some Specific Problems

Four significant areas of research* requiring ocean wave data have been selected for review: 1) properties of successions of individual waves, 2) wave interactions with other environmental aspects, 3) extremal probabilities for coastal flooding, and (4) wave directionality, in general.

Sequences of Waves

It has long been suspected that storm damage to structures as diverse as offshore oil rigs and coastal breakwaters may be as much related to the particular sequences of waves as to the intensity of individual waves. Wave grouping, in both height and direction, may be a major determinant of breakwater damage, for example. It is common to find in field measurements that the highest was not the most forceful wave. One may conjecture that the flow structure of preceding waves set the stage for a very intense horizontal surge of water in the present wave.

To study this problem adequately, more data are needed than present technology can provide, although oil companies have recently made intensive efforts to study the total assemblies of wave properties in a "bump" of water as it strikes a fixed-leg platform.

---

*The brevity of this review and the number of investigators who have made important contributions to these topics preclude a complete historical account.

The difficulties are conceptual as well as related to the lack of data. How should the direction of an individual, short-crested wave be defined as it impinges on the structure? What is the detailed water-particle-velocity structure within the moving mound of water? What are the multivariate probability laws relating the various geometric properties of a succession, or group, of these short-crested waves as they reach the structure? Perhaps some sort of rapid, computerized scan is needed of the two-dimensional water-level elevation in or surrounding the structure as a function of time. Certainly, a substantial amount of theoretical and conceptual development is required for interaction with data collection. The integration of the concept of individual wave-travel direction with the probabilities of other wave properties is itself a relatively undeveloped subject. The same can be said of the probabilities related to sequences of waves.

Collecting data to answer these questions would entail innovative techniques applied very intensively for short periods of time. It would probably not be appropriate to extend such an effort over many years, unless the data collection could be automated and managed via radar or some similar shore-mounted system.

Interaction of Waves and Other Aspects of the Environment

Investigating the interaction of waves with currents, bottom bathymetry, winds, shoaling, and other aspects of the environment demands statistical analysis or a deterministic Fourier decomposition, since a mixture of waves with different frequencies and travel directions is usually present. Nonlinearities, in particular, and the apparently statistical nature of the data need to be resolved. This problem area is really the battleground of coastal processes, since it relates directly to coastal erosion and breakwater damage, and to diverse operations on most of the continental shelf. The extrapolation of deep-water wave forecasts over the shelf to the shore, as well as shallow-water wave-generation processes, is pertinent to problems of interaction, especially if site-specific wave predictions are to be made in very shallow water.

The data for this area of research should be gathered over a long-term period covering many seasons, and directional measurements should be among the data collected. It would be desirable to select one area of coast for a fairly dense array of instrumentation, both alongshore and extending to relatively deep water. Much more would be learned from an area-intensive deployment of instrumentation than from the same instrumentation spread thinly over all coasts. A good argument can be made for several clusters of instrumentation at various typical coastal sites; nevertheless, a "critical mass" of instrument density is necessary for real progress in understanding coastal interactions. An instrument density below this critical mass is relatively ineffective and might as well be replaced with a few gauges placed to gather climatological data. If funds are limited, it would be better to

instrument one area adequately, and deploy a few gauges over the rest of the area for fundamental climatological data.

Extremal Statistics of Coastal Flooding and Associated Wind Waves

Long-term climatological extremes are significant in coastal flooding and coastal erosion, but extreme events are rare, and difficult to intercept with operating instrumentation. In addition, highly site-specific characteristics of the nearshore bathymetry, the topography of the land, and the pattern of vegetation influence the severity of flooding and associated wave attack. An unusual amalgam of deterministic long-wave surge theory, extremal statistics, and storm wind-wave climatology is required. More accurate storm hindcasting and the further development of joint probabilities for storm path, intensity, and scale characterizations are needed.

Two types of data measurements could be used to make more accurate predictions of the extremes of coastal flooding. One would be from rather evenly spaced nets of wave-measurement devices along the coasts of flood-prone areas. These would need to be maintained continuously and routinely, as is the present tide-gauge system. Both the long-wave surge and the shorter wind-wave activity would need to be recorded. The wind-wave measurements would also be useful for calibrating and verifying storm wave hindcasts and storm routing when extreme events do occur.

The second type of useful data measurement would be performed after extreme coastal flooding occurs. Immediately after the storm, a team of specialists would document the magnitude of flooding and any special features with photographs and measurements. These would subsequently be compared with mathematical and statistical models. Some such activities are undertaken, of course, by the concerned government agencies and other interested researchers. Further standardization of procedures and improved methods for data dissemination and follow-up studies are called for, as well as sustained support.

Wave Directionality

The general topic of wave directionality is not particular to singular geographic settings; rather it has direct pertinence to all scales of research and engineering problems respecting waves, from wave generation in major storm systems to the study of individual waves surging against a breakwater.

The three most important geometrical characteristics of an individual wave are height, period, and direction. One might also add crest height and some measure of short-crestedness. Of these, wave direction appears to be the most significant parameter that is not routinely measured, although short-crestedness is also rarely determined. Both are strongly related to the directional mixture of waves present.

Most investigators of wave effects have recognized the importance of wave direction, but it is difficult to measure routinely. Buoys, arrays of wave gauges, and instrument arrays, including subsurface current meters, have all been used to determine the characteristics of wave direction. Most systems require careful, continuous attention to keep the instrumentation operational. Three techniques appear to offer promise for successful routine operations: the tilt-and-roll buoy (van der Vlugt et al., 1982), a fixed-space array of bottom-pressure cells (Seymour and Higgins, 1978), and a platform-mounted wave staff with velocity gauges measuring horizontal water-particle-velocity components at several depths beneath the staff (Forristall et al., 1978). All three systems have been used by various investigators in more or less routine measurement programs, but some development research would still be desirable.

The data measurements needed for wave-directionality studies entail continued use of these systems in a variety of environments to gain more information about their accuracy and reliability.

One other system for measuring wave direction, at least in the high-frequency end of the spectral density, should be mentioned: shore-based or airborne radar. It appears to offer the substantial advantages of being operable in severe weather and giving good regional pictures of wave directionality. Its primary disadvantages appear to be cost and certain frequency resolution problems.

For in situ instrumentation such as wave gauges, there is a point of diminishing return in increasing the number of instruments in the array: not only are there more instruments to maintain, but other problems arise. If the instruments are too close together, they carry the same informational content as other gauges nearby. On the other hand, if the gauges are too far apart, apparent spatial nonstationarity in the random wave field is often encountered. Thus, the three systems mentioned earlier appear to represent the cost-effective compromise for routine measurements. However, for special, one-time studies, more elaborate systems may well be appropriate.

General Comments

The accuracy needed in wave measurements varies with the application. However, measurements of low accuracy collected routinely are often more useful than those of higher accuracy gathered sporadically. Often, some type of replication and statistical processing can provide accuracy sufficient for parameter estimates, even if considerable noise affects the data. A well-known example is the average of a random sample of size n. The arithmetic average has a standard deviation of $\sigma/n^{\frac{1}{2}}$, although the original data have a standard deviation of σ. The population mean is determined with substantially more precision than the scatter of the raw data.

The same general comments apply to determining the principal direction of wave travel and the dispersion of wave energy about that direction from wave measurements with a tilt-and-roll buoy. The

apparent spreading function for the directional spectrum as determined from the first two Fourier harmonics may be quite broad. In spite of this, the principal direction and dispersion may be determined with substantially better precision. Some examples of this are presented in Table 1 (Borgman et al., 1982). The root-mean-square error in determination of principal direction and dispersion was determined both analytically and by simulations to obtain the results listed. The rms errors of 4^{o}-10^{o} are quite acceptable for most applications.

Considering the substantial experience of most of the participants in the meeting, it appears unnecessary to emphasize the regular calibration of in situ ocean instruments before, during, and after data collection. Many problems with data analysis and interpretation are related to inadequacy of calibration procedures. In fairness to investigators, it should be mentioned that lack of critical calibration may be owing to circumstances beyond the control of the data collection personnel.

Whatever efforts are dedicated to collecting data, the data may become useless in time. Every researcher is aware of large bodies of data, collected at substantial cost, that are quietly becoming obsolete in storage, as the personnel who know the format and special features of the data disperse to other jobs and other concerns. Insufficient money was set aside for analysis. This may be true even if the data were completely analyzed for the particular purpose for which they were collected. It is the author's strong opinion that at least some portion of each data collection budget should be dedicated to further analysis of the data as they pertain to the general fields of ocean science and engineering. This final analysis phase may be difficult to justify to research administrators, but the value to the profession makes the effort worthwhile. An independent facility is best suited to perform the analysis to extract the aspects of the data of general usefulness. About 5-10 percent of the total budget might be a good figure to set aside for this general post-analysis.

Epilogue

The research parable beginning this discussion continues:

"When the three climbers reached the top, they saw that they were not really at the mountain top. The slope dropped slightly to a saddle and then rose steeply to a much higher crest. And they proceeded again to learn new techniques so they could ascend this new crest."

The final obvious point to the story is that in research there are always new problems to solve and new techniques to develop. The participants are invited to gather on the promontory to which we have climbed and plan our ascent to the next higher crest.

Table 1 Accuracy of determination of directional spreading function parameters by a tilt-and-roll buoy* ($N = 1024$, $\Delta t = 1$ s)

Case 1 (Symmetric, unimodal) (57° effective width)

Fourier Coefficients: $\pi a_1 = -.923$, $b_1 = 0$, $\pi a_2 = .725$, $b_2 = 0$

Parameter:	Principal Direction	Dispersion
rms error		
- by theory	3.6°	2.5°
- by simulation	3.7° 3.6°	2.7° 2.7°

Case 2 (Symmetric, bimodal)

Fourier Coefficients: $\pi a_1 = -.462$, $\pi b_1 = -.462$, $a_2 = 0$, $b_2 = 0$

Parameter:	Principal Direction	Dispersion
rms error		
- by theory	9.8°	4.1°
- by simulation	10.6° 10.2°	5.4° 4.5°

Case 3 (Nonsymmetric, bimodal) (82° effective width)

Fourier Coefficients: $\pi a_1 = -.839$, $\pi b_1 = -.084$, $\pi a_2 = .593$, $b_2 = 0$

Parameter:	Principal Direction	Dispersion
rms error		
- by theory	4.9°	5.2°
- by simulation	4.7° 4.7°	5.4° 4.1°

*SOURCE: L. E. Borgman, R. Hagan, and A. J. Kuik (1982), "Statistical Precision of Directional Spectrum Estimation with Data from a Tilt-and-Roll Buoy," Advanced Topics in Ocean Physics (in press).

References

Borgman, L. E., R. Hagan, and A. J. Kuik (1982), "Statistical Precision of Directional Spectrum Estimation with Data from a Tilt-and-Roll Buoy," Advanced Topics in Ocean Physics (Scheduled for publication by the Italian Physical Society).

Forristall, G. Z., E. G. Ward, V. J. Cardone, and L. E. Borgman (1978), "Directional Spectra and Kinematics of Surface Gravity Waves in Tropical Storm Delia," J. Phys. Oceanogr., 8: 889-909.

Seymour, R. J. and A. L. Higgins (1978), "Continuous Estimation of Longshore Sand Transport," Proceedings: Coastal Zone '78, 3: 2308-2318.

van der Vlugt, A. J. M., A. J. Kuik, and L. H. Holthuijsen (1982), "The WAVEC Directional Buoy under Development," Directional Wave Spectra Applications (New York: American Society of Civil Engineers), pp. 50-60.

SURVEY OF REMOTE SENSING TECHNIQUES FOR WAVE MEASUREMENT

Norden E. Huang[1]

1. Introduction

Remote sensing, by definition, is to sense or measure something without direct physical contact by the instrument or the observer. By this criterion, remote sensing of ocean waves is not only the most widely used method, but also the oldest one--visual observations made with human eyes. Visual observations of sea state are routinely recorded by all research vessels and oceangoing ships. These data constitute the bulk of the existing data base used by engineers as well as scientists (Wiegel, 1974).

As our interactions with the ocean increase, the need for detailed quantitative sea-state data also increases. The data base and sources of data are woefully inadequate for several reasons, among them the subjective nature of visual observation. Statistical analysis of the distribution of visually observed data reveals large variations and significant bias (Parsons, 1979). Second, the geographical distribution of the data sources is quite uneven. Observations are abundant in the heavily used sea lanes, but hardly available in meaningful quantity elsewhere. This leaves vast areas, including some near-coastal regions, grossly underrepresented in the data base, or not represented at all (Meserve, 1974). Third, the historical data base derived from visual observations is biased low owing to practices of ship routing that seek to avoid extreme sea states. Nevertheless, extreme sea states provide the most important of needed information. Before quantitative remote sensing technologies and methods came of age, in situ methods were studied intensively. In situ methods were reviewed recently by Ribe (1979).

The most critical problem with in situ methods is the limited area of coverage. Not all ocean surface areas are equally accessible. Even unattended buoys cannot achieve the desired coverage, nor can they provide sea-state data globally. The need for more versatile measurement methods and the advancement of radar and space technology in recent years have led to the rapid development of quantitative remote sensing methods for ocean wave measurements. The advantages of remote sensing methods for oceanographic studies have been discussed by various investigators, such as McGoogan (1975), Apel (1976, 1980), and Huang (1979). This discussion will be limited to wave measurements.

---

[1]NASA Goddard Space Flight Center, Wallops Flight Facility

Surface waves are ubiquitous. Because the ocean wave is a surface phenomenon, it is ideally suited to measurement by remote sensing techniques. Waves are not just the source of information for remote sensing, but also a source of noise. For example, wind speed at the ocean surface measured by a scatterometer depends on short-wave intensity (Jones and Schroeder, 1978). Wave Doppler shift measured by radar provides surface current information (Stewart and Jay, 1974). On the other hand, ocean surface waves influence measurements of mean sea level by an altimeter (Jackson, 1979a). The study of waves by any means is thus a necessary step in establishing remote sensing techniques to monitor the oceans.

A brief review of the principles of remote sensing techniques for ocean waves is offered in the succeeding section, followed by a summary of remote sensing instruments and recent results. The last section discusses new approaches to wave studies in light of newly available information and promising developments.

2. The Principles of Remote Sensing Techniques for Ocean Wave Measurements

Great progress has been made in the study of ocean waves since World War II. Scientific progress can only be commensurate with observational techniques, and improved understanding of ocean wave phenomena leads to demands for better measurements. New observational methods using electromagnetic (EM) waves to make ocean wave measurements are among the latest developments in ocean wave studies.

The commonly used EM wave ranges and their wavelength-frequency designations, according to the Radio Regulations of the International Telecommunications Union (see, for example, Westman, 1974), are given in Figure 2.1. Since all EM waves in ocean water for ocean wave measurements have to rely on the information from backscattering at the ocean surface, the key to establishing any EM remote sensing technique is a clear understanding of the physical processes involved in the interaction of electromagnetic and ocean waves.

This interaction is basically the backscattering processes, reviewed recently by Valenzuela (1978). When the EM wave encounters the ocean surface, a certain portion of its energy will be reflected by the random ocean surface. This reflected EM wave contains useful information about the reflecting surface. The scattering of the EM wave from a rough surface is a classical problem. General reviews of this subject can be found in Beckmann and Spizzichino (1963), Shmelev (1972), and Long (1975). A solid foundation of theoretical work has been laid for using the backscattered EM signal as an information source to measure ocean waves (Barrick, 1968a,b, 1970, 1972a,b; Barrick and Peake, 1968; Brown, 1978; Mikhailov, 1960; Moore, 1978; Rice, 1951; Valenzuela, 1967, 1968, 1978; Wait, 1971; Wright, 1968).

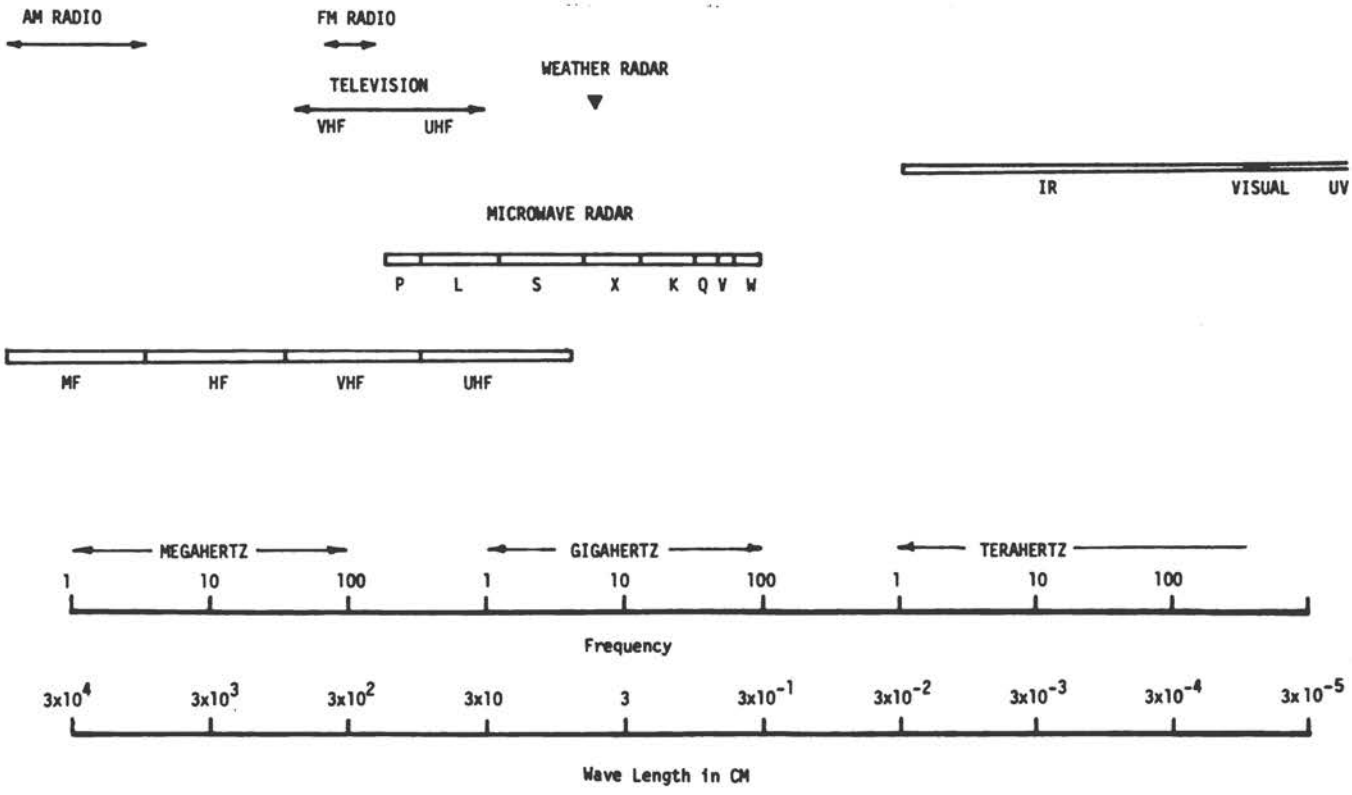

Figure 2.1 Electromagnetic wave ranges and their wavelength-frequency designations, according to the Radio Regulations of the International Telecommunications Union

In simple terms, there are two basic backscattering processes, specular and Bragg scattering (shown in Figure 2.2). Specular scattering is limited by

$$\theta_i \leq \left\{ \overline{\left(\frac{\delta\zeta}{\delta r}\right)^2} \right\}^{\frac{1}{2}} \tag{2.1}$$

but

$$\theta_i = \frac{\delta\zeta}{\delta r} \tag{2.2}$$

where θ_i is the angle of incidence of the EM waves with respect to the vertical, ζ is the surface elevation, r is the radial distance from the nadir point, and the over-bar designates the mean. As the incidence angle increases, the scattering process becomes the resonant Bragg type. For this case, θ_i is limited by

$$\left\{ \overline{\left(\frac{\partial\zeta}{\partial r}\right)^2} \right\}^{1/2} \leq \theta_i \leq 70^{\circ} \tag{2.3}$$

and the scattering is generated only by those waves that satisfy the resonant condition given by

$$k = 2k_e \sin\theta_i \tag{2.4}$$

where k_e is the wavenumber of the EM wave and k is the wavenumber of the ocean waves. All these scattering processes are incorporated by Brown (1978) in an elegant composite rough-surface model. As the amplitude of the ocean wave increases, the second- and higher-order contributions to the scattering processes will become more obvious. In fact, this higher-order backscattering process is basic to certain techniques for measuring the ocean wave spectrum. The details of the mathematical derivations and expressions can be found in Valenzuela (1978) and Barrick (1978). Most of the predominant remote sensing techniques for measuring the ocean's wave field use the microwave portion of the EM system, and can be described generally as radar. "Radar" will be used in this paper as a convenient label for remote sensing techniques, but the reader should understand that instruments using other portions of the EM spectrum are included.

Since the backscattered EM wave is the only source of information about ocean waves collected by a remote sensor, measurements must be based on the EM wave processes of transmission and reflection. Two basic measurement techniques are used in any active EM remote sensing system, as described in the succeeding subsections.

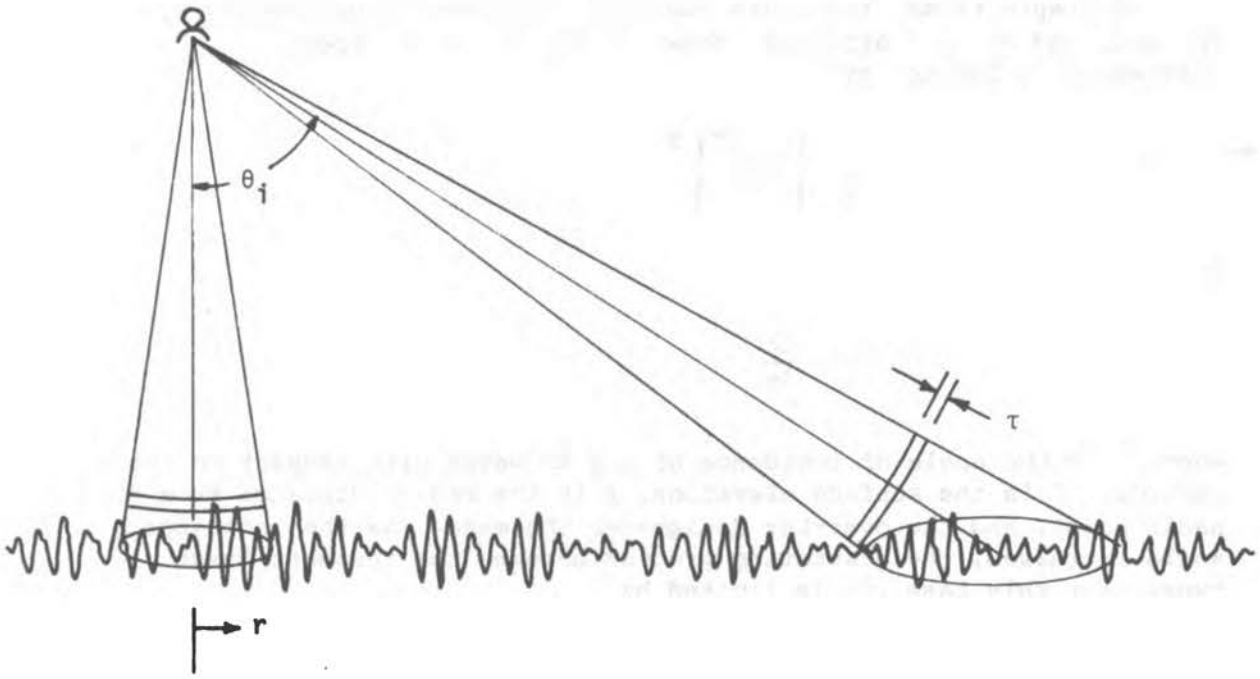

SPECULAR		BRAGG
$\theta_i \leq \left\{\overline{\left(\frac{\partial \zeta}{\partial r}\right)^2}\right\}^{\frac{1}{2}}$	Range	$\left\{\overline{\left(\frac{\partial \zeta}{\partial r}\right)^2}\right\}^{\frac{1}{2}} \leq \theta_i \leq 70°$
$\theta_i = \frac{\partial \zeta}{\partial r}$	Condition	$K = 2 K_e \sin \theta_i$

Figure 2.2 The principal backscattering processes

2.1 Ranging

The most important and basic function of a radar is to measure the distance between the radar and the target by transmitting a pulse and measuring the time elapsed between transmission and return. The return pulse is recorded by a set of range gates, each with a specific width, but usually fixed at the same value, designated as pulse duration width. The minimum distance ΔR between two points on the ground that a radar can discriminate can be calculated as

$$t = \frac{2R}{c}$$
$$t + \tau = \frac{2(R + \Delta R)}{c} \tag{2.5}$$

where c is the speed of light (3×10^8 m/s). Therefore,

$$R = \frac{ct}{2} \tag{2.6}$$

and

$$\Delta R = \frac{c\tau}{2} \tag{2.7}$$

If the radar sends the pulse at repetition periods of T seconds, then the maximum unambiguous distance that can be measured is given by

$$R_{max} = \frac{cT}{2} \tag{2.8}$$

Equation (2.6) gives the range information, (2.7) the resolution limit, and (2.8) the range limit. To achieve better resolution, a narrow pulse is necessary. This was made possible by the pulse-compression technique, which reduces the pulse width to a few nanoseconds (see, for example, Skolnik, 1962). Besides these theoretical limitations, practical limitations of power and pulse shape are important criteria in radar design. Details can be found in standard references on radar systems, such as Skolnik (1962).

Although ranging is the most elementary function of radar, practical problems arise in attempting to use the ranging technique for wave measurements. To measure the height of individual waves, for example, the radar footprint must be small in comparison to the ocean wavelength, and meeting this requirement demands a very large radar antenna. For a dense set of data, the radar will have to have very high pulse repetition. Both requirements make a direct range device to profile individual waves from satellites infeasible. However, successful airborne systems have been designed and constructed using both laser (Hoge et al., 1980) and radar (Kenney et al., 1979).

It should be pointed out that the range gates could be used to measure the stretching of the returned pulse by the ocean waves. This

is a variation of the ranging technique that will yield wave-height statistics. A detailed discussion is given in a subsequent section.

Finally, the range information can also be obtained by continuous-wave (CW) radar or amplitude-modulated (AM) and frequency-modulated (FM) radars using phase-shift information. This will be discussed together with the Doppler effect in the next section.

2.2 Doppler Effect

The relative motion of the radar and the target produces the Doppler effect--a frequency shift, or a rate of change of phase. Consider a radar signal of the form

$$S(t) = S_o \sin 2\pi f_o t \tag{2.9}$$

where f_o is the frequency of the EM wave transmitted. For a moving target traveling at a velocity, V, the range between the radar and the target is changing constantly as

$$R = R_o + Vt \tag{2.10}$$

If the signal is sent by the radar and reflected by the target, the reflected signal at time t would be

$$S_r(t) = S_o \sin [2\pi(f_o(t - \Delta t)] \tag{2.11}$$

(The signal was sent at $t - \Delta t$.) Since

$$\Delta t = \frac{2R}{c} = \frac{2\ (R_o + Vt)}{c} \tag{2.12}$$

then (2.11) and (2.12) will give the returned signal as

$$S_r(t) = S_o \sin \left[2\pi\left(f_o - \frac{2f_oV}{c}\right) t - \left(\frac{4\pi f_o R_o}{c}\right)\right] \tag{2.13}$$

Thus, the returned signal would have a different frequency

$$f_r = f_o - \frac{2f_oV}{c} \tag{2.14}$$

and a phase shift, given by

$$\phi_r = 4\pi \frac{f_o R_o}{c} \tag{2.15}$$

The difference between the transmitted and returned frequency is the Doppler shift, f_d, or

$$f_d = f_r - f_o = -\frac{2f_o V}{c} = -\frac{2V}{\lambda_r} \tag{2.16}$$

where $\lambda_r = c/f_o$ is the wavelength of the transmitted EM wave. The Doppler shift is directly related to the relative velocity of the radar and the target, and inversely proportional to the EM wavelength. The target velocity can be measured by using the relationship given in (2.16). One of many examples of Doppler-effect applications is the measurements of wave-phase velocity made by Wright and Keller (1971).

By use of the phase shift given by (2.15), distance can be calculated in terms of the EM wavelength as

$$R_o = \frac{\phi r}{4\pi} \cdot \lambda_r \tag{2.17}$$

Thus, by monitoring the phase shift, the distance can also be measured. In real applications, the phase shift can be derived from the phase change from an amplitude-modulated CW signal. Then, the phase tracking will be with respect to the envelope of the modulated signal rather than the carrier. The phase shifts of a CW laser and radar have been used by Ross et al. (1970) and Barnett and Wilkerson (1967).

A combination of the basic techniques is used for ocean wave measurements in most applications. These are described in the succeeding sections.

3. Instruments and Results

Although the basic techniques of radar measurements are simple, a variety of different combinations of the basic techniques have been used in design and construction of instruments for actual wave measurements. This section reviews the available instruments and results. For the reader's convenience, a few commonly used classification schemes of radars are given first.

3.1 Classification of Radars

Radars can be classified by various characteristics. The following commonly used criteria of radar classification define instrument functions and their products.

3.1.1 By the EM Wave Signal Source Radar systems can be classified as active and passive devices. The active device has both a transmitter and a receiver. The signal received is sent and controlled by the transmitter, which is an integrated part of the instrument system. The transmitter and the receiver usually employ a single antenna, as in most radars, but this is not necessary. The transmitted EM waves can be in any EM wave range, such as visible laser light, microwaves, and high frequency (HF). In general, the transmitted EM wave serves as the active probing agent of the instruments. Active devices are designed to measure the changes in geometric shape and spatial location of the target, and are therefore ideal for wave measurements.

The passive device has only a receiver. The signal is either from emissions or reflection of other natural EM wave sources. Since most of the emission processes are controlled by physical properties of the target, such as temperature, color, or salinity, they are usually not good sources of wave information. The results are subject to wide variation in uncontrollable environmental conditions because of the unknown quality and quantity of the EM wave source. Consequently, most wave-measurement instruments are active devices. The only passive devices used for deducing wave-field characteristics are limited to various photographic methods--stereo photography, for example (Cote et al., 1960), and still photographs (Stilwell, 1969).

3.1.2 By the EM Wave Characteristics Many characteristics are used to specify the EM waves; the two most common are the waveform and wavelength.

Radars can be divided by waveform used into pulse and CW radars. The CW radars include the amplitude-modulated and frequency-modulated variations, in which wave information is given by phase and Doppler shifts. The pulse radars can be further divided into beam-limited and pulse-limited radars, as shown in Figure 3.1. A beam-limited radar requires a large antenna to focus the beam and produce a small footprint. In close-range measurements--from aircraft, for example--the footprint could be much smaller than the ocean wavelength. Thus, the ranging information could effectively profile the ocean surface (as in most profilometers and their variations). The pulse-limited radar derives statistical wave information from the incoherent reflection of EM waves that stretches the returned pulse. Since there is no need for a large antenna to focus the beam, this technique is better suited to space applications. Using pulse-compression techniques, the pulse can be narrowed to as little as 3 nanoseconds, the pulse of the Seasat-1 altimeter.

If radar is classified by EM wavelength, the principal types rely on microwave and HF waves. The visual band is limited to cameras or laser devices.

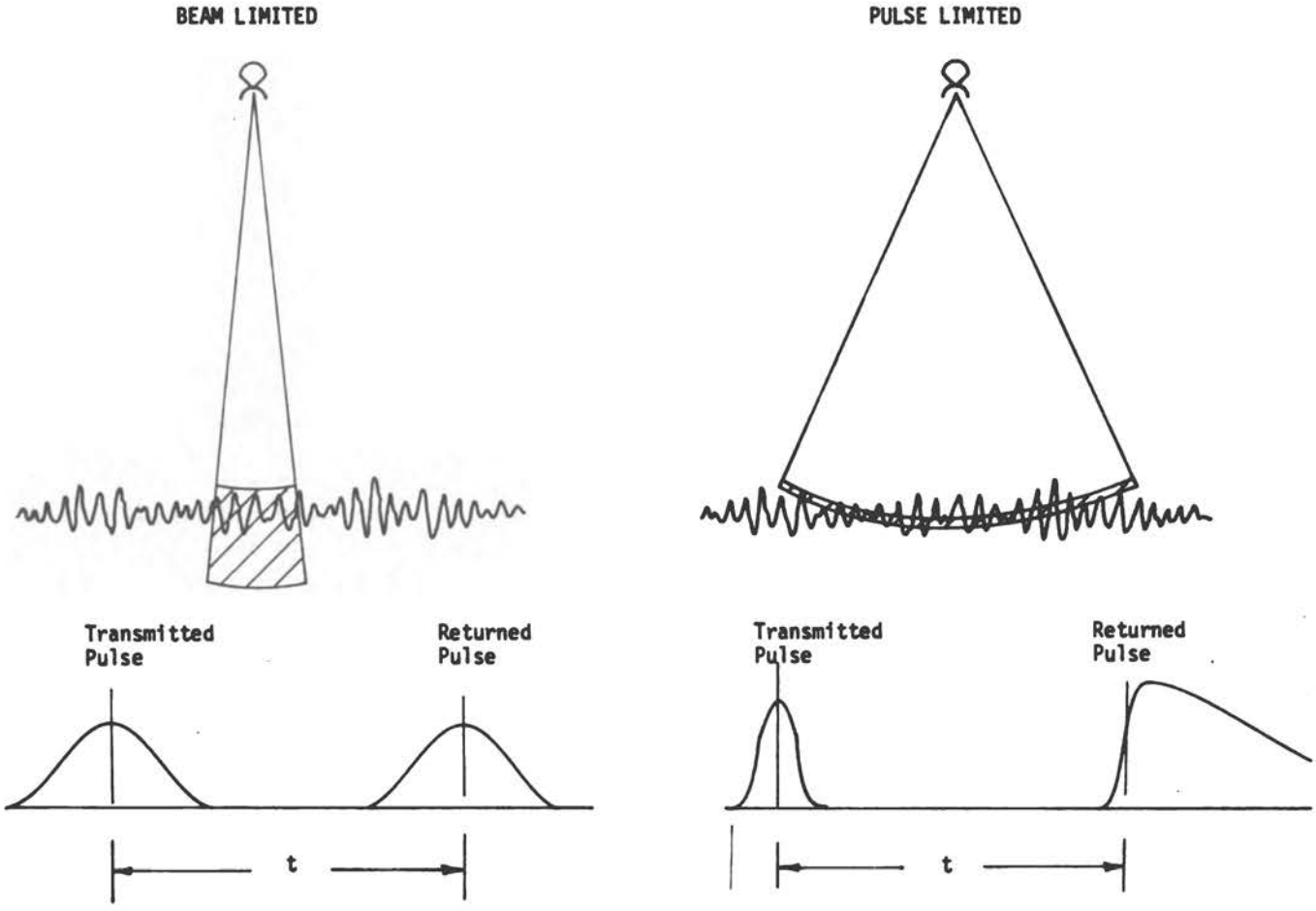

Figure 3.1 The principles of beam- and pulse-limited radars

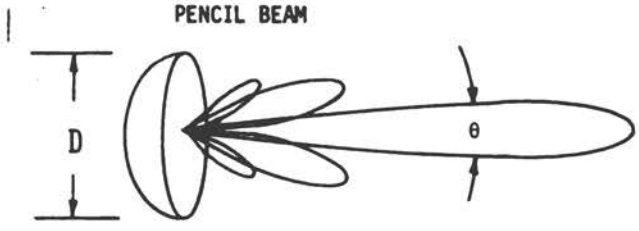

Angular Resolution

$$\Theta = \lambda r / D$$

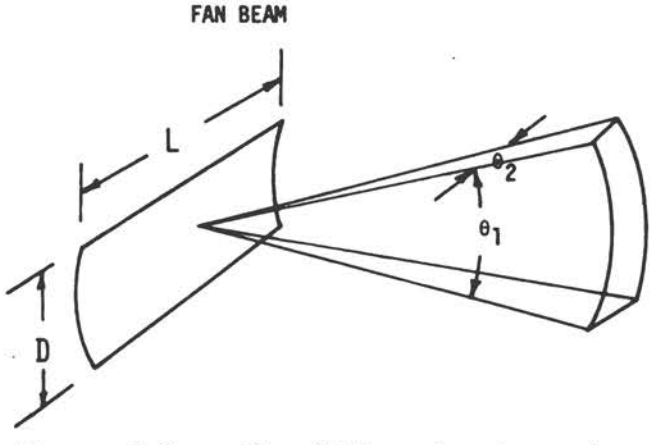

$$\Theta_1 = \lambda r / D$$

$$\Theta_2 = \lambda r / L$$

Figure 3.2 The different antenna beam patterns

3.1.3 By Antenna Characteristics The geometric shape of the radar antenna controls the transmitted and backscattered EM beam shapes. Depending on the shape of their antennas, radars can be classified as pencil beam or fan beam, both shown in Figure 3.2. The pencil-beam radars need large antennas to focus on the sea surface. The beam width, θ, or the angular resolution is given by

$$\theta = \frac{\lambda_r}{D} \tag{3.1}$$

where D is the diameter of the antenna. The fan-beam radars have asymmetric antennas. The resolution power of the beam is unequal, but can be determined by the different linear dimensions of the antennas using equation (3.1).

Beam width is not the only way to limit the footprint of a radar in ocean wave measurements. The pulse width should also be considered. A narrow-pulse radar will also have a limited footprint, even if the beam width is large.

Other than the geometric shapes, the relative locations of transmitter and receiver are also used to classify radars, as shown in Figure 3.3. Most radars are monostatic. Bistatic radars are common in ground-based systems. The sweep aperture radar employs a multiple transmitter/receiver system and the motion of the platform to create an effectively stationary radar. This greatly facilitates the Doppler measurements of target motion from a moving radar. However, in order to use the sweep aperture, the height of the spacecraft, H, has to be known precisely to determine the antenna separation, L. The formula is simply

$$L = \frac{2VH}{c} \tag{3.2}$$

This concept is discussed in detail by Bush and MacArthur (1979).

Synthetic aperture radars use a single antenna for transmitter and receiver. The information received is processed coherently to produce an image of the ocean. This technique is discussed in detail in Section 3.2.8.

3.1.4 By Look Angle The radars can be classified according to the look angle of the transmitter and receiver as nadir-looking, side-looking, and scanning. Most nadir-looking devices to measure waves are based on ranging, or a variation of ranging such as pulse stretching. Altimeters and profilometers are nadir-looking radars.

There is a much wider variety of side-looking devices. Almost all the side-looking devices use the Bragg scattering process to generate the returned signal, and the measured quantities are derived by a combination of ranging and the Doppler effect. The beam width can be narrow, as in the real aperture radar, or wide, as in the synthetic aperture radar. For the real aperture, the antenna can be rotated to generate a scanning pattern of footprints.

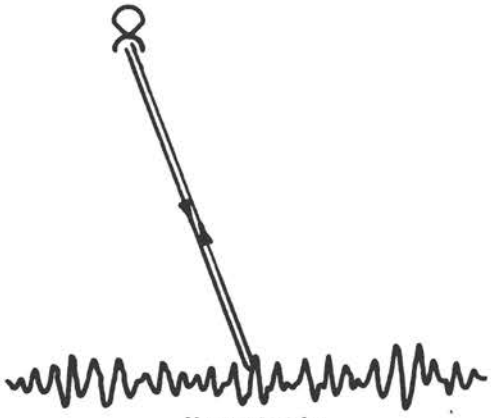

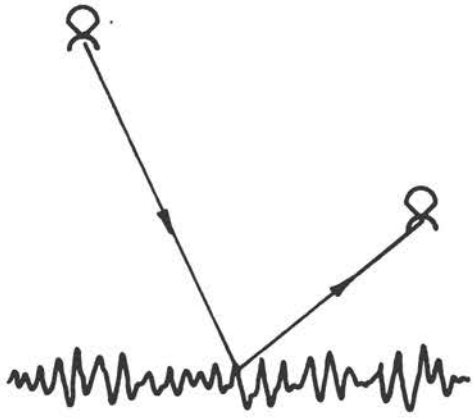

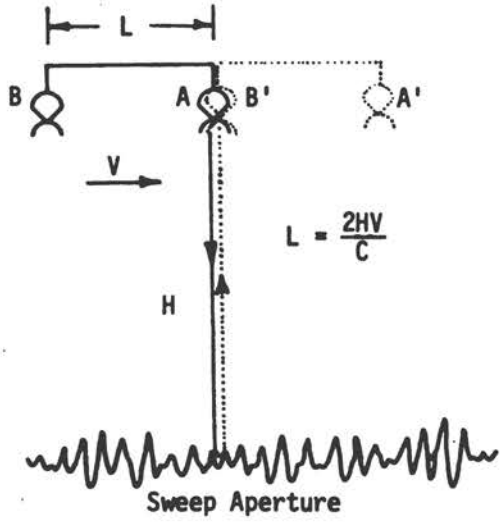

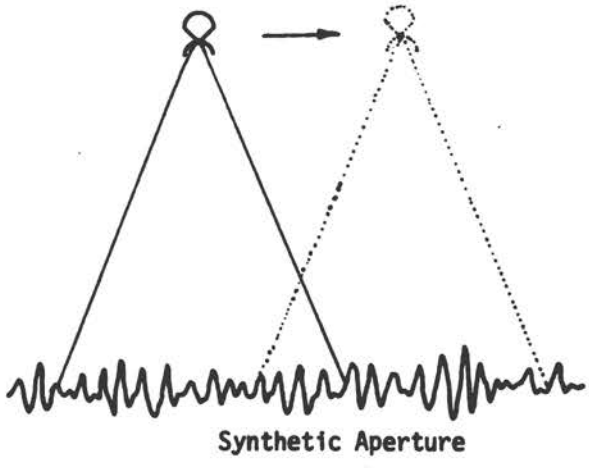

Figure 3.3 The different transmitter/receiver arrangements

A variation of the side-looking technique is the near-grazing-angle radar, used principally in ground-based systems. In this case, the radar beam is almost parallel to the surface. The Bragg resonant condition approaches

$$k = 2k_e \tag{3.3}$$

These near-grazing-angle radars can transmit the EM wave directly as ground waves or surface waves with very limited ranging (less than 100 miles) or indirectly as sky waves reflected from the ionosphere, extending the range to a few thousand miles.

3.1.5 By Outputs Classified by their outputs, radars can be divided into imaging and nonimaging devices. Most of the imaging radars are active side-looking devices. The ranging resolution is achieved by transmitting a short pulse: resolution of a few meters can easily be accomplished. The azimuth resolution for the image can be achieved two different ways, as shown in Figure 3.4. One is by using a real aperture. According to the antenna theory, the angular resolution is given by (3.1). Thus, the spatial resolution is

$$\Delta R = \frac{R\lambda_r}{D} \tag{3.4}$$

The real aperture radar uses a fan beam to increase its resolution power in the azimuthal direction. However, even with the fan beam, the minimum separable target distance increases directly with the range. This requirement makes the use of real aperture radar cumbersome for satellite-borne systems.

The second method to achieve azimuth resolution is by using synthetic aperture. Details of the synthetic aperture technique can be found in many of the standard references; for example, Rihaczek (1969), Harger (1970), Kovaly (1976), and Hovanessian (1980). The synthetic aperture technique is basically that of sensing the Doppler effect on the backscattered signal from different looking angles, and processing the information coherently. The theoretically attainable spatial resolution in the azimuthal direction is given by

$$\Delta R = \frac{D}{2} \tag{3.5}$$

The amazing fact is that the resolution is independent of the range. However, owing to the curvature of the pulse front, the phase shifts are different for different looking angles. This effect is called unfocusing. An unfocused radar can only achieve a spatial resolution of

$$\Delta R = \frac{1}{2}(R\lambda_r)^{\frac{1}{2}} \tag{3.6}$$

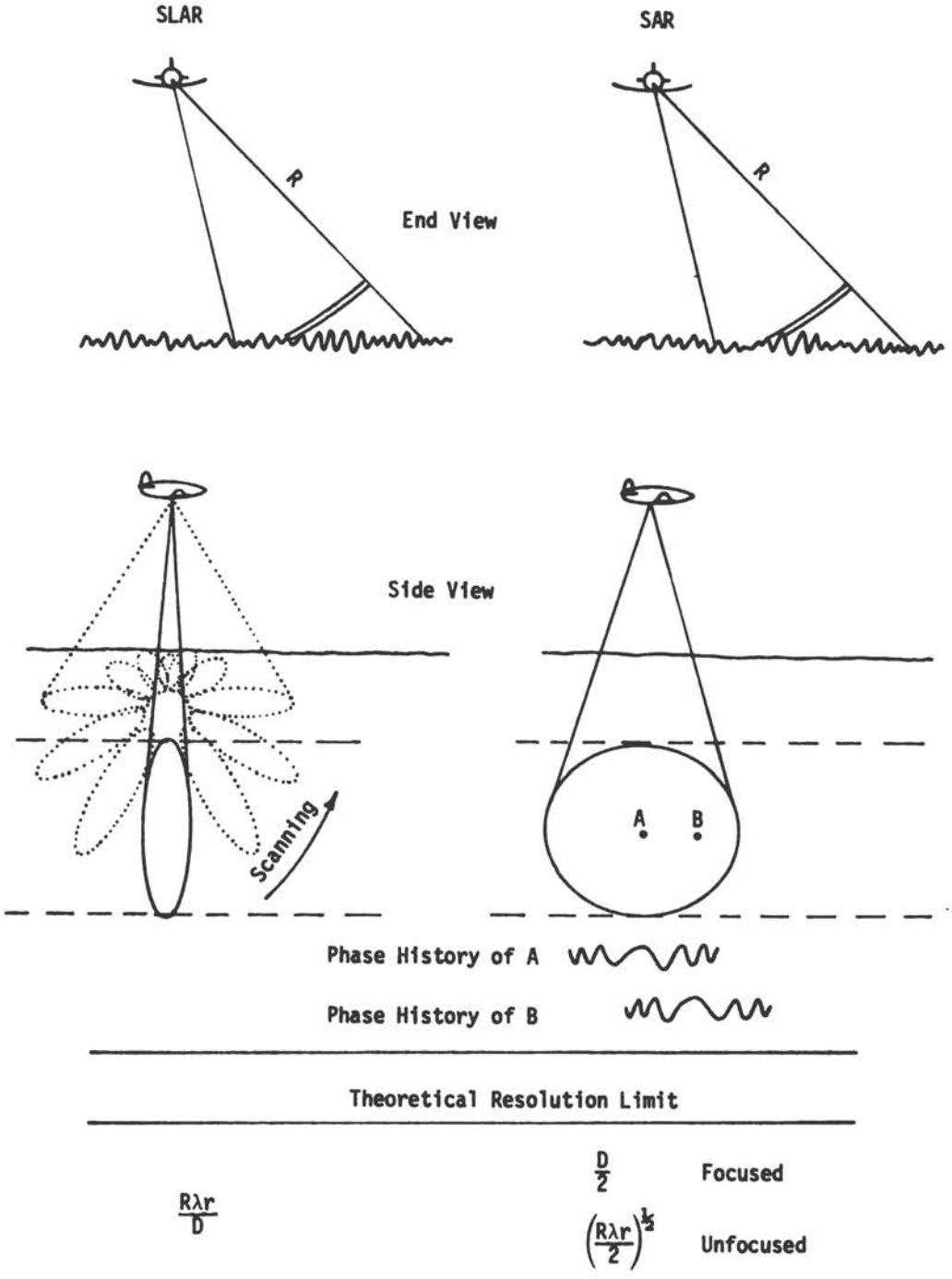

Figure 3.4 The principle of SLAR and SAR operations

The unfocusing effect can be corrected if the relative speed of the radar with respect to the target is known. Owing to the antenna pattern of the radar beam, the best actually achievable spatial resolution for a focused radar is approximately

$$\Delta R = \frac{3D}{2} \tag{3.7}$$

Since R is almost always much larger than D, the resolution power of even an unfocused synthetic aperture radar is much better than that of a real aperture system. Because of the coherent processing of the information, the data reduction task is a much more complicated process for synthetic aperture radars.

In addition to radars, cameras are also image-forming devices. All methods other than those mentioned in this section produce nonimaged outputs.

3.2 Some Remote Sensing Instruments for Wave Measurement and Results

Having classified the instruments by their characteristics, we can now discuss some of the specifics of the instruments and offer examples of the results they produce.

3.2.1 Camera Cameras using the visible region of the EM spectrum under natural illumination are obvious extensions of human eyes. The first known serious attempt to use the camera as an instrument to study waves was made by Schumacher (1928) with stereo photos. The areas imaged were too small to be of any practical use. Later, photos were taken from aircraft by Cox and Munk (1954a,b). In this set of experiments, the sun glitter pattern was used to deduce the probability density function of the surface slope distribution of surface waves. The results are classical pieces of work that are still in use today.

Cox and Munk's pioneering work was followed by another ambitious project in the late fifties known as the Stereo Wave Observation Project, or SWOP (Cote et al., 1960). Synchronized cameras on two airplanes produced stereo-pairs of pictures that were then used to construct the ocean wave-height contour. Three-dimensional wave-elevation data were painstakingly read from the stereo pattern, and two-dimensional wavenumber spectra were made. Typical results of the SWOP project can be found in Neumann and Pierson (1966). The results of this project also became classical examples of early attempts to study the ocean wave field. The cumbersome data processing procedures required by the stereo photographic method favored the development of other remote sensing methods.

Stilwell proposed using a single snapshot of the ocean surface wave pattern. A wavenumber spectrum is then produced by optical Fourier analysis. Considerable research has been conducted to automate the data analysis as reported by Stilwell and Pilon (1974),

Sugimori (1972, 1973, 1975, 1976), Kasevich (1975), and Peppers and Ostrem (1978). Efforts to use satellite photographs were reported by Noble (1970) and Apel et al. (1975).

Although a wide range of wave-related phenomena was studied by photographic methods, including directional spectrum, directional spectrum evolution under shear current, and even the detection of internal waves, none has ever become a serious mainstream remote sensing technique for waves. The principal shortcomings of photographic methods are the uncontrollable source of natural illumination and requirements for clear visibility of the field. For quantitative data, natural light has to be uniform, the camera must be pointed at the optimal angle with respect to the waves, and the visibility must be good. After these conditions are met, the brightness of the negative has to be rigorously controlled. Even under ideal conditions, the spectrum produced cannot be assigned an absolute scale of energy content. Consequently, the results are largely qualitative in nature and thus fail to meet the quantitative requirements of many applications. A recent summary of photographic techniques can be found in Monaldo and Kasevich (1981).

For certain applications, such as those described by Gotwols and Irani (1979) and many coastal wave pattern studies (Stafford et al., 1973), cameras are still very powerful and economical tools compared to other methods.

3.2.2 Laser or Radar Profilometer The principle of a profilometer is use of a beam-limited ranging device to measure the distance between a moving platform and the ocean surface. By virtue of the small footprint of the beam-limited device, its measurements are a faithful profile of the surface. To measure the wave profile precisely, the beam has to be as narrow as possible, and the distance between the platform and ocean moderate. As profilometers were developed, laser devices were heavily favored to meet these conditions, but the limitations lasers suffer because of low power and cloud interference have recently made radars as attractive as lasers for profilometry.

Profilometers using radar (Barnett and Wilkerson, 1967) and laser (Schule et al., 1971; Liu and Ross, 1980) have provided many important results in wind-wave studies, especially on the generation and growth of waves as functions of fetch. Because the profilometer collects data along the flight line only, the value of the data would be seriously degraded for a complicated wave field consisting of more than one wave component coming from different directions. This complication has limited the application of profilometry in the past to sea states dominated by a locally generated wind-wave field, and limited the measurements to the upwind and downwind directions. Even in these restricted applications, Hammond and McClain (1980) have shown that aliasing in the data still occurs owing to the finite angular spreading of the wave field.

Two recent developments have considerably enhanced the role of the profilometer in wave studies. One is using a single profilometer to profile the wave field in more than three directions. On each flight

track, a special projection of the total wave field can be obtained. With the geometry of the flight tracks known, data from multi-projections along the tracks provide the necessary information for determination of the mean directions and energy levels of any number of wave components. A recent experiment carried out at the Grand Banks by McClain et al. (1982) produced quantitative results that were used not only to delineate the various directions of propagation for the wave components, but also for a wave-current interaction study.

The second development is conversion of the beam transmitter from a fixed position to a scanning pattern, allowing the radar or laser beam to profile an area rather than a single line. These data can be used to reconstruct the three-dimensional surface of the ocean. A laser device has been constructed by Hoge et al. (1980), and a corresponding radar device, the surface contour radar (SCR), is now fully operational and can produce a two-dimensional wavenumber spectrum in near real time (Kenney et al., 1979).

Since the results of a profilometer depend critically on the measured distance between the radar and the surface spot profiled, the motion of the platform becomes an important source of error. Various schemes have been proposed to deal with the problem; for example, by Walsh (1977) and McClain et al. (1980). Although a complete resolution has still not been achieved, the results are highly accurate for many applications. A more severe restriction of the profilometer is its footprint size. Owing to the limitations of angular resolution inherent in radars and the power limitations of lasers, today's profilometers cannot be used in space. For regional measurements, however, the SCR can provide the most complete and reliable data on the directional wave spectrum available.

3.2.3 Radar Altimeter The radar altimeter is a simple nadir-looking, pulse-limited radar. It was first proposed by Godbey (1965) and Frey et al. (1965) for measuring mean sea level, and for calculation of the geostrophic current at the ocean surface (Huang et al., 1978).

Through the pioneering work of Miller and Hayne (1972), Miller and Hammond (1972), Yaplee et al. (1971), Barrick (1972a,b), Godbey et al. (1970), and McGoogan (1974), it was shown that the stretching of the returned pulse shape recorded by the range gates can be processed to produce the probability distribution function of the surface wave elevation. The first successful measurement was made by Walsh (1974) using the Naval Research Laboratory radar with a pulse width of 1 nanosecond. Subsequently, the radar altimeter on board the satellite Geos-3 with a pulse width of 12 nanoseconds produced the first successful quantitative wave-height measurement from space. The results can be found in papers by Fedor et al. (1979) and Parsons (1979). Seasat-1 also provided highly accurate significant wave-height data (Townsend, 1980). As a result of these satellite missions, the altimeter is regarded as an operational instrument for wave-height measurements.

Recent developments by Walsh (1979), Huang and Long (1980), Huang et al. (1981a,b), and Huang (1981) could extend the results of altimetry far beyond the original concepts, as described in Section 4.

3.2.4 Doppler Radar The Doppler radar is a CW, side-looking, nonimaging device designed with the simple idea of measuring the Doppler effect produced by the relative motion between the radar and the target. Since it is side-looking, the returned signal comes primarily from those waves that satisfy the Bragg condition. Different components of waves can be measured by using different radar frequencies. Ground-based Doppler radar has been used extensively by the Naval Research Laboratory: Wright (1966, 1968, 1978), Pidgeon (1968), Wright and Keller (1971), Keller and Wright (1975), Larson and Wright (1975), Plant and Wright (1977, 1979), Lee (1977), and Plant et al. (1978). Theoretical work has been done by Hasselmann (1971), who proposes using second-order backscattering to measure the wave spectrum. The theoretical analysis has been extended by Valenzuela (1974).

The radars as used now in the laboratory or the field are fixed, and the Doppler effect is thus produced by the wave motions alone. Specific results produced so far constitute the most detailed studies of interaction between EM and ocean surface waves. Among these results are discovery of the upwind propagation of wave components in an active generating wave field, the growth of spectral components as a function of time, and the modulation of short waves by long ones. Since the Doppler radars measure the particle and phase velocities and frequency of the waves, it is possible to use linear wave theory to deduce the amplitude of the wave observed. Spectra can also be deduced from such information as shown in Figure 3.5.

A recent study by Plant has extended the application of the Doppler radar to moving platforms, such as aircraft and satellites. Since the speed of the platform, whether aircraft or satellite, is much higher than that of wave motion, the Doppler effect could be treated as produced by the platform motion alone. Active research is still under way to make the system operational.

3.2.5 Dual-Frequency Spectrometer The dual-frequency spectrometer is a CW, side-looking, nonimaging radar. The technique uses the Bragg scatter condition matched by the EM wavelength at the difference of the frequencies transmitted. The condition is given as

$$k = 2 \cdot \frac{2\pi \Delta f_r}{c} \sin \theta_i \tag{3.8}$$

where k is the ocean wavenumber and Δf_r is the radar wave frequency difference. By varying the frequency difference of the transmitted EM waves, as well as the incidence angles and the azimuth angle of the antenna axis, the full two-dimensional gravity wave spectrum can be determined from a moving platform.

This method was first proposed by Ruck et al. (1972) for a stationary platform. Later, theoretical and experimental studies by Weissmann (1973), Weissmann and Johnson (1977), Schuler (1978), and Hasselmann (1978), Plant (1977), Plant and Schuler (1980), and

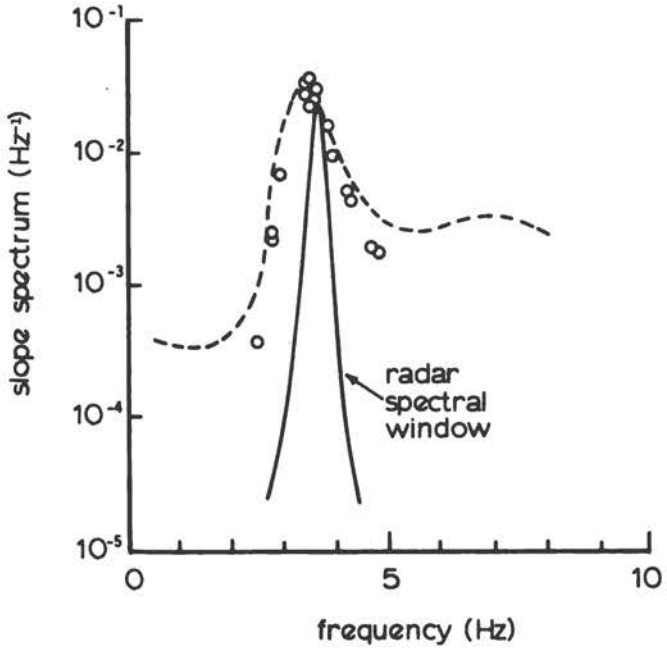

Figure 3.5 Wave-slope spectrum as determined by the Doppler radar*

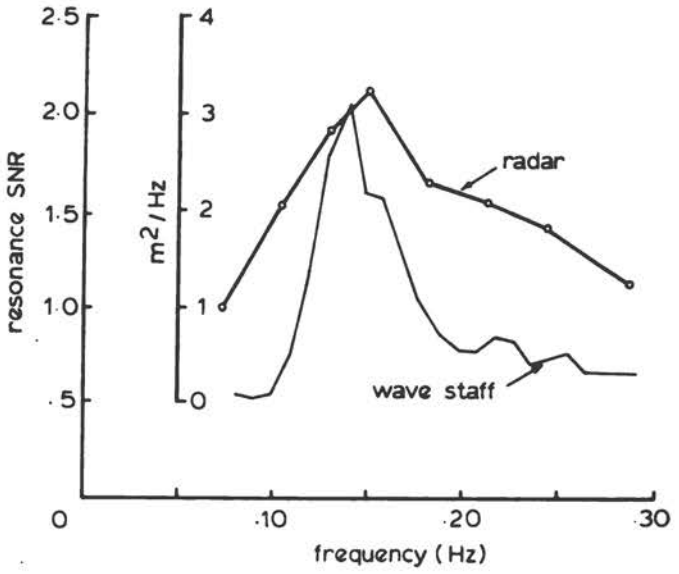

Figure 3.6 Wave spectrum as determined by the ΔK spectrometer**

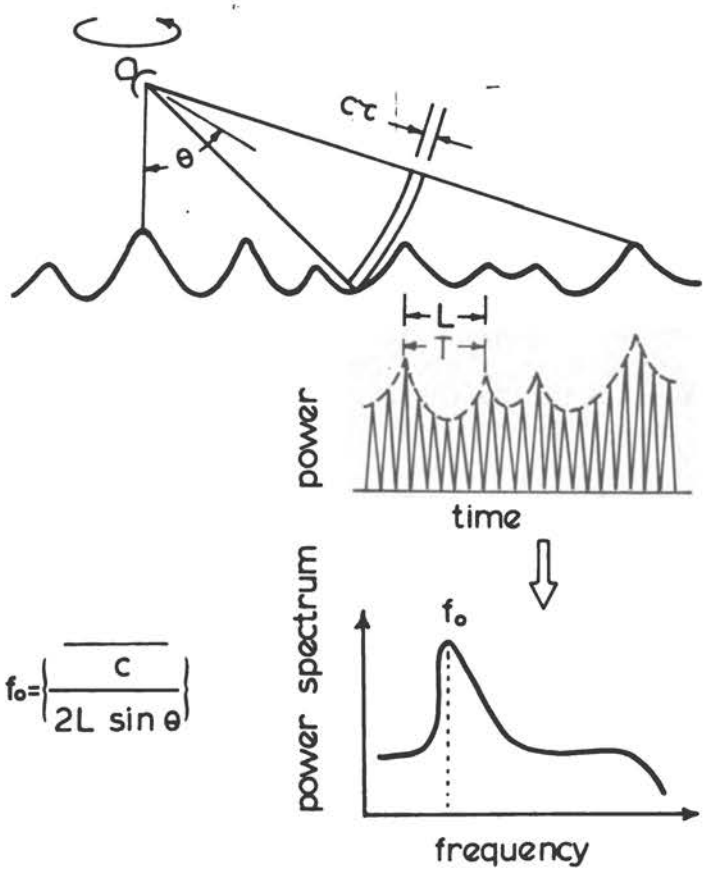

Figure 3.7 The schematic of the short-pulse radar spectrometer system

*SOURCE: W. J. Plant and J. W. Wright (1979), "Growth and Equilibrium of Short Gravity Waves in a Wind-Wave Tank," J. Fluid Mech., 82: 767-793.

**SOURCE: J. W. Johnson, W. L. Jones, and D. E. Weissman (1981), "Dual-Frequency (Delta K) Microwave Scatterometer Measurements of Ocean Wave Spectra from an Aircraft," Oceanography from Space, J. F. R. Gower, ed. (New York: Plenum Press), pp. 607-616.

Johnson et al. (1981) have substantially extended the original ideas and established the feasibility of using the dual-frequency techniques from moving platforms.

Recent experiments with aircraft measurements by Johnson et al. (1981) showed that the location of the resonant line agrees exactly with the theoretically predicated value given in equation (3.8). However, the signal-to-noise ratio of the preliminary data is still quite low. An example of the spectrum is given in Figure 3.6. Additional work in the data-reduction algorithm is needed to make this technique fully operational. The method could be coupled with the scanning short-pulse spectrometer to become an inexpensive, low data-rate system for directional wave-spectrum measurements.

3.2.6 Short-Pulse Spectrometer The short-pulse (SP) spectrometer is a near-nadir looking, pulse-limited, scanning, nonimaging radar. In fact, the first SP spectrometer tested was identical to the altimeter flown on Geos-3, the only difference being that in the spectrometer mode the radar looks slightly off-nadir. The basic idea of the SP spectrometer is to detect the modulation of backscattered power caused by the reflectivity changes induced by large gravity waves. The measurement principle is shown in Figure 3.7. To the first approximation, the measured result is proportional to the large wave slope in the plane of incidence. A directional wave spectrum can be obtained by rotating the antenna.

The idea of the SP spectrometer was first proposed by Tomiyasu (1971), using a wide-band radar model. The theoretical analysis was extended by Jackson (1974), and preliminary field tests were performed by LeVine (1974) and Harger and LeVine (1975) in the nonscanning mode. The major breakthrough in use of the SP spectrometer was not made until Jackson (1979b, 1981) applied the Doppler filter technique proposed by Alpers and Hasselmann (1978) for the dual-frequency radar to the SP spectrometer. Theoretical analysis by Jackson showed that a good directional slope spectrum could be obtained for radar incidence angles between 8° and 15°. However, because the modulation of reflected power by the large waves depends on the existence of small waves to serve as reflectors, the method would not work well for low winds ($w \leq 5$ m s^{-1}) or high values of wave steepness ($(\overline{\zeta^2})^{1/2}/\lambda_o \leq 0.015$), where ζ is the surface elevation and λ_o is the length of the energy-containing waves).

Field testing of the SP spectrometer has been quite successful. Details of the results can be found in Jackson's paper in these proceedings ("Aircraft and Satellite Measurement of Ocean Wave Directional Spectra..."). The major difficulty in the interpretation of the spectrometer results is in the accurate transformation of the spectrum pattern into absolute energy units. The absolute energy level could be provided by the addition of an altimeter operated in conjunction with the spectrometer. Even with this difficulty, the scanning SP spectrometer will still be an important wave-measuring instrument because it is inexpensive, because it has a low data rate, and because it produces a directional spectrum of ocean waves.

3.2.7 Side-Looking Airborne Radar (SLAR) SLAR is a short-pulse, fan-beam, side-looking, real aperture, imaging radar. It has long been used for military surveillance purposes (see, for example, Skolnik, 1962). Application of SLAR to ocean wave measurements was suggested by Moore and Simonett (1967). A more detailed discussion was given recently by DeLoor and Brunsveld van Hulten (1978). Owing to the limited spatial resolution of the real aperture radar (as discussed in Section 2), the SLAR can only be used from an airplane for wave measurements.

The spatial resolution is not the only problem with SLAR. The SLAR technique depends on the coherent processing of variations in the scattered power induced by the small scatterers and modulated by the large waves. The distribution of the scatterers varies considerably for any independent sample. Any average of the samples will have to be made within the de-correlation time scale. For the open ocean, this time scale is of the order of milliseconds (Long, 1975). Furthermore, the existence of the scatterers depends on wind conditions. Experiments have shown that SLAR can only obtain usable images in conditions of light and moderate winds. For high winds, the image is too speckled to show any wave pattern. Even with a perfect wave image, determining the absolute energy level of the spectrum is an unsettled issue. Because of these problems, SLAR has not been seriously developed for general ocean wave measurements. For certain applications in coastal areas, where the wave patterns are more predictable, SLAR can be very valuable. An example of a wave image derived from SLAR is shown in Figure 3.8.

3.2.8 Synthetic Aperture Radar (SAR) The need for finer spatial resolution and practical limitations on the size of antennas make the synthetic aperture technique a logical choice for radar development. The early history of SAR development can be found in Sherwin et al. (1962). Recent reviews have been made by Cutrona (1970), Harger (1970), and Hovanessian (1980).

The application of SAR to ocean wave measurement was suggested by Cutrona (1970). The first demonstration was made by Moskowitz (1973). Accelerated development of SAR was prompted by the Seasat-1 project. Brown et al. (1976) reported good examples of wave measurements by SAR.

SAR is a side-looking, narrow-pulse, wide-beam, synthetic aperture, imaging radar. The range resolution is achieved by the narrow pulse, and the azimuth resolution develops from the coherent processing of the image from different look angles. The theoretical limit of the spatial resolution is the antenna size. SAR is a potentially powerful instrument for ocean studies, and its applications are not limited to waves. The richness of the information contained in the data collected from Seasat-1 is still dizzying to ocean scientists; nevertheless, interpreting the SAR image for wave measurements is not free of problems.

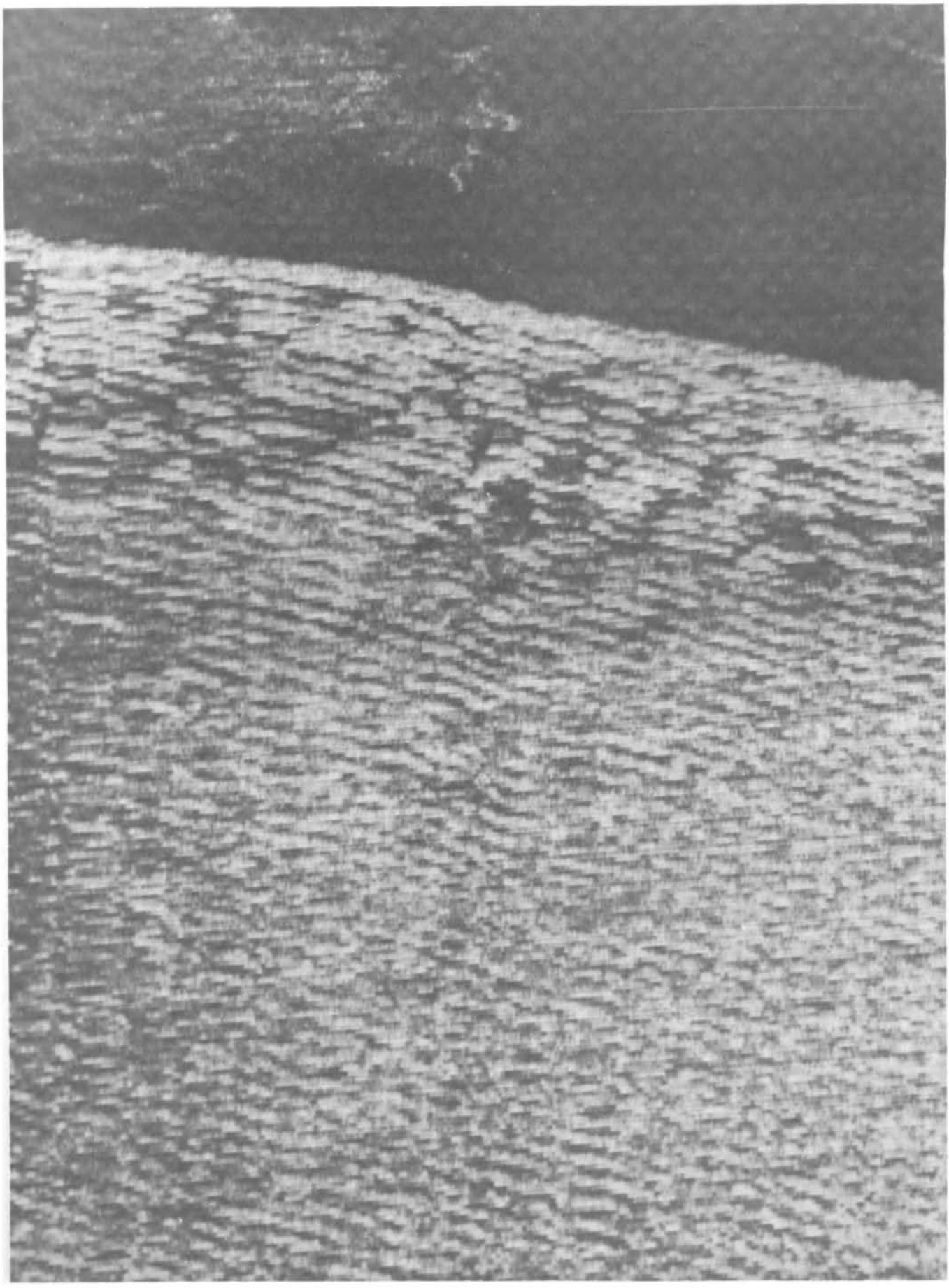

Figure 3.8 The ocean wave patterns determined by X-band SLAR at a height of 300 m from an airplane

Some uncertainty exists about the exact image-forming mechanism. Generally accepted models of modulated power returned from scatterers by long waves were used in most of the theoretical studies, such as those of Elachi and Brown (1977) and Valenzuela (1980). Since the detailed modulation mechanism is still unknown for an active wind-wave field, the interpretation of the image produced is subject to some question. Attempts to determine the absolute energy level of the spectrum measure by Jain (1977) have been unsuccessful. So far, the most complete formulation of image formation by SAR is that proposed by Valenzuela (1980). The results indicate a number of potential sources of image distortions. The effect of orbit motions helps to both form the image and degrade it to give false wavelength and wave patterns, as reported by Jain (1978), Alpers and Rufenach (1979), Raney (1971), and Swift and Wilson (1979).

Conflicting requirements of the SAR design place an inherent limit on the image quality. For finer resolution, SAR needs a longer integration time, but the motion of the waves could cause defocusing if the integration time overlaps with the frequency of the waves to be imaged.

Furthermore, the SAR image is influenced by the scatterer distribution. Although high sea-state data have been collected by Elachi et al. (1977), the quality of the image deteriorates quickly with higher wind speed. Other effects on the scatterer distribution are the SAR look angles and the influence of other dynamic processes in the ocean. Since the scatterers consist of small waves, any other motions in the ocean, such as currents or fronts, will all influence the image quality. The sensitivity of the SAR image is certainly an asset, but sometimes has detrimental side effects.

The data processing requirement for a SAR image is also a problem deserving proper attention for any applications.

Even with these problems, SAR still emerges as the leading candidate for a global ocean wave-measurement system. Recent studies by Beal (1980), Brown et al. (1976), Elachi (1976, 1978), Elachi et al. (1977), Shemdin et al. (1978), and Shuchman and Zelenka (1978) have proved the value of SAR in wave measurements despite the problems. A very complete description of SAR in the whole spectrum of ocean studies can be found in Beal et al. (1981).

The generation area of the waves is pinpointed by the directional distributions of the spectra. A detailed spectrum is shown in Figure 3.9b. SAR has great promise for other applications, such as detection of shear current, ocean eddies, frontal boundaries, bottom topographic features, ice, and wind.

3.2.9 High-Frequency (HF) Ground-Based Radar The term high frequency is loosely used here to designate any frequency between 3 and 30 MHz with wavelength between 10 and 100 m. The basic principle of the HF radar is the strong Doppler effect on the Bragg-scattered signal at both first and second order. Since it is ground-based, the radar beam is always nearly parallel to the ocean surface. The Doppler shift in the Bragg line of the returned power is given by

$$\Delta f = \frac{2C_o}{\lambda_r} \tag{3.9}$$

where C_o is the phase velocity of the ocean waves that satisfy the Bragg condition. Since the Bragg resonant condition requires $\lambda_r = \lambda/2$, and the dispersion relationship also relates the phase velocity with length of the wave as

$$C_o = \left(\frac{g\lambda}{2\pi}\right)^{\frac{1}{2}} \tag{3.10}$$

the return signal of the HF radar could be used to measure the existence of a particular wave component using equations (3.9) and (3.10). This phenomenon was discovered by Crombie (1955). His report was one of the first addressed to quantitative remote sensing of ocean waves.

Later theoretical work by Wait (1966) related the strength of the returned signal voltage at the Doppler peak to the height of the ocean waves. Subsequent work by Barrick and Peake (1968) and Barrick (1972b) has further extended the analysis to bistatic configurations of the radar system.

More significantly, Barrick (1971, 1972b), Trizna et al. (1977), and Lipa (1977) extended the analysis to the second order and established the relationship between the second-order Doppler spectrum and the directional wave-height spectrum of the ocean waves. In the higher-order analysis of data, a minute over-all shift of the spectrum was found to relate to the ocean surface current. The ability of HF radar to measure surface current and vertical current shear was studied by Stewart and Joy (1974) and Barrick et al. (1974).

Because the spatial resolution is determined by the EM wavelength and the antenna dimension, as in equation (3.1), the long EM wavelength of HF radar requires an antenna of unreasonable size to achieve acceptable beam width for spatial resolution. To solve this problem, a Stanford-Scripps team developed a synthetic aperture technique that employs a small omnidirectional receiving antenna moving along various directions at a constant speed. The Doppler shift induced by this motion can be related to the wave direction of a specific wavelength range. The results are reported by Teague et al. (1973) and Tyler et al. (1974).

The long wavelength used by HF radar also makes both direct ground-wave and indirect sky-wave propagation possible. The sky wave depends on the refraction of HF waves by the ionosphere, which is almost invisible to microwaves. The sky wave can propagate a long distance (4000 km maximum) from a single reflection, making measurements possible at a distance, even for ground-based systems. To achieve spatial resolution in the sky-wave mode, the antenna has to be rather long. Earlier results by Tveten (1967) and Ward (1969) have proved the feasibility of this method. However, due to the motion and the inhomogeneities of the ionosphere, as well as the layered structure of the atmosphere, high-quality data are not available all the time.

Other drawbacks of the HF technique are its susceptibility to external noise interference and the limited range of ground-wave propagation ($\sim$200 km). Even with these limitations, the simplicity of the system, the low data rate, the versatility of operational modes, and the richness of the information offered all make the HF radar an attractive choice for regional monitoring of ocean waves.

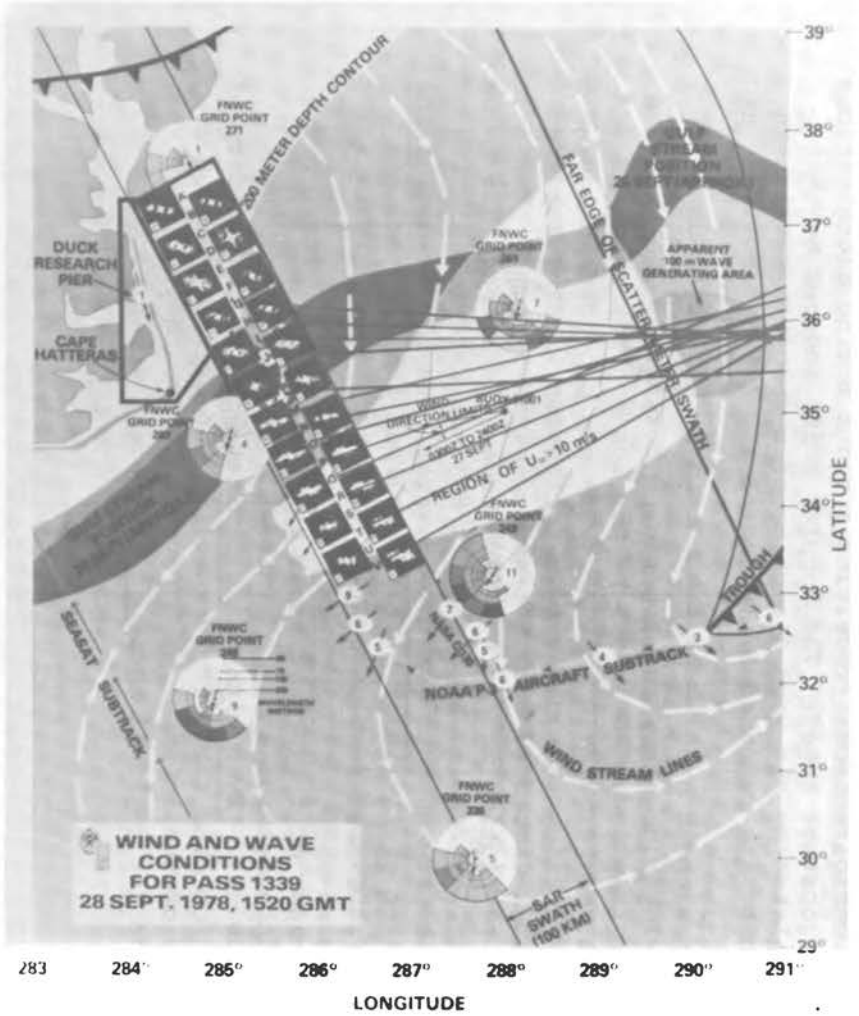

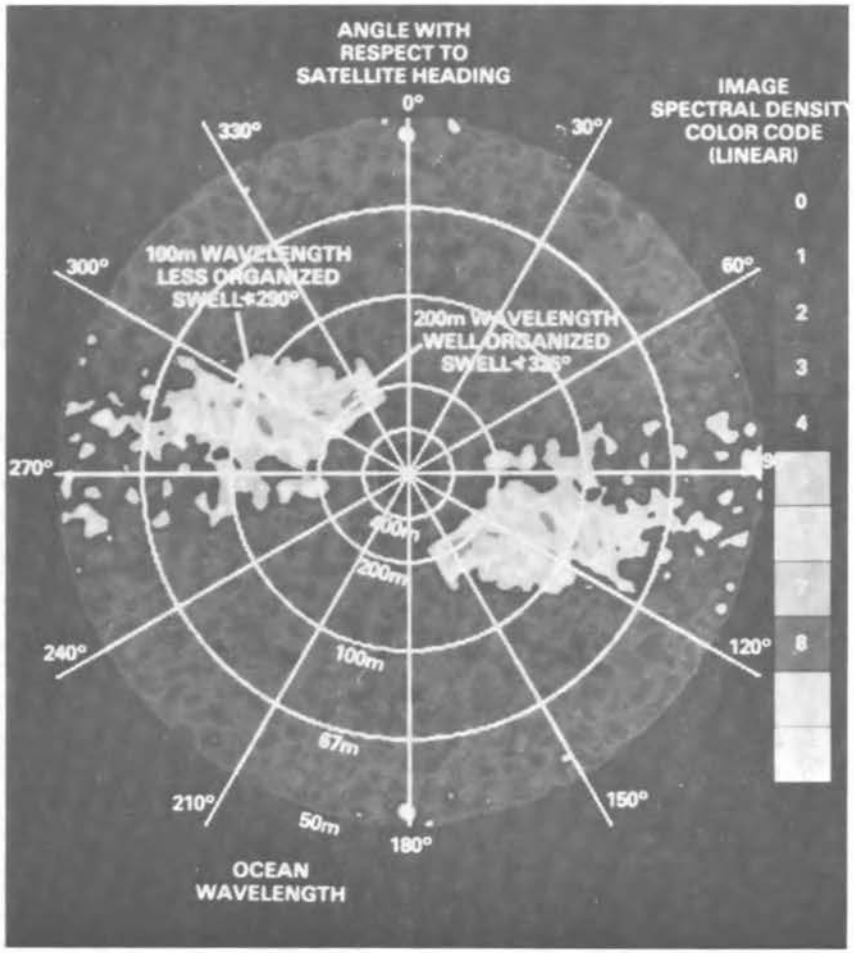

SEASAT SAR
TYPICAL OCEAN WAVE SPECTRUM
SEPT 28, 1978, 1520 GMT
36.2°N, 75.0°W

Figure 3.9 A case study of storm waves by SAR from Seasat-1 (a), and a typical wave spectrum as determined by SAR (b)*

*SOURCE: R. C. Beal, P. S. DeLeonibus, and I. Katz, eds. (1981), Spaceborne Synthetic Aperture Radar for Oceanography (Baltimore: The Johns Hopkins University Press).

An excellent review of HF radar techniques can be found in Barrick (1978). A more detailed report of recent developments is given by Barrick in these proceedings ("Status of HF Radars for Wave-Height Directional Spectral Measurements").

3.2.10 Acoustic Methods This review centers on the use of EM waves for sensing, but the same principles and techniques can readily be applied to acoustic waves. In fact, owing to the limited propagation of EM waves in water, sonar was developed before radar, and remains the principal method of underwater detection today. A summary of the sonar method can be found in Creasey (1976).

Although acoustic waves have superior propagating properties underwater, problems militate against using acoustic waves to measure surface waves. If the sonar is located underwater to measure waves from below, the beam-bending caused by variations in temperature and salinity as a function of depth forms a shadow zone near the surface layer. Bending of the beam can also cause errors in measuring the slant range. If the sonar is used in the air above the water surface, the propagation range is limited to about 10 m. Furthermore, the signal-to-noise ratio is always a problem for acoustic methods in monitoring a natural phenomenon such as surface waves (Little, 1969). Finally, for the underwater techniques, platform mobility is also a problem.

Although there have been some efforts to develop the acoustic counterpart of EM instruments by Essen (1974, 1979), Essen and Hasselmann (1970), and Essen et al. (1978), the acoustic method has never been seriously considered as a surface wave measurement technique, particularly in comparison to the EM methods. The only application of the acoustic method in wave measurements today is in small-scale laboratory experiments.

4. New Approaches to Wave Study and Uses of Wave Data Suggested by Remote Sensing Techniques

The traditional solution to obtaining wave information over a large area is to make a limited number of direct wave measurements, and to close the data gaps between observation stations using models such as those of Pierson and Moskowitz (1964) or JONSWAP spectral functions (Hasselmann et al., 1976). The inputs for these models are all from external variables such as wind speed, duration, and fetch. Such models are also used for wave predictions. The rationale for this approach is obvious. Wave data of any form are not readily available everywhere, but wind data in some form are. Since ocean waves are generated primarily by wind, the available wind field data should enable one to obtain the ocean wave field. It is all very logical.

On closer examination, flaws become evident in this approach. To begin, the validity of existing models is contingent on satisfying restrictive conditions. More fundamentally, the lack of detailed understanding of the wind-wave generation, propagation, and decay mechanism makes the models based on external variables uncertain even

in the most favorable conditions. But real situations are far from ideal. The lack of reliable observations of atmospheric conditions over the vast ocean area makes geostrophic wind prediction less than perfect. Coupling the high-level wind speed to the surface through a planetary boundary model is also fraught with uncertainties. Remote sensing techniques such as scatterometry have been developed to provide direct wind data (see, for example, Jones and Schroeder, 1978; Jones et al., 1979). Although derived wind speeds are inferred from sea states, these data have greatly improved the input quality of the models.

With advanced development of remote sensing techniques, an entirely new source of wave data has become available. This new source provides wave data directly, and almost as frequently as wind data. Thus, remote sensing techniques offer an internal wave-data source rather than the purely external environmental conditions. The usefulness of the internal variables can be illustrated by considering the output of altimeters.

As discussed briefly in Section 3, the altimeter is a simple nadir-looking, pulse-limited radar. Wave information is contained in the stretched returned pulse waveform, as shown in Figure 4.1. The waveform of the returned pulse has been analyzed extensively by Brown (1978) and Hayne (1980). With detailed calibration data on the transmitted pulse shape, and the record of the satellite pointing angles and the returned wave shape, a successful deconvolution can produce the true probability density function of the surface elevation, as shown in Figure 4.2. Recent experimental and theoretical studies by Walsh (1979), Jackson (1979a), Huang and Long (1980), Huang et al. (1981b), and Huang (1981) have shown that various wave and wave-related phenomena can be modeled with an internal parameter of the wave field, the significant slope, defined as

$$\S = \frac{(\overline{\zeta^2})^{\frac{1}{2}}}{\lambda_o} \tag{4.1}$$

This variable can be derived from the altimeter data by calculating both the rms wave height (Parsons, 1979) and the skewness, K_3 (Walsh, 1979), from the probability density function. Theoretical and experimental studies by Longuet-Higgins (1963), Huang and Long (1980), and Huang et al. (1981a) have shown that

$$K_3 = 8\pi\S \tag{4.2}$$

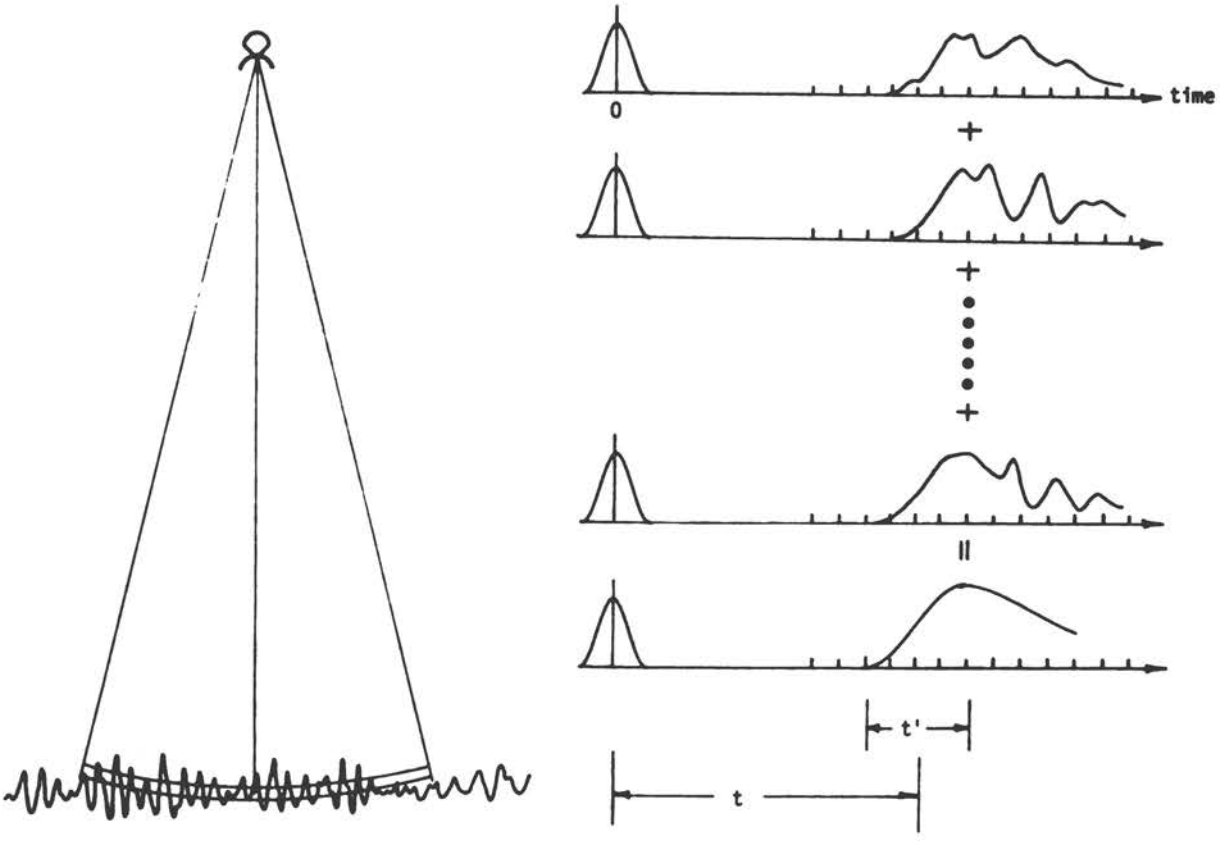

Figure 4.1 The schematic of the short-pulse altimeter system

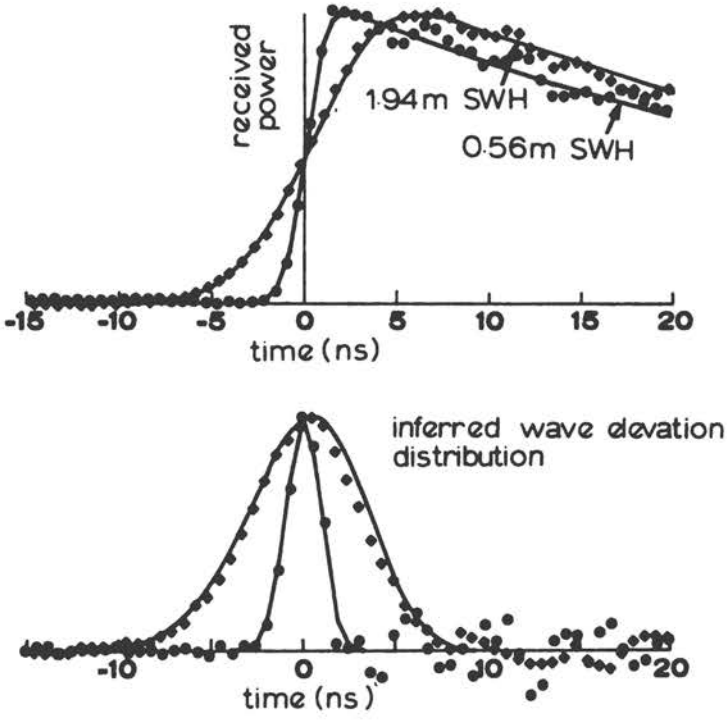

Figure 4.2 The mean return pulse and the inferred wave-elevation distribution function*

*SOURCE: E. J. Walsh (1974), "Analysis of Experimental NRL Radar Altimeter Data," Radio Science, 15: 711-722.

Thus, using (4.1) and (4.2), one can solve for λ_o with $(\overline{\zeta^2})^{\frac{1}{2}}$ given. Then by the dispersive relationship for a random wave field (see, for example, Huang and Tung, 1976), the frequency of the energy-containing waves can be calculated. With this information, a generalized spectrum model would yield the frequency spectrum for the wave field. An example of the spectrum given by this approach and comparison to field data from JONSWAP can be found in Huang et al. (1981a).

A family of new models for the dynamics of the upper ocean has been proposed by Huang (1981), based on the availability of values for the significant slope and the breaking-wave theory developed by Longuet-Higgins (1969). Of crucial importance to wave studies is calculation of the wave attenuation rate from energy loss by wave breaking, as this determines wave propagation and decay characteristics.

In addition, by considering the nonlinear effects, various statistical properties of waves as derived by Longuet-Higgins (1957, 1963, 1975, 1980) can be parameterized by the internal variable. These properties include the group length of the wave field and extreme wave conditions. Such information is of great use to ship operations and engineering activities. Besides its role in theoretical studies, the internal variable has also been found to control the empirical relationship between nondimensional energy, fetch, and frequency, as reported by Huang et al. (1981b).

The altimeter data collected by Geos-3 over three and a half years provided a rich global data base of wave climate. This data base was analyzed and compiled by McMillan (1981). The density of data distribution is shown in Figure 4.3, and a map of percentage of waves higher than 3.5 m distribution is shown in Figure 4.4. Utt (1980) used this data base to extract the probability of occurrence of significant wave height for Heather Field in the North Sea. The agreement between satellite and conventional data suggested that altimeter data are as reliable as any existing data, as shown in Figure 4.5.

Remote sensing techniques have made progress in the last two decades, and promise more: the instruments available today are an incipient sample of what might be possible. With the successful test flights of the Space Shuttle, it now becomes practical to put antennas 100 m or more in diameter into orbit. New approaches to remote sensing must now be considered. The Large Antenna Real Aperture Radar (LARAR) discussed by McGoogan and Walsh (1978) is an attractive option. Using a contiguous active pushbroom radar system, a radar can use an array feed system. With the sweep aperture concept developed by Bush and MacArthur (1979) to cancel forward motion, the satellite can be treated as a stationary platform for Doppler measurements of wave motion. Combining these capabilities into a single system, the LARAR could provide wave-motion data, imaging, and contouring and monitoring of roughness changes at a low data rate, and in a real aperture mode. Within the next two decades, the increasing capability offered by the Shuttle will be fully explored.

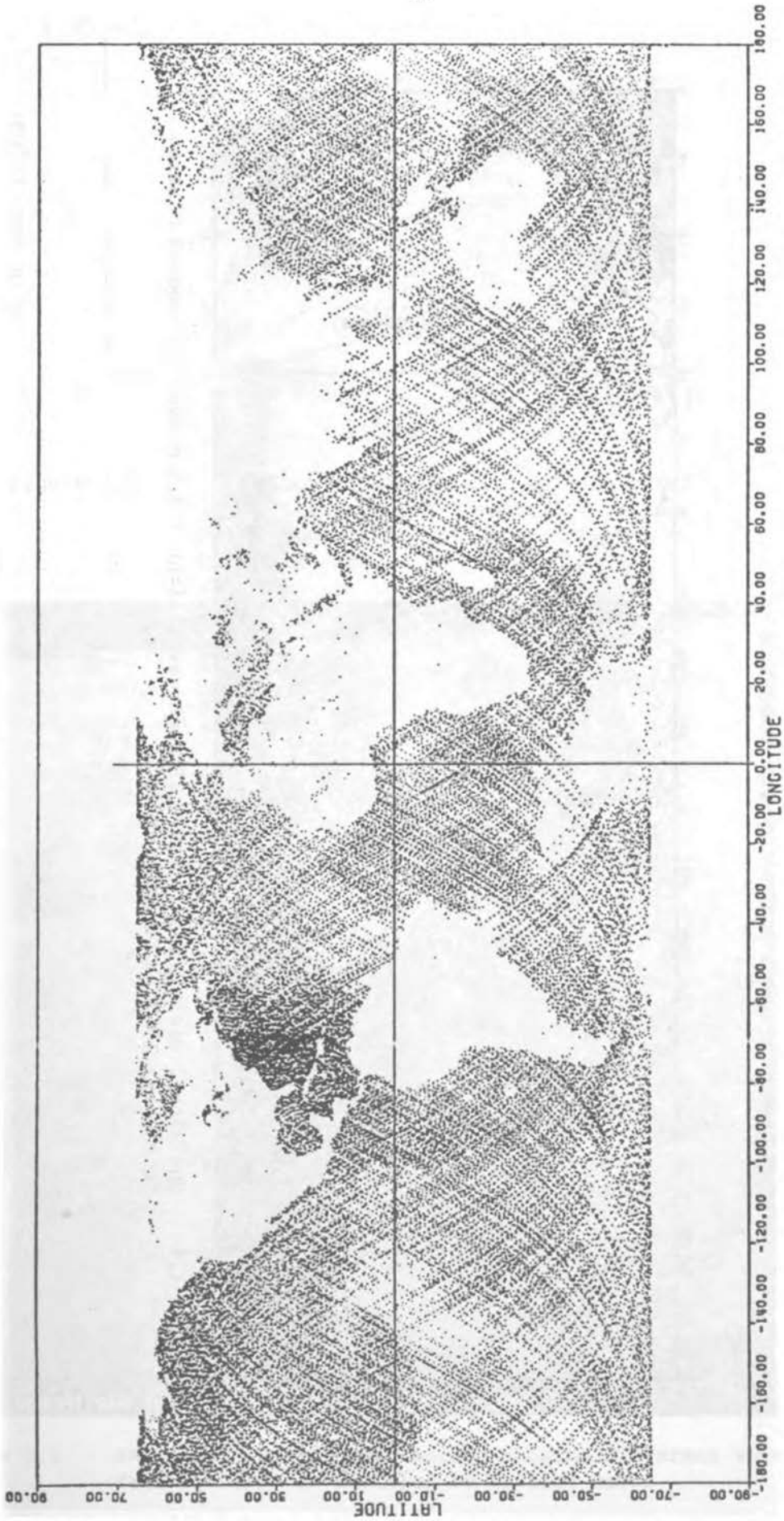

Figure 4.3 Significant wave-height data distribution from Geos-3 satellite. Each dot represents 10 wave records.

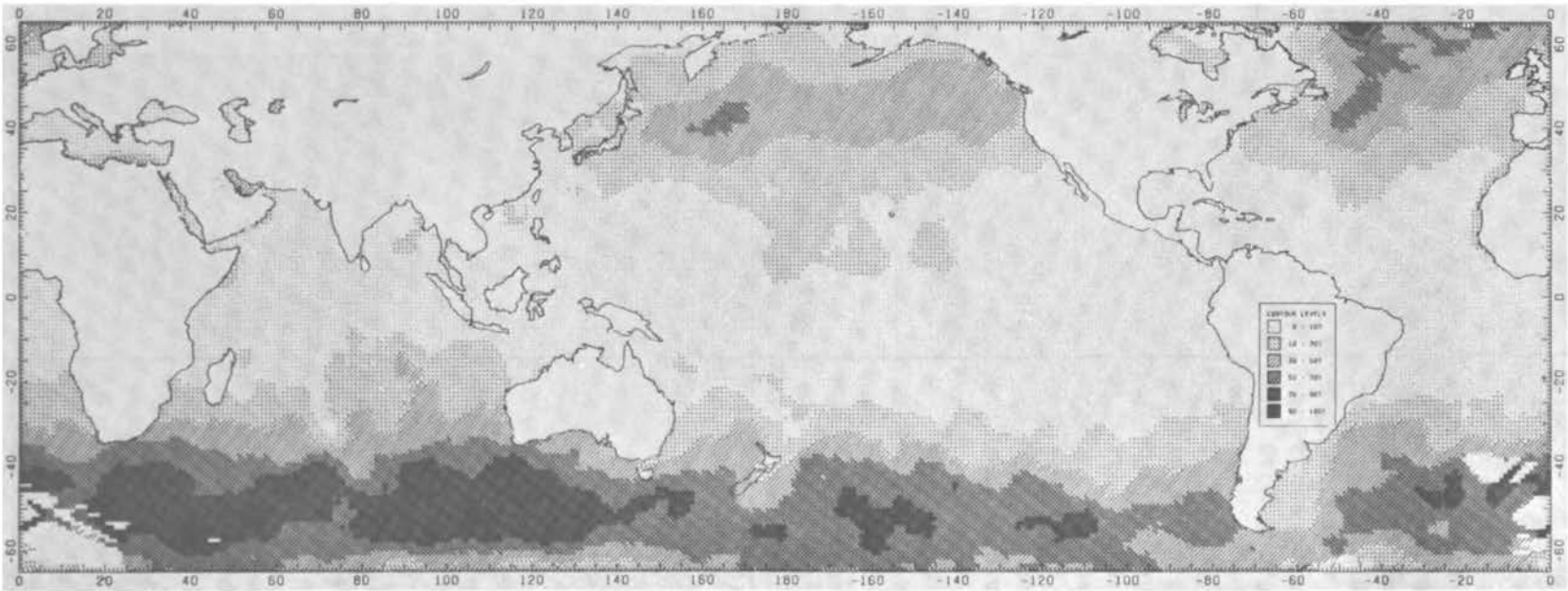

Figure 4.4 The global distribution of significant wave height > 3.5 m over the Geos-3 mission from April 1975 to December 1978

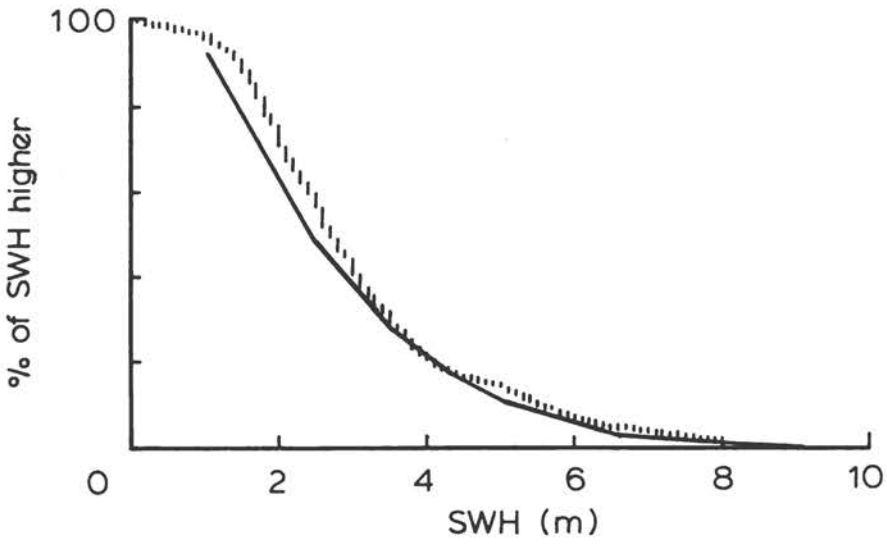

Figure 4.5 Comparison of significant wave-height frequency between Geos-3 satellite altimeter (——) and historical data (----) at a North Sea site

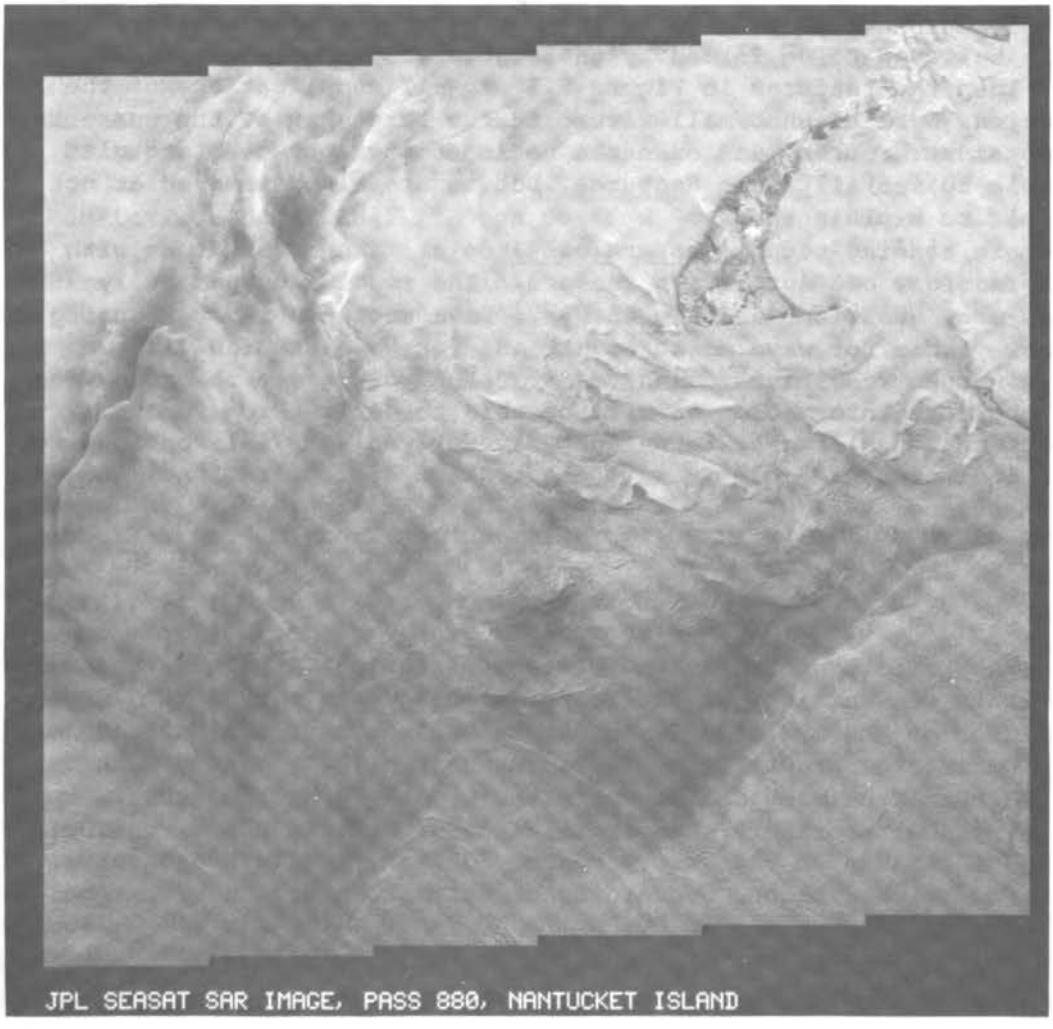

Figure 5.1 SAR image of Nantucket Island showing different surface features in addition to surface waves

SAR and operational spaceborne Doppler radar and spectrometers are also under active study. Applications of SAR to ocean studies have already been demonstrated by Beal et al. (1981). The next 20 years will witness more quantitative results from the mature remote sensing techniques. Even before the absolute calibration of the remote sensing techniques is established, an orbiting satellite instrument will provide a uniform standard for sea-state measurements that will allow expeditious intercomparisons to be made of different measurement systems at various locations in the world.

5. Conclusion

The progress of science has always advanced in step with the progress of observational methods. Wave study is certainly not an exception. During the last two decades, remote sensing techniques have provided us with more and more quantitative data. Their rapid development has in some respects outstripped not only some of the older and established in situ wave-measurement methods, but also our understanding of wave phenomena and dynamics. Interpretation of the remotely sensed data depends crucially on this understanding. The SAR image shown in Figure 5.1 clearly demonstrates the power and powerlessness of the remote sensing techniques in their present stage. As discussed earlier, a SAR image is believed to be formed by the scatterers, i.e., the small waves. Then the features in Figure 5.1 are all complications of the interactions between the small waves and the large waves, the currents, the frontal structures, and even the bottom topography. We are glad to be able to see all these features, but we are also dismayed at not being able to explain them.

Remote sensing techniques are only tools. They provide us with raw information, but not always answers. The results occasionally raise as many questions as they answer. Nevertheless, remote sensing opens new vistas for wave measurements and for wave studies. The remotely sensed results force us to more study of waves; the more we learn, the more information we will be able to derive from remote sensing techniques. These techniques have played and will continue to play an indispensible role in wave observations for operational and research purposes.

6. Acknowledgments

This summary report on the status of remote sensing techniques for wave measurements was carried out under the encouragement of Robert G. Dean, the chairman of the symposium, and Aurora Gallagher of the Marine Board. During the preparation of this manuscript, I received much unselfish help from many colleagues--Robert Beal, Johns Hopkins Applied Physics Laboratory; Gaspar Valenzuela, William Plant, and Dale Shuler, Naval Research Laboratory; James Johnson, Langley Research Center; Frederick Jackson, Goddard Space Flight Center; and John Apel

of NOAA. Of course, I would like to thank my colleagues at Wallops Flight Center, Joseph McGoogan, Chester Parsons, Ray Stanley, Edward Walsh, and George Hayne, who over the last decade not only devoted their time in development of the techniques, but also spent countless hours teaching me how remote sensors work.

This work is part of the NASA Supporting Research Technology Program, Ocean Processes Office.

References

Alpers, W. and K. Hasselmann (1978), "The Two Frequency Microwave Techniques for Measuring Ocean-Wave Spectra from an Airplane or Satellite," Boundary-Layer Meteorol., 13: 215-230.

Alpers, W. R. and C. L. Rufenach (1979), "The Effect of Orbital Motions on Synthetic Aperture Radar Imagery of Ocean Waves," IEEE Trans., AP-27: 685-690.

Apel, J. R. (1976), "Ocean Science from Space," Trans. AGU, 57: 612-624.

Apel, J. R. (1980), "Satellite Sensing of Ocean Surface Dynamics," Ann. Rev. Earth Planet. Sci., 8: 303-342.

Apel, J. R., H. M. Byrne, J. R. Proni, and R. L. Charnell (1975), "Observations of Oceanic Internal and Surface Waves from the Earth Resource Technology Satellite," J. Geophys. Res., 80: 865-881.

Barnett, T. P. and J. C. Wilkerson (1967), "On the Generation of Ocean Wind Waves as Inferred from Airborne Radar Measurements of Fetch-Limited Spectrum," J. Marine Res., 25: 292-328.

Barrick, D. E. (1968a), "Rough Surface Scattering Based on the Specular Point Theory," IEEE Trans., AP-16: 449-454.

Barrick, D. E. (1968b), "Relationship between Slope Probability Density Function and the Physical Optics Integral in Rough Surface Scattering," Proc. IEEE, 56: 1728-1729.

Barrick, D. E. (1970), Radar Cross Section Handbook (New York: Plenum Press).

Barrick, D. E. (1971), "Dependence of Second-Order Sidebands in HF Sea Echo Upon Sea State," IEEE Trans., G-AP: 194-197.

Barrick, D. E. (1972a), "Remote Sensing of Sea State by Radar," Remote Sensing of the Troposphere, V. E. Derr, ed. (Washington, D.C.: Government Printing Office).

Barrick, D. E. (1972b), "First-Order Theory and Analysis of MF/HF/VHF Scatter from the Sea," IEEE Trans., AP-20: 2-10.

Barrick, D. E. (1978), "HF Radio Oceanography--A Review," Boundary-Layer Meteorol., 13: 23-43.

Barrick, D. E., J. M. Headrick, R. W. Bogle, and D. D. Crombie (1974), "Sea Backscatter at HF: Interpretation and Utilization of the Echo," Proc. IEEE, 62: 673-680.

Barrick, D. E. and W. H. Peake (1968), "A Review of Scattering from Surfaces with Different Roughness Scales," Radio Science, 3: 865-868.

Beal, R. C. (1980), "Spaceborne Imaging Radar: Monitoring of Ocean Waves," Science, 208: 1373-1375.

Beal, R. C., P. S. DeLeonibus, and I. Katz, eds. (1981), Spaceborne Synthetic Aperture Radar for Oceanography (Baltimore: The Johns Hopkins University Press).

Beckman, P. and A. Spizzichino (1963), The Scattering of Electromagnetic Waves from Rough Surfaces (New York: MacMillan Co.).

Brown, G. S. (1978), "Backscattering from a Gaussian Distributed Perfectly Conducting Rough Surface," IEEE Trans., AP-26: 472-482.

Brown, W. E., C. Elachi, and T. W. Thompson (1976), "Radar Imaging of Ocean Surface Pattern," J. Geophys. Res., 81: 2657-2667.

Bush, G. B. and J. L. MacArthur (1979), Evaluation of the Airborne Wave Motion Sensor, TM SIR 79-032 (Laurel, Md.: Applied Physics Laboratory, The Johns Hopkins University).

Cote, L. J., J. O. Davis, W. Marks, R. J. McGough, E. Mehr, W. J. Pierson, J. F. Ropek, G. Stephenson, and R. C. Vetter (1960), "The Directional Spectrum of a Wind-Generated Sea as Determined from Data Obtained by the Stereo Wave Observation Project," Meteorological Papers, 2(6), College of Engineering, New York University.

Cox, C. S. and W. H. Munk (1954a), "Measurement of the Roughness of the Sea Surface from Photographs of the Sun's Glitter," J. Optical Soc. Am., 44: 838-850.

Cox, C. S. and W. H. Munk (1954b), "Statistics of the Sea Surface Derived from Sun Glitter," J. Marine Res., 13: 198-227.

Creasey, D. J. (1976), Remote Sensing for Environmental Sciences, E. Schanda, ed. (Berlin: Springer-Verlag).

Crombie, D. D. (1955), "Doppler Spectrum of Sea Echo at 13.56 MC/S," Nature, 175: 681-682.

Cutrona, L. J. (1970), "Synthetic Aperture Radar," Radar Handbook, Chapter 23, M. I. Skolnik, ed. (New York: McGraw-Hill).

DeLoor, G. P. and H. W. Brunsveld van Hulten (1978), "Microwave Measurements over the North Sea," Boundary-Layer Meteorol., 13: 119-131.

Elachi, C. (1976), "Wave Patterns across the North Atlantic on September 28, 1974, from Airborne Radar Imagery," J. Geophys. Res., 81: 2655-2656.

Elachi, C. (1978), "Radar Imaging of the Ocean Surface," Boundary-Layer Meteorol., 13: 165-179.

Elachi, C. and W. E. Brown (1977), "Models of Radar Imaging of the Ocean Surface Waves," IEEE Trans., AP-25: 84-95.

Elachi, C., T. W. Thompson, and D. King (1977), "Ocean Wave Patterns Under Hurricane Gloria: Observation with an Airborne Synthetic Aperture Radar," Science, 198: 609-610.

Essen, H. H. (1974), "Wave-Facet Interaction Model Applied to Acoustic Scattering from a Rough Sea Surface," Acustica, 31: 107-113.

Essen, H. H. (1979), "Theoretical Investigations on Acoustic Remote Sensing of Ocean Surface Waves," Z. Geophys., 45: 183-198.

Essen, H. H. and K. Hasselmann (1970), "Scattering of Low-Frequency Sound in the Ocean," Z. Geophys., 36: 655-678.

Essen, H. H., F. Schirmer, and J. Siebert (1978), "Measurements of Ocean Surface Waves with an Acoustic Range," Dt. Hydrog. Z., 31: 7-15.

Fedor, L. S., T. W. Godbey, J. F. R. Gower, R. Guptill, G. S. Hayne, C. L. Rufenach, and E. J. Walsh (1979), "Satellite Altimeter Measurements of Sea State: An Algorithm Comparison," J. Geophys. Res., 84: 3991-4001.

Frey, E. J., J. V. Harrington, and W. S. von Avx (1965), "A Study of Satellite Altimetry for Geophysical and Oceanographic Measurement," 16th International Astronautical Congress Proceedings, pp. 53-72.

Godbey, T. W. (1965), "Oceanographic Satellite Radar Altimeter and Wind Sea Sensor," Oceanography from Space, G. C. Ewing, ed. (Woods Hole, Mass.: Woods Hole Oceanographic Institution), pp. 21-26.

Godbey, T. W., E. L. Hofmeister, B. N. Keeney, and W. J. Kelly (1970), "Radar Altimeter Study, Phase II Final Report," Contract No. NAS 12-683, General Electric Company, Utica, N.Y.

Gotwols, B. L. and G. B. Irani (1979), "Optical Determination of the Phase Velocity of Short Gravity Waves," J. Geophys. Res., 85: 3964-3970.

Hammond, D. L. and C. R. McClain (1980), "Spectral Distortion Inherent in Airborne Profilometer Measurements of Ocean Wave Heights," Ocean Engineering, 7: 99-108.

Harger, R. O. (1970), Synthetic Aperture Radar Systems, Theory and Design (New York: Academic Press).

Harger, R. O. and D. M. LeVine (1975), "Microwave Radar Sea State Sensing at Intermediate Incidence Angles," NASA-X-952-75-228.

Hasselmann, K. (1971), "Determination of Ocean Wave Spectra from Doppler Radio Return from the Sea Surface," Nature Phys. Sci., 229: 16-17.

Hasselmann, K., D. B. Ross, P. Müller, and W. Sell (1976), "A Parametric Wave Prediction Model," J. Phys. Oceanogr., 6: 200-228.

Hayne, G. S. (1980), "Radar Altimeter Mean Return Waveforms from Near-Normal Incidence Ocean Surface Scattering," IEEE Trans., AP-28: 687-692.

Hoge, F. E., R. M. Swift, and E. B. Frederick (1980), "Water Depth Measurement Using an Airborne Pulsed Neon Laser System," Applied Optics, 19: 871-883.

Hovanessian, S. A. (1980), Introduction to Synthetic Array and Imaging Radars (Dedham, Mass.: Artech House, Inc.).

Huang, N. E. (1979), "New Developments in Satellite Oceanography and Current Measurements," Rev. Geophys. Space Phys., 17: 1558-1568.

Huang, N. E. (1981), "On the Influence of Breaking Waves on the Dynamics of the Upper Ocean," NASA IP WFC-300-81-002.

Huang, N. E., C. D. Leitao, and C. G. Parra (1978), "Large-Scale Gulf Stream Frontal Study Using GEOS-3 Radar Altimeter," J. Geophys. Res., 83: 4673-4682.

Huang, N. E. and S. R. Long (1980), "An Experimental Study of the Surface Elevation Probability Distribution and Statistics of Wind-Generated Waves," J. Fluid Mech., 101: 179-200.

Huang, N. E., S. R. Long, C. C. Tung, Y. Yuen, and L. F. Bliven (1981a), "A Unified Two-Parameter Wave Spectral Model for a General Sea State," J. Fluid Mech., in press.

Huang, N. E., S. R. Long, and L. F. Bliven (1981b), "On the Importance of the Significant Slope in Empirical Wind Wave Studies," J. Phys. Oceanogr., 11: in press.

Huang, N. E. and C. C. Tung (1976), "The Dispersion Relation for a Nonlinear Random Gravity Wave Field," J. Fluid Mech., 75: 337-345.

Jackson, F. C. (1974), "Directional Spectra of Ocean Waves for Microwave Backscatter," Proc. URSI Specialist Meeting: Microwave Scattering and Emission from the Earth, E. Shanda, ed.

Jackson, F. C. (1979a), "The Reflection of Impulses from a Nonlinear Random Sea," J. Geophys. Res., 84: 4939-4943.

Jackson, F. C. (1979b), "Directional Spectra of Ocean Waves from Microwave Backscatter: A Physical Optics Solution with Application to the Short-Pulse and Two-Frequency Measurement Techniques," NASA TM-80295.

Jackson, F. C. (1981), "An Analysis of Short Pulse and Dual Frequency Radar Techniques for Measuring Ocean Wave Spectra from Satellites," Radio Science, 16: 1385-1400.

Jain, A. (1977), "Determination of Ocean Wave Heights from Synthetic Aperture Radar Imagery," Applied Phys., 13: 371-382.

Jain, A. (1978), "Focusing Effects in the Synthetic Aperture Radar Imaging of Ocean Waves," Applied Phys., 15: 323-333.

Johnson, J. W., W. L. Jones, and D. E. Weissman (1981), "Dual-Frequency (Delta K) Microwave Scatterometer Measurements of Ocean Wave Spectra from an Aircraft," Oceanography from Space, J. F. R. Gower, ed. (New York: Plenum Press).

Jones, W. L. and L. C. Schroeder (1978), "Radar Backscatter from the Ocean: Dependence on Surface Friction Velocity," Boundary-Layer Meteorol., 13: 133-149.

Jones, W. L. et al. (1979), "SEASAT Scatterometer: Results of the Gulf of Alaska Workshop," Science, 204: 1413-1415.

Kasevich, R. S. (1975), "Directional Wave Spectra from Daylight Scattering," J. Geophys. Res., 80: 4535-4541.

Keller, W. C. and J. W. Wright (1975), "Microwave Scattering and the Straining of Wind-Generated Waves," Radio Science, 10: 139-147.

Kenney, J. E., E. A. Uliana, and E. J. Walsh (1979), "The Surface Contour Radar, A Unique Remote Sensing Instrument," IEEE Trans., MTT-27: 1080-1092.

Kovaly, J. J. (1976), Synthetic Aperture Radar (Dedham, Mass.: Artech House, Inc.).

Larson, T. R. and J. W. Wright (1975), "Wind-Generated Gravity-Capillary Waves: Laboratory Measurements of Temporal Growth Rates Using Microwave Backscatter," J. Fluid Mech., 70: 417-436.

Lee, P. H. Y. (1977), "Doppler Measurements of the Effects of Gravity Waves on Wind-Generated Ripples," J. Fluid Mech., 81: 225-240.

LeVine, D. M. (1974), "Spectrum of Power Scattered by a Short Pulse from a Stochastic Surface," NASA X-952-74-299.

Lipa, B. J. (1977), "Derivation of Directional Ocean Wave Spectra by Integral Inversion of Second Order Echo," Radio Science, 12: 425-433.

Little, C. G. (1969), "Acoustic Methods for Remote Probing of the Lower Atmosphere," Proc. IEEE, 57: 571-578.

Liu, P. C. and D. B. Ross (1980), "Airborne Measurements of Wave Growth for Stable and Unstable Atmospheres in Lake Michigan," J. Phys. Oceanogr., 10: 1842-1853.

Long, M. W. (1975), Radar Reflectivity of Land and Sea (Lexington, Mass.: D. C. Heath Co.).

Longuet-Higgins, M. S. (1957), "The Statistical Analysis of a Random Moving Surface," Phil. Trans. Roy. Soc., A 249: 321-387.

Longuet-Higgins, M. S. (1963), "The Effect of Non-Linearities on Statistical Distributions in the Theory of Sea Waves," J. Fluid Mech., 17: 459-480.

Longuet-Higgins, M. S. (1969), "On Wave Breaking and the Equilibrium Spectrum of Wind-Generating Waves," Proc. Roy. Soc., A 310: 151-159.

Longuet-Higgins, M. S. (1975), "On the Joint Distribution of the Periods and Amplitudes of Sea Waves," J. Geophys. Res., 80: 2688-2694.

Longuet-Higgins, M. S. (1980), "On the Distribution of the Heights of Sea Waves: Some Effects of Nonlinearity and Finite Band Width," J. Geophys. Res., 85: 1519-1523.

McClain, C. R., D. T. Chen, and D. L. Hammond (1980), "Gulf Stream Ground Truth Project: Results of the NRL Airborne Sensors, Ocean Engineering, 7: 55-97.

McClain, C. R., N. E. Huang, and P. E. LaViolette (1982), "Measurements of Sea State Variations Across Oceanic Fronts Using Laser Profilometry," J. Phys. Oceanogr., in press.

McGoogan, J. T. (1974), "Precision Satellite Altimetry," IEEE Intercon., 74: Session 34/3.

McGoogan, J. T. (1975), "Satellite Altimetry Applications," IEEE Trans., MTT-23: 970-978.

McGoogan, J. T. and E. J. Walsh (1978), "Real-Time Determination of Geophysical Parameters from a Multibeam Altimeter," AIAA/NASA Conference on Smart Sensors, Nov. 14-16, 1978, Hampton, Virginia.

McMillan, J. D. (1981), "A Global Atlas of GEOS-3 Significant Waveheight and Comparison of the Data with National Buoy Data," Ph.D. Dissertation, University of Texas at Austin.

Meserve, J. M. (1974), U.S. Navy Marine Climatic Atlas of the World, I: North Atlantic Ocean, NAVAIR 50-1C-528 (Washington, D.C.: Government Printing Office).

Mikhailov, V. I. (1960), "On the Theory of Scattering of Electromagnetic Waves on the Sea Surface," Izv. Geophys. Ser., 1229-1233.

Miller, L. S. and D. L. Hammond (1972), "Objectives and Capabilities of the Skylab S-193 Altimeter Experiment," IEEE Trans. Geo. Electron., 73-79.

Miller, L. S. and G. S. Hayne (1972), "Characteristics of Ocean-Reflected Short Radar Pulses with Applications to Altimetry and Surface Roughness Determination," Sea Surface Topography from Space, 1, NOAA TR ERL-228-AOML 7, pp. 12-1 - 12-7.

Monaldo, F. M. and R. S. Kasevich (1981), "Daylight Imagery of Ocean Surface Waves for Wave Spectra," J. Phys. Oceanogr., 11: 272-283.

Moore, R. K. (1978), "Active Microwave Sensing of the Earth's Surface--A Mini Review," IEEE Trans., AP-26: 843-849.

Moore, R. K. and D. S. Simonett (1967), "Potential Research and Earth Resource Studies with Orbiting Radar: Results of Recent Studies," Meeting Paper AIAA No. 67-676, Proc. AIAA 4th Annual Meeting.

Moskowitz, L. I. (1973), "The Feasibility of Ocean Current Mapping Via Synthetic Aperture Radar Methods," Proc. Amer. Soc. Photogrammetry, Fall 1973, Part 2, pp. 760-771.

Neumann, G. and W. J. Pierson, Jr. (1966), Principles of Physical Oceanography (Englewood Cliffs, N.J.: Prentice-Hall).

Noble, V. E. (1970), "Ocean Swell Measurements from Satellite Photographs," Remote Sensing of Environ., 1: 151-154.

Parsons, C. L. (1979), "GEOS-3 Wave Height Measurements: An Assessment During High Sea State Conditions in the North Atlantic," J. Geophys. Res., 84: 4011-4020.

Peppers, N. A. and J. S. Ostrem (1978), "Determination of Wave Slopes from Photographs of the Ocean Surface: A New Approach," Applied Optics, 17: 3450-3458.

Pidgeon, V. W. (1968), "Doppler Dependence of Radar Sea Return," J. Geophys. Res., 73: 1333-1341.

Pierson, W. J. and L. Moskowitz (1964), "A Proposed Spectral Form for Fully Developed Wind Sea Based on the Similarity Theory of S. A. Kitaigorodskii," J. Geophys. Res., 69: 5181-5190.

Plant, W. J. (1977), "Studies of Backscattered Sea Return with a CW Dual-Frequency, X-Band Radar," IEEE Trans., AP-25: 28-36.

Plant, W. J., W. C. Keller, and J. W. Wright (1978), "Modulation of Coherent Microwave Backscatter by Shoaling Waves," J. Geophys. Res., 83: 1347-1352.

Plant, W. J. and D. L. Schuler (1980), "Remote Sensing of the Sea Surface Using One and Two Frequency Microwave Techniques," Radio Science, 15: 605-615.

Plant, W. J. and J. W. Wright (1977), "Growth and Equilibrium of Short Gravity Waves in a Wind-Wave Tank," J. Fluid Mech., 82: 767-793.

Plant, W. J. and J. W. Wright (1979), "Spectral Decomposition of Short Gravity Wave Systems," J. Phys. Oceanogr., 9: 621-624.

Raney, R. K. (1971), "Synthetic Aperture Imaging Radar and Moving Targets," IEEE Trans., AES-7: 499-505.

Ribe, R. L. (1979), "Wave Sensor Survey," NOAA TR NOS78.

Rice, S. (1951), "Reflection of Electromagnetic Waves from Slightly Rough Surfaces," Comm. Pure and Appl. Math., 4: 351-378.

Rihaczek, A. W. (1969), Principles of High-Resolution Radar (New York: McGraw-Hill).

Ross, D. B., J. Conaway, and V. J. Cardone (1970), "Laser and Microwave Observations of Sea-Surface Conditions for Fetch-Limited 17 to 25 m/sec Winds," IEEE Trans., GE-8: 326-336.

Ruck, G., D. E. Barrick, and T. T. Kalisvewskii (1972), "Bistatic Radar Sea State Monitoring," Battelle Tech. Report, Columbus, Ohio.

Schule, J. J., L. S. Simpson, and P. S. DeLeonibus (1971), "A Study of Fetch-Limited Wave Spectra with an Airborne Laser," J. Geophys. Res., 76: 4160-4171.

Schuler, D. L. (1978), "Remote Sensing of Directional Gravity Wave Spectra and Surface Currents Using a Microwave Dual-Frequency Radar," Radio Science, 13: 321-331.

Schumacher, A. (1928), "Die stereogrammetrische Wellenaufnahmen der deutschen Atlantischen Expedition," Zeit f.d. Gesellschaft f. Erdkunde zu Berlin, 3: 105-120.

Shemdin, O. H., W. E. Brown, F. G. Staudhammer, R. Shuchman, R. Rawson, J. Zelenka, D. B. Ross, W. McLeish, and R. A. Berles (1978), "Comparison of In Situ and Remotely Sensed Ocean Waves Off Marineland, Florida," Boundary-Layer Meteorol., 13: 193-202.

Sherwin, C. W., J. P. Ruina, and R. D. Rawcliffe (1962), "Some Early Developments in Synthetic Aperture Radar Systems," IRE Trans., MIL-6: 111-115.

Shmelev, A. B. (1972), "Wave Scattering by Statistically Uneven Surfaces," Usp. Fiz. Nauk., 106: 459-480.

Shuchman, R. A. and J. S. Zelenka (1978), "Processing of Ocean Wave Data from a Synthetic Aperture Radar," Boundary-Layer Meteorol., 13: 181-191.

Skolnik, M. I. (1962), Introduction to Radar Systems (New York: McGraw-Hill).

Stafford, D. B., R. O. Bruno, and H. M. Goldstein (1973), "An Annotated Bibliography of Aerial Remote Sensing in Coastal Engineering," CERC MP Paper Z-73.

Stewart, R. H. and J. W. Joy (1974), "HF Radio Measurements of Surface Currents," Deep-Sea Res., 21: 1039-1049.

Stilwell, D., Jr. (1969), "Directional Energy Spectra of the Sea from Photographs," J. Geophys. Res., 74: 1974-1986.

Stilwell, D. and R. O. Pilon (1974), "Directional Spectra of Surface Waves from Photographs," J. Geophys. Res., 79: 1277-1284.

Sugimori, Y. (1972), "Application of Hologram Method to the Analysis of the Directional Spectrum of the Surface Wave," La Mer, 10: 9-20.

Sugimori, Y. (1973), "Dispersion of the Directional Spectrum of Short Gravity Waves in the Kuroshio Current," Deep-Sea Res., 20: 747-756.

Sugimori, Y. (1975), "A Study of the Application of the Holographic Method to the Determination of the Directional Spectrum of Ocean Waves," Deep-Sea Res., 22: 339-350.

Sugimori, Y. (1976), "Two-Dimensional Surface Wave on the Shari Current," Report Nat. Res. Cent. for Disaster Prevention, 13: 75-87.

Swift, C. T. and L. R. Wilson (1979), "Synthetic Aperture Radar Imaging of Moving Ocean Waves," IEEE Trans., AP-27.

Teague, C. C., G. L. Tyler, J. W. Joy, and R. H. Stewart (1973), "Synthetic Aperture Observations of Directional Height Spectra for 7s Ocean Waves," Nature, 244: 98-100.

Tomiyasu, K. (1971), "Short Pulse Wide-Band Scatterometer Ocean Surface Signature," IEEE Trans., GE-9: 175-177.

Townsend, W. F. (1980), "An Initial Assessment of the Performance Achieved by the SEASAT-1 Radar Altimeter," IEEE Trans., OE-5: 80-92.

Trizna, D. B., J. C. Moore, J. M. Headrick, and R. W. Bogle (1977), "Directional Sea Spectrum Determination Using HF Doppler Radar Techniques," IEEE Trans., AP-25: 4-11.

Tveten, L. H. (1967), "Ionospherically Propagated Sea Scatter," Science, 157: 1302-1304.

Tyler, G. L., C. C. Teague, R. H. Stewart, A. M. Peterson, W. H. Munk, and J. W. Joy (1974), "Wave Directional Spectra from Synthetic Aperture Observations of Radio Scatter," Deep-Sea Res., 21: 989-1016.

Utt, M. E. (1980), "Satellite Wind and Wave Data," TM E&PP 80-71M, Union Oil Co.

Valenzuela, G. R. (1967), "Depolarization of EM Waves by Slightly Rough Surfaces," IEEE Trans., AP-15: 552-557.

Valenzuela, G. R. (1968), "Scattering of Electromagnetic Waves from a Tilted Slightly Rough Surface," Radio Science, 3: 1057-1066.

Valenzuela, G. R. (1974), "The Effect of Capillarity and Resonant Interactions on the Second Order Doppler Spectrum of Radar Sea Echo," J. Geophys. Res., 79: 5031-5037.

Valenzuela, G. R. (1978), "Theories for the Interaction of Electromagnetic and Oceanic Waves--A Review," Boundary-Layer Meteorol., 13: 61-85.

Valenzuela, G. R. (1980), "An Asymptotic Formulation for SAR Images of the Dynamical Ocean Surface," Radio Science, 15: 105-114.

Wait, J. R. (1966), "Theory of HF Ground Wave Backscatter from Sea Waves," J. Geophys. Res., 71: 4839-4892.

Wait, J. R., ed. (1971), Electromagnetic Probing in Geophysics (Boulder, Colo.: The Golem Press).

Walsh, E. J. (1974), "Analysis of Experimental NRL Radar Altimeter Data," Radio Science, 9: 711-722.

Walsh, E. J. (1977), "Problems Inherent in Using Aircraft for Radio Oceanography Studies," IEEE Trans., AP-25: 145-149.

Walsh, E. J. (1979), "Extraction of Ocean Wave Height and Dominant Wavelength from GEOS-3 Altimeter Data," J. Geophys. Res., 84: 4003-4010.

Ward, J. F. (1969), "Power Spectra from Ocean Movements Measured Remotely by Ionospheric Radio Backscatter," Nature, 223: 1325-1330.

Weissmann, D. E. (1973), "Two Frequency Radar Interferometry Applied to the Measurement of Ocean Wave Height," IEEE Trans., AP-21: 649-656.

Weissmann, D. E. and J. W. Johnson (1977), "Dual Frequency Correlation Radar Measurements of the Height Statistics of Ocean Waves," IEEE Trans., AP-25: 74-83.

Westman, H. P., ed. (1974), Reference Data for Radio Engineers, 5th ed. (Indianapolis: Howard W. Sams and Co.).

Wiegel, R. L. (1974), "Engineers' Concern with Waves and their Measurement," Proc. Symp. Ocean Wave Measurement and Analysis '74, Vol. II, ASCE, 1974, New Orleans, pp. 1-22.

Wright, J. W. (1966), "Backscattering from Capillary Waves with Application to Sea Clutter," IEEE Trans., AP-14: 749-754.

Wright, J. W. (1968), "A New Model for Sea Clutter," IEEE Trans., AP-16: 217-223.

Wright, J. W. (1978), "Detection of Ocean Waves by Microwave Radar: The Modulation of Short-Gravity-Capillary Waves," Boundary-Layer Meteorol., 13: 87-105.

Wright, J. W. and W. C. Keller (1971), "Doppler Spectra in Microwave Scattering from Wind Waves," Phys. Fluids, 14: 466-474.

Yaplee, B. S., A. Shapiro, D. L. Hammond, B. D. Au,, and E. A. Uliana (1971), "Nanosecond Radar Observations of the Ocean Surface from a Stable Platform," IEEE Trans., GE-9: 170-174.

REMOTE SENSING OF OCEAN WAVES BY SURFACE CONTOUR RADAR

Edward J. Walsh[1]

Introduction

The Surface Contour Radar (SCR), developed jointly by NASA Wallops Flight Center (WFC) and the Naval Research Laboratory, is an airborne, computer-controlled 36 GHz bistatic radar that produces a real-time topographical map of the surface beneath the aircraft. Figure 1 shows a nominal measurement geometry. The SCR, described in detail by Kenney et al. (1979), was designed to measure the directional wave spectra of the ocean surface. Of the remote sensing instruments described in these proceedings, the SCR operates by the simplest measurement concept and offers the greatest ease of data interpretation, since it involves a direct range measurement.

SCR System

The SCR is flown in a WFC P-3 aircraft. An oscillating mirror scans a $0.85^{o} \times 1.2^{o}$ pencil beam laterally, measuring the elevations at 51 evenly spaced points on the surface below the aircraft within a swath approximately as wide as half the aircraft's altitude. Figure 2 shows the horizontal resolutions in terms of the aircraft altitude, h. At each point, the SCR measures the slant range to the surface, correcting in real time for the off-nadir angle of the beam to determine the elevation of the point with respect to the horizontal reference.

The elevations are false-color coded and displayed on the SCR's color TV monitor to allow real-time estimates to be made of significant wave height (SWH), dominant wavelength, and direction of propagation. These estimates allow the aircraft altitude and flight lines to be optimized during the flight, freeing the operations from dependence on prior knowledge of wave conditions. As the SCR can also map terrain, it is well suited for work in coastal areas.

Correction for Aircraft Motion

The aircraft generally experiences some altitude variation as data are being acquired that contaminates the elevation measurements. An extreme example is shown in the top curve of Figure 3, an elevation

---

[1]NASA Goddard Space Flight Center, Wallops Flight Facility

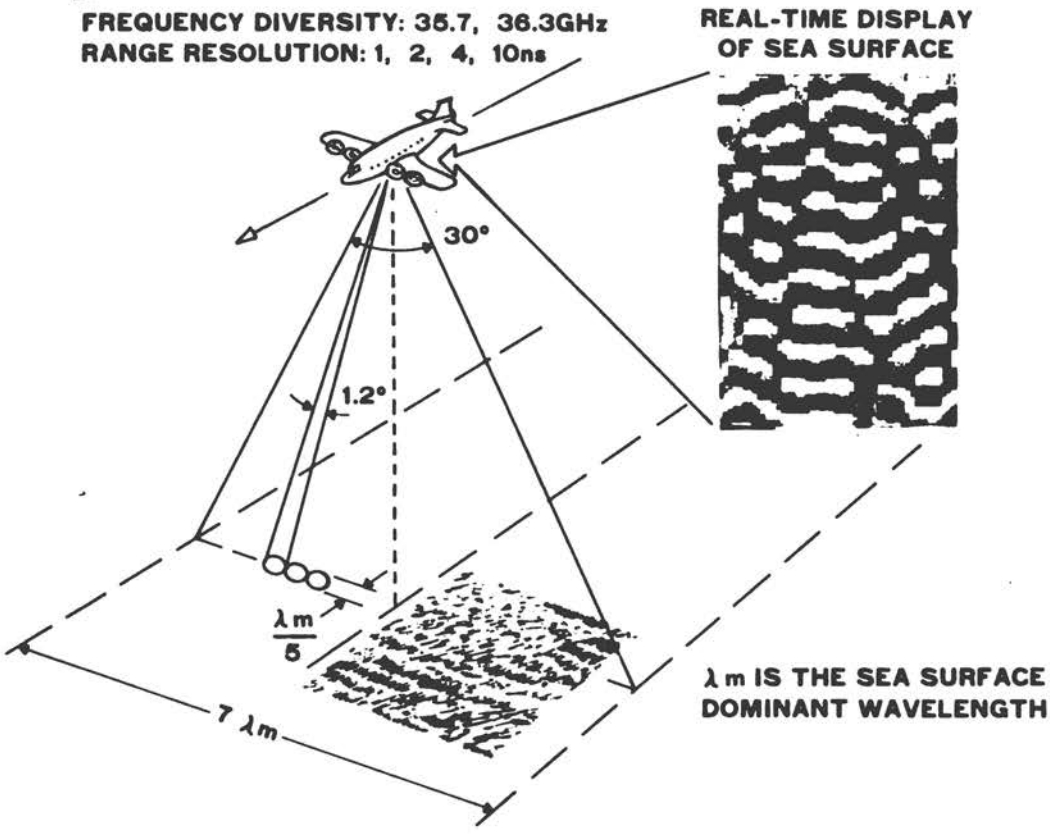

Figure 1 The basic measurement geometry of the Surface Contour Radar (SCR)

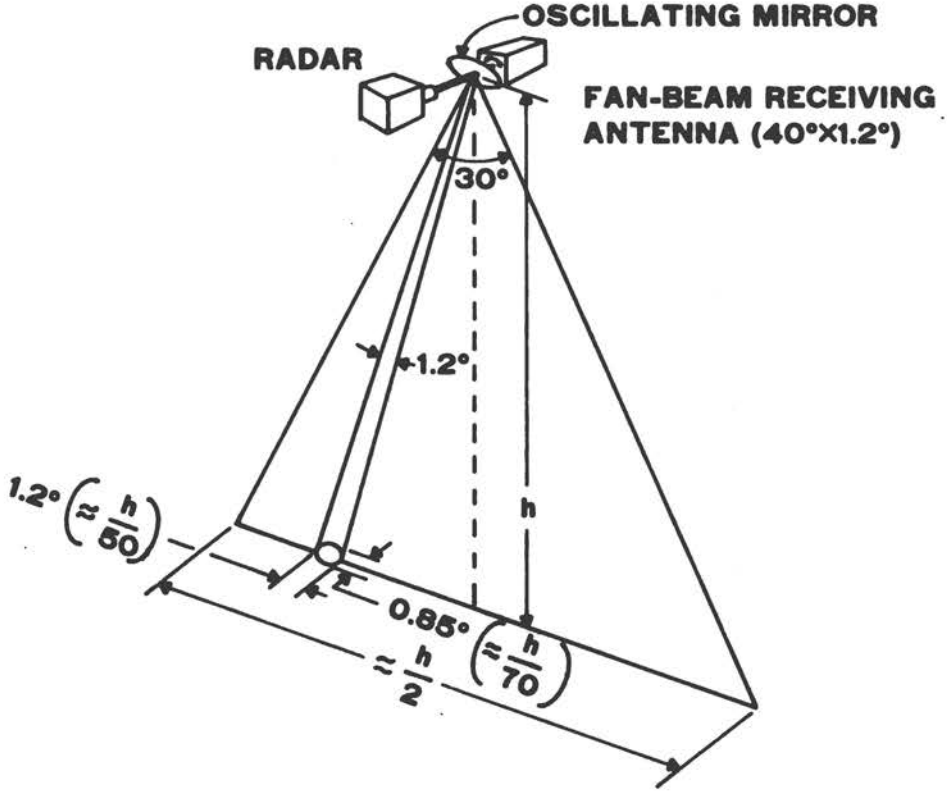

Figure 2 The SCR antenna and mirror orientation, and the spatial resolution in terms of aircraft altitude (h)

profile from the center of the swath: the aircraft was flying parallel to the crests of a 5.5 m SWH sea whose dominant wavelength was 140 m. In this example, it would clearly be difficult to remove the aircraft motion from the elevation data by high-pass filtering of the raw data. An independent estimate of aircraft motion is obtained by doubly integrating the output of a vertically mounted accelerometer. The bottom curve in Figure 3 shows the result when the accelerometer-determined aircraft motion has been subtracted from the raw elevation data. A parabola of the form $a_o + a_1 y + a_2 y^2$ (where y is the alongtrack distance) that was least-squares fitted over the data span has also been removed from the elevation data. This procedure compensates for any uncertainties in the initial values of aircraft altitude and vertical velocity and the accelerometer constant. The resulting elevation data may still contain some small residual aircraft motion, but it is obvious that they are much lower in amplitude and in frequency than the wave data.

Airborne Oceanographic Lidar

Figure 4 shows a more typical set of data, taken when the aircraft was traveling perpendicular to the crests of waves of wavelengths approximately 45 m. The aircraft motion is apparent in these uncorrected elevation data. Also shown is a comparison between the SCR elevation data and elevation data from the WFC Airborne Oceanographic Lidar (AOL) which is also on the P-3 aircraft. The AOL elevation data were acquired in profiling mode using 200 pulses per second. The general agreement is excellent, although the instruments are separated by 8 m along the center of the aircraft (the data sets have been shifted into alignment). The AOL also has a scanning mode using a 5 Hz conical scan at 15° off-nadir rather than the 10 Hz raster scan employed by the SCR. In its scanning mode at 420 m altitude, the AOL would look at the waves 1 s before and 1 s after the SCR encountered them. The AOL can also measure fluorescence (Hoge and Swift, 1981) and bathymetry (Hoge et al., 1980). The instruments are quite complementary: the SCR cannot see through water; the AOL cannot see through clouds.

Results

Figure 5 shows close-up views of grey-scale-coded SCR elevation data taken on the same day within minutes of each other during the Atlantic Remote Sensing Land-Ocean Experiment (ARSLOE). The wind was blowing from approximately 45° at 9 m/s; SWH was 1.6 m, and the dominant wavelength was 65 m. The data were taken at a 215 m altitude (ALT) along the three different aircraft ground tracks (GTK) indicated in the headers. The troughs are dark and the crests are light so that the data have the visual appearance of waves illuminated by a low-angle sun. Distance along the ground track increases to the right in each case by approximately 5 m per line (the ground speed (GS) divided by L/S, the number of scan lines per second). The data point separation on the display is approximately the same alongtrack

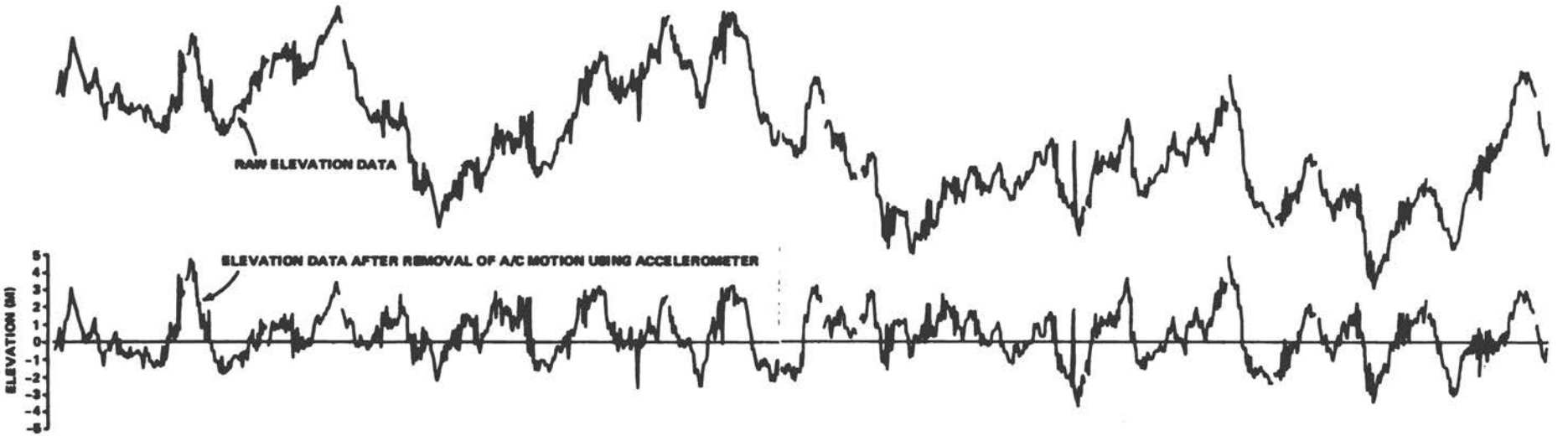

Figure 3 Center swath profile of SCR elevation data before (top) and after (bottom) removal of aircraft motion using accelerometer data

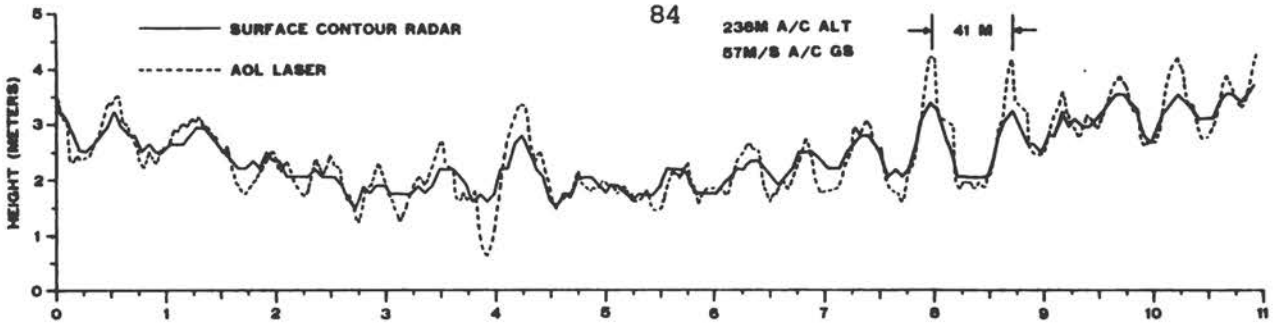

Figure 4 Comparison of center-swath elevation data from SCR and a profiling AOL laser system

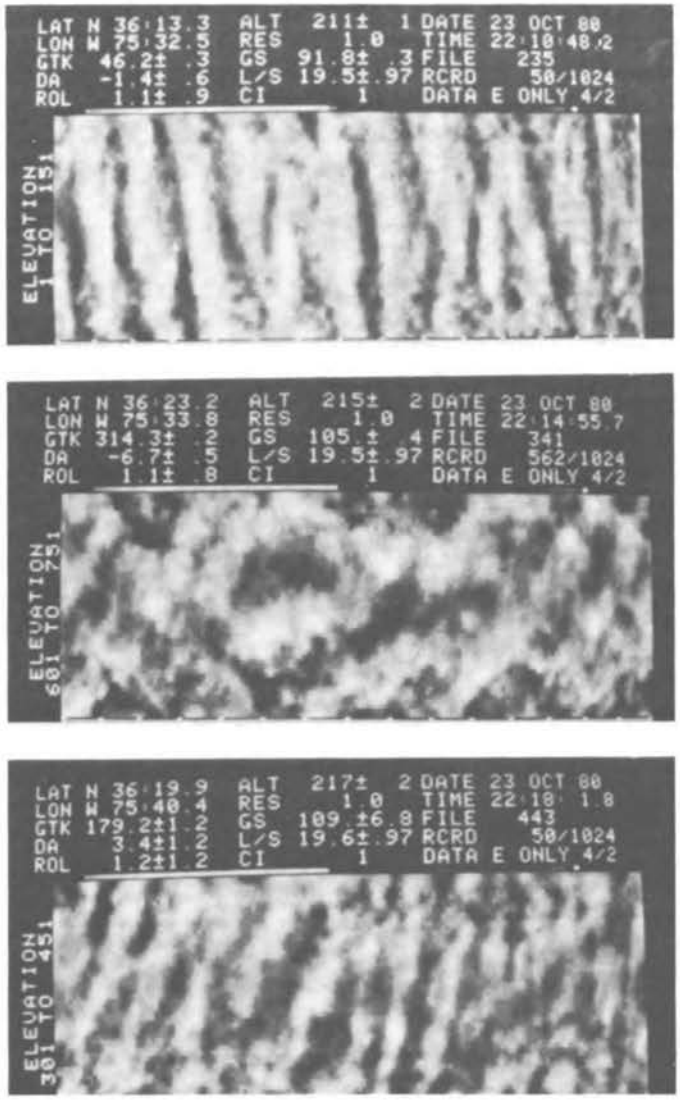

Figure 5 Grey-scale-coded elevation data taken at 215 m altitude for three different flight directions. The header information indicates latitude (LAT), longitude (LON), aircraft ground track (GTK), drift angle (DA), roll (ROL), altitude (ALT) in m, range resolution (RES) in ns, ground speed (GS) in m/s, and the contour interval (CI) by which the data are divided before being displayed. The angles are in degrees. There is considerable distortion, owing to the disparity between alongtrack and crosstrack dimensions.

and crosstrack. The actual crosstrack spacing of the 51 elevation points is the altitude divided by 100, which means that there is quite some geometric distortion in the displays. The lateral dimension has been exaggerated by a factor of approximately 2 relative to the alongtrack dimension, which makes the waves appear long-crested in the case of the aircraft ground track of 45° and short-crested in the case of the 314° ground track. The exaggeration also distorts the apparent angle of propagation in the data displayed for a 179° ground track.

Two-dimensional fast Fourier transforms (FFTs) are performed on groups of 1024 scan lines, as shown in Figure 6 for four elevation data sets taken at 400 m altitude, where there is little geometric distortion in the elevation display. The data have been oriented in the proper ground track directions. The alongtrack dimension of approximately 5 km produces an alongtrack spectral resolution of $2\pi/5000$ m^{-1} in wavenumber space, whereas the crosstrack resolution is approximately $2\pi/200$ m^{-1}; thus, the grid of FFT points is badly out of proportion.

Figure 7 shows a grey-scale-coded raw spectrum in which the alongtrack and crosstrack separation of the FFT points is about the same. The altitude for the data set associated with this FFT was only 211 m, so the swath width was approximately 110 m. The alongtrack distance was 4.8 km, giving a geometric distortion in Figure 7 of approximately 44:1. At the origin of the FFT can be seen a bright region which is due to residual aircraft motion that the accelerometer did not remove.

When displaying the final spectrum on the color TV monitor, the spectrum is oriented with respect to true north and data points are filled in crosstrack, so the display is in proportion. Figure 8 shows false-color-coded spectra for three different aircraft ground tracks (the directions are indicated by the white radials from the origin) and two different altitudes, 400 m and 200 m. The actual spectrum in k-space is taken to be in the direction toward which waves are traveling, not the direction from which they are coming. This means, for example, that the actual spectra are in the third quadrant in Figure 8. The 180° ambiguity in the first quadrant is an artifact of the FFT process, since the same elevation data could represent waves traveling in either direction. The elimination of this ambiguity is discussed in a succeeding section that describes correction of such "encounter" spectra for the effects of aircraft velocity and drift angle (the difference between the aircraft's heading and the aircraft's ground track).

It is reassuring that essentially the same spectrum is obtained independent of altitude and heading. The noise in the spectra can be reduced by increasing the number of degrees of freedom through incoherent averaging of a number of spectra for the same flight direction. Figure 9 shows the results of averaging four spectra taken on a 315° ground track at 215 m altitude. It is a false-color-coded variance spectrum in which 10 color levels change at the 1, 4, 9, 16, 25, 36, 49, 64, and 81 percent levels relative to the spectral maximum. The banding in Figure 9 parallel to the aircraft ground track is the effect of the poor lateral spectral resolution. Even so, the spectrum is still well defined.

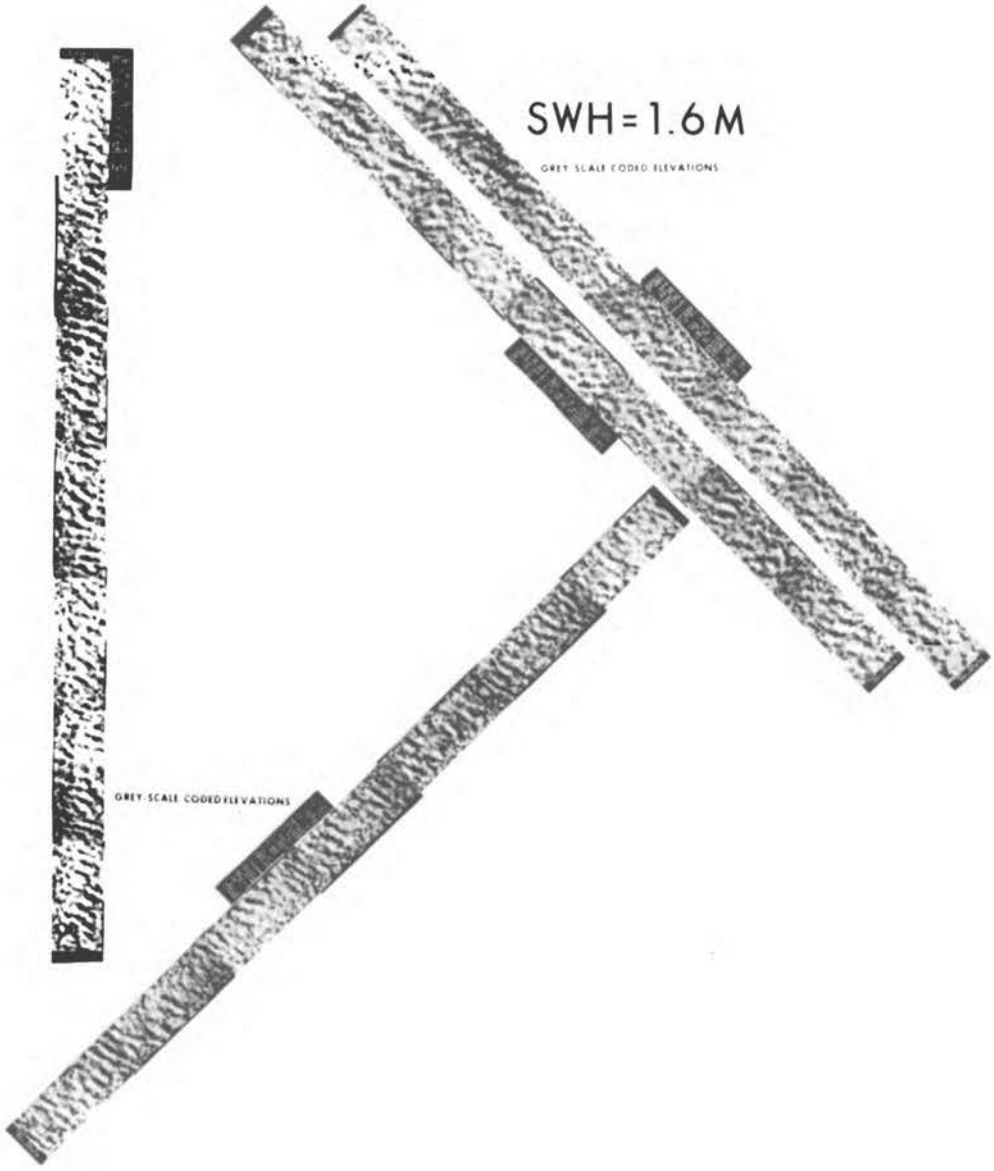

Figure 6 Grey-scale-coded elevation data acquired October 23, 1980, at 400 m altitude (where the geometric distortion is small). The data are oriented in the directions of the aircraft ground tracks, with north the ordinate.

Figure 7 Grey-scale-coded variance spectrum before corrections for geometric distortion and rotation (to orient with respect to true north)

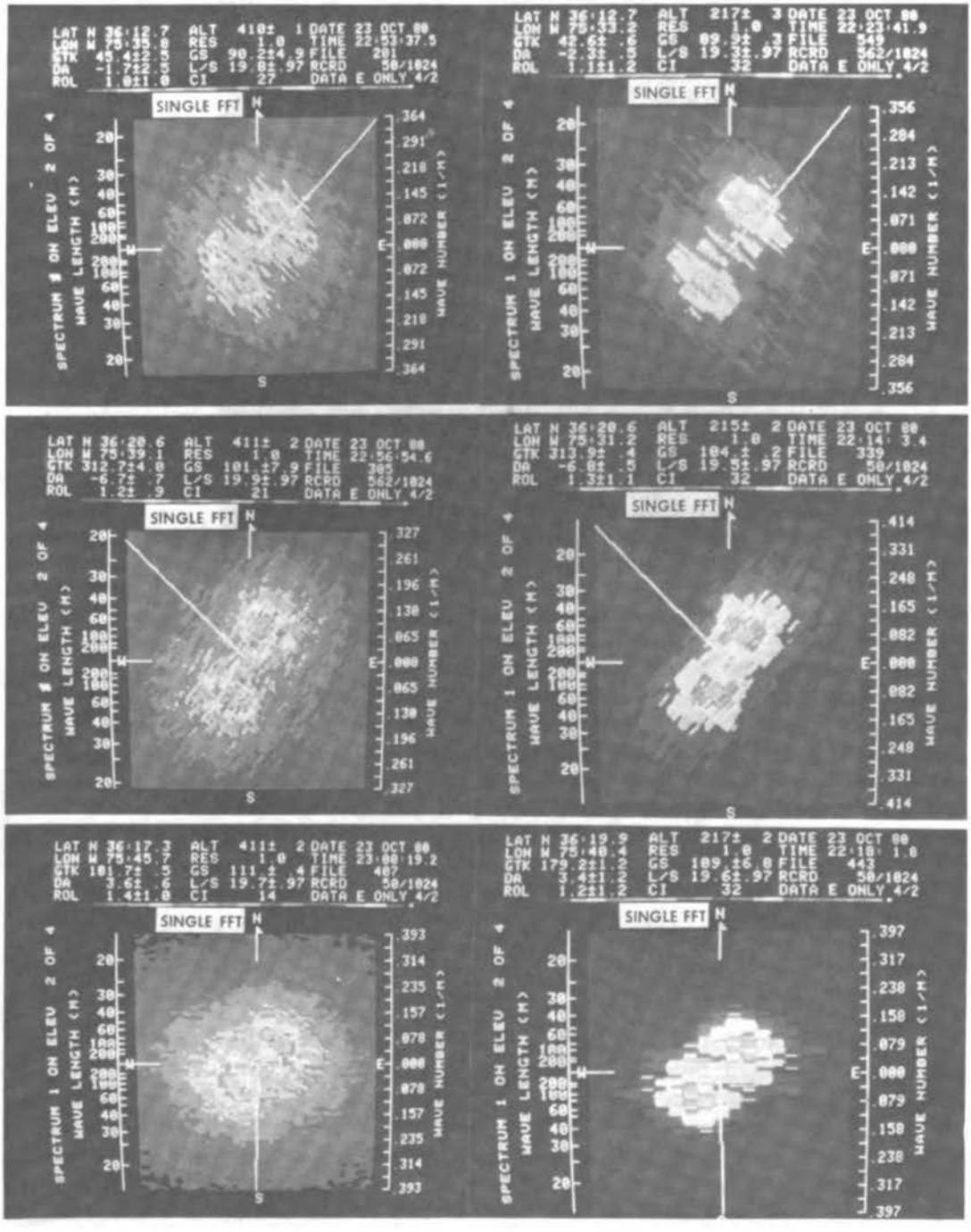

Figure 8 False-color-coded variance spectra for two altitudes and three flight directions (here reproduced in black and white)

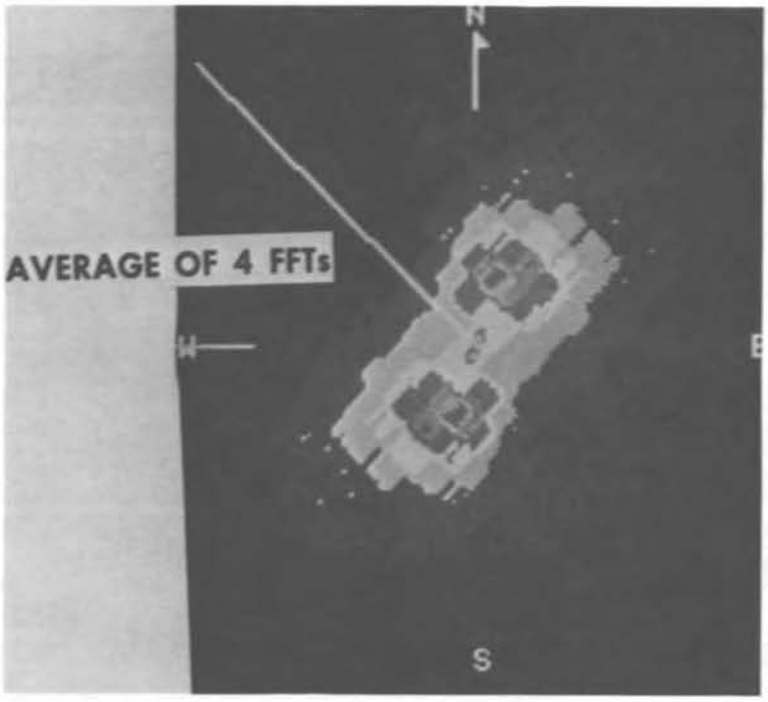

Figure 9 The average of four false-color-coded variance spectra (here reproduced in black and white). Data taken at 215 m altitude for the flight direction indicated by the white radial. The color changes at the 1, 4, 9, 16, 25, 36, 49, 64, and 81 percent levels relative to the spectral peak.

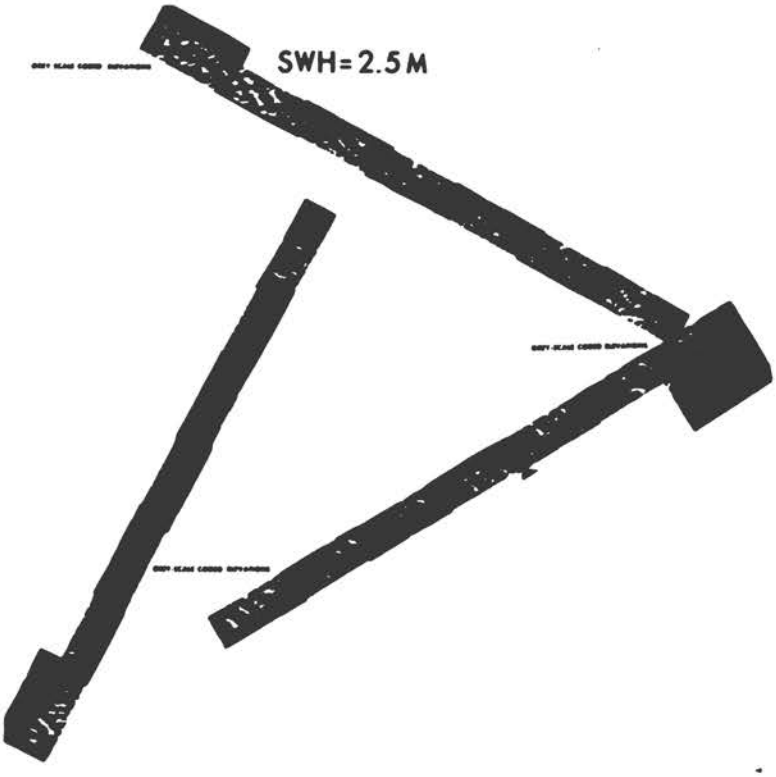

Figure 10 Grey-scale-coded elevation data, acquired November 12, 1980, at 400 m altitude

Figure 10 shows data from another ARSLOE set, taken at 400 m altitude. The wind was blowing at about 9 m/s from about 350° and the SWH was approximately 2.5 m. Figure 11 shows the average of four variance spectra for each of two different flight directions (false-color coded as in the preceding example). The agreement between flight directions is excellent. Figure 12 shows the same spectra with a grey-scale coding where the grey-scale is cycled through slightly more than twice. The spectral peak is black and the first transition between white and black occurs at the 25 percent level relative to the spectral peak. If one examines the Figure 12 spectra carefully, it is apparent that the encounter spectrum (in the third quadrant) and the 180° ambiguity of the image (in the first quadrant) are more widely separated for the northeast ground track than for the southeast ground track. Also, the radial joining the spectral peaks is rotated clockwise in the southeast ground track spectrum relative to the northeast ground track. These changes are caused by the aircraft velocity and drift angle, and must be corrected to obtain the actual spectrum from the encounter spectrum.

Correction for Aircraft Velocity and Drift Angle

Figure 13 shows the migration of a representative sampling of points in k-space. The base of each vector is the original spectral component position. The arrowhead shows the apparent position to which that component would shift owing to an aircraft ground speed of 100 m/s when there is no drift angle (top) and when there is a 10° drift angle (bottom). When the aircraft follows its nose, the drift angle is zero. If there is a crosswind from the left, the aircraft ground track will drift to the right relative to its heading. For no drift angle, all the points in k-space migrate antiparallel to the aircraft ground track: the magnitude of the change is proportional to the magnitude of the original k-vector (Long, 1979). When the drift angle is nonzero, the k-vectors additionally rotate in the direction opposite to the aircraft heading relative to the ground track.

Figure 14 shows overlaid plots in k-space of the encounter spectra of Figure 11. The curves in Figure 14 extending from the lower right to upper left correspond to the northeast ground track, and the curves extending from the lower left to upper right correspond to the southeast ground track. The curves are linear in variance, plotted as the "third" dimension, so the ordinate represents both variance and a direction of 73°. Each set of curves shows the high alongtrack resolution and the coarse crosstrack resolution (indicated by the wide lateral separation of the adjacent curves). A 7-point smoothing filter has been applied to the curves in the alongtrack direction, and wavenumbers smaller than $2\pi/500$ have been arbitrarily set to zero. The SWH observed on the southeast ground track was higher than that observed on the northeast ground track. Because it was started from the end of the northeast ground track, the southeast ground track was farther from shore, and the increased wave height was probably a fetch-limited effect. To compensate crudely for that effect, all the

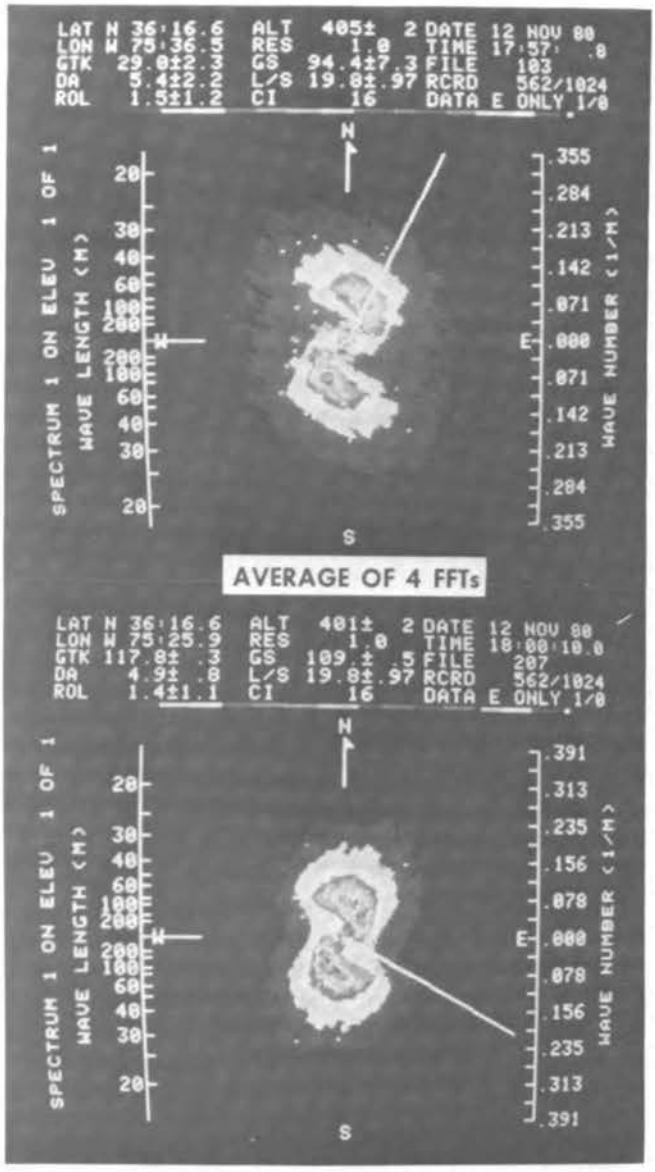

Figure 11 False-color-coded variance spectra (here reproduced in black and white) which are the average of four spectra for each of the indicated aircraft ground tracks (indicated by the white radial)

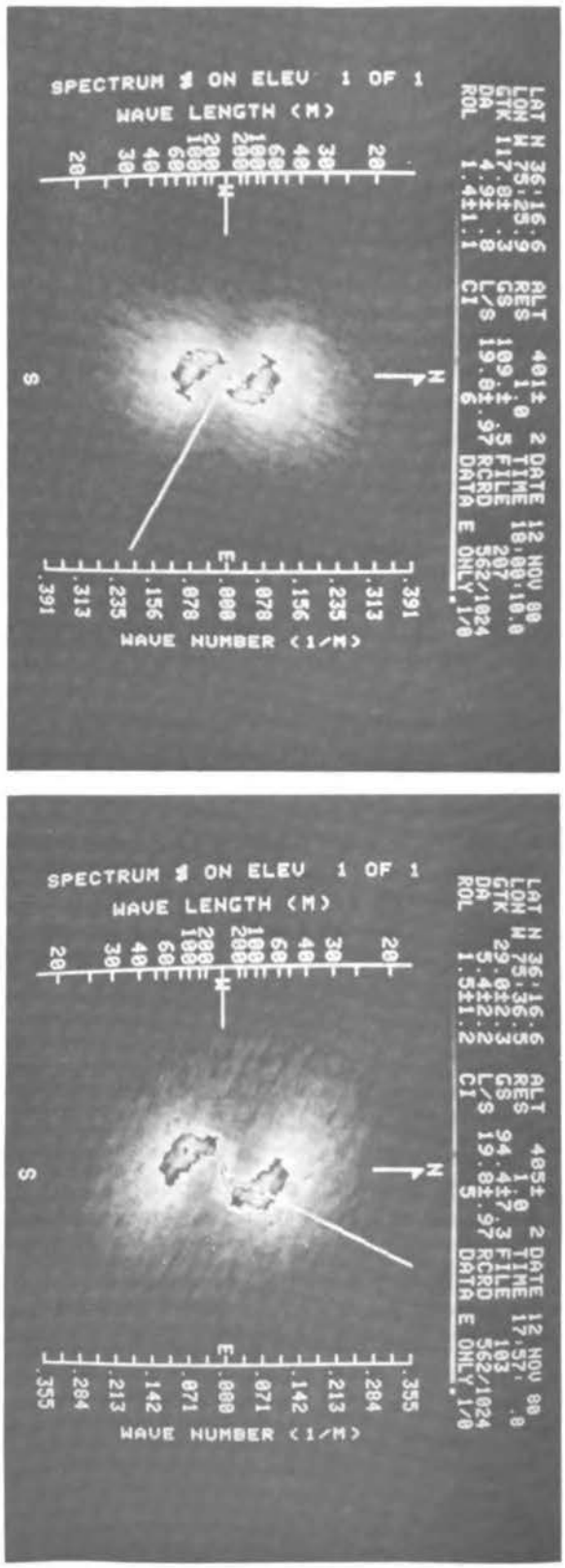

Figure 12 The same variance spectra as Figure 11, but grey-scale coded: the spectral peak is black and the first transition from white to black is at the 25 percent level relative to the spectral peak.

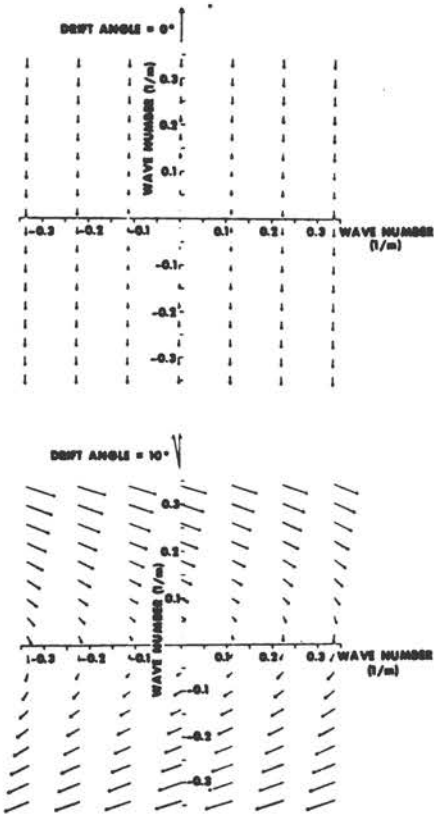

Figure 13 The migration of points in k-space for aircraft ground speed of 100 m/s and drift angles of 0° and 10°. The ordinate is the direction of the aircraft's ground track.

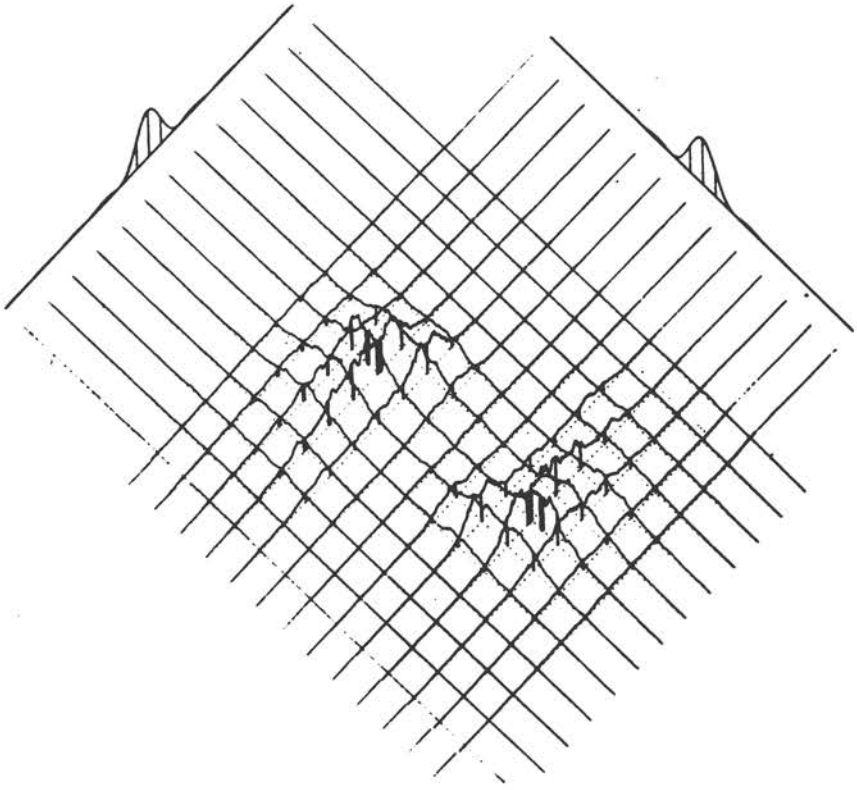

Figure 14 Overlay of the variance spectra of Figure 11 before the corrections of Figure 13

variance values in the FFT for the southeast ground track were reduced by 20 percent before plotting them relative to those for the northeast ground track. The actual encounter spectra for the two flight directions are in the lower right, and the 180° ambiguous spectra are in the upper left. The heavy pairs of vertical lines represent arbitrary reference points for the two ground tracks.

Figure 15 pictures the same data as Figure 14 after they have been corrected in the manner indicated in Figure 13. In applying the corrections no a priori knowledge of the direction of propagation was assumed. In effect, all the data were assumed to be real and corrected accordingly. It can be seen that the corrections have caused the two reference lines to coalesce in the actual spectrum of the lower right, while they are spread farther apart in the 180° ambiguous spectrum in the upper left. The corrections compensate the actual spectrum, but are in the wrong direction for the other, and worsen the disparity between the flight directions. Rejection of the ambiguous lobe of the spectrum can be done by computer, comparing the squares of the differences at the crossing points for perpendicular flight lines on the spectral lobes. The procedures to combine the two flight directions into a single spectrum for comparison with the ARSLOE in situ data are now being developed.

Figure 16 shows some false-color-coded data (here in black and white) taken at an altitude of 800 m with SWH of approximately 5 m, and dominant wavelength of 220 m. By varying the aircraft altitude, the spatial resolution and swath width can be adjusted as dictated by the sea state.

Other Features

Another feature of the SCR is that it acquires backscattered power information simultaneously and perfectly registered with the elevation data. By banking the plane, backscattering information from nadir to about 27° off-nadir can be obtained together with detailed information on the surface elevation variation. As the plane turns in a circle, the radar will pass through all azimuthal directions relative to the local wind. This should be a very powerful technique for interpreting SAR and SLAR data.

Conclusions

The SCR offers a convenient means of making direct measurements with high resolution of directional wave spectra. It requires no calibration against sea-truth data, and may, in fact, find important application in verifying the measurements of other remote sensing systems.

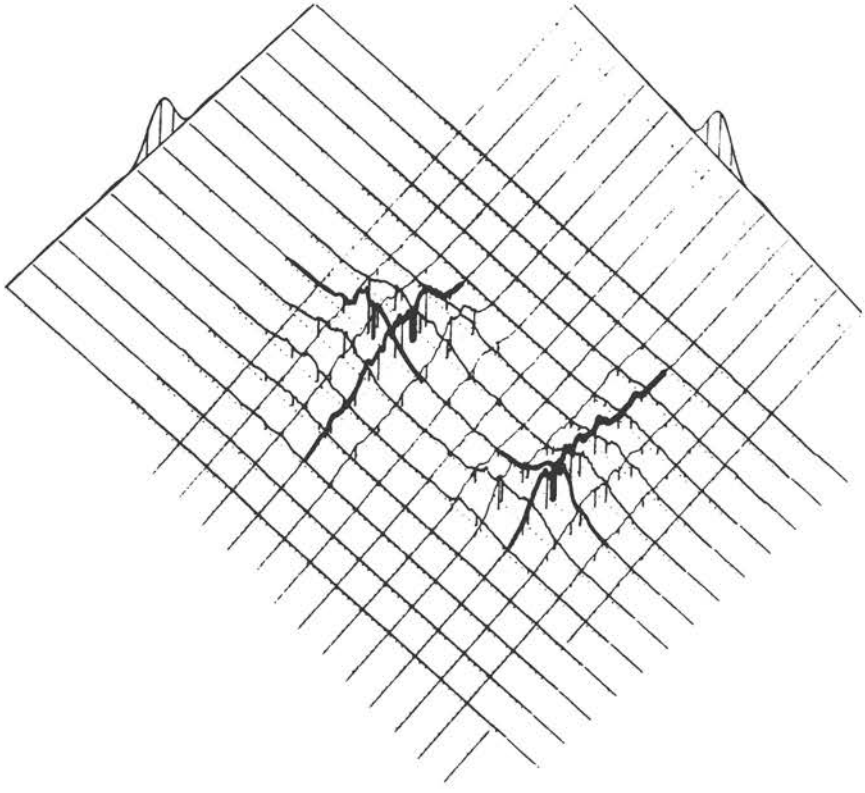

Figure 15 Overlay of the variance spectra of Figure 11 after the corrections of Figure 13

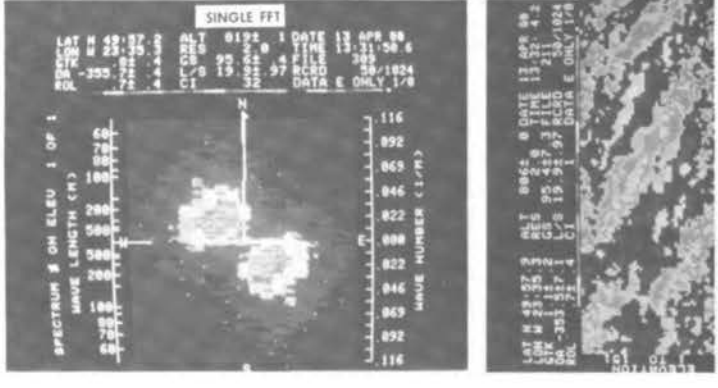

Figure 16 False-color-coded elevation data (here reproduced in black and white) acquired at 800 m altitude, and the variance spectrum for a day when the significant wave height (SWH) was 5 m, and the dominant wavelength was 220 m.

References

Hoge, F. E. and R. N. Swift (1981), "Absolute Tracer Dye Concentration Using Airborne Laser-Induced Water Raman Backscatter," Applied Optics, 20: 1191-1202.

Hoge, F. E., R. N. Swift, and E. B. Frederick (1980), "Water Depth Measurement Using Airborne, Pulsed Neon Laser System," Applied Optics, 19: 871-883.

Kenney, J. E., E. A. Uliana, and E. J. Walsh (1979), "The Surface Contour Radar, A Unique Remote Sensing Instrument," IEEE Trans., MMT-27: 1080-1092.

Long, R. B. (1979), "On Surface Gravity Wave Spectra Observed in a Moving Frame of Reference," NOAA Technical Memorandum ERL AOML-38.

THE USE OF SYNTHETIC APERTURE RADAR (SAR) TO MEASURE OCEAN GRAVITY WAVES

R. A. Shuchman,*[1] E. S. Kasischke,[1]
J. D. Lyden,[1] and G. A. Meadows[2]

Abstract

This paper reviews the use of synthetic aperture radar (SAR) to detect water gravity waves. SAR data, collected by aircraft and satellites during a series of oceanographic experiments, have been used to demonstrate the ability of this imaging remote sensor to measure water gravity waves in a variety of sea states. For example, wave refraction was successfully documented in the coastal regions near Cape Hatteras, North Carolina, using Seasat SAR satellite data. SAR has also been successfully used to measure internal gravity waves and long-period "surf beats." Several parameters determine the visibility of gravity waves in SAR images: radar wavelength and polarization, angle of incidence and radar look direction (relative to the wave propagation direction), as well as ocean wavelength, wave height, and wind speed and direction. In general, waves traveling toward or away from the SAR line of sight are more visible in the imagery than waves traveling perpendicular to the SAR line of sight.

Introduction

Considerable research during the past decade has explored SAR's ability to detect and measure gravity waves on the oceans and Great Lakes. The purpose of this paper is to review this research and to identify areas where additional study is needed.

SAR is a coherent airborne (or spaceborne) radar that uses the motion of a moderately broad physical antenna beam to synthesize a very narrow beam, thus providing fine azimuthal (alongtrack) resolution (Brown and Porcello, 1969; Harger, 1970). Fine range (crosstrack) resolution is achieved by transmitting either very short pulses or longer coded pulses which are compressed by matched-filtering techniques into equivalent short pulses. The coded pulse is usually a waveform linearly modulated in frequency.

---

*Presenter

[1]Radar and Optics Division, Environmental Research Institute of Michigan

[2]Department of Atmospheric and Oceanic Science, University of Michigan

The phase history of a scattering point in the scene is either recorded on photographic film as an anamorphic (astigmatic) Fresnel zone plate or on digital tapes. The parameters of the phase histories are set in the azimuth direction by the Doppler frequencies produced by the relative motion between the sensor and the point scatterer, and in the range direction by the structure of the transmitted pulses. These optically recorded SAR phase histories are a collection of superimposed zone plates, representing the collection of point scatterers in the scene. SAR optical processing is described by Kozma et al. (1972). Digital processing techniques are reviewed by Ausherman (1980).

The principle in imaging any surface with a radar is that the backscatter of microwave energy (echo) received by the radar receiver mostly contains information about the roughness characteristics (shapes, dimensions, and orientations) of the reflecting area. The parameters that influence the SAR image of the ocean surface include the motion of the scattering surfaces, the so-called speckle effect, system resolution, and noncoherent integration, as well as contributions attributable to wind, waves, surface currents, and surface tension. The orientation of ocean waves to the radar look direction must also be considered. Attempts to understand the SAR ocean-wave-imaging mechanism entail consideration of factors pertaining to wave orbital velocity, Bragg-scatterer velocity, and long (or resolvable) wave-phase velocity (Teleki et al., 1978).

This review paper discusses the use of both aircraft and spaceborne synthetic aperture radars. The aircraft data here presented were collected by the ERIM* X-L SAR, flown at the time in an ERIM-owned C-46, and now installed in the CV-580 aircraft of the Canada Centre for Remote Sensing (CCRS). This X-L system, described by Rawson et al. (1975), consists of a dual-wavelength and dual-polarization synthetic aperture radar that simultaneously images at X-band (3.2 cm) and L-band (23.5 cm). (A C-band [5.6 cm wavelength] capacity was recently added to the system.) Alternate X- and L-band pulses (chosen to be either horizontally or vertically polarized) are transmitted and reflections of both polarizations are received; thus, four channels of radar imagery are simultaneously obtained. Both polarizations of X-band are recorded on one film, and both polarizations of L-band on another. The data presented in this paper were obtained from the horizontal-transmit, horizontal-receive channel (HH) of both the X- and L-band receivers. Polarization effects have not been analyzed. The resolution of the ERIM aircraft SAR system is approximately 3 m in both range and azimuth. The swath width of the X-L system is approximately 6 km.

Two other aircraft SAR systems routinely collect ocean gravity wave information. One is an X-band military system (UPD-4), flown on an RF-4 jet. The characteristics of this Goodyear-built system are similar to those of the X-band portion of the ERIM SAR system, with

*ERIM: Environmental Research Institute of Michigan

the exception that the swath width is 18.5 km. The Jet Propulsion Laboratory (JPL) also operates an L-band SAR for gravity wave measurement (Shemdin, 1980a,b). This system has a resolution of approximately 15 m and a swath width of approximately 10 km.

A spaceborne SAR system specifically designed to image ocean gravity waves was launched in June of 1978 as part of the NASA Seasat* satellite (Jordan, 1980). This SAR operated at L-band and produced imagery with a ground resolution of 25 m by 25 m. The Seasat SAR imagery had a swath width of 100 km and lengths of up to a few thousand kilometers.

Theory

Although the SAR wave-imaging mechanism is not completely understood, several theories have been proposed that appear to explain the modulation of the radar backscatter, which leads to the wave patterns observed in SAR images (Raney, 1971; Elachi and Brown, 1977; Raney and Shuchman, 1978; Alpers and Rufenach, 1979; Harger, 1981; Valenzuela, 1980; Jain, 1978; Shuchman et al., 1981).

The fundamental backscatter mechanism is believed to be Bragg scattering (Wright, 1966); that is, transmitted radar energy with wavenumber K interacts in a resonant or constructive interference fashion with ocean surface waves with wavenumber K_w such that

$$K_w = 2K \sin \theta$$

where $K_w = 2\pi/L$ and $K = 2\pi/\lambda$ are the wavenumbers; L and λ are the wavelengths, respectively, of the ocean wave and the radar; and θ is the incident angle. For the X- (3.2 cm) and L-band (23.5 cm) SAR considered in this study, with a nominal incidence angle of 45°, the equation leads to Bragg water waves of 2 and 17 cm (for the X- and L-bands, respectively). These correspond to the capillary and ultra-gravity wavelength regions which are typically abundant in the presence of wind fields of low to moderate strength.

In general, three mechanisms contribute to wave patterns observed on SAR imagery: 1) tilt modulation, 2) hydrodynamic modulation, and 3) velocity bunching effects. Tilt modulation refers to periodic variation in the local incident angle caused by the long gravity waves. As the incident angle changes, it modulates the cross-section of the surface that backscatters the microwaves.

Hydrodynamic modulation, as reported by many investigators (Alpers et al., 1981; Alpers and Hasselmann, 1978; Phillips, 1981), refers to straining of the small ocean Bragg waves due to divergence of the surface velocity field due to the long gravity waves. This straining can be considered as a modulation of the height of the Bragg ocean wave.

---

*The entire Seasat satellite system suffered a catastrophic power loss approximately 100 days after launch.

It has been suggested by Phillips (1981) and several others that the short capillary and ultra-gravity waves are modulated by the longer gravity waves. Phillips suggests that the gravity waves compress the small waves and increase their height in the crest region of the gravity wave, and likewise, elongate the shorter waves and decrease their height in the trough region. This compression and expansion is thought to result from the straining of the shorter waves by the orbital velocity of the gravity wave (Wright et al., 1980; Alpers and Rufenach, 1979).

The greater the compression and expansion of these small wave structures, the higher the contrast on the SAR imagery, as compression and expansion cause certain portions of the long wave to contain a higher amplitude of Bragg (resonant) scatterers than other parts of the wave, leading to a modulated image that closely corresponds to the prevalent gravity wave field.

The velocity bunching effect refers to a periodic azimuthal target displacement on the imagery. This displacement (the well-known "train off the track" phenomenon) is caused by a radial component (parallel to the radar line of sight) of the orbital motion of the long gravity waves (Alpers et al., 1981; Shuchman et al., 1981; Vesecky and Stewart, 1982; Raney, 1980; Harger, 1981).

Tilt and hydrodynamic modulation are maximum for range-traveling waves and minimum for azimuth-traveling waves. The velocity bunching effect is maximum for waves traveling at approximately 45^{o} to the range direction.

Synthetic aperture radars are sensitive to velocity components present in the imaged scene. Effects of wave motions present in SAR imagery may include: 1) image displacement, smearing and loss of focus in the azimuth direction; and 2) loss of focus in the range direction. Some of these effects can be removed during processing of the SAR signal histories by making appropriate adjustments to the processor. The effects that cannot be removed during processing may reduce the detectability of gravity waves, and can also influence the wave spectral estimates obtained from SAR wave data.

When using a SAR system to image moving targets such as ocean waves, unique problems occur in correlating the signal data. Because moving targets perturb the Doppler frequencies, and hence the phase histories recorded by the signal receiver, conventional processing of these signal histories produces images of the waves that are defocused relative to a stationary target. Defocusing by the alongtrack (azimuth) velocity of the moving ocean waves can be refocused by re-adjusting the azimuth (cylindrical) focus by an amount proportional to the relative velocity of the wave train with respect to the SAR platform velocity.

Similarly, the radial motion of a moving ocean wave imaged by a SAR will also perturb the signal history of a scatterer. Radial wave velocity (motion toward or away from the radar look direction) produces an apparent tilt to the phase history as well as azimuthal shift in the image. Essentially, the scatterer history shifts across the signal record. This is referred to as "range walk" and can be compensated for by a rotation of the cylindrical optics in the processing of the signal histories. The azimuthal image shift is not correctable.

A number of investigators (Shuchman, 1981; Shuchman et al., 1979; Jain, 1978; Shuchman and Zelenka, 1978) designed and evaluated algorithms to enhance SAR-imaged gravity waves through focusing (i.e., accounting for water-wave motion). The investigators generally agree that azimuth- and range-traveling waves can be better detected, respectively, by adjustment of focal distance and by rotation of the cylindrical telescope in the SAR processor. Enhancement of ocean waves has been successfully attempted using these techniques on JPL's L-band and ERIM's X- and L-band data (Jain, 1978; Kasischke et al., 1979).

The importance of the defocusing effect owing to azimuth and range wave motion is twofold. First, it can be used to determine the direction of ocean wave propagation. Second, it can be used to make a rough estimate of the phase velocity associated with these waves.

Analysis Techniques to Extract Gravity Wave Information from SAR Data

It should be noted that SAR-derived spectral estimates of water gravity waves are wavenumber directional spectra of the radar return intensity. The spectral estimates obtained do not represent wave-height information, at least not in an easily extracted form. The modulation transfer function (i.e., SAR gravity-wave-imaging mechanism) is not yet totally understood. The determination of this transfer function, as well as determination of wave height using SAR data, will be a major scientific advancement. It will then be possible to use SAR gravity wave data to obtain power spectral density estimates of the sea surface.

There are four recognized techniques for extracting estimates of wave period and direction of the dominant gravity wave from SAR data. These are two-dimensional Fourier transforms, both optical and digital, a semi-causal technique, and a new one-step spectral estimation routine that extracts the wavenumber directly from the SAR signal histories.

By passing a monochromatic, collimated beam of light through the film image of the gravity waves imaged by the SAR, a two-dimensional optical Fourier transform (OFT) of the image is created (Barber, 1949; Shuchman et al., 1977). If a digital image is made, the same process can be accomplished on a computer by taking a fast Fourier transform (FFT) of the data (Shuchman et al., 1979). Producing an FFT has the advantage over an OFT of allowing distributional wave spectra, as a function of wave frequency or direction, to be generated in addition to the dominant wavelength and direction. Figure 1 presents an example of actual wave images from the Seasat SAR and the resulting OFT and FFT generated from the data.

A new two-dimensional spectral-estimation algorithm related to maximum entropy, called the semi-causal model (Jain and Ranganath, 1978), has been applied to SAR imagery of ocean waves (Jackson and Shuchman, 1982). The spectral estimates generated with this technique were compared to FFT-derived estimates of identical data sets and reference functions. Results indicate the semi-causal model can

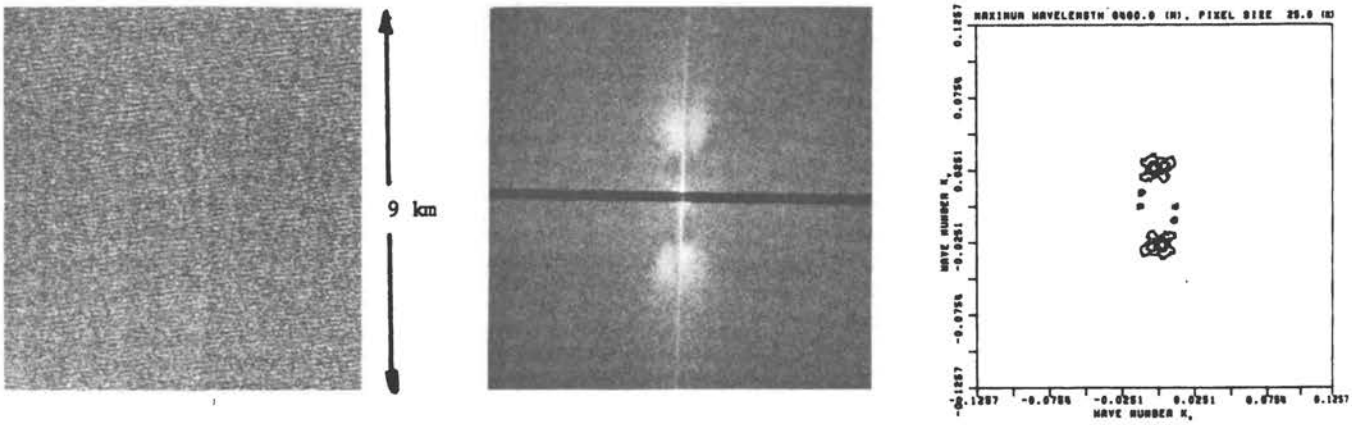

Figure 1 Seasat SAR image of ocean gravity waves and their resultant two-dimensional Fourier transforms (Seasat Rev. 762, 19 August 1978)

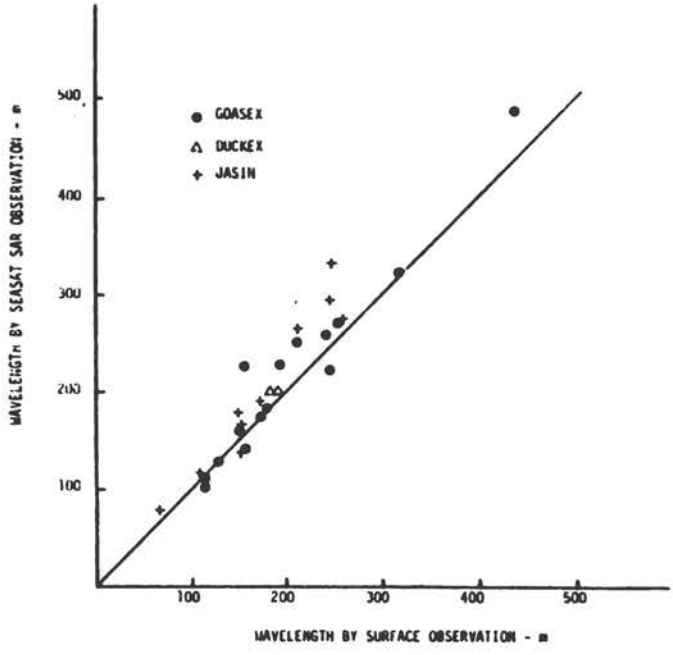

Figure 2 Plot of wavelength, SAR versus sea truth, for L-band Seasat data*

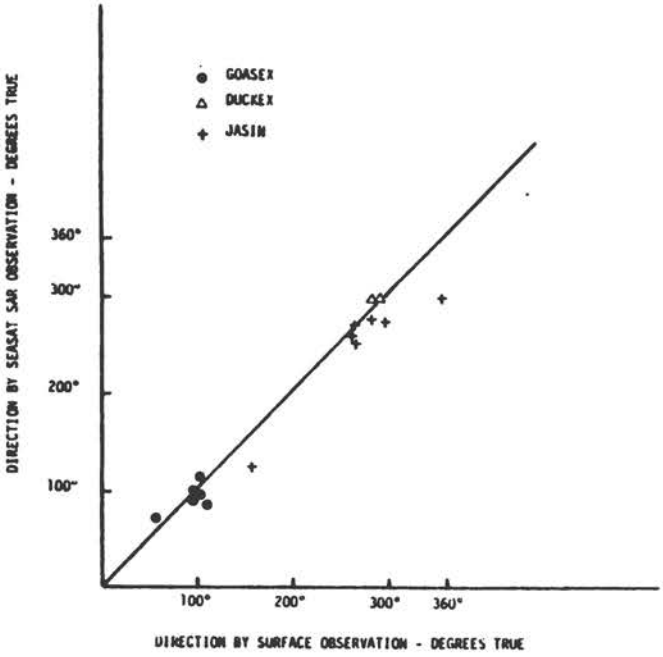

Figure 3 Plot of wave direction, SAR versus sea truth, for L-band Seasat data*

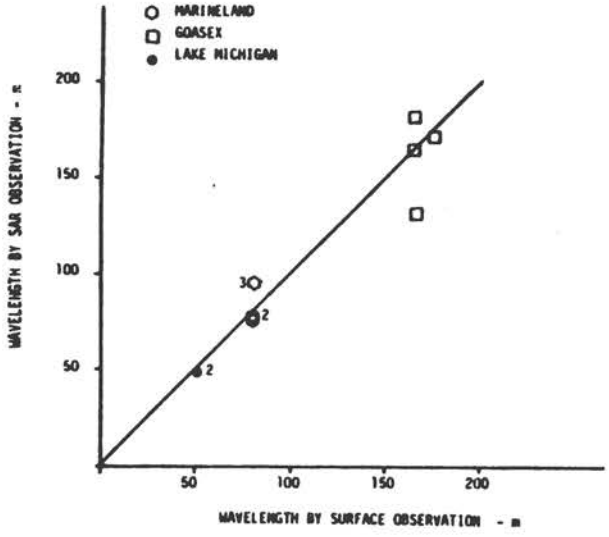

Figure 4 Plot of wavelength, SAR versus sea truth, for X-band aircraft data

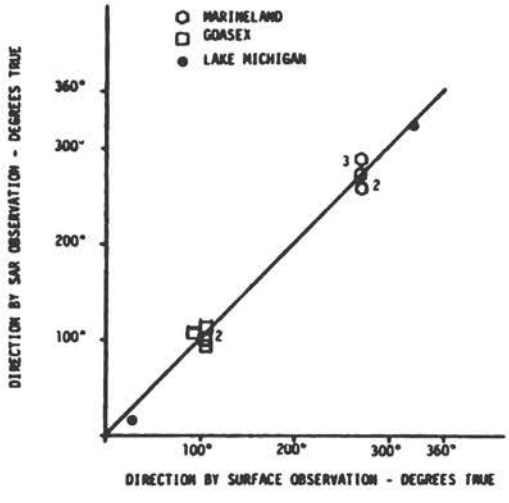

Figure 5 Plot of wave direction, SAR versus sea truth, for X-band aircraft data

*SOURCE: J. F. Vesecky and R. H. Stewart (1982), "The Observation of Ocean Surface Phenomena Using Imagery from the Seasat Synthetic Aperture Radar--An Assessment," J. Geophys. Res., 87: 3397-3430.

successfully produce spectral estimates of truncated data sets (i.e., 1-2 wave cycles). However, as with one-dimensional maximum entropy, the two-dimensional semi-causal model is sensitive to the autoregressive order and to noise, and exhibits spectral splitting in some cases.

A new technique has been proposed by Hasselmann (1980) to extract spectral wave information from SAR. Hasselmann has derived a simple method for determining the two-dimensional surface-image spectrum from the return signal of a SAR without explicitly forming an image. This algorithm, called a signal-image Fourier transform (SIFT), has recently been programmed at ERIM, and is being tested and evaluated using Seasat SAR data.

Recent investigations have explored several possible methods of measuring wave height from SAR through detailed examination of various system and image parameters. Jain et al. (1982) showed that speckle correlation techniques applied to SAR data are a possible means of obtaining wave height. Harger (1982) showed that phase information in the SAR-recorded signals can be related to wave height. Thomas (1982) statistically correlated the image contrast in digitally processed Seasat SAR wave data to wave height. Although preliminary results are promising, each of the methods is still considered experimental.

SAR Versus Sea-Truth Spectral Comparisons

A series of experiments has been carried out over the past seven years to demonstrate that SAR can be used to determine the wavelength and direction of gravity waves. Among these experiments are Marineland, West Coast (Shemdin, 1980a,b); DUCKEX (Mattie et al., 1980); GOASEX (Gonzalez et al., 1981); JASIN (Allan and Guymer, 1980); MARSEN (Anonymous, 1980); and ARSLOE (Baer, 1981).

Figure 2 (after Vesecky and Stewart, 1982) is a scatterplot of ocean wavelength information obtained from the Seasat SAR compared to *in situ* ocean wavelength sea-truth data obtained from a pitch-and-roll buoy. Figure 3 (after Vesecky and Stewart, 1982) is the direction of wave propagation obtained from the Seasat SAR, again compared to sea-truth measurements. Based on these data, Seasat SAR estimates of wavelength are biased slightly high; the average error is about 12 percent. For wave direction, there appears to be no significant bias; the average error is about 15°. The Seasat SAR wave analysis indicates that dominant wavelength and direction can be measured by the Seasat SAR, provided the waves in question are evident in the SAR image (Vesecky et al., 1981). Directional wave information provided by a SAR has a 180° ambiguity, but selective Doppler processing, as reported earlier (Shuchman and Zelenka, 1978), can resolve it. The data included in Figures 2 and 3 represent significant wave heights in the 1 m to 5 m range. Ocean wavelengths shorter than 100 m in length were not observed by the Seasat SAR. The wind speed for all the observations mentioned exceeded 3 m/s.

Figures 4-7 are scatterplots of SAR-derived estimates of wavelength and direction versus sea truth for X- and L-band data of Marineland, GOASEX (aircraft), and Lake Michigan experiments. Neither wavelength nor directional information appears biased: accuracies are about 13 percent and 10 percent, respectively.

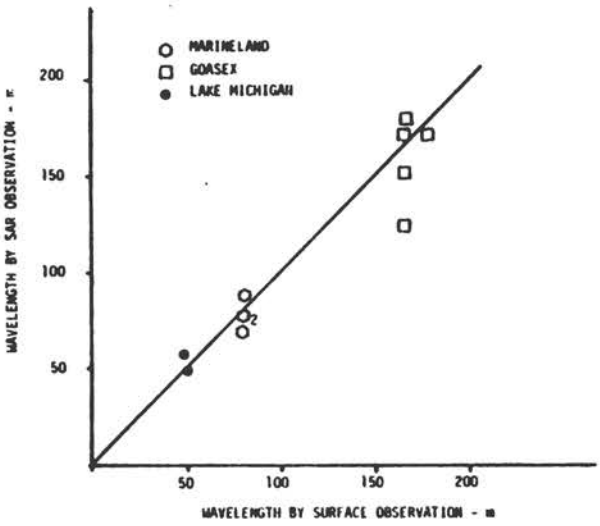

Figure 6 Plot of wavelength, SAR versus sea truth, for L-band aircraft data

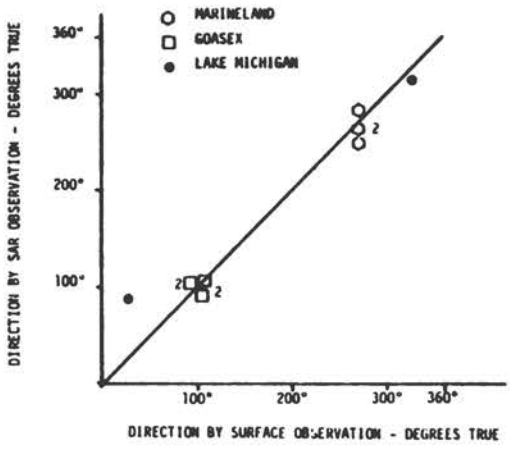

Figure 7 Plot of wave direction, SAR versus sea truth, for L-band aircraft data

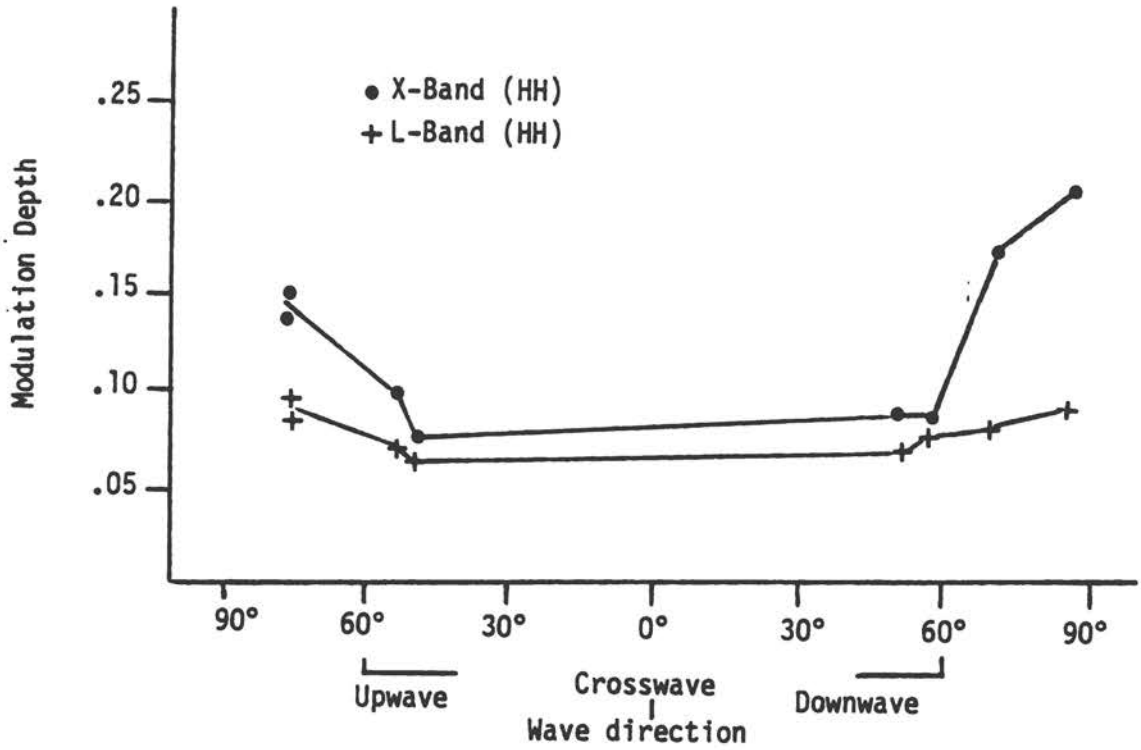

Figure 8 Modulation depth at X-band and L-band as function of the direction of wave propagation

Determination of Wave Refraction and Long-Period Gravity Waves

Recently completed work by Shuchman and Kasischke (1981) has revealed that SAR imagery can be used to document refraction of gravity waves as they enter shallow coastal waters. Images of waves approaching Cape Hatteras, North Carolina (from the Seasat SAR), were analyzed for measurements of wave direction and length. These compared favorably to those computed by classical wave-refraction techniques. The correlation coefficients of SAR-derived and model-derived parameters were 0.76 for wavelength and 0.55 for wave direction (significant at $\rho = 0.99$). Recent investigations (Meadows et al., 1982a) indicate that the correlations can be improved significantly by taking into account the modifying effects on gravity waves of traversing the Gulf Stream.

Additional studies by Schwab et al. (1980) and Shuchman and Meadows (1980) have shown that aircraft SAR directional wave spectra approaching the Lake Michigan shoreline do correlate with predicted wave refraction.

SAR data have also been demonstrated to be capable of discriminating long-period internal waves off the coast of southern California (Apel, 1981) as well as in every major ocean basin imaged by Seasat. Recent work by Meadows et al. (1982b) has demonstrated the ability of SAR X-band data to successfully image low-amplitude, long-period signals. The signals appear to correspond to a "surf beat" generated by the incident wind-wave field.

Limitations of SAR in Detecting Gravity Waves

There are limits to using a SAR to image gravity waves that are still being defined. An example is the recent JASIN experiment during which the Seasat SAR successfully imaged gravity waves in 13 of 18 possible opportunities (Vesecky et al., 1982). A study of the sea-truth data for those occasions when the Seasat failed to image gravity waves revealed that one of two conditions prevailed: either the waves had a very low significant wave height ($H_{1/3} < 1.3$ m), or the waves were traveling in a direction close to azimuth with respect to the radar line of sight. Additionally, wind speed and direction with respect to the gravity wave appeared to be influencing factors. Kasischke and Shuchman (1981) found a significant linear correlation between wave contrast (or wave detectability) on the SAR data and wave height. Earlier studies by Teleki et al. (1978) revealed that for X-band SAR data (collected by an aircraft-mounted SAR), gravity waves were more clearly visible when the waves were traveling in a range direction with respect to the radar line of sight.

Work has also been carried out to determine the sensitivity of various radar parameters to the discrimination of gravity waves. The important radar parameters include the radar wavelength, SAR platform velocity, radar look direction, polarization, and angle of incidence. Working with Marineland data, Teleki et al. (1978) concluded that optimum wave images result when the radar is looking primarily upwave

or downwave; that is, when waves propagate toward or away from the aircraft in the range direction. Figure 8 (after Teleki et al., 1978) is a graph of modulation depth (wave crest-to-trough contrast) versus radar look direction for X- and L-band airborne SAR data collected at Marineland. Observe in Figure 8 that when the SAR is looking upwave or downwave (i.e., when the SAR line of sight is perpendicular to the wave crests), higher contrast or more visible waves result. It should be noted that the significant wave height is approximately 1.5 m for the 8 s swell presented in Figure 8. Range-traveling waves are more clearly discernible in SAR imagery because in the range direction, the SAR uses a train of very short pulses. Therefore, waves traveling in range appear quasi-stationary relative to the sampling time. Differences in the modulation depth of range-traveling waves (Figure 8) also indicate that better-quality wave images can be generated with X- than with L-band data. Consequently, wave spectral peaks derived from X-band images can usually be more accurately defined than those from L-band images.

A possible explanation for the higher quality of X-band imagery was given by Shuchman and Zelenka (1978), who suggested that X-band data have a greater depth of focus than L-band data; therefore, the waves moving in the azimuth direction are not appreciably defocused, as commonly occurs in L-band images of comparable resolution. The X-band also incorporates a shorter synthetic aperture length or integration time than L-band, hence reducing motion errors.

A further X- and L-band comparison is given in Figure 9. Figure 9 represents a two-dimensional fast Fourier transform (FFT) of simultaneously obtained X- and L-band SAR data from GOASEX. The data, all collected within 30 minutes, represent a 10.2 s swell with a 2.5 m significant wave height. Note from the figure that for this higher wave height and longer ocean wavelength, SAR imaging of the gravity waves is less sensitive to frequency and radar look direction (compared to the Marineland data). Figure 10 represents one-dimensional directional distributions (180^{o}) of the relative magnitude of energy at the dominant wavenumber of the data presented in Figure 9. Also plotted are the wavenumbers immediately above and below this peak value. Figure 10 indicates there is no significant change in the directional spectral width of the six SAR-derived ocean spectra.

Summary and Recommendations

This paper presents evidence that both aircraft and spaceborne SARs have the ability to detect the wavelength and direction of gravity waves. It should be mentioned that the spectral estimates presented are wavenumber and directional spectra of the radar return intensity. The data do not represent wave-height information in a direct sense. SAR intensities (i.e., crest-to-trough modulation) have been successfully correlated to wave heights, but the exact mathematical modulation transfer function (i.e., SAR gravity-wave-imaging mechanism) is not totally understood. Obviously, a mathematical expression describing the SAR imaging mechanism of ocean waves needs to be developed.

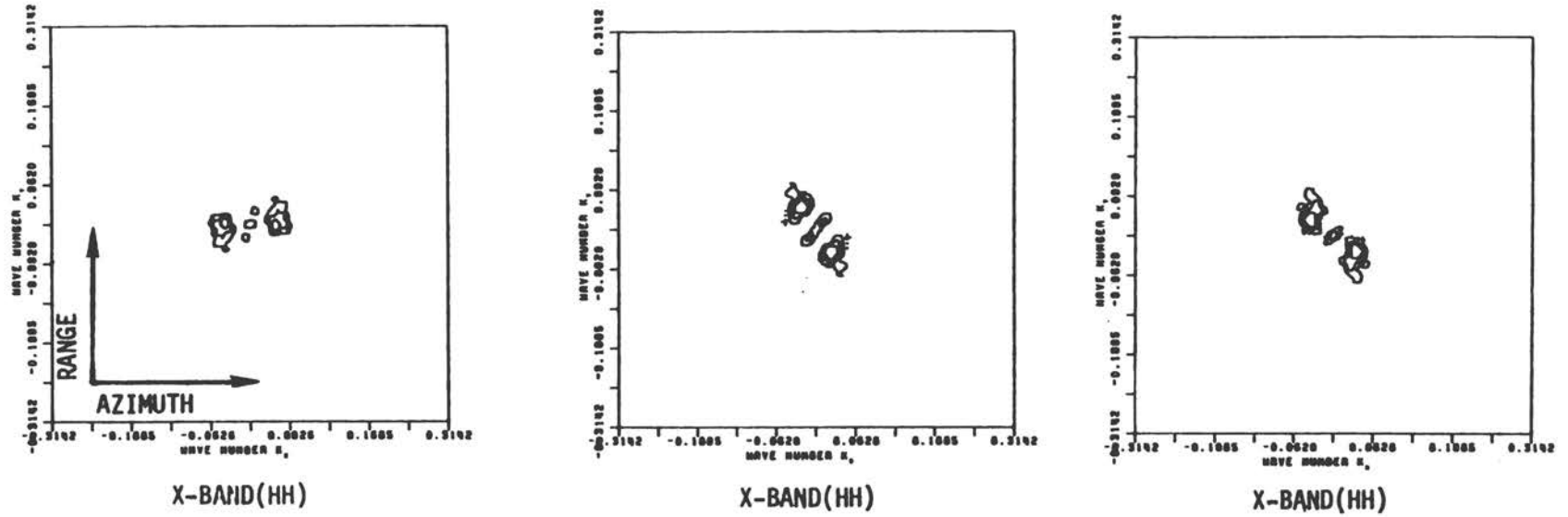

NOTE: Each vertical pair is simultaneously obtained.

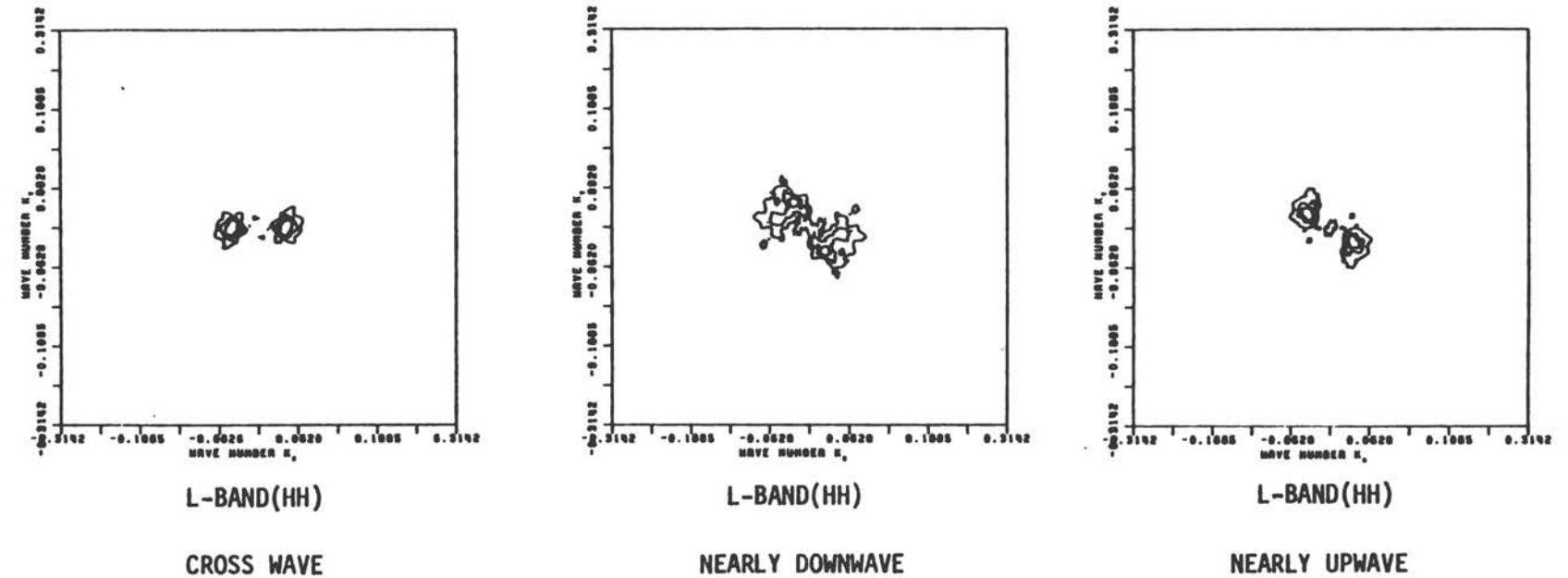

Figure 9 Two-dimensional fast Fourier transforms (FFTs) of simultaneously collected X- and L-band (HH) SAR wave data from GOASEX (September 23, 1978)

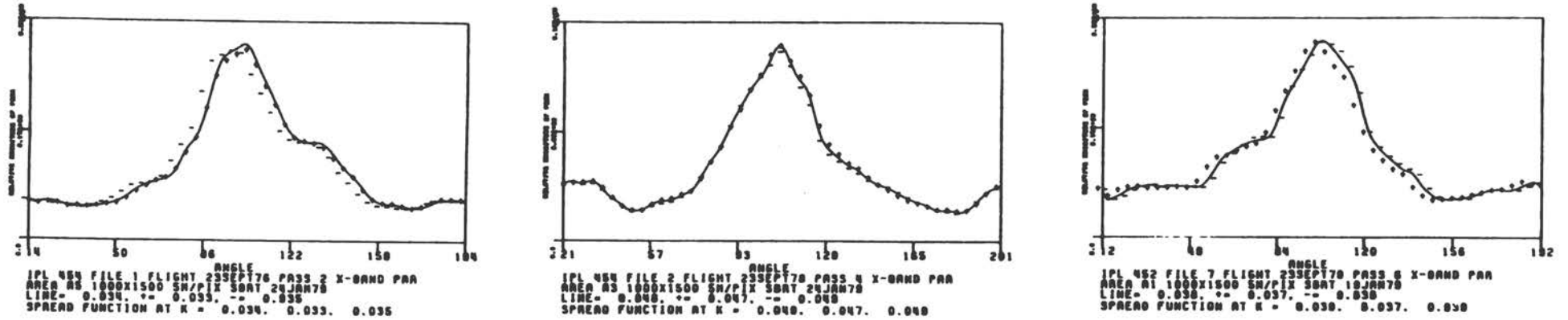

NOTE: Each vertical pair is simultaneously obtained.

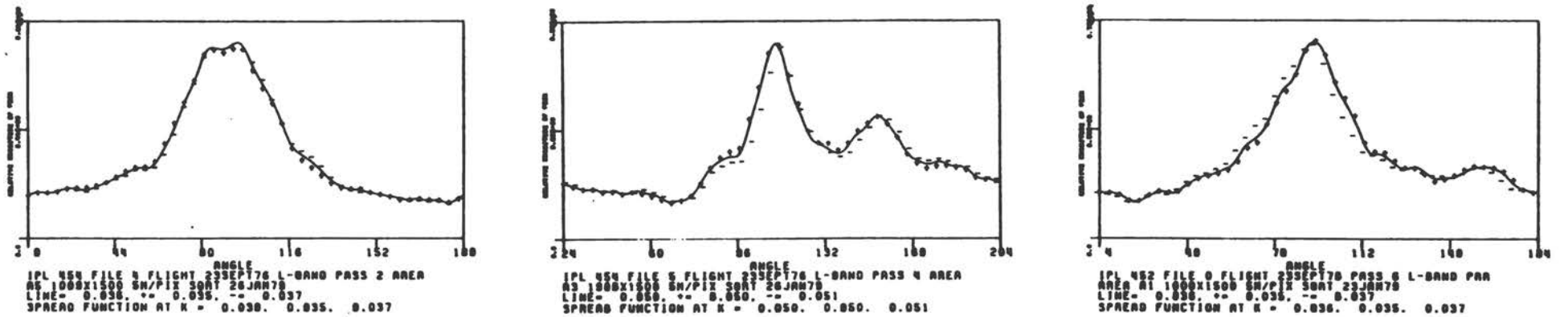

Figure 10 One-dimensional directional distributions (180^{o}) of FFTs presented in Figure 9

When ocean waves are visible in the SAR imagery, the imagery generally represents the dominant wavelength and direction indicated by in situ sea truth. The accuracy of the SAR estimate of dominant wavelength is typically within 15 percent, and the direction of propagation within about 12°.

The ability of SAR to image gravity waves successfully depends on parameters of the physical environment as well as parameters of the SAR system. Generally, waves propagating either toward or away from the radar line of sight are most easily detected by the SAR.

More research is needed exploring the use of SAR to detect wave height so that true power spectral density can be obtained. The spectrum of SAR intensity is not now being fully used. The spectrum shape as reported by McLeish et al. (1980) and Vesecky et al. (1981) more closely resembles a wave-height spectrum than a slope spectrum. A mathematical expression for the SAR imaging mechanism would be quite useful in better explaining the SAR-derived ocean surface wave spectrum.

SARs hold promise for remote sensing of dominant ocean gravity waves and the direction of their propagation throughout the ocean basins. SARs now have a prohibitively large data rate when operated from satellites. Techniques need to be explored to lower these data rates, yet still obtain the required geophysical information. An example of such a technique is Hasselmann's SIFT algorithm.

Acknowledgments

The ERIM SAR ocean wave work reported in this paper was supported by ONR Contract N00014-76-C-1048. The ONR technical monitor is Hans Dolezalek.

References

Allan, T. D. and T. H. Guymer (1980), "Seasat and JASIN," Int. J. Remote Sensing, 1: 261-267.

Alpers, W. E. and K. Hasselmann (1978), "The Two-Frequency Technique for Measuring Ocean Wave Spectra from an Airplane or Satellite," Boundary-Layer Meteorol., 13: 215-230.

Alpers, W. E., D. B. Ross, and C. L. Rufenach (1981), "On the Detectability of Ocean Surface Waves by Real and Synthetic Aperture Radar," J. Geophys. Res., 86: 6481-6498.

Alpers, W. E. and C. L. Rufenach (1979), "The Effect of Orbit Motions on Synthetic Aperture Radar Imagery of Ocean Waves," IEEE Trans., AP-27: 685-690.

Anonymous (1980), "MARSEN Data Analysis and Research Plan," Pasadena, California.

Apel, J. (1981), "Nonlinear Features of Internal Waves as Derived from the Seasat Imaging Radar," Oceanography from Space, J. F. R. Gower, ed. (New York: Plenum Press), pp. 525-533.

Ausherman, D. A. (1980), "Digital versus Optical Techniques in Synthetic Aperture Radar (SAR) Data Processing," Optical Eng., 19: 157-167.

Baer, L. (1981), "Informal Proceedings of the Atlantic Remote Sensing Land-Ocean Experiment Data and Analysis Workshop," Virginia Beach, Virginia.

Barber, N. F. (1949), "A Diffraction Analysis of a Photograph of the Sea," Nature, 164: 485.

Brown, W. J. and L. Porcello (1969), "An Introduction to Synthetic Aperture Radar," IEEE Spectrum, 6: 52-66.

Elachi, C. and W. E. Brown (1977), "Models of Radar Imaging of the Ocean Surface Waves," IEEE Trans., AP-25: 84-95.

Gonzalez, F. I., R. A. Shuchman, D. B. Ross, C. L. Rufenach, and J. F. R. Gower (1981), "Synthetic Aperture Radar Wave Observations During GOASEX," Oceanography from Space, J. F. R. Gower, ed. (New York: Plenum Press), pp. 511-523.

Harger, R. O. (1970), Synthetic Aperture Radar Systems: Theory and Design (New York: Academic Press).

Harger, R. O. (1981), "SAR Ocean Imaging Mechanisms," Spaceborne Synthetic Aperture Radar for Oceanography, R. C. Beal, P. S. DeLeonibus, and I. Katz, eds. (Baltimore: The Johns Hopkins University Press), pp. 41-52.

Harger, R. O. (1982), "A Sea Surface Height Estimator Using SAR Complex Imagery," IEEE J. Oceanic Eng., in press.

Hasselmann, K. (1980), "A Simple Algorithm for the Direct Extraction of the Two-Dimensional Surface Image Spectrum from Return Signal of a Synthetic Aperture Radar," Int. J. Remote Sensing, 1: 219-240.

Jackson, P. L. and R. A. Shuchman (1982), "High Resolution Spectral Estimates of SAR Ocean Wave Imagery," J. Geophys. Res., in press.

Jain, A. (1978), "Focusing Effects in Synthetic Aperture Radar Imaging of Ocean Waves," J. Appl. Phys., 15: 323-333.

Jain, A., G. Medlin, and C. Wu (1982), "Ocean Wave Height Measurement with Seasat SAR Using Speckle Diversity," IEEE J. Oceanic Eng., OE-7: 103-107.

Jain, A. K. and S. Ranganath (1978), "Two-Dimensional Spectral Estimation," Proc. of the RADC Spectrum Estimation Workshop, pp. 151-157.

Jordan, R. L. (1980), "The Seasat-A Synthetic Aperture Radar System, IEEE J. Oceanic Eng., OE-5: 154-164.

Kasischke, E. S., A. Klooster, and R. A. Shuchman (1979), "Verification of Synthetic Aperture Radar Focusing Algorithms," Proc. Thirteenth Int. Symp. Remote Sensing Environ., Ann Arbor, Michigan, pp. 1077-1092.

Kasischke, E. S. and R. A. Shuchman (1981), "The Use of Wave Contrast Measurements in SAR/Gravity Wave Models," Proc. Fifteenth Int. Symp. Remote Sensing Environ., Ann Arbor, Michigan, pp. 1187-1206.

Kozma, A., E. N. Leith, and N. G. Masey (1972), "Tilted Plane Optical Processor," Applied Optics, 11: 1766.

Mattie, M. G., D. E. Lichy, and R. C. Beal (1980), "Seasat Detection of Waves, Currents and Inlet Discharge," Int. J. Remote Sensing, 1: 377-398.

McLeish, W., D. Ross, R. A. Shuchman, P. G. Teleki, S. V. Hsiao, O. H. Shemdin, and W. E. Brown (1980), "Synthetic Aperture Radar Imaging of Ocean Waves: Comparison with Wave Measurements," J. Geophys. Res., 85: 5003-5011.

Meadows, G. A., R. A. Shuchman, Y. S. Tseng, and E. S. Kasischke (1982a), "The Observation of Gravity Wave-Current Interactions Using Seasat Synthetic Aperture Radar," submitted to J. Geophys. Res.

Meadows, G. A., R. A. Shuchman, and J. D. Lyden (1982b), "Analysis of Remotely Sensed Long-Period Wave Motions," J. Geophys. Res., 87: 5731-5740.

Phillips, O. M. (1981), "The Structure of Short Gravity Waves on the Ocean Surface," Spaceborne Synthetic Aperture Radar for Oceanography, R. C. Beal, P. S. DeLeonibus, and I. Katz, eds. (Baltimore: The Johns Hopkins University Press), pp. 24-31.

Raney, R. K. (1971), "Synthetic Aperture Imaging Radar and Moving Targets," IEEE Trans. Aerospace Elect. Syst., AES-7: 499-505.

Raney, R. K. (1980), "SAR Response to Partially Coherent Phenomena," IEEE Trans., AP-28: 777-787.

Raney, R. K. and R. A. Shuchman (1978), "SAR Mechanism for Imaging Waves," Proc. Fifth Canadian Symp. on Remote Sensing, Victoria, B. C.

Rawson, R. F., F. Smith, and R. Larson (1975), "The ERIM X- and L-Band Dual Polarized Radar," Proc. IEEE 1975 International Radar Conference, Arlington, Virginia, pp. 505-510.

Schwab, D. J., R. A. Shuchman, and P. L. Liu (1980), "Wind Wave Directions Determined from Synthetic Aperture Radar Imagery and from a Tower in Lake Michigan," J. Geophys. Res., 85: 2059-2064.

Shemdin, O. H. (1980a), "The Marineland Experiment: An Overview," Trans. AGU, 61: 625-626.

Shemdin, O. H. (1980b), "The West Coast Experiment: An Overview," Trans. AGU, 61: 649-651.

Shuchman, R. A. (1981), "Processing Synthetic Aperture Radar Data of Ocean Waves," Oceanography from Space, J. F. R. Gower, ed. (New York: Plenum Press), pp. 477-496.

Shuchman, R. A., P. L. Jackson, and G. B. Feldkamp (1977), "Problems of Imaging Ocean Waves with Synthetic Aperture Radar," ERIM Interim Technical Report No. 124300-1-T, Ann Arbor, Michigan.

Shuchman, R. A. and E. S. Kasischke (1981), "Refraction of Coastal Ocean Waves," Spaceborne Synthetic Aperture Radar for Oceanography, R. C. Beal, P. S. DeLeonibus, and I. Katz, eds. (Baltimore: The Johns Hopkins University Press), pp. 128-135.

Shuchman, R. A., K. H. Knorr, J. C. Dwyer, P. L. Jackson, A. Klooster, and A. L. Maffett (1979), "Imaging Ocean Waves with SAR--A SAR Ocean Wave Algorithm Development," ERIM Interim Technical Report No. 124300-5-T, Ann Arbor, Michigan, p. 123.

Shuchman, R. A., A. L. Maffett, and A. Klooster (1981), "Static and Dynamic Modeling of a SAR Imaged Ocean Scene," IEEE J. Oceanic Eng., OE-6: 41-49.

Shuchman, R. A. and G. A. Meadows (1980), "Airborne Synthetic Aperture Radar Observations of Surf Zone Conditions," Geophys. Res. Letters, 7: 857-860.

Shuchman, R. A. and J. S. Zelenka (1978), "Processing of Ocean Wave Data from a Synthetic Aperture Radar," Boundary-Layer Meteorol., 13: 181-191.

Teleki, P. G., R. A. Shuchman, W. E. Brown, Jr., W. McLeish, D. Ross, and M. Mattie (1978), "Ocean Wave Detection and Direction Measurements with Microwave Radars," Oceans '78, IEEE/MTS, pp. 639-648.

Thomas, M. H. B. (1982), "The Estimation of Wave Height from Digitally Processed SAR Imagery," Int. J. Remote Sensing, 3: 63-68.

Valenzuela, G. R. (1980), "An Asymptotic Formulation for SAR Images of the Dynamical Ocean Surface," Radio Science, 15: 105-114.

Vesecky, J. F., H. M. Assal, and R. H. Stewart (1981), "Remote Sensing of Ocean Wave-Height Spectrum Using Synthetic-Aperture-Radar Images," Oceanography from Space, J. F. R. Gower, ed. (New York: Plenum Press), pp. 449-457.

Vesecky, J. F. and R. H. Stewart (1982), "The Observation of Ocean Surface Phenomena Using Imagery from the Seasat Synthetic Aperture Radar--An Assessment," J. Geophys. Res., 87: 3397-3430.

Vesecky, J. F., R. H. Stewart, H. M. Assal, R. A. Shuchman, E. S. Kasischke, and J. D. Lyden (1982), "Gravity Waves, Large-Scale Surface Features and Ships Observed by Seasat During the 1978 JASIN Experiment," 1982 Int. Geoscience and Remote Sensing Digest, Munich, Germany, pp. WP3, 1.1-1.6.

Wright, J. W. (1966), "Backscattering from Capillary Waves with Application to Sea Clutter," IEEE Trans., AP-14: 749-754.

Wright, J. W., W. J. Plant, W. C. Keller, and W. L. Jones (1980), "Ocean Wave-Radar Modulation Transfer Functions from the West Coast Experiment," J. Geophys. Res., 85: 4957-4966.

STATUS OF HF RADARS FOR WAVE-HEIGHT DIRECTIONAL SPECTRAL MEASUREMENTS

Donald E. Barrick[1]

Introduction

This manuscript is a concise review of the status of high-frequency (HF) radars for measuring various descriptors of the ocean wave-height directional spectrum. It is not intended as a historical account of the many developments and contributors to the subject over the past three decades; other reviews serve that purpose (e.g., Barrick, 1978; Barrick and Lipa, 1979a; Georges, 1980). Nor is it meant to develop the theory and techniques of HF radar in sufficient detail for planning HF radar programs; again, other published research papers and reports serve this purpose. Finally, no attempt is made to review every MF/HF experiment performed or analyzed, although several very clever techniques have been tried (e.g., bistatic arrangements, synthetic aperture systems, and balloon-borne antennas); rather, techniques are discussed that appear to have potential for practical, operational ocean monitoring.

The next section reviews very briefly the principles of HF radar sea echo that make it possible to measure the wave-height directional spectrum. The section following discusses the capability and status of sky-wave (over-the-horizon) radar for making wide-area ocean surface measurements. The final section discusses the application of HF ground-wave radars to measuring the wave-height directional spectrum, both for coastal use and for deployment from offshore platforms or ships, and their accuracy. In all cases, the limitations as well as the advantages of HF radars are indicated.

Background Physics

At high frequencies, the highly conducting sea favors vertically polarized electromagnetic waves, in both propagation and scattering. For sky-wave radars, where the energy incident to the ocean from the ionosphere is generally randomly polarized, vertical polarization is selected from the incoming radiation, and scattered back toward the radar. In nonionospheric propagation, as from a coastal radar out to an ocean patch 40 km from shore, vertical polarization is intentionally transmitted and received. This mode is called "ground wave" or "surface wave," in contrast to the sky-wave mode. At high frequencies, vertically polarized surface-wave radiation will propagate a considerable distance beyond the horizon of the mean spherical sea owing to diffraction. As a result, given moderate amounts of transmitted

[1]Wave Propagation Laboratory, National Oceanic and Atmospheric Administration

power (e.g., 100 W average), a coastal backscatter radar at water level can obtain usable sea echo out to a distance of 60 km from shore at a frequency of 25 MHz.

The sea is a strong scatterer of high frequencies; in fact, the backscattered power per unit area from the ocean is generally greater than that for land, even when the land includes mountains, tall buildings, or trees. It is the motion of the ocean wave scatterers, however, that gives the sea echo the unique characteristic that allows extraction of wave-height directional spectra, surface currents, and wind patterns. This unique characteristic is the spectral spread in echo energy due to the Doppler effect of moving targets.

The scattering mechanism itself is the Bragg effect. Only wave trains of a given wavelength (period) and direction of propagation--either singly or in combination--can contribute to the backscattered signal. The strength of the signal is proportional to the heights of the waves in these spectral wave trains. Since the velocity of a wave train is proportional to the square root of its wavelength, however, different wavelength/direction combinations in the wave-height directional spectrum yield their signal echo energy at unique, mathematically determinable positions in the echo spectrum.

To first order, the radar wave is backscattered by two wave trains--or Fourier components of the wave spectrum: wave trains moving toward and away from the radar whose ocean wavelengths are half the radar wavelength. This is shown schematically in Figure 1. These two wave trains produce two sharply peaked spectral echoes symmetrically placed about the transmitter frequency; their amplitudes are proportional to the heights of the wave trains moving toward and away from the radar. At 25 MHz radar frequency, these echoes therefore originate from wave trains whose wavelengths are 6 m. When a current is present, it imparts an additional common velocity to these wave trains, resulting in a further symmetrical shift of the two peaks to one side, as shown in the bottom half of Figure 1. This additional frequency shift, Δf, is directly proportional to the component of current velocity pointing toward the radar, v_{cr}. It is this latter shift, Δf, that has been exploited by HF coastal radars (Barrick et al., 1977) to map surface currents.

The wave-height directional spectrum is extracted from a different part of the echo spectrum, that produced by the simultaneous interaction of two ocean wave trains. The mathematical expression for the echo spectrum in this case is an integral involving the wave-height directional spectrum twice; all of the mathematical factors appearing in this integral are determined from fundamental hydrodynamic and electromagnetic principles, and are completely known. Therefore, this integral equation can be inverted (and has been, with success) to give the wave-height directional spectrum.

Status of Sky-Wave Radars

HF radio signals of frequency less than 25 MHz can be totally reflected from the ionosphere, which is a layer of charged particles whose

effective reflective height (7 MHz and 25 MHz) lies between 100 and 300 km above the earth. Thus, a single reflection from the ionosphere can extend radar surveillance of the ocean to distances of 3000 km from the station.

The ionosphere, however, is a highly variable factor in the radar equation. Its density varies from day to night, summer to winter, with latitude, and in response to solar storms and their resulting emissions. Although average ionospheric conditions can be predicted or measured (by ionospheric soundings), temporal variations of the order of tens of seconds over spatial scales of the order of a few kilometers are largely unpredictable. These unknown variations in the effective reflecting layer produce Doppler spectral distortions in the signal of the same order as the expected variations produced by the sea echo. Therefore, the extraction of useful sea-state and current information is complicated by the ionosphere itself.

A joint research program of the Wave Propagation Laboratory (NOAA) and the Remote Measurement Laboratory (SRI International) has attempted to develop techniques for coping with the ionospheric distortions, and to determine the resulting accuracy of sky-wave radar for wide-area ocean wave measurements. Other countries also have active sky-wave programs for sea-state monitoring. A recent review of sky-wave sea-state radars is offered by Georges (1980).

Sky-wave radars have measured wave height to an accuracy of 3%, dominant (long-wave) direction to an accuracy of 3^{o}, and dominant period to an accuracy of 1.0 s (Lipa et al., 1981). In another situation, sky-wave radars measured wave height to an accuracy of 7%, and measured the five parameters of a nondirectional wave-height directional spectral model: agreement with buoy measurements was quite good (Maresca and Georges, 1980). However, both sets of experiments were conducted under favorable ionospheric conditions. Furthermore, the data were analyzed in a research mode in which echo time series taken in the field were later reduced and interpreted on computers in the laboratory.

Experiments to study the limitations, utility, and accuracy of real-time operation of sky-wave radars began in 1981. Software was developed that allowed the radar operator to scan a large ocean sector (out to 3000 km) at a pre-selected grid of points, in order to map wave height in real time. Preliminary analysis indicates that reasonable and accurate wave heights were mapped over several days as winter storms moved across the North Pacific. An exact assessment of accuracy is difficult to make. The only comparative wave-height information available for most of this wide area was provided by NOAA and Navy wave forecasts, and a few ship reports, both sources that are known to be quite inaccurate. All the general wave patterns recorded agree very well, however, demonstrating that ionospheric conditions can be sufficiently compensated to permit daily, real-time, synoptic maps of wave height, the single most important parameter of the wave-height directional spectrum. Wind direction maps (from sky-wave radar measurements of short wave directions) can also be made available in real time. Future real-time software should allow extraction of other important wave descriptors; it is not now clear, however, whether the entire

wave-height directional spectrum can be routinely measured with sky-wave radar, owing to ionospheric distortions.

Status of Ground-Wave Radars

The physical interaction of HF radar waves with the sea surface is the same for sky-wave radars and ground-wave radars. Therefore, if the distortions imposed on the sky-wave signal by the ionosphere can be removed, the remaining echo for both systems is effectively the same, and the methods of analysis discussed in this section are applicable to either system.

Narrow-Beam Ground-Wave Radars

The fundamental theoretical solutions for first- and second-order sea backscatter at high frequencies assume that a finite patch of ocean surface is viewed from a single, fixed direction (Barrick, 1972a,b, 1978; Barrick and Lipa, 1979a). This is what a narrow-beam radar does: an antenna whose aperture length is many wavelengths forms a beam whose angular width is a few degrees. The effective pulse width at a given time delay after pulse transmission thus defines an approximately rectangular patch of sea surface, whose dimensions typically vary from several kilometers to several tens of kilometers on a side. The requirement that antenna sizes be many wavelengths to form a narrow beam means the physical dimensions of antennas must be hundreds of meters at high frequencies.* Several such systems have been used in the past to obtain ground-wave HF sea echo. Because the mathematical expressions for the back-scattered signal spectrum are most straightforward for narrow-beam geometries, initial investigations of obtaining wave-height directional spectral parameters concentrated on measurements taken from those narrow-beam experiments.

If a given patch of sea can be observed by one radar from only a single direction, then only limited information about wave directional spectra can be obtained for that patch. There is a right-left ambiguity in wave direction about the line of sight. This means that when the directional spectrum is expanded in an angular Fourier series about the look direction to the patch, all odd (i.e., sine) coefficients in the series are indeterminate. Furthermore, some inaccuracy can occur in retrieving the even coefficients when the data are noisy (Lipa and Barrick, 1982). Nonetheless, success at extracting the most important wave directional spectral parameters has been achieved, vindicating the theoretical methods.

*It is possible to circumvent the requirement for large antennas--for example, by synthetically forming a large aperture by driving a receiver along a road several kilometers long (Tyler et al., 1974). While of limited interest for research experiments, the methods are impractical for routine, long-term, operational monitoring.

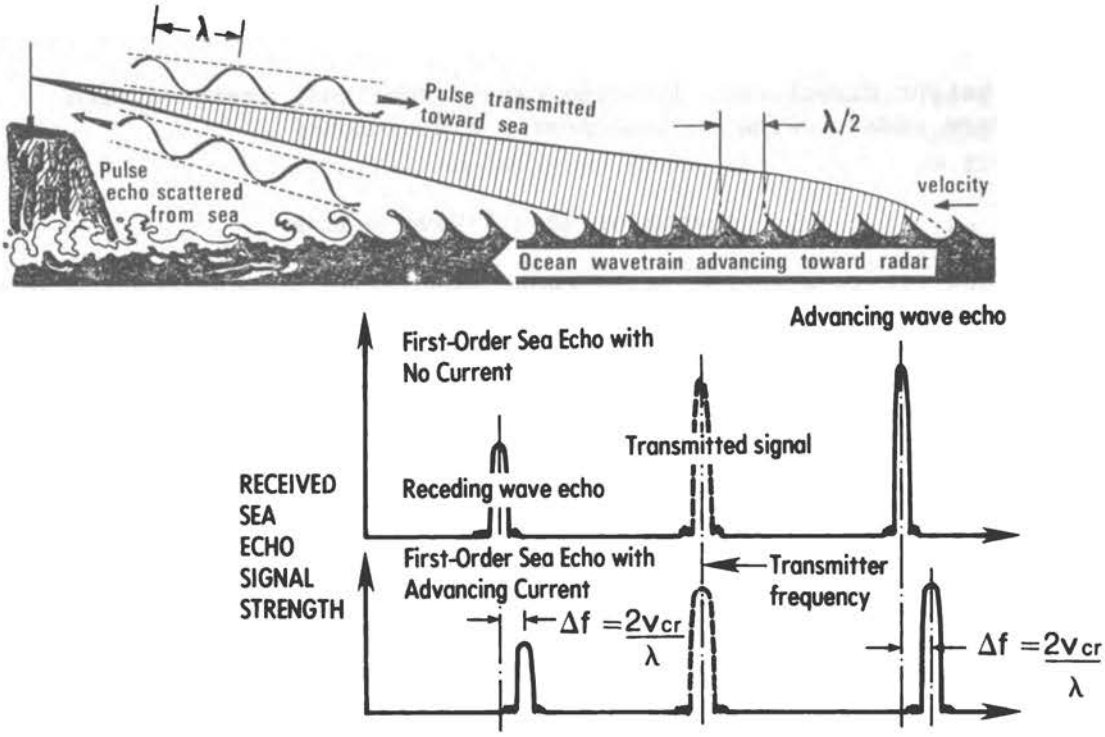

Figure 1 Sketch showing principles of first-order Bragg backscatter from the sea. Upper plot shows positions of echo energy in the signal spectrum from wave trains half the radar wavelength traveling toward and away from the radar. Lower plot shows symmetrical shift of these peaks by a current whose radial speed is v_{cr}.

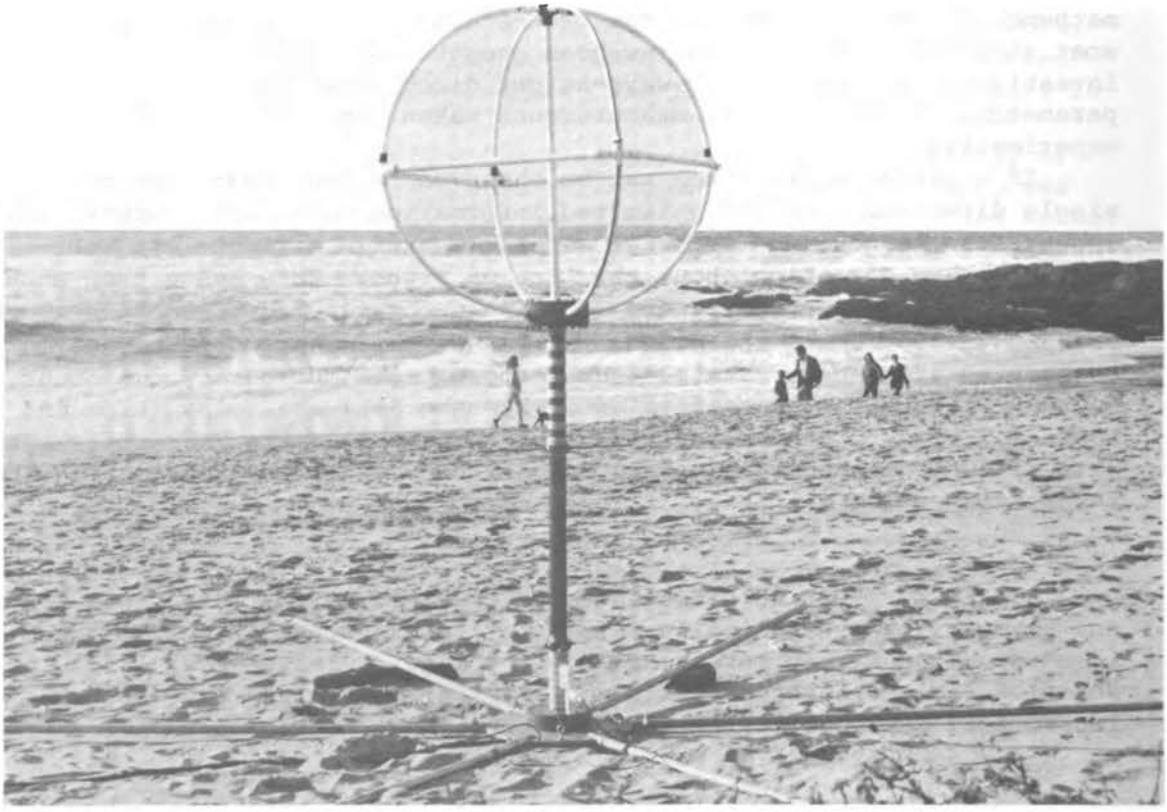

Figure 2 Photograph of compact crossed-loop/monopole antenna system for coastal wave-height directional spectral measurements, as operated at Pescadero, California, during January 1978. The antenna is less than 2 m tall.

Data from three narrow-beam radars have been analyzed and compared to heave-pitch-roll buoy requirements in the scatter area. One set was taken from a series of experiments done at San Clemente Island (off California) by a westward-looking NOAA/Navy/ITS ground-wave facility in 1972. A second was from a northwest-looking ground-wave system operated by Stanford University off Pescadero, California, between 1976 and 1978. The third set is narrow-beam sky-wave radar results from the Wide Aperture Radar Facility in California (owned by SRI International), selected for minimal ionospheric distortions.

Theoretical methods for inverting data from narrow-beam systems were developed by Lipa and Barrick (1980) for wave periods 10 s and greater. In this region, the integral equation is simplified by linearization. These methods were applied to the data from the three experiments by Lipa et al. (1981). The results confirm the theoretical methods, and show, for example, that wave height can be measured to an accuracy of ±5% (rms), wave period to ±0.5 s (rms), and direction within 7° (rms).

Some external means of resolving the left-right directional ambiguity was of course required. Lipa (1978) developed and demonstrated inversion techniques for extracting accurate wave-height directional spectral information (based on the Stanford system) for wave periods down to 3 s, cases for which linearization of the integral equation is not possible.

Broad-Beam, Scanning, Ground-Wave Radars

Ground-wave radars with vertical polarization must have their antennas on the beach, as close to the seawater as possible, in order to achieve maximum distance. The large antenna sizes required for a narrow-beam system, as discussed above, make such systems uneconomical and environmentally unattractive for coastal or offshore sites. The most compact and unobtrusive antenna system that can provide the same angular information for wave spectra as a pitch-roll buoy is the crossed-loop/monopole technique discussed by Barrick and Lipa (1979b). Use of this configuration for both transmitting and receiving reduces the size of the antenna system further, and increases the angular resolution. A picture of such a system, operated at Pescadero, California, in 1978, is shown in Figure 2. Although this antenna system does not mechanically rotate, digital switching of signals among the three antenna elements (under microprocessor control) causes a broad beam to rotate in angle.

An HF radar with a compact antenna system such as this is ideally suited to coastal observations of wave-height directional spectra. In fact, the crossed-loop/monopole technique has been employed in two experiments for directional wave-field measurements: at Pescadero, California, in 1978, and at Duck, North Carolina, in 1980. Operation in coastal waters, however, requires accounting for a number of factors in analysis of the data.

Evaluation of the accuracy of the wave directional spectral measurements using the crossed-loop/monopole coastal HF radar under fetch-limited and current-distorted regimes is not yet completed.

Also, development and evaluation of software for this system for measuring waves with 9 s periods and less are still under way. However, the success so far achieved indicates that the system will be an ideal tool for detailed research investigations of coastal wave processes, and also for routine monitoring of wave directional spectra.

Use of this system from offshore platforms promises to be even simpler for the following reasons: 1) the water in the area is usually deep; 2) fetch variations are rarely present over the small areas of radar coverage; 3) current patterns are uniform over the area covered. Experiments in 1983 will employ the system on an offshore platform to evaluate its performance in this important application.

References

Barrick, D. E. (1972a), "First-Order Theory and Analysis of MF/JF/VHF Scatter from the Sea," IEEE Trans., AP-20: 2-10.

Barrick, D. E. (1972b), "Remote Sensing of Sea State by Radar," Remote Sensing of the Troposphere, V. E. Derr, ed. (Washington, D.C.: U.S. Government Printing Office).

Barrick, D. E. (1978), "HF Radio Oceanography--A Review," Boundary-Layer Meteorol., 13: 23-43.

Barrick, D. E., M. W. Evans, and B. L. Weber (1977), "Ocean Surface Currents Mapped by Radar," Science, 205: 138-144.

Barrick, D. E. and B. J. Lipa (1979a), "Ocean Surface Features Observed by HF Coastal Ground-Wave Radars: A Progress Review," Ocean Wave Climate, M. D. Earle and A. Malahoff, eds. (New York: Plenum Press), pp. 129-152.

Barrick, D. E. and B. J. Lipa (1979b), "A Compact Transportable HF Radar System for Directional Coastal Wave Field Measurements," Ocean Wave Climate, M. D. Earle and A. Malahoff, eds. (New York: Plenum Press), pp. 153-201.

Georges, T. M. (1980), "Progress Toward a Practical Skywave Sea-State Radar," IEEE Trans., AP-28: 751-761.

Lipa, B. J. (1978), "Inversion of Second-Order Radar Echoes from the Sea," J. Geophys. Res., 83: 859-862.

Lipa, B. J. and D. E. Barrick (1980), "Methods for the Extraction of Long-Period Ocean-Wave Parameters from Narrow-Beam HF Radar Sea Echo," Radio Science, 15: 843-853.

Lipa, B. J. and D. E. Barrick (1982), "Simplified Interpretation of Skywave Radar Sea-State Observations," submitted to Radio Science.

Lipa, B. J., D. E. Barrick, and J. W. Maresca, Jr. (1981), "HF Radar Measurements of Long Ocean Waves," J. Geophys. Res., 86: 4089-4102.

Maresca, J. W. and T. M. Georges (1980), "Measuring RMS Wave Height and the Scalar Ocean Wave Spectrum with HF Skywave Radar," J. Geophys. Res., 85: 2759-2771.

Tyler, G. L., C. C. Teague, R. H. Stewart, A. M. Peterson, W. H. Munk, and J. W. Joy (1974), "Wave Directional Spectra from Synthetic Aperture Observations of Radio Scatter," Deep-Sea Res., 21: 989-1016.

AIRCRAFT AND SATELLITE MEASUREMENT OF OCEAN WAVE DIRECTIONAL SPECTRA USING SCANNING-BEAM MICROWAVE RADARS

Frederick C. Jackson,*[1] W. Travis Walton,[1]
and Paul L. Baker[2]

Abstract

A microwave radar technique for remotely measuring the vector wavenumber spectrum of the ocean surface is described. The technique, which employs short-pulse, noncoherent radars in a conical scan mode near vertical incidence, is shown to be suitable for both aircraft and satellite application. The technique has been validated at 10 km aircraft altitude, where we have found excellent agreement between buoy and radar-inferred absolute wave-height spectra.

1. Introduction

For several years, we have been endeavoring to develop a microwave radar technique for measuring ocean wave directional spectra that would be suitable for satellite application. Basically, we have been seeking to define an alternative to the coherent imaging radar approach that was adopted for Seasat, the nation's first oceanographic satellite (Beal et al., 1981). Our motivation has been to find an alternative measurement approach that would at the same time 1) be simpler and less costly, 2) be capable of truly global measurements, and 3) be more accurate.

In this we believe we have been successful. Theoretically, and on the basis of aircraft flight experiments, we have determined that such global-scale satellite measurements are feasible. The measurements can be made with relatively simple, noncoherent short-pulse radars operating in a conical scan mode near vertical incidence, $\theta \sim 10^{\circ}$. No new technological developments are required. Rather, these measurements can be made with existing space-qualified hardware. For example, with some relatively minor modifications such as the addition of a modest-gain scanning antenna, the Seasat altimeter can be adapted to perform these measurements. The measurements are inherently of high resolution spectrally in both wavenumber and direction, and as we shall see, they will be remarkably accurate as well.

A typical satellite measurement geometry is illustrated in Figure 1. For the assumed satellite altitude of 700 km and incidence angle of 10°, the radius of the scan pattern on the ocean surface is approximately 130 km. A 3 rpm antenna rotation rate is selected as a

---

*Presenter

[1]Laboratory for Atmospheric Sciences, NASA Goddard Space Flight Center

[2]Computer Sciences Corporation

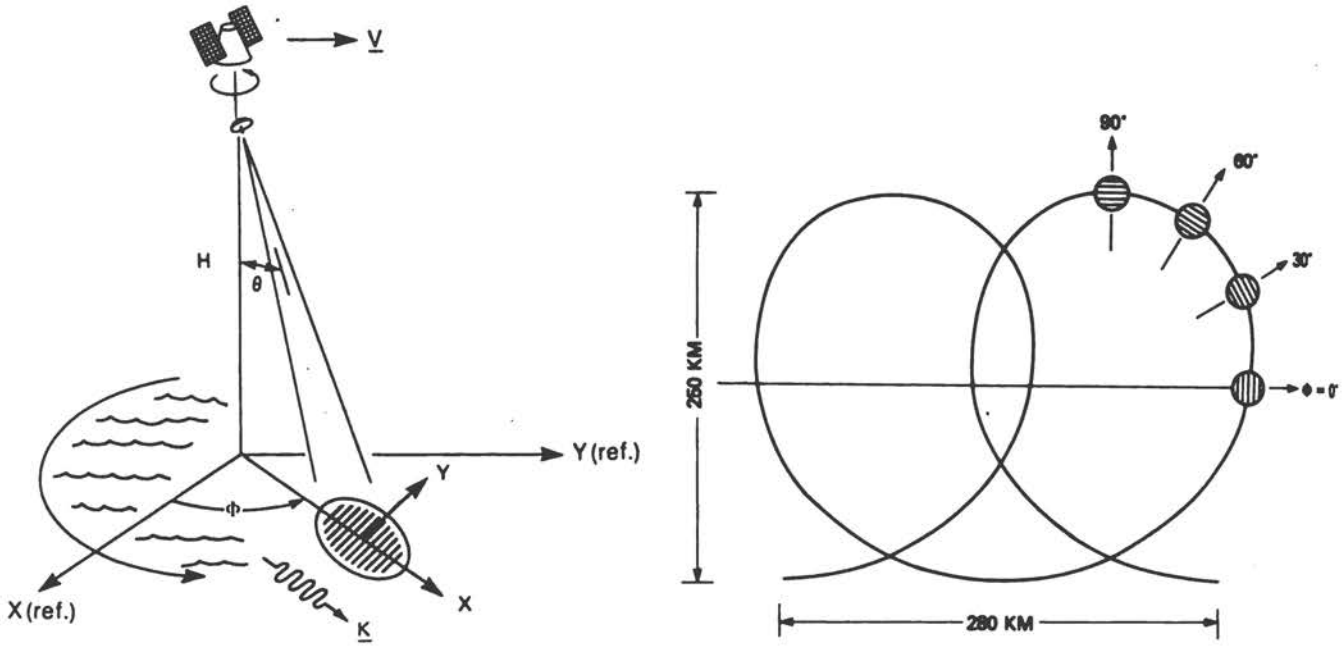

Figure 1 (a) Typical satellite measurement geometry; (b) scan pattern on the ocean surface, 700 km altitude, 10° incidence angle, and 3 rpm scan rate

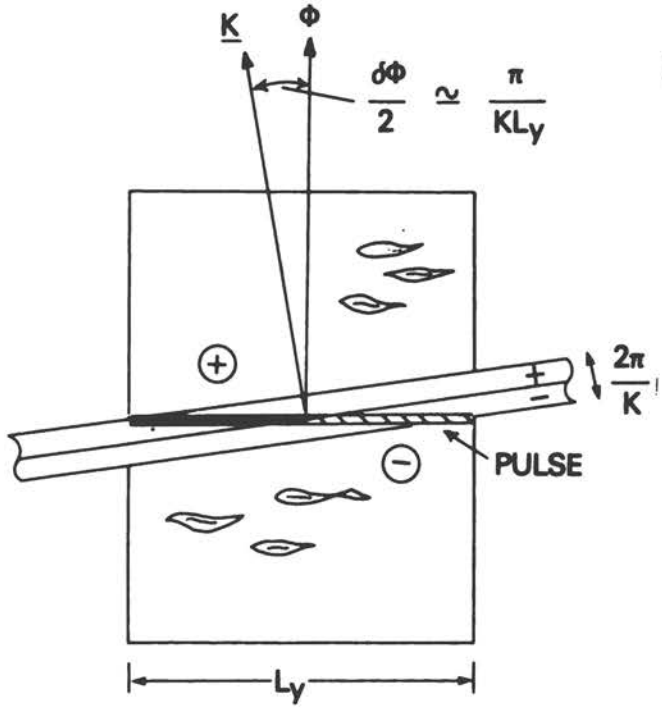

Figure 2 Illustrating directional selectivity by phase-front matching of EM and ocean wave components. For the rectangular illumination pattern illustrated here, the angle of the first null is as indicated.

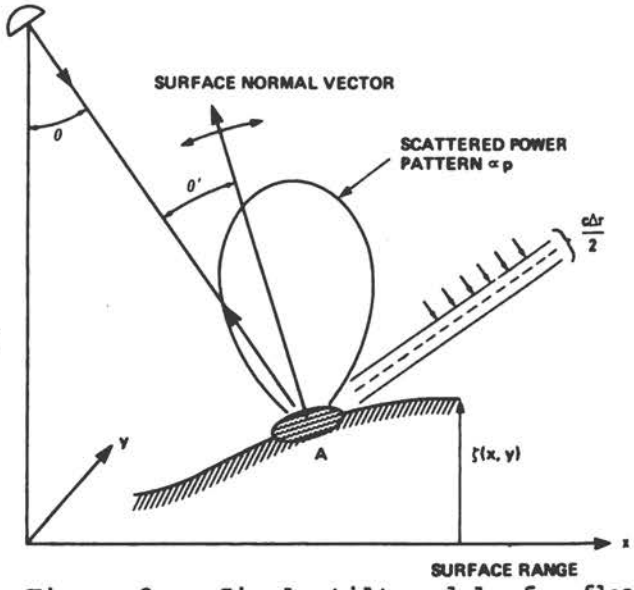

Figure 3 Simple tilt model of reflectivity modulation

reasonable compromise between coverage and integration time requirements. The measurement cells (not to be confused with the instantaneous field of view, or antenna "footprint") are roughly 130 km squares situated one on either side of the subsatellite track. Basically, the measurement product consists of two statistically stable estimates of the polar-symmetric vector wavenumber spectrum, one on either side of the subsatellite track. If less than 180° of look is allowed, then these measurements can be confined to an area considerably smaller than the nominal 130 km square, as is evident from Figure 1.

Although the technique we shall be considering employs short-pulse waveforms, it is not in its most fundamental aspect different from the two-frequency technique investigated theoretically by Alpers and Hasselmann (1978) and experimentally by Johnson et al. (1981). In both techniques the basic measurement principle is the same. This is the directional selectivity that results as a natural consequence of the phase-front matching of electromagnetic and ocean wave components. The choice of waveforms, and the manner of detection, are, however, critical. Jackson (1981)--hereinafter referred to as J--has shown that the narrow-band two-frequency technique has, inherently, a very low signal-to-noise ratio (SNR) compared to the short-pulse technique. Basically, this is because the sea spectrum is relatively broad-band, whereas the two-frequency beat-wave signal is comparatively narrow-band. For large footprint dimensions this results in modulation signal power being detected only in a very narrow spectral band, and consequently, the signal energy is small compared to the fading variance.

Our work differs from that of Alpers and Hasselmann (1978) in another important respect. This is in the choice of incidence angles. Alpers and Hasselmann (1978) were concerned with large-angle measurements, whereas our concern is with small angles of incidence. There are several reasons why we have chosen to study small-angle scatter. First, as should be apparent from the above discussion of the measurement geometry, small angles of incidence are necessary at satellite altitudes in order to keep the scan radius to a minimum. If the nadir angle is too large, the scan pattern on the surface may exceed the scale of homogeneity of the wave field. Second, the reflectivity modulation mechanism in near-vertical backscatter is simpler and more predictable than it is in large-angle backscatter. In the near-vertical, specular backscatter regime, the contrast modulation does not depend on the strong--and essentially unpredictable--hydrodynamic modulation of the short Bragg-diffracting water wave. The modulation mechanism is primarily a geometrical tilting effect, and consequently, it is more amenable to accurate modeling. Another reason for choosing small incidence angles is an obvious one, that the greater cross-section and lower link loss near nadir demand less transmitter power and antenna gain. This is an important consideration in the wide-band measurement approach that we are advocating.

In succeeding sections, we will discuss the three major conceptual elements that constitute the measurement technique, namely, 1) the principle of directional selectivity, 2) the modulation mechanism in near-vertical backscatter, and 3) the use of short-pulse waveforms to detect the range reflectivity modulation. The discussion is intended to provide a basic understanding of the measurement technique and to provide such results and formulas as will be found useful in the analysis of the aircraft data. For a fuller and more detailed theoretical treatment, the reader is referred to J.

2. The Measurement Technique

2.1 The Principle of Directional Selectivity

We are concerned with fairly narrow antenna beams in a high-altitude measurement geometry. The relevant geometry is illustrated in Figure 1. The situation desired is one where 1) the antenna footprint is large compared to the scale of the waves, and 2) the curvature of the wave front is small compared to the directional spread of the waves. Now obviously, if the lateral beam spot dimension is large compared to the scale of the waves, then the waves cannot be resolved in azimuth (short of resorting to synthetic aperture). Rather, the wave contrasts will be averaged laterally across the beam. What is the effect of this lateral averaging? To understand the effect, imagine a Fourier decomposition of the two-dimensional reflectivity field into an angular spectrum of plane contrast waves. (The reflectivity field can be imagined to be that measured by a very high resolution, real aperture, imaging radar looking in the same azimuth direction.) Referring to Figure 2, it is apparent that the effect of the lateral averaging is to eliminate or "cancel out" any plane surface contrast wave that is not aligned with the beam direction. Only those surface waves whose phase fronts are "matched" to the electromagnetic (EM) phase front can survive the lateral averaging. The effect of the broad footprint is then to isolate or resolve surface contrast wave components whose wave vectors $\underline{K} = (K, \Phi)$ are aligned with the beam direction.

The directional resolution is determined by and limited by 1) the finiteness of the beam spot size in azimuth L_y, and 2) the curvature of the wave front within the beam spot. If we assume a Gaussian-shaped azimuth gain pattern,

$$G(y) = \exp\ (-y^2/2L_y^{\,2}) \tag{2.1}$$

then it follows (e.g., from the Fresnel zone solution in J) that the directional resolution $\delta\Phi$, defined as the half-power spectral window width in azimuth, is given by

$$\delta\Phi \sim \delta K_y/K = 2\sqrt{2\ \ln\ 2}\ [(KL_y)^{-2} + (L_y\ \cot\ \theta/2H)^2]^{\frac{1}{2}} \tag{2.2}$$

where H is the altitude. The first and second terms in (2.2) derive from the finite-footprint and wave-front curvature effects, respectively. In our aircraft experiment geometry, $H \sim 10$ km, $\theta \sim 13^\circ$, and $L_y \sim 300$ m (half-power width $L_y^* = 2\sqrt{2 \ln 2}\, L_y \sim 700$ m). For a typical 200 m water wave, we have $\delta\Phi \sim 17^\circ$. In a typical satellite measurement, $H = 700$ km, $\theta = 10^\circ$, and $L_y = 8.5$ km ($L_y^* = 20$ km), in which case $\delta\Phi \sim 5^\circ$.*

2.2 The Reflectivity Modulation in Near-Vertical Backscatter

Near vertical incidence, $\theta \lesssim 15^\circ$, microwave backscatter from the sea occurs by means of quasi-specular reflections from wave facets oriented normal to the radar's line of sight. The average backscatter cross-section σ^o is proportional to the probability density function (pdf) of orthogonal surface slopes satisfying the specular condition for backscatter: $\delta\zeta/\delta x = \tan\theta$; $\delta\zeta/\delta y = 0$. The cross-section is given by (e.g., Valenzuela, 1978)

$$\sigma^o(\theta,\Phi) = \rho\pi \sec^4\theta p(\tan\theta, 0) \qquad (2.3)$$

where p is the slope pdf expressed in the radar's coordinate system, x is the plane of incidence, and ρ is a (diffraction) modified, normal-incidence Fresnel reflectivity (Brown, 1978).

Hydrodynamic modulation is a second-order effect in near-vertical backscatter. Consider that, first, for most microwave frequencies, the most strongly forced waves, the gravity-capillary waves, lie under the diffraction limit--about three EM wavelengths in the horizontal, according to Brown (1978). Thus, they are only weakly sensed, and to the extent that they are, it is via a diffuse diffraction field that can be only very weakly modulated by geometrical tilting. Second, the specular component derives from the entire wave ensemble, including waves on all scales, from the scale of the dominant waves we are seeking to measure down to the scale of the diffraction limit. For this large ensemble of waves, it is reasonable to assume that hydrodynamic forcing and wave-wave interaction effects are of secondary importance. To the extent that hydrodynamic nonlinearities affect the EM modulation, they are to be attributed to the entire wave ensemble rather than a particular water-wave component. Neglecting second-order effects, the surface can be treated as a free-wave superposition possessing Gaussian statistics. If the large-wave slopes are then assumed to be small compared to the total rms surface slope, the modulation can be modeled by the following linear "tilt model."

The backscatter cross-section of a small patch of sea surface of area A (cf. Figure 3) is given by $\sigma = \sigma^o A$, where the normalized cross-section σ^o is assumed to be the average σ^o of the sea surface

*The directional resolution quoted in J (equation 79) is wrong.

in a tilted reference frame. Thus, if θ' and Φ' are the local incidence and azimuth angles, we suppose that $\sigma^o(\text{patch}) = \sigma^o(\theta', \Phi')$. For small large-wave tilts δ, the fractional cross-section variation is given by

$$\frac{\delta\sigma}{\sigma} \simeq \frac{\delta\sigma^o}{\sigma^o} + \frac{\delta A}{A} \tag{2.4}$$

The elementary surface area is that area contained in the range interval $c\Delta\tau/2$. To first order in δ, A is given by $\Delta y(c\Delta\tau/2)\csc\theta'$. Provided that $\delta << \theta$, the local incidence angle can be approximated by $\theta' \sim \theta - \delta\zeta/\delta x$. Thus, to first order in δ it follows that $\delta A/A = \cot\theta\ \delta\zeta/\delta x$. Since the azimuthal dependence of σ^o is small compared to the θ dependence, it follows that the tilt term $\delta\sigma^o/\sigma^o$ is also proportional to the large-wave slope component in the plane of incidence. From (2.3),

$$\frac{\delta\sigma^o}{\sigma^o} = -\frac{1}{p}\frac{\delta p}{\delta \tan\theta}\frac{\delta\zeta}{\delta x} + O(\delta^2) \tag{2.5}$$

The fractional range reflectivity modulation seen by the radar is $\delta\sigma/\sigma$ averaged laterally across the beam:

$$m(x, \Phi) = \frac{\int G^2(y)\,(\delta\sigma/\sigma)\,dy}{\int G^2(y)\,dy} \tag{2.6}$$

The directional modulation spectrum is defined by

$$P_m(K, \Phi) = (2\pi)^{-1} \int \langle m(x, \Phi) m(x + \xi, \Phi)\rangle \exp(-iK\xi)\,d\xi \tag{2.7}$$

where the angle brackets denote ensemble average. Now let G be given by the Gaussian pattern (2.1), and consider the limiting case of very large footprints, $KL_y >> 1$. It is easy to show then that P_m is proportional to the directional slope spectrum as

$$P_m(K, \Phi) = \frac{\sqrt{2\pi}}{L_y}\left[\cot\theta - \frac{\partial \ln p}{\partial \tan\theta}\right]^2 K^2 F(K, \Phi) \tag{2.8}$$

where F is the two-sided, polar-symmetric height spectrum defined so that the height variance

$$\langle\zeta^2\rangle = \int_0^\infty\int_0^\pi 2F(K, \Phi)K\,dK\,d\Phi \tag{2.9}$$

The rms modulation depth, by definition, is given by

$$\mu(\Phi) = \langle m^2(x, \Phi)\rangle^{1/2} = \left[\int_0^\infty 2P_m(K, \Phi)\,dK\right]^{1/2} \tag{2.10}$$

It should be pointed out that, strictly, the large-footprint limiting form is valid only if L_y is much larger than the lateral

de-correlation scale of $\delta\zeta/\delta x$. This is equivalent to the condition $KL_y >> 1$ in the general case of directionally spread seas, but not in the case of unidirectional, long-crested swell. We have encountered such a swell in our aircraft experiment, where the crest length was very long compared to the antenna beam width. In such a case a separate calculation must be carried out, one which accounts for the curvature of the EM wave front. But as the case we encountered was exceptional among our data, we have neglected to perform such a calculation.

Now it is only consistent at this point to assume that the slope pdf is Gaussian. Indeed, it would be inconsistent to assume otherwise, since the tilt model is predicated on an assumption of free, noninteracting waves, and this can only imply normal statistics. The K_u-band scatterometer data of Jones et al. (1977) analyzed by Wentz (1977) show in fact that the pdf is nearly normal. More interesting though, the data indicate that the pdf at K_u-band frequencies is very nearly isotropic. This is convenient, as it simplifies the measurement of bi- or multi-modal directional spectra, since the sensitivity is independent of azimuth, and no relative weighting of different directional components is required. If the slope pdf is Gaussian and isotropic, then the sensitivity coefficient, the factor of K^2F in (2.8), can be written as

$$\alpha \equiv \frac{\sqrt{2\pi}}{L_y}\left[\cot\theta + \frac{2\tan\theta}{\langle|\nabla\zeta|^2\rangle}\right]^2 \qquad (2.11)$$

where $\langle|\nabla\zeta|^2\rangle$ is the mean-square wave slope effective at the particular radar operating frequency (diffraction-effective mean-square slope).

The linear tilt model solution (2.8) is identical to the first term in the series expansion of the geometrical optics solution obtained by J. The second-order terms consist of an EM and a hydrodynamic (hydro) term. The two terms are of comparable magnitude, both scaling as the large-wave steepness $\delta_o \equiv K_o\langle\zeta^2\rangle^{\frac{1}{2}}$ to the fourth power. The EM term is independent of hydrodynamic nonlinearity and arises in scattering from a normally distributed sea surface. The hydro term is due to the non-Gaussian statistics associated with hydrodynamic nonlinearity, and is given in terms of various third-moment statistics in wave height and slope. Since these statistics scale with δ_o (see J; also Huang and Long, 1980), the result is that both EM and hydro terms scale as δ_o^4. The calculations of the second-order EM term carried out in J indicate that, first, the term is generally small, and second, the least harmonic distortion occurs in the neighborhood of 10^o incidence. The smallness of the second-order terms requires that the following inequalities should be satisfied:

$$\text{i)}\quad \delta_o \cot\theta << 1$$

$$\text{ii)}\quad \frac{\delta_o \tan\theta}{\langle|\nabla\zeta|^2\rangle} << 1 \qquad (2.12)$$

If i) is violated seriously, an obvious consequence is that the phase front, or pulse, may intersect the surface at more than one point. A less extreme but more general consequence of violating i) is the confounding of the surface range coordinate with the wave height. The range coordinate will suffer a displacement $\delta x = \zeta \cot \theta$. The net result will be a dispersion of the range coordinate by an amount $\langle \zeta^2 \rangle^{\frac{1}{2}} \cot \theta$. This dispersion will represent a limit to the smallest wavelengths observable by this technique. Since $\langle \zeta^2 \rangle^{\frac{1}{2}} = \delta_o / K_o$, it follows that the upper limit on wavenumber as a function of the peak wavenumber is of the order of

$$K_{max}/K_o \simeq (\delta_o \cot \theta)^{-1} \tag{2.13}$$

For example, if $\theta = 10^o$ and $\delta_o \sim 0.05$ (fully arisen seas), then $K_{max} \sim 3.5\ K_o$. In steep developing seas, $\delta_o \sim 0.1$, in which case $K_{max} \sim 1.75\ K_o$. To illustrate the nature of the spurious response associated with the violation of ii), take the extreme case of swell under calm conditions. Obviously, if $\tan \theta > \delta_o$, then no backscatter occurs, since there are no wave slopes satisfying the specular condition. If $\tan \theta < \delta_o$, the backscatter will now occur in periodically spaced bursts at points on the swell profile satisfying the specular condition. The backscatter will look like a string of delta functions, and will bear little resemblance to the swell profile save in its periodicity. Clearly, for the measurement to have decent fidelity (to the slope spectrum) there must be sufficient small-scale roughness, or in other words, a sufficient density of specular points. Practically, this means that the local wind speed should be in excess of several meters per second.

Some guide to the selection of the "best" incidence angle may be had by assuming that the effects of violating i) and ii) are equally undesirable. Then we can minimize the sum i) + ii) with respect to θ. This yields $\tan \theta = \langle |\nabla \zeta|^2 \rangle$. For example, if the wind speed is 10 m s^{-1} then using (4.8) we get $\theta = 10^o$. More work along the lines established in J is required to get a better idea of what is really the best angle for minimizing the measurement nonlinearities. Unfortunately, the aircraft data are of little or no use to us here. This is because at the relatively low aircraft altitudes, the elevation beam width must be fairly broad in order to generate a sufficiently large beam spot for wavenumber resolution. In our aircraft experiment geometry, the 10^o elevation beam width makes it virtually impossible to establish the optimal angle, since the likely range of θ lies within the beam width.

2.3 The Short-Pulse Technique

In principle, the range reflectivity modulation spectrum $P_m(K, \Phi)$ can be measured by either short-pulse or two-frequency techniques. However, as shown by J, the narrow-band two-frequency technique has, inherently, a poor measurement SNR (signal-to-noise ratio) compared to the short-pulse technique. This is due to the use of narrow-band waveforms that completely fill the beam. The analysis bandwidth δK

in this case is equal to the reciprocal of the range footprint dimension--the "record length." Hence the SNR $\propto P_m(K)\delta K$ will neccessarily be small when the footprint dimension is large. Since $P_m \propto L_y^{-1}$ and $\delta K \propto L_x^{-1}$, it follows that the two-frequency SNR is inversely proportional to the footprint area, as noted by Alpers and Hasselmann (1978).

In the short-pulse technique,* wide-bandwidth, short pulses are used to resolve the wave structure in range. Backscattered pulses are integrated in surface-fixed range bins, and the range modulation spectrum is computed digitally from the observed sample of the range modulation $m(x, \Phi)$. For narrow pencil beams, the curvature of the wave front can be neglected, and the surface range can be taken to be a linear function of the signal delay time τ. If the motion of the platform is accounted for, then

$$x = c\tau/(2 \sin \theta) + Vt \cos \Phi \equiv x' + Vt \cos \Phi \qquad (2.14)$$

where c is the speed of light, V is the platform speed, and x and τ are referred to the center of the beam spot at $t = 0$. The coherency of the radiation results in random signal fading akin to the speckle observed when a coherent laser illuminates a "rough" surface, such as an ordinary piece of bond paper. The backscattered field statistics are complex Gaussian, the amplitude is Rayleigh-distributed, and the detected power is exponentially distributed (Moore et al., 1975). If the measurement integration time is short (< 1 s), the surface can be regarded essentially as frozen. Consider the backscatter of a short pulse of length $\Delta\tau$. The surface range resolution cell is given by

$$\Delta x = c\Delta\tau/(2 \sin \theta) \qquad (2.15)$$

It is assummed that Δx is small compared to the dominant wavelength. The backscattered power in a pulse transmitted at a time t_i can be modeled as a weakly modulated noise process of the form

$$W_i(x', \Phi) = W_o(x', \Phi)[1 + m(x, \Phi)]w(x, t_i) \qquad (2.16)$$

where $W_o \propto G^2(x)\sigma^o(\theta, \Phi)$ is the average backscattered power profile and w is the unit exponential fading process. The de-correlation length of the w-process is equal to the range resolution; more generally, if excess bandwidth is employed, the de-correlation length is given by the reciprocal of the pulse bandwidth (Moore et al., 1975). Since the auto-correlation function of the fluctuating component of the w-process is concentrated near the origin, it follows that the spectrum of the (normalized) backscattered power is given by

$$P_i(K, \Phi) \simeq \delta(K) + P_m(K, \Phi) + [1 + \mu^2(\Phi)]P_w(K) \qquad (2.17)$$

where δ is the Dirac delta function. The fading spectrum is essentially

*The terminology may be due to Tomiyasu (1971).

the spectrum of the transmitted pulse. This follows because the backscattered field is given by the convolution of the pulse waveform with the surface impulse response, which, in the absence of modulation, is a complex Gaussian white noise process. For a Gaussian pulse shape with half-power width $\Delta\tau$ one finds (cf. J, equations 5 and 70 et seq.):

$$P_w(K) = \frac{\Delta x}{2\sqrt{2\pi \ln 2}} \exp\left[-(K\Delta x)^2/8 \ln 2\right] \tag{2.18}$$

An integration of N independent pulses will reduce the fading variance by a factor of N^{-1}. Because of the platform motion, the backscattered pulses must be integrated in range bins that are fixed in the surface; otherwise the wave contrasts will be smeared out by range walk. This can be accomplished simply by delaying or advancing the trigger signal to the sampling gates according to the line-of-sight relative speed between the platform and the surface. The N pulse average can be expressed as

$$W_N(\tau) = N^{-1} \sum_{i=1}^{N} W_i(\tau + \dot{\tau} t_i) \tag{2.19}$$

where the rate of change of signal delay $\dot{\tau} = -(2V/c) \sin\theta \cos\Phi$. Omitting the dc term and neglecting μ^2, then the spectrum of the N-pulse average is given by

$$P_N(K, \Phi) \simeq P_m(K, \Phi) + N^{-1} P_w(K) \tag{2.20}$$

If thermal noise is negligible, then the SNR is just the ratio of the signal spectrum to the residual fading spectrum, $SNR = NP_m/P_w$. Using (2.18) for P_w and assuming $K \ll 2\pi/\Delta x$, we have

$$SNR = \frac{2\sqrt{2\pi \ln 2}}{\Delta x} N P_m(\underline{K}) \tag{2.21}$$

The number of independent pulses depends on the pulse repetition frequency (PRF), the Doppler bandwidth B_d, and the integration time T_{int}. If the PRF $> 2B_d$, the signal is essentially continuously sampled, and hence $N = B_d T_{int}$. If the PRF $\ll B_d$, then the individual pulses are independent, in which case $N = PRF \times T_{int}$. The Doppler bandwidth is determined by the interference rate of waves backscattered from the lateral extremities of the range resolution cell. From elementary considerations, or from equation 72 in J,

$$B_d = (2V/\lambda)\beta_\phi |\sin\Phi| \tag{2.22}$$

Here B_d is the half-power, post-detection Doppler spread in hertz, λ is the EM wavelength, and $\beta_\phi \equiv (L_y^*/H) \cos\theta$ is the half-power azimuth beam width.

The measurement integration time is limited by the azimuth scan rate, which in turn is driven by coverage requirements. The integration time should not be longer than the time it takes to move one footprint dimension. The modulation signal can only be built up coherently when the radar is viewing the same portion of the surface. When the beam moves to view a new, statistically independent patch of sea, the range modulation signal will evolve randomly, and further integration will proceed in an incoherent fashion, not only with respect to the scintillation or fading noise, but with respect to the modulation signal as well. Thus both P_m and P_w will be driven down as N^{-1}. Thus, as the beam moves to view a new piece of the surface, the signal strength goes down as $1/T_{int}$ while the SNR approaches an asymptotic value. Since the antenna rotation is generally more rapid than the beam's translation, the azimuth scan rate determines the choice of integration time. Let us arbitrarily require that the beam move no more than one-half of its azimuth dimension. Then the integration time is set by

$$T_{int} \leq \Delta\Phi/2\dot{\Phi} = \beta_\phi \csc\theta/2\dot{\Phi} \tag{2.23}$$

An interesting consequence of (2.23) is that the SNR is independent of the footprint dimensions and hence of the antenna gain. This follows because the integration gain $N \propto T_{int} \propto L_y$, while the signal spectrum $P_m \propto L_y^{-1}$. Thus, while the azimuth beam width affects the modulation signal strength (weakly as $L_y^{-\frac{1}{2}}$), it does not affect the measurement SNR.

The number of degrees of freedom (DOF) in a measurement of $P_m(\underline{K})$ is determined by the number of elementary wavenumber bands $\delta K \sim 2\pi/L_x^*$ contained in the spectral estimate. For example, consider an analysis with 25% resolution. Then the DOF of the estimate is given by (Blackmann and Tukey, 1958)

$$DOF \sim 2(0.25)/\delta K \sim KL_{x^*}/4\pi \tag{2.24}$$

For example, if $L_x^* = 20$ km and $K = 2\pi/200$ m, then DOF ~ 50.

3. A Satellite System

These measurements can be made with a modified Seasat-class radar altimeter. The pertinent Seasat altimeter characteristics are (Townsend, 1980):

Frequency:	13.5 GHz
Pulse type:	Linear FM, 1000:1 pulse compression
Pulse length:	3.2 ns compressed
Peak power:	2.0 kW
PRF:	1000 Hz
Detection:	Noncoherent square law

One can modify the Seasat altimeter* in such a way that it can perform a dual function, first as an altimeter per se, and second as a "directional wave spectrometer." In the conventional altimeter mode, mean altitude and wave height are determined from the delay time and broadening of the leading edge of the averaged return of nadir-directed pulses. There are several ways whereby transmitted pulses may be shared between the instrument's nadir altimeter mode and off-nadir spectrometer mode; for example, by power dividing or time sharing. Modification would entail the addition of a separate receiving section (post IF) and microprocessor as well as a separate rotating antenna. Pulse tracking, integration, and spectral analysis functions would be incorporated in the separate microprocessor. As an example, let us consider adding a 1 m diameter, 3 rpm rotating antenna to the existing instrument. If we assume a 700 km satellite altitude and 10° nadir angle, then the measurement geometry is that of Figure 1, and the relevant measurement parameters are:

Velocity:	$V = 7$ km s^{-1}
Beam width:	$\beta_\theta = \beta_\phi = 1.6^\circ$
Spot size:	$L_x^* \sim L_y^* = 20$ km
	$(L_x \sim L_y = 8.5$ km)
Rotation rate:	$\dot{\Phi} = 360^\circ/20$ s
Range resolution:	$\Delta x = 2.8$ m (from 2.15)
Doppler bandwidth:	$B_d = 18 \lvert \sin \Phi \rvert$ kHz (from 2.22)
Integration time:	$T_{int} = 0.26$ s (from 2.23)

The PRF equals B_d at $\Phi \sim 3^\circ$ of foreward or aft. For most azimuths the PRF $<<$ B_d so that the number of independent samples is given by

$$N = \text{PRF} \times T_{int} = 260 = +24 \text{ dB}$$

For illustrative purposes let us assume a Phillips cutoff spectrum with a $\cos^4$ spreading factor:

$$F(K, \Phi) = \begin{cases} 0.005(4/3\pi)\cos^4(\Phi - \Phi_o)K^{-4}, & K \geq K_o \\ 0, & K \leq K_o \end{cases}$$

Assume a 200 m water wavelength and upwave/downwave looks. Let the mean-square slope as a function of wind speed be given by (4.8) and let $U = 10$ m s^{-1}. Then we have (cf. 2.8, 2.10, and 2.21):

$$P_m = (2.95 \times 10^{-4} \text{ m}^{-1})(5.67 + 9.53)^2(2.15 \text{ m}^2) = 0.15 \text{ m}$$

$$\mu = 10^\circ$$

$$\text{SNR} = 260 \times 0.22 = +18 \text{ dB}$$

---

*Unfortunately, the Seasat engineering unit is no longer available for this purpose.

The directional resolution given by (2.2) is $\delta\Phi = 4.7^{o}$, but this assumes no rotation of the beam. Since the beam moves about 5^{o} during the integration time, the actual resolution will be somewhat less. We have already calculated the DOF in the last section: DOF $\sim$ 50. At 10^{o} incidence, $\sigma^{o} \sim +5$ dB and is very nearly independent of wind speed. A link equation assuming 3 dB in losses and a noise factor of F = 6 dB gives a signal-to-thermal-noise ratio of + 6 dB. Thus, thermal noise is not a problem, even if half the transmitter power is shared with the altimeter mode.

The spectrometer mode does not require the full pulse compression. For example, a partial compression of the chirped waveform to 20 ns (17.3 m surface range resolution) would be quite adequate. The excess bandwidth, of course, is still useful for reducing the fading variance. With 20 ns resolution, something like 1024 sample gates would adequately sample the return (17.7 km of surface range). The spectrometer mode data can be merged with the altimeter mode data stream in a way that is compatible with the existing instrument's data system. For example, the spectrometer data might consist of 58 6% bandwidth spectral estimates covering the wavelength range 50-1000 m output at a nominal four frames per second. These data can easily be merged with the altimeter data without exceeding the 10 kb s^{-1} data rate of the existing system. Thus, onboard recording, and hence fully global coverage, is possible.

The above figures clearly indicate that these measurements are feasible. Yet, have we missed something, erred in our thinking somehow? The aircraft data to be presented below convince us that we have not.

4. Aircraft Validation

4.1 The Fall '78 CV-990 Mission

The Goddard K_u-band Short-Pulse Radar was built up from the Geos-3 satellite altimeter breadboard obtained from General Electric Co. in 1974, and it shares the following characteristics with the spacecraft instrument:

Frequency:	13.9 GHz
Pulse type:	Linear FM, 100:1 pulse compression
Pulse length:	12.5 ns compressed
Peak power:	2.5 kW
PRF:	100 Hz
Detection:	Noncoherent square law

Prior to 1978, the radar was flown on several aircraft missions with fixed-azimuth, variable-elevation antennas. A description of the Goddard radar as it was configured in 1975 is given by LeVine et al. (1977). A major breakthrough in our program occurred in 1978, when we

had an opportunity to fly piggyback, free of charge, on the 1-month-long Convair-990 Nimbus-7 Underflight Mission. For this mission, one of the fixed-azimuth printed-circuit antennas was modified (by sawing it in half) and adapted to an azimuth scan. Also, the data system was redesigned to allow continuous recording at the full PRF. Figure 4 shows the rotating antenna installed in the CV-990's instrument "sled." It is shown surrounded by a cylindrical baffle which was designed to protect a neighboring radiometer from possible RFI. Also shown in Figure 4 is a 12^o x 12^o, nadir-directed rectangular horn antenna, which served in our instrument's "altimeter" mode. The nadir horn and rotating antennas are shown connected by a wave-guide switch; this switch could be activated by a mode-change command from the radar's control panel in the aircraft cabin. The rotating antenna characteristics are:

Boresight incidence angle:	$\theta_o = 15.8^o$
Azimuth beam width:	$\beta_\phi = 4^o$
Elevation beam width:	$\beta_\theta = 10^o$
Rotation rate:	$\Phi = 6$ rpm

The boresight angle was chosen so that an elevation sidelobe at 15.8^o to the main-beam axis would be directed toward nadir. The return from the sidelobe, which was recorded in the same frame as the main-beam return, allowed us to calculate the range on the surface without having to calibrate for absolute time delay. This is important in the relatively low-altitude (10 km) aircraft geometry where a rather broad elevation beam width is required to generate a large enough range footprint extent for wavenumber resolution. Thus in the aircraft geometry, wave-front curvature in the elevation plane is not negligible, and if not properly accounted for, the curvature will result in a considerable dispersion of the surface wavenumber. If τ is the time elapsed from the time of the nadir sidelobe return, then given the aircraft altitude from the plane's operational altimeter, the surface range x as measured from the nadir point can be calculated according to the equation

$$x^2 + H^2 = (c\tau/2 + H)^2 \qquad (4.1)$$

Of course, in the satellite measurement geometry, we can linearize (4.1) to get (2.14). The aircraft measurement geometry is illustrated in Figure 5. At the nominal aircraft altitude of 10 km, the footprint dimensions are $L_x^* = 1500$ m and $L_y^* = 700$ m, approximately. Because of the rapid roll-off of σ^o with θ, the backscattered power peaks inward of the boresight angle. Generally, the peak return occurs in the vicinity of 13^o incidence. The metallic baffle and the poor radome environment in general spoiled the gain pattern to such an extent that we have not attempted to measure σ^o either as a function of elevation or azimuth angle. Figure 6 is an example of the (azimuthally averaged) average backscattered power profile: the large $\sim 3^o$ ripple near the beam axis caused by diffraction by the

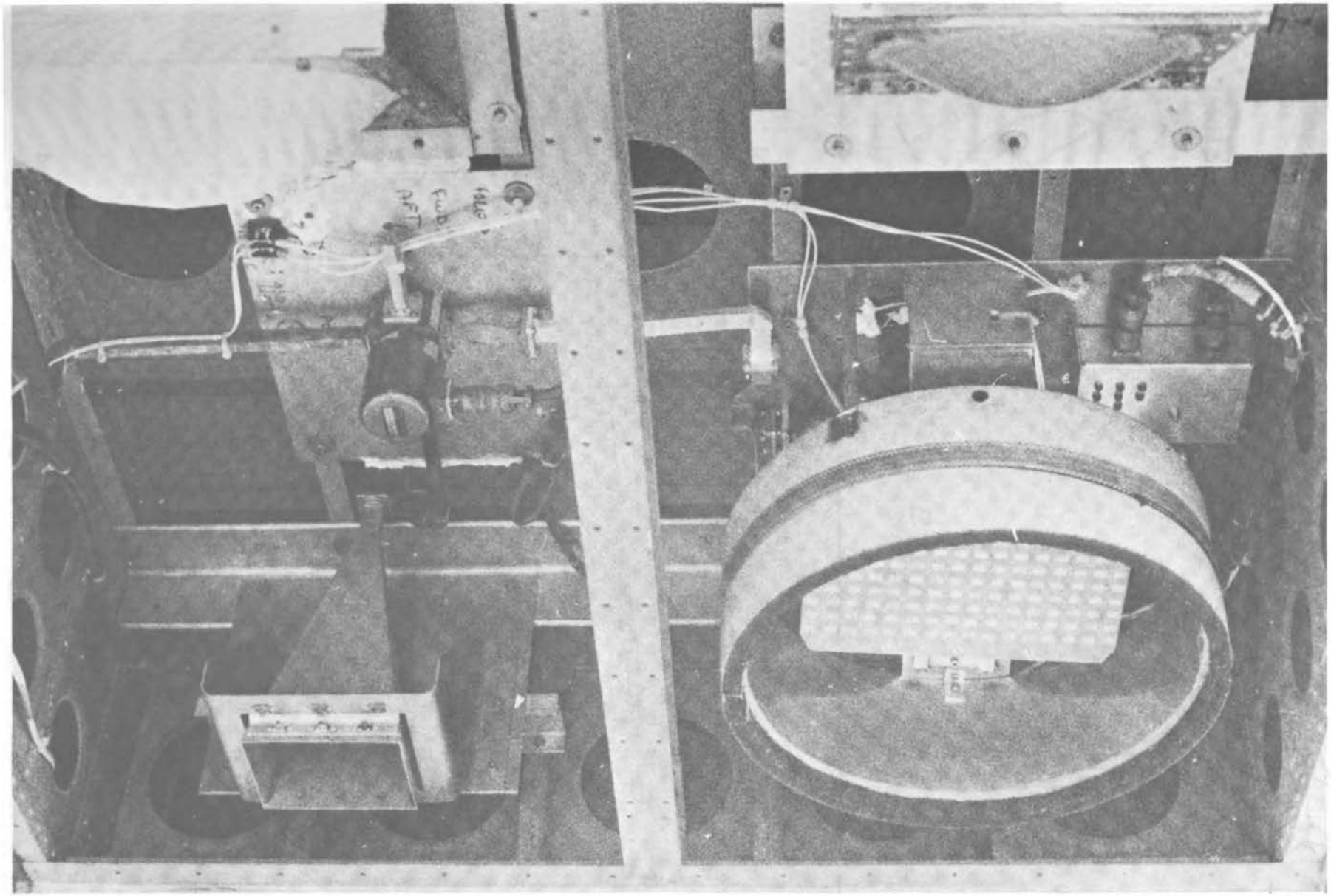

Figure 4 Antennas mounted in the CV-990 instrument "sled." View is upward, looking into the sled with the radome cover removed. The rotating antenna is surrounded by a cylindrical baffle. The nadir-pointing horn antenna is connected to the rotary antenna by a wave-guide switch. The other antennas shown belong to the SMMR (simulator microwave radiometer).

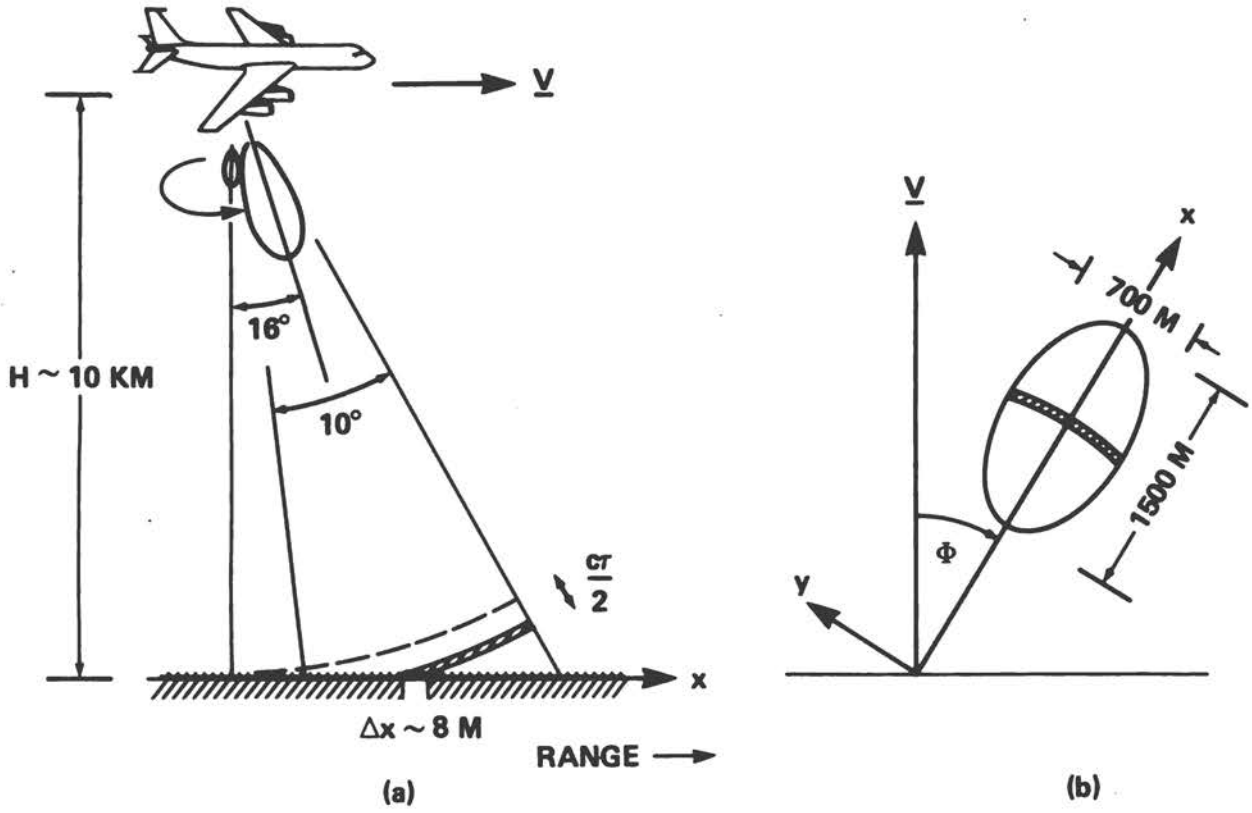

Figure 5 Aircraft measurement geometry: (a) elevation view; (b) plan view

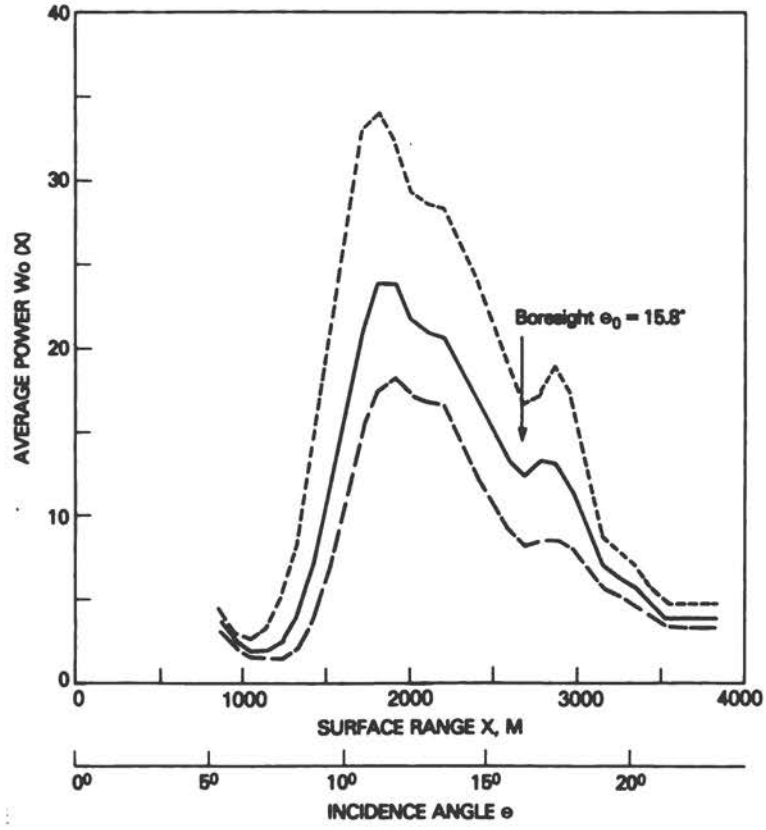

Figure 6 Azimuthally averaged, average backscattered power profile, Tape 37/File 1. The upper and lower dashed curves represent, respectively, the average maximum and minimum values over 360° of azimuth.

baffle is obvious. The poor gain pattern is unfortunate, as, ideally, we want to estimate the tilt model sensitivity term $\delta \ln p/\delta \tan \theta$ directly from the observed cross-section roll-off. The gradient of the slope pdf and mean-square slope are internal parameters of the measurement; yet, in the analysis to follow we shall have to rely on external parameters in order to calculate the tilt model sensitivity α. That is, we will have to use a mean relationship between the mean-square slope and the buoy-observed wind speed in order to verify the prediction of the tilt sensitivity coefficient (2.11).

The digital data system consisted of a high-speed waveform sampler (Biomation Co.), two 6 k-byte buffers, and a high-speed (75 ips) 1600 bpi tape drive. The Biomation sample gates were selectable and could be set to 2, 5, 10, or 20 ns. Quantization was 6 bits and the maximum frame size was 1024 samples. Generally, we recorded in the spectrometer mode at a 5 or 10 ns rate, taking 512 samples at the full PRF. Shaft encoder and other housekeeping data were recorded in the first two tape tracks.

The Fall '78 Mission took in 19 flights of approximately 5 hours' duration in the period October 24 to November 19, 1978. About half these flights were over ice, the remainder over water. Approximately fifty 2400-ft tapes were written with ocean backscatter data; roughly half these data were taken in the instrument's spectrometer mode and the remainder in the altimeter mode. The spectrometer files are by and large 1-2 minutes long. The 1 minute files, amounting to only six antenna rotations, are a bit short on equivalent DOF, and consequently the spectra from these files are noisy.

In this paper we are only concerned with validating the technique, and so we shall be examining only a small subset of the Fall '78 Mission data set; that is, we shall be examining only those files for which we have corroborative "surface truth." Table 1 is a summary of the surface-truth data set (spectrometer mode). This data set consists of overflights of three types of wave-recording buoys, including two NOAA data buoys (N.E. Pacific), a Waverider (Norwegian Sea), and a pitch-roll buoy (N.E. Pacific). Colocation was generally within 100 km spatially and within 1 hour temporally.

4.2 Data Analysis

The digital flight tapes were reformatted and compressed by averaging 3 consecutive pulses. Also, the spectrometer mode data were standardized to 10 ns resolution. Figure 7 is an example of the backscatter data contained on the reformatted tapes. The figure shows 1500 pulse returns, intensity-coded, and stacked vertically, on a CRT display. These (essentially raw) data were further processed on a general-purpose computer as follows:

1) The equally spaced array in time $W(m\Delta\tau)$, $m = 1, 2, \ldots, 512$, is converted to an equally spaced array in surface range according to (4.1). The nominal surface range resolution $\Delta x = 8.1$ m at 13° incidence; however, it was more convenient to array the data in equally spaced 12 m surface range bins.

Table 1 Fall '78 Mission Surface-Truth Data Summary (Spectrometer Mode)

Flt.	Tape/ File	Date (1978)	GMT Start	GMT Stop	(mean) Lat.	(mean) Lon.	Alt. [km]	Hdg. [°T]	Buoy ID[a]	GMT	H_s [m]	Wind speed[b] [m s^{-1}]	Wind dir.[b] [°T]	Colocation Dist. [km]	Colocation Time [hrs]	Note
6	27/1	10/30	1801:13	-04:32	71.6°N	19.0°E	5.7	248	TROMSO	1725	4.2	10.1	330	3	0.6	c
7	29/1	11/01	0840:12	-42:20	72.4	23.2	9.5	051	"	0825	2.4	4.6	240	100	0.3	c
9	36/1	11/03	0811:45	-18:32	71.3	18.2	9.4	247	"	0831	9.4	18.4	280	13	0.3	
10	45/2	11/06	0950:00	-50:45	71.2	18.9	9.5	356	"	0818	3.1	11.5	190	11	1.5	
11	-/3	"	0954:30	-55:30	71.8	19.2	"	011	"	1118	2.8	"	"	10	1.4	
									"	1132	2.3	"	"		1.6	
17	85/10	11/17	0001:30	-02:30	42.2	131.7°W	9.6	071	EB-16	0000	2.2	7.9	325	14	0.0	
"	86/4	"	0036:49	-37:45	45.2	130.8	9.5	345	EB-21	0000	1.9	6.1	009	29	0.6	
"	-/6	"	0049:15	-50:15	45.9	129.9	9.5	091	"	"	"	"	"	83	0.8	
18	89/2	"	2135:30	-36:30	50.0	145.1	9.3	267	PAPA	2104	3.5	8.8-12.9	130	6	0.5	d
"	89/3	"	2142:45	-44:15	50.2	145.6	4.5	96	"	2138	3.3	"	"	42	0.0	d
"	90/7	11/18	0000:30	-01:30	46.3	131.5	8.4	134	EB-21	0000	1.3	5.7	189	41	0.0	e
"	-/9	"	0007:00	-07:46	45.9	130.5	8.4	104	"	"	"	"	"	14	0.1	e
19	91/6	11/19	2026:40	-27:40	45.6	131.6	8.7	232	"	2100	4.2	14.4	003	65	0.6	
"	94/2	"	2315:40	-17:14	41.9	128.9	8.7	128	EB-16	2400	4.0	10.3	333	119	0.7	

[a] TROMSO = Waverider buoy, weather station Tromsoflaket, 71.5°N, 19.0°E
EB-16 = NOAA data buoy 46002, 42.5°N, 130°W
EB-21 = NOAA data buoy 46005, 46.0°N, 131°W
PAPA = NOAA pitch-roll buoy, weather station PAPA, 50.0°N, 145.0°W

[b] Wind speed and direction at nearest 3-hourly reporting time (no height or stability corrections applied)

[c] Unresolved data problem (possibly high A/D bias level)

[d] Wind speed = 8.8 m s^{-1} at 2138Z; 12.9 m s^{-1} at 2029Z

[e] Unidirectional, monochromatic swell--Eq. (2.8) not applicable; see text

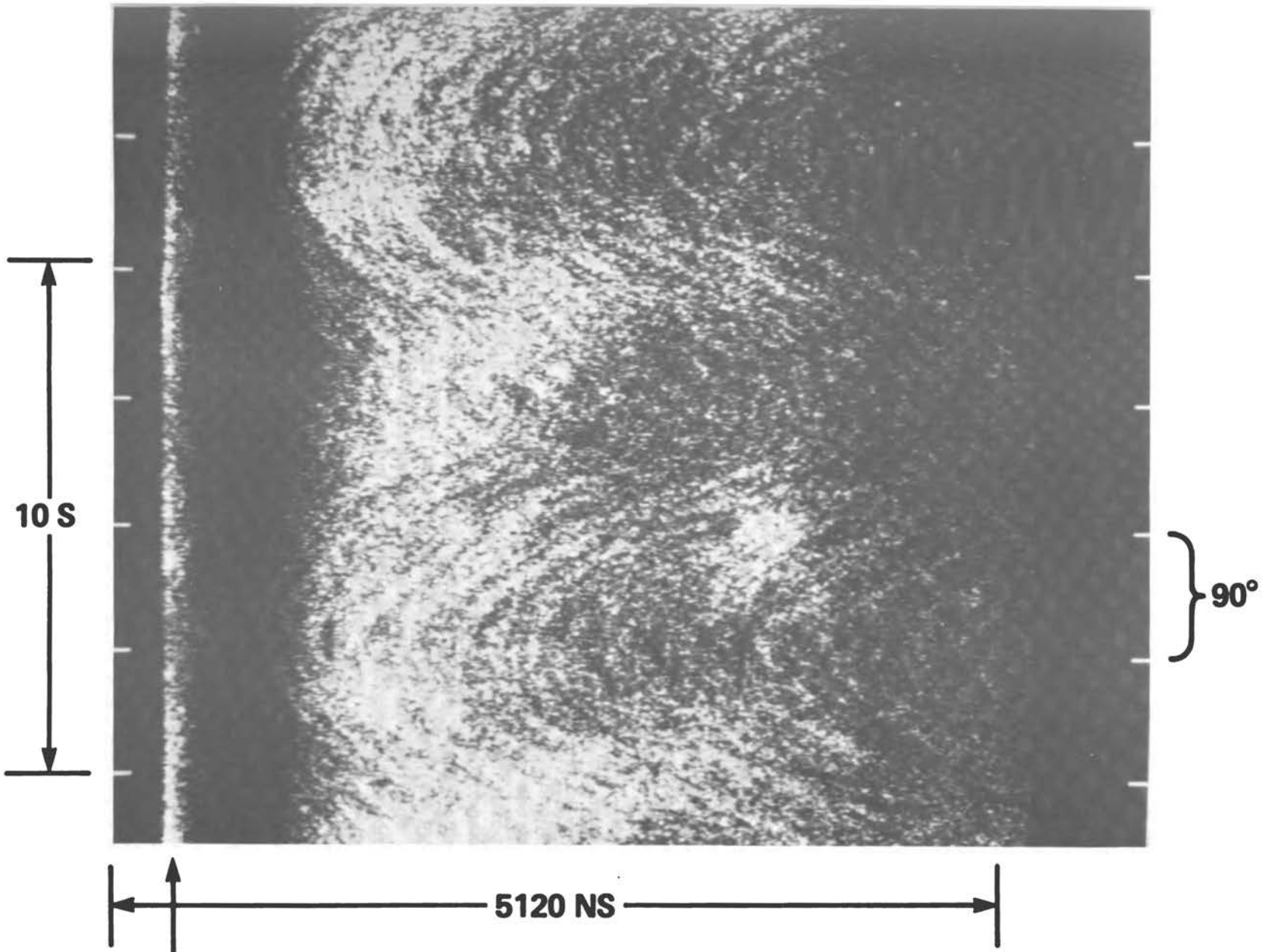

Figure 7 CRT display of 3-pulse average backscatter data. The sample gate setting is 10 ns and the frame size is 512. The display represents 512 consecutive 3-pulse averages stacked vertically. The tick marks are placed every 250 pulses, or, equivalently, every 90° of antenna rotation. The "S" pattern is the result of antenna rotation combined with aircraft motion.

2) The geometrically corrected data are then subjected to two algorithms. In the first, no motion correction is applied; the data are smoothed in range, and averaged over the several rotations of the antenna. This produces an estimate of the average backscattered power $W_o(x, \Phi)$. In the second algorithm, the motion compensation is applied. That is, the array is transformed according to $x \leftarrow x + Vt \cos \Phi$. The data have been processed in 15° azimuth blocks; given the 6 rpm rotation rate, this means we have integrated N = 42 independent pulses. (The pulses are generally independent even for forward/aft looks, since the sea-Doppler spread is generally greater than 100 Hz.) The decision to process in 15° blocks was made some time ago; this seemed reasonable, as the nominal directional resolution is about 17° (200 m wave) and tests indicated no loss of signal strength. However, this is about equal to the angle subtended by the footprint, and therefore the 15° is at odds with our prior dictum (2.23) to allow no more than half a beam width's movement in azimuth. Thus, the problem of the appropriate integration time for the aircraft data is still somewhat open, and requires a second and more careful examination. (As discussed in Section 2, choosing too long an integration time will not affect the spectral shape, only the signal strength; that is, the signal strength will start to drop as the integration becomes incoherent with respect to the modulation signal. Thus, it is possible that we may have to re-examine our conclusions about the precise values of the sensitivity coefficient.)

3) The accumulated N-pulse average is normalized by the the estimate of the average power $W_o(x, \Phi)$, and unity is subtracted. (The azimuthal dependence of W_o is probably mostly due to asymmetry in the radome environment.) The data are then rewindowed by a cosine-squared window. In the high altitude range (8-10 km) the window end points are taken to be x = 800 m and x = 3872 m, and at the low altitudes (4-6 km) these values are halved. The midpoint of the window corresponds roughly to $\theta = 13.5°$.

4) Estimates of $P_N(K, \Phi)$ for each 15° azimuth block are computed using a 256-point fast Fourier transform. These estimates are then ensemble-averaged over the several rotations of the antenna.

Figures 8a-8f are polar contour plots of the processed directional spectra $P_{42}^*(K, \Phi)$ in units of meters, where $P_N^* \equiv 4\pi P_N$ is the one-sided (in K) spectrum as a function of wavenumber in cycles per meter. The noise background has not been subtracted in these plots, but as the SNR is quite high (+ 10-20 dB), the background noise level is insignificant. Thus, these spectra can be viewed as directional slope spectra (one need only supply the "calibration constant" α). Figure 8a is the directional spectrum of a storm sea, significant wave height H_s = 9.4 m, dominant wavelength = 330 m. This spectrum (Tape 36/File 1) was produced from a long run, and hence it is very stable. Figures 8b and 8e are examples of bimodal spectra. Figure 8c represents a fairly low sea state (H_s = 1.9 m). The "rattiness" of this spectrum is characteristic of the noisy spectra from the short files (< six rotations). Figure 8f is an interesting example. It is the observed spectrum of a unidirectional, ∿330 m monochromatic

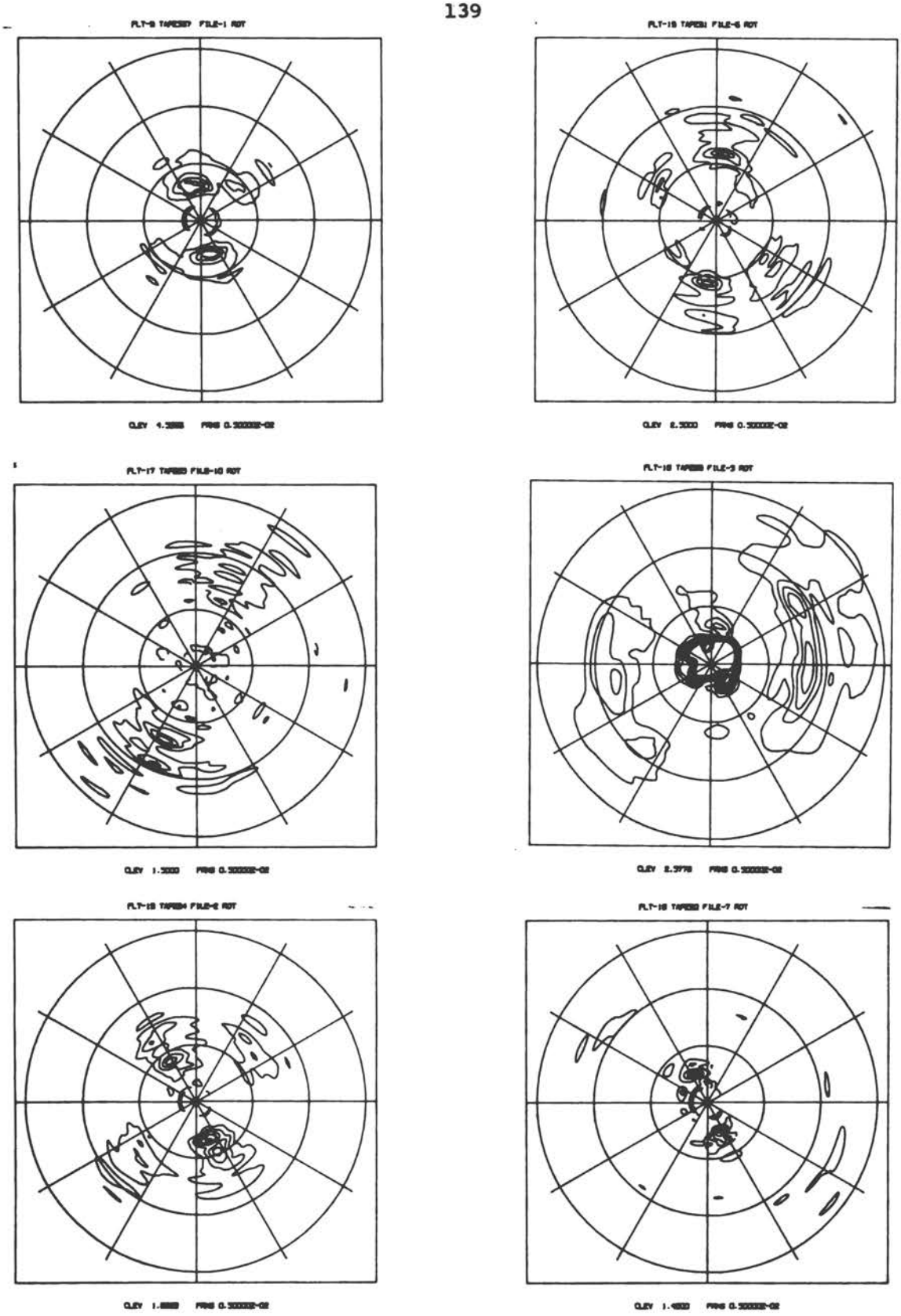

Figure 8 Polar contour plots of the (one-sided) directional spectra $4\pi P_{42}(K, \Phi)$ in units of meters. Top of the figures is 0^{o} radar azimuth = aircraft heading. The wavenumber rings are spaced every 0.005 cpm (first ring, 200 m wavelength; second, 100 m; and third 66.7 m). The labeled contour level (CLEV) increments are low by a factor of 2; they should read: (a) Tape/File = 36/1, CLEV = 9.08 m; (b) Tape/File = 91/6, CLEV = 5.00 m; (c) Tape/File = 85/10, CLEV = 3.00 m; (d) Tape/File 89/3, CLEV = 5.16 m; (e) Tape/File 90/7, CLEV 2.8 m.

swell running under fairly light winds. Visually, from the vantage point of 8.4 km, the sea surface had the striking appearance of a diffraction grating. The crest length was for all practical purposes infinite (> 40 km). (The eye can easily detect any deviations from a straight line.) It follows then that if the radar system's response were perfect, the observed spectrum would be a symmetrical pair of delta functions. The blossoming in Figure 8f thus represents, in effect, the system transfer function (for this 330 m wave).* According to (2.2), the directional dispersion should be approximately 30° for this wave; indeed, this is the amount of dispersion seen in the spectrum. The wavenumber dispersion is determined by the finite-range footprint dimension of 1500 m. If we figure roughly a dispersion $\delta K \sim 1/L_x^* \sim 7 \times 10^{-4}$ cpm, this accords with the observed wavenumber dispersion in Figure 8f.

Lastly, respecting Figure 8, we note the asymmetry that is evident in several of the spectra. This is obviously related to asymmetry in in the wave-slope distribution. What is significant here is that the asymmetry is by and large rather small, and this would indicate that, by and large, the second-order hydrodynamic effects are small.

Figure 9 is a series of cuts through the directional spectrum $P_N(K, \Phi)$ of Tape 36/File 1. The figure is intended here to show that the forward face of the (slope) spectrum is sharply defined and stands clearly away from the residual antenna-pattern energy near dc. This rather "clean" situation will not obtain for the nondirectional spectra we shall be computing in the following.

4.3 Absolute Nondirectional Comparisons

For these comparisons, we will need to take a closer look at the residual fading spectrum which must be subtracted from P_N to give the directional modulation spectrum P_m. Because of the nonlinear time delay versus surface range relationship (4.1) that obtains in the aircraft geometry, the formula (2.18) for P_w will not be exact. The pulse spectrum in the surface wavenumber domain will be similar to the pulse spectrum only when there is a linear relationship between surface range and delay time. Nevertheless, (2.18) may stand as a fair approximation. If we assume as a nominal range resolution the resolution at 13.5° incidence, i.e., $\Delta x = 8.14$ m, then (2.18) gives (with N = 42)

$$\frac{4\pi P_w}{N} = 0.58 \text{ [m]} \exp\left[-0.5(K/0.033)^2\right] \tag{4.2}$$

where K is given in cpm. Figure 10 is a plot of the azimuthally integrated value of P_N in the wavenumber band 0.0218-0.0250 cpm

*Actually, this is the spectral window; one might also refer to Figure 8f as a map of the spectral "point spread function," to borrow a term from the visible imagery people.

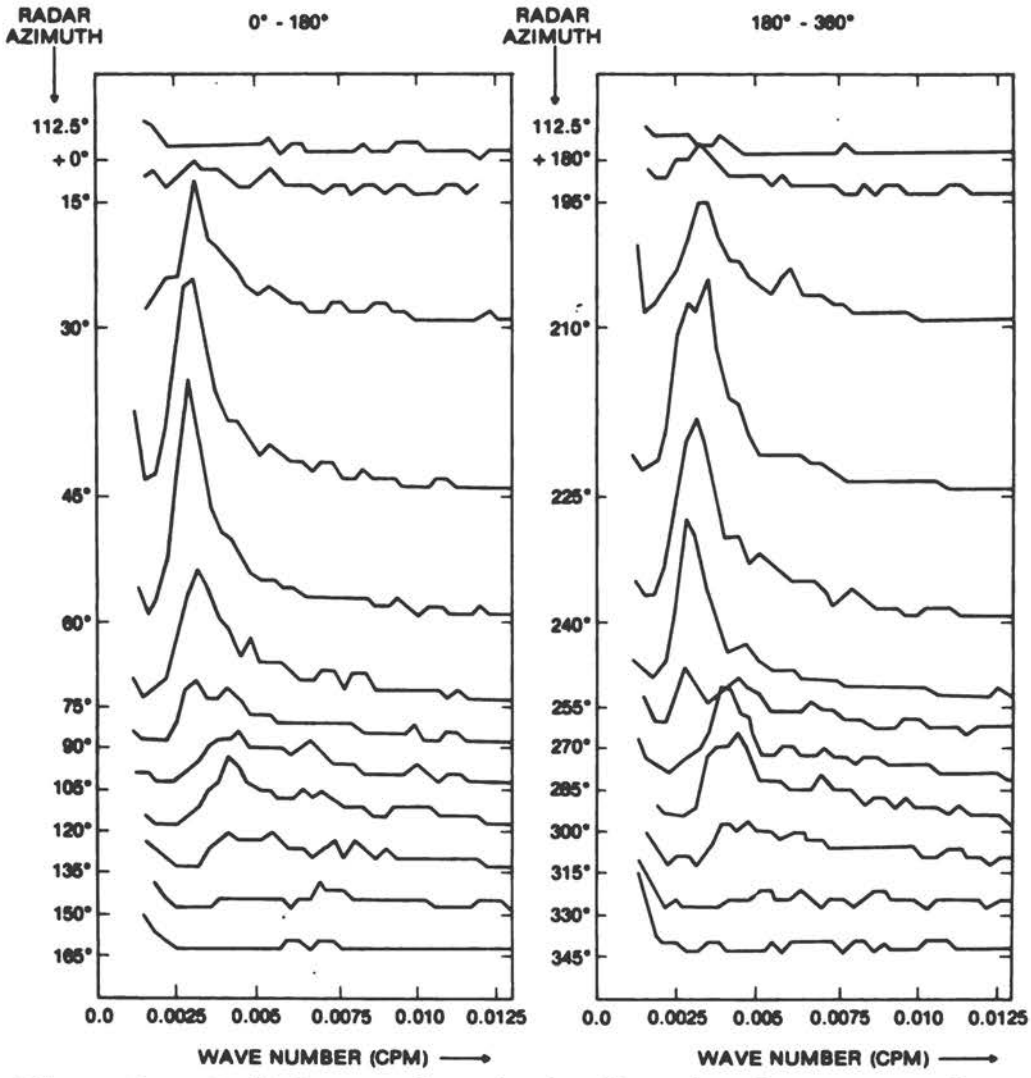

Figure 9 Radial cuts through the directional spectrum of Figure 8a

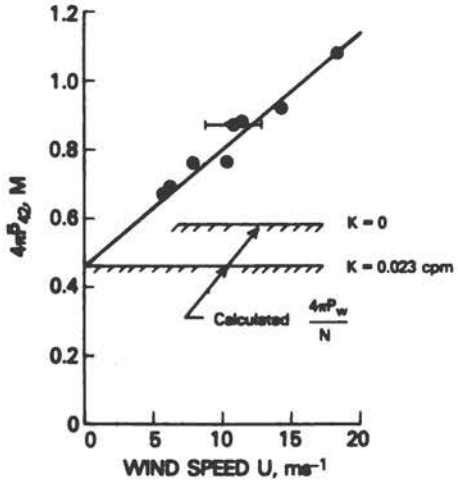

Figure 10 Estimation of the background fading noise level. The level of the azimuthally averaged directional spectrum in the wavenumber band 0.0218-0.0250 cpm for 12 files is plotted versus buoy-observed wind speed. The data from the adjacent files 45/2 & 3, 86/4 & 6, 89/2 & 3, and 90/7 & 9 have been averaged together. An eyeball extrapolation to zero wind speed yields the value of the residual fading variance spectrum predicted by equation (4.2).

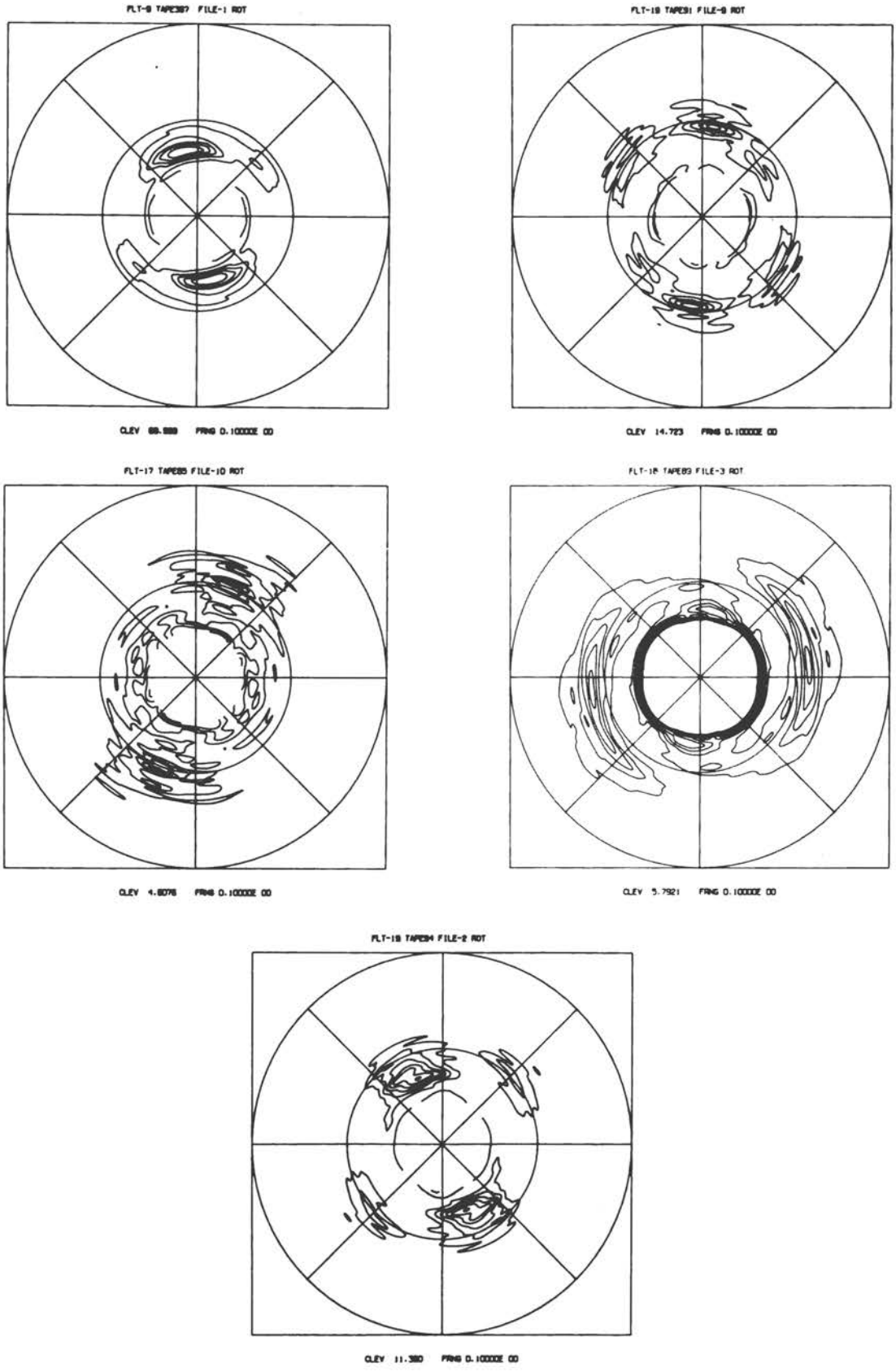

Figure 11 Polar-symmetric directional height spectra S(f, Φ), corresponding to Figures 8a-8e. The frequency rings are 0.1 Hz and 0.2 Hz. The equally spaced contour levels (CLEV), in units m^2/Hz/rad, have been multiplied by a factor of 2π.

(center frequency = 0.19 Hz) for several files, where the buoy-observed wind speed is used as an ordering parameter. From the plot, one sees that an extrapolation of the observed P_N to zero wind speed (and hence, presumably, to zero modulation depth) yields the value of the residual fading variance predicted by (4.2). The pulse spectrum roll-off between zero wavenumber and 0.023 cpm (42 m wavelength) is about 20%.

With P_m computed from P_N by subtracting (4.2), the directional height-frequency spectrum $S(f, \Phi)$ is computed using the tilt model solution (2.8). Assuming the linear, deep-water dispersion relationship, it follows that

$$S(f, \Phi) = (2/\alpha f)P_m(K, \Phi) \tag{4.3}$$

where S is the polar-symmetric spectrum expressed in $m^2/Hz/rad$. In computing (4.3), the measured modulation spectrum is symmetrized according to

$$P_m \leftarrow 0.5[P_m(K, \Phi) + P_m(K, \Phi + 180^\circ)] \tag{4.4}$$

Symmetrizing the spectrum, of course, has the advantage of doubling the DOF. The nondirectional spectrum is now computed according to

$$\begin{aligned} \bar{S}(f) &= (\alpha f)^{-1}(1/12)\sum_{i=1}^{12} 4\pi P_m(K, \Phi_i) \\ &\equiv 4\pi \bar{P}_m(K)/\alpha f \end{aligned} \tag{4.5}$$

As we have pointed out before, the sensitivity coefficient α should ideally be calculated on the basis of the observed cross-section roll-off, but the poor antenna gain pattern has made this virtually impossible. Thus, we will have to make do here with an indirect means of verifying the tilt model predictions. First, let us measure α by taking the ratio of the area under the radar spectrum to the area under the buoy spectrum. That is, let

$$\alpha_{meas} = \frac{\int_{f_c}^{0.2\ Hz} 4\pi \bar{P}_m(K)\ d\ \ln f}{\int_{f_c}^{0.2\ Hz} \bar{S}(f)\ df} \equiv \frac{\alpha H_s^2(radar)}{H_s^2(buoy)} \tag{4.6}$$

where f_c is a low-frequency cutoff, and the significant wave height $H_S \equiv 4\langle\zeta^2\rangle^{1/2}$ (where the low-frequency deficit is understood). The low-frequency cutoff is necessary because the antenna-pattern effects can be quite severe in the nondirectional spectra computed according to (4.5). This is because the antenna-pattern energy is omni-directional and therefore makes a large contribution to the azimuthal average. This should be apparent from Figures 8, 9, and 11. (Also, the 1/f factor in going to the height spectrum will magnify any errors

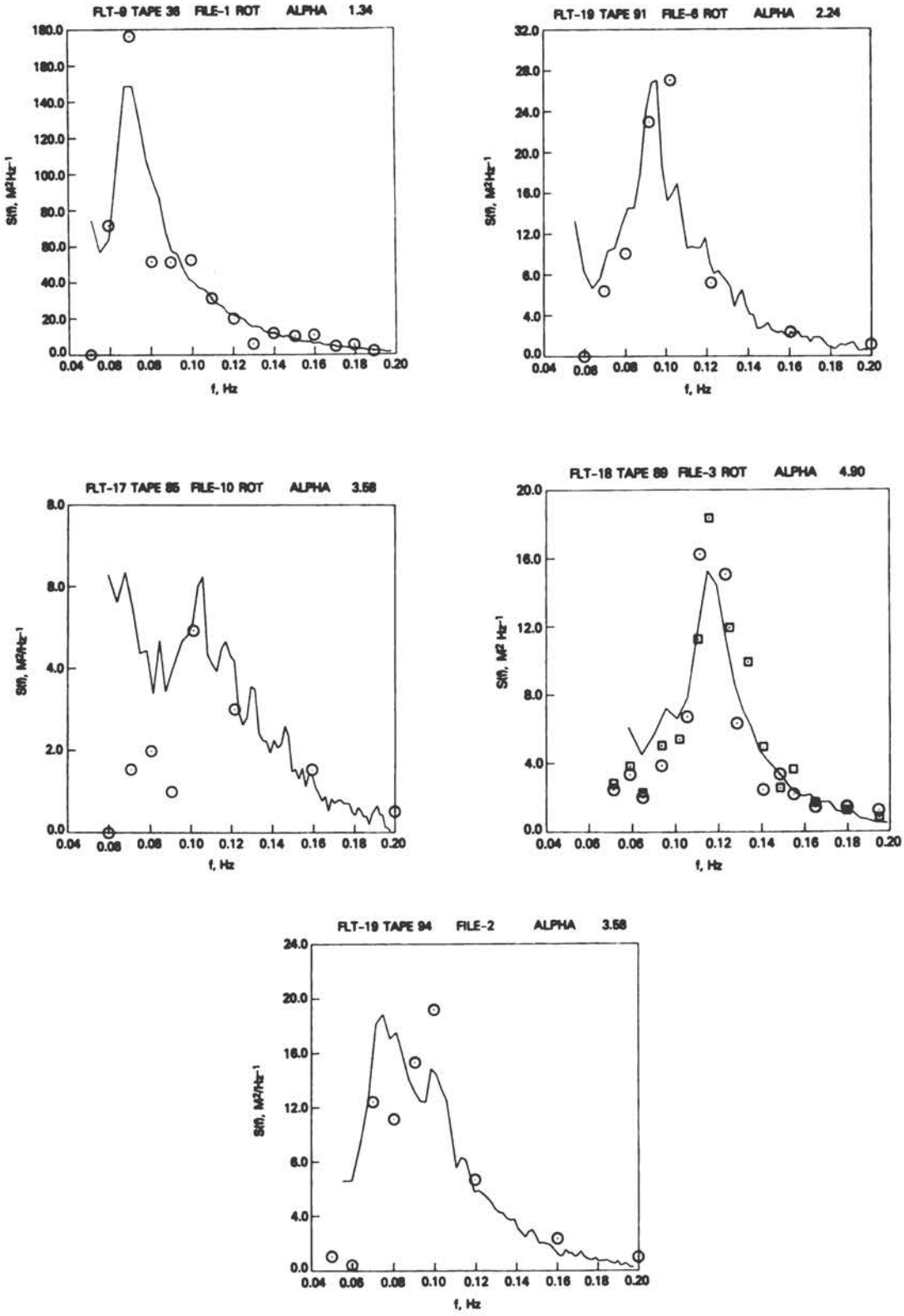

Figure 12 Comparisons of radar-inferred (solid line) and buoy (circles) nondirectional height spectra $\bar{S}(f)$ using the measured alphas. Figures 12a through 12e correspond to Figures 11a through 11e. In (d), the circles and squares stand for the buoy records at 2138 Z and 2104 Z, respectively. The 2138 Z data have been smoothed by a 2-point average in the vicinity of the peak.

Table 2 Measured Versus "Theoretical" Sensitivity Coefficient

Radar Tape/File	Low-frequency cutoff f_c [Hz]	Measured $\sqrt{\alpha}H_s$		Buoy H_s [m]		α_{meas} [m^{-1}]	Inferred $\langle \lvert \nabla\zeta \rvert^2 \rangle$		α_{theo} [m^{-1}]	Inferred H_s [m]	Altimeter mode H_s [m]
36/1	0.055	10.90		9.4		1.34	0.061		1.36	9.35	--
45/2	0.070	4.55	4.47	3.1	2.95	1.64	0.041		2.27	2.97	2.52
-/3	0.067	4.39		2.8							
85/10	0.080	4.16		2.2		3.58	0.030		3.42	2.25	2.31
86/4	0.090	3.72	3.80	1.9		4.00	0.028		4.57	1.78	--
-/6	0.085	3.86									
89/2	0.090	4.87		3.1[a]		2.47	0.039	0.041	2.48[b]	3.09	3.1[a]
-/3	0.085	6.86				4.90	0.042		5.12[b]	3.03	--
91/6	0.060	6.29		4.2		2.24	0.044		1.92	4.54	4.78
94/2	0.055	6.38		4.0		2.74	0.041		2.81	3.80	3.66

[a] H_s with energy below f_c subtracted (ΔH_s = -0.2 m)

[b] Average wind speed of 10.9 m s^{-1} assumed

Mean ΔH_s	= 0.00 m
Rms ΔH_s	= 0.16 m

in the specification of the fading noise background level, producing, in effect, a "1/f noise" background.)

Table 2 lists the measured alphas for 10 files, representing basically seven independent observations. The cutoff frequency in each case is chosen arbitrarily as the frequency of the minimum between the dc and the spectral peak. Figure 11 gives five examples of the inferred directional height spectra based on the measured alphas. Figures 12a-12e compare the inferred nondirectional spectra with buoy observations. The five examples shown are plotted auto-scaled, linear-linear; they cover a range of sea states from H_s = 1.9 m to 9.4 m, and include a variety of spectral forms. It is seen that the agreement is generally excellent over the entire range from f_c to 0.2 Hz. The minor discrepancies that are apparent in some of these comparisons can be attributed, for the most part, to sampling variability, geophysical variability (colocation error), and antenna-pattern contamination. One does not need to look for explanation in terms of second-order scattering effects. These effects are by and large so small as to be masked by the larger errors. For example, consider sampling variability. The 90% confidence interval on the buoy spectrum in Figure 12a is (0.6 S, 1.9 S). Thus the confidence interval on the peak of the spectrum is 130% of the full scale of the figure! The pattern contamination is evident in all figures, but it is only severe in the case of Figure 8c. Here, the frequency is low and the spectral density is low. If one examines all the figures, it appears that the antenna-pattern-related dc component has a spectral density of about 2 m^2/Hz in the vicinity of 0.08 Hz; this would account for the apparent discrepancy in Figure 8c. Yet, there still may be a real low-frequency whitening due to second-order scattering effects (intermodulation products--see J); however, it is not possible with the present data to distinguish the real whitening from antenna-pattern contamination. One would need a much larger footprint to reduce the dc component. There does, on the other hand, seem to be evidence of second-order effects on the high-frequency side: these are manifest in the slightly more rapid roll-off of the radar spectrum. This apparent "droop" is related to (2.13) and has been predicted by J. (We will defer for the moment a discussion of the colocation errors.)

From these comparisons, we conclude that the measurements can be made with good spectral fidelity. But, what about absolute spectral levels? Let us check the measured alphas. How do they compare with (2.11)? An immediate check on the $1/L_y$ dependence is possible with files 89/2 and 89/3. The ratio of the altitudes is 9.3/4.5 = 2.07; the ratio of the alphas is 4.90/2.47 = 1.98 (a 4% difference). Thus, the asymptotic $1/L_y$ dependence is verified. Now, using (2.11) let us infer a mean-square slope from the measured alphas. Let us assume a nominal incidence angle of 13^o. Then, inverting (2.11), we obtain

$$\langle|\nabla\zeta|^2\rangle = \frac{2 \tan 13^o}{\left[\frac{L_y \alpha_{meas}}{\sqrt{2\pi}}\right]^{\frac{1}{2}} - \cot 13^o} \qquad (4.7)$$

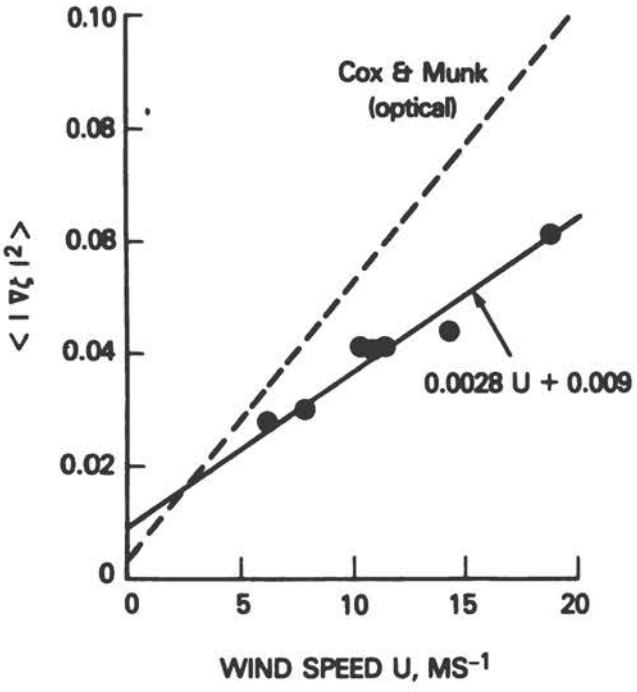

Figure 13 Mean-square slopes inferred from the measured alphas versus wind speed

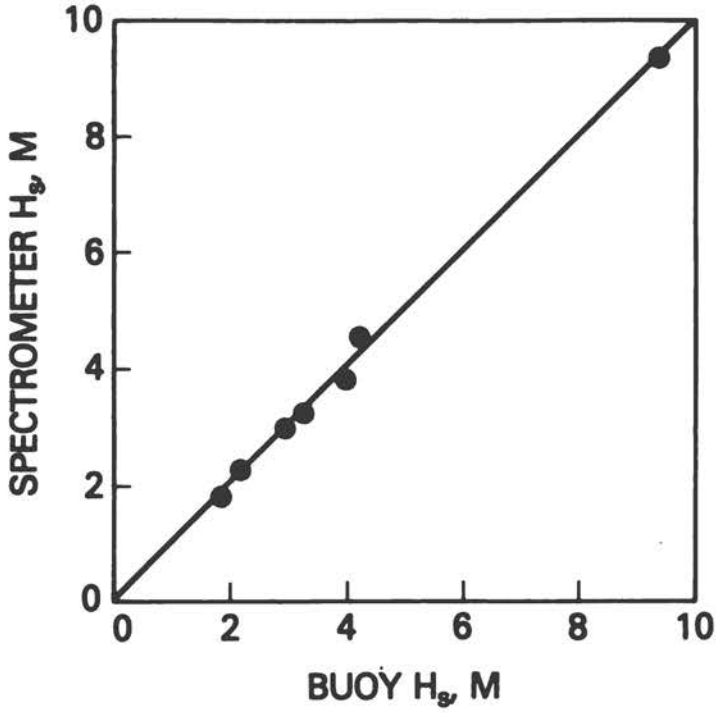

Figure 14 Radar-inferred versus buoy significant wave height (spectrometer mode). Data from adjacent files have been averaged together (cf. Table 2).

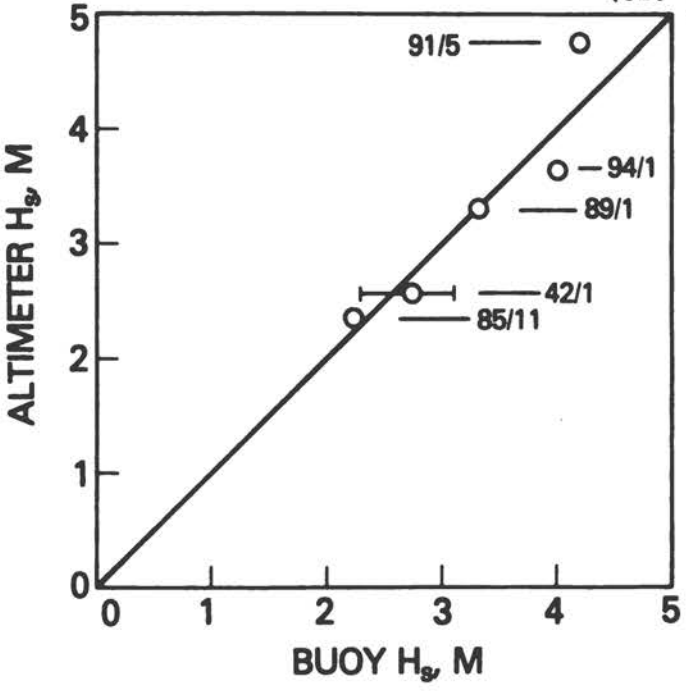

Figure 15 Radar-inferred versus buoy significant wave height (altimeter mode)

The inferred mean-square slope values are tabulated in Table 2 and plotted in Figure 13 as a function of the buoy-observed wind speed. No corrections were made for anemometer height or atmospheric stability. An eyeball regression yields the relationship

$$\langle|\nabla\zeta|^2\rangle = 0.0028U\ [\text{m s}^{-1}] + 0.009 \tag{4.8}$$

for the wind speed range of approximately 5-20 m s^{-1}. Equation (4.8) is in perfect agreement with the K_u-band scatterometer data analyzed by Wentz (1977), at least up to the largest wind speed (12 m s^{-1}) in Wentz's data set. In fact, Wentz's data are not plotted, because they are sensibly no different, and would only clutter the plot. Equation (4.8) also agrees with Wilheit's (1979) analysis of passive microwave data. It predicts slope variances that are $\sim$ 60% of the optical values reported by Cox and Munk (1954) and which, interestingly, lie between their "clean" and "slick" surface observations. Our inferred mean-square slope values (4.8) are thus consistent with our knowledge of what the K_u-band effective slopes should be and strongly support our conclusion that the tilt model solution (2.8) is a correct first-order relationship.*

Now let us use the regression result (4.8) in (2.11) to compute a "theoretical" alpha. The "theoretical" alpha can then be used to compute a "radar-inferred" absolute height spectrum and significant wave height. Table 2 is a tabulation and Figure 14 is a plot of the results for the "inferred" wave height for the seven independent cases analyzed. Over the wave-height range 1.9-9.4 m the mean difference between the radar-inferred and buoy H_s is 0.00 m (sic) and the rms difference is 0.16 m. This is truly remarkable considering that 1) we are using only a first-order, back-of-the-envelope theory, 2) our measurement geometry is not ideal (broad elevation beam width), 3) we have had to rely on external parameters (buoy wind speeds) rather than internal parameters (cross-section roll-off), and 4) the data are subject to sampling variability as well as geophysical variability (colocation errors). Some information as to the last source of error is available to us through the instrument's altimeter mode. The altimeter mode algorithm consisted of epoch realignment, and an iterative least-squares fitting of an error function to the leading edge of the average pulse return. H_s was computed from the measured temporal dispersion σ according to

$$H_s = [4c^2\sigma^2 - H_p^2]^{\frac{1}{2}} \tag{4.9}$$

where H_p = 4.91 m (compare with Fedor et al., 1979). The altimeter wave heights are shown in the last column of Table 2 and are plotted in Figure 15. The altimeter H_s show a positive correlation with the spectrometer mode minus buoy H_s residuals indicating that colocation errors are a significant component of the error budget. This probably

*A factor of 2 error in the computation of P_m from the FFT led to the wrong result for mean-square slope in Jackson et al. (1981).

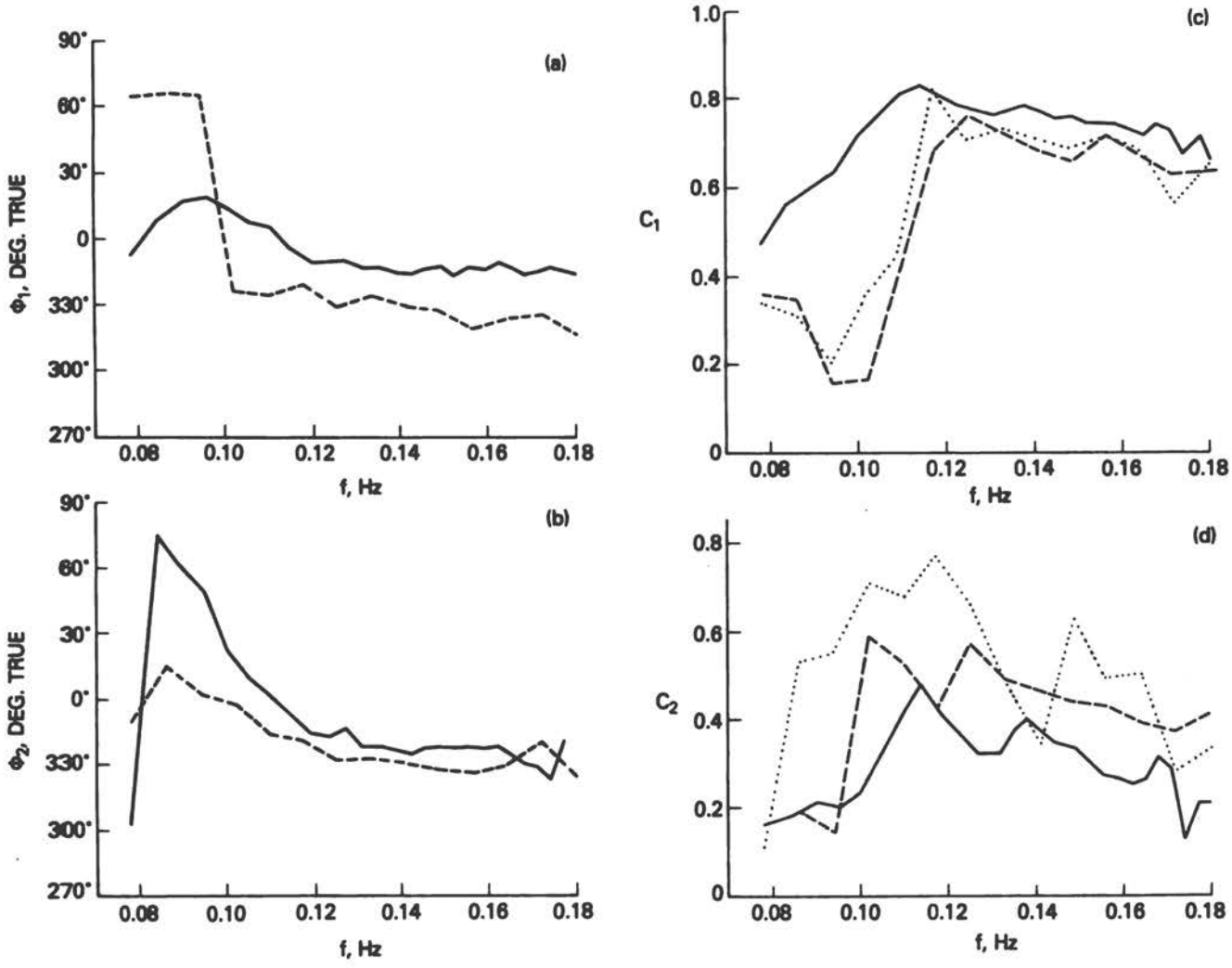

Figure 16 First and second harmonics of radar angular distribution compared to pitch-roll buoy data. Solid line (——) is from radar file 89/3; dashed line (----) is from average of five buoy records; and dotted line (····) is from buoy record at 2104 Z. Figures 16a and 16b, phases; Figures 16c and 16d, amplitudes.

explains the discrepancy in the bimodal spectrum comparison of Figure 12e. However, there does remain the possibility that the sensitivity coefficient is not truly isotropic. Data from future flights with an improved radome should enable us to resolve this question.

4.4 Directional Comparison

The single directional comparison available to us is with a pitch-roll buoy operated by Duncan Ross of NOAA's Miami Labs. The buoy was deployed from OWS PAPA in the Pacific. It produced five records in a several-hour period up to and including the time of overflight. Two radar files, 89/2 and 89/3, are available for comparison, but 89/3 is preferred because of its greater length, even though it is at the lower altitude. The directional height spectrum from 89/3 is shown in Figure 11d, and the nondirectional comparison is made in Figure 12d. Because of the basic 180° ambiguity in the radar spectrum, a true direction of wave travel must be assumed if first harmonics are to be compared. (As suggested by Prof. W. J. Pierson (personal communication), perhaps the most objective way to compare buoy and radar data is on the basis of the first two angular harmonics, since these are linearly related to the slope auto- and cross-spectra obtained from the buoy record.) To facilitate the comparison, the radar spectrum is set identically equal to zero in the half-space which the buoy indicated to be opposite to the direction of dominant wave travel. Because the sea is rather broadly spread in this case (apparently due to wind turning) and because there is swell running at $\sim 90^{\circ}$ to the dominant wave direction, this ad hoc procedure will necessarily result in some error, particularly at the low swell frequencies.

The amplitudes and phases of the first and second harmonics of the angular distribution are compared to the buoy data in Figure 16. The reason that there is a bias in direction is apparently due to the fact that the buoy's compass card had slipped, and true direction was figured after the fact from the general meteorological conditions. There is evidently good agreement in first-harmonic amplitudes from the peak to 0.2 Hz, but the second-harmonic amplitudes disagree by almost a factor of 2 over most of the range. Why? Our guess is that the problem is with the buoy, but the reader may judge for himself. A standard practice in the analysis of pitch-roll buoy data is to assume a model angular distribution function such as the following

$$D(f, \Phi) = \cos^{2s}[(\Phi - \Phi_o)/2] \qquad (4.10)$$

The first and second harmonics of this distribution can then be equated to the observed first and second harmonics to give two estimates, s_1 and s_2, of the spreading parameter s as a function of frequency (Cartwright, 1963). If the two s-parameters are identical, then the actual angular distribution is perfectly represented by the model function (4.10). Figure 17 is a plot of the two s-parameters for the radar data. They are practically equal over the entire range of

frequencies. This makes sense, since according to Figure 18, the radar data do appear to be consistent with a cosine-power distribution. But now, the buoy data do not appear to be consistent with a cosine-power model. This is apparent from Figure 19, which shows the radar data falling neatly on Cartwright's (1963) curve, while the buoy data scatter over a large area above the curve.

This consistency of the radar data versus that of the buoy data naturally inclines us to believe more in the radar results, especially as we are biased in that direction. Nonetheless, we should avoid drawing hasty conclusions. In truth, the disagreement here is not as great as Figure 19 might lead one to believe. First, there is agreement in the first harmonic and s_1 values. At the peak, $s_1 = 4.9$, which implies a half-power spread of 85°. Second, the half-power spread is not very sensitive to the s-value, at least for $s > 5$ or so. While the buoy s-values scatter considerably, they average about $s_2 = 10$ near the peak. This implies a spread of 59°, which, really, is not so far away from 85°. Further, the average of the two values, 72°, is quite close to the observed radar half-power spread of 67° at 0.114 Hz.

Still, we are skeptical of obtaining from buoys the kind of intercomparison data we need to gain a full understanding of the limits of accuracy of these radar measurements. We are looking forward to getting these intercomparison data from the NASA Surface Contour Radar (Walsh et al., 1981).

5. Conclusion

We have described a rather simple microwave radar technique for measuring directional wave spectra. We have shown that satellite measurements on a truly global scale are possible with this technique, and we have, in our opinion, provided a firm theoretical and experimental basis for the technique. While further aircraft experimentation is warranted and desirable, we are going to be limited by the constraints of the relatively low aircraft altitudes. That is, at aircraft altitudes in a near-nadir geometry, there is no way to avoid both a relatively broad beam width on the one hand and a relatively small footprint on the other. Both of these factors make it difficult to investigate second-order scattering effects: we may have the theory, but we will be unable to verify it satisfactorily. Without a space experiment, there is little reason to expand the theory of measurement further; that is, to go beyond Jackson's (1981) theory.

We do intend, however, to improve the aircraft radar system. For example, we are replacing the 12° nadir horn antenna with a much broader beam-width, standard-gain horn. This should permit accurate measurements of the isotropic cross-section roll-off and mean-square slope for better estimates of the first-order sensitivity coefficient. This type of measurement has been described by Hammond et al. (1977).

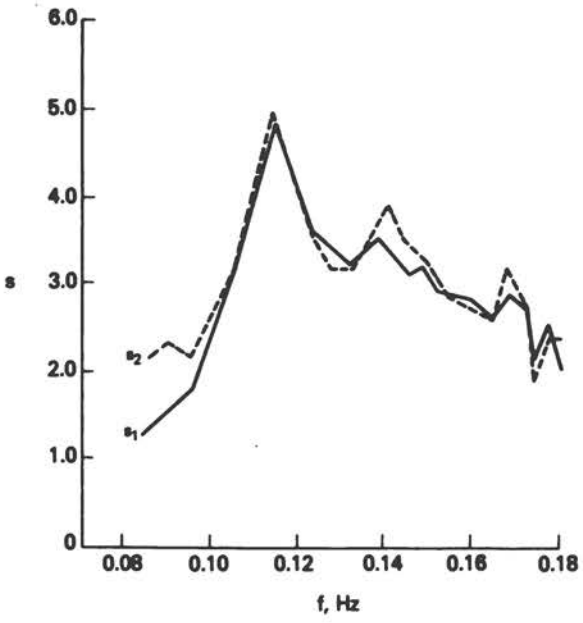

Figure 17 Radar-observed spreading parameters corresponding to the first and second harmonics shown in Figure 16

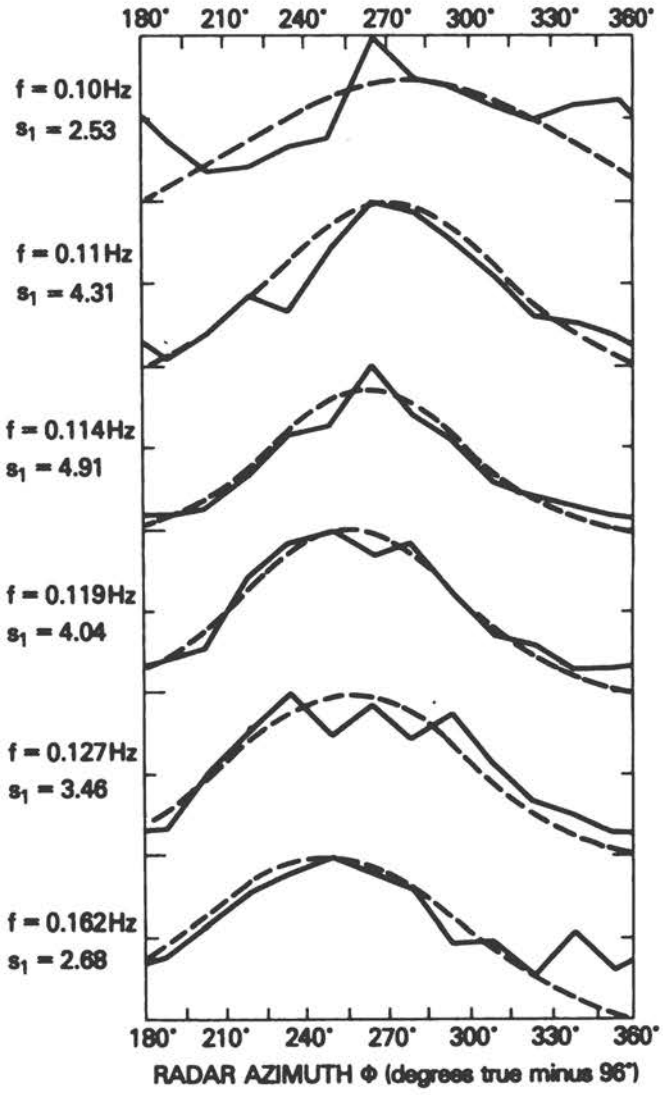

Figure 18 Radar-observed directional distributions (Tape/File = 89/3) compared to cosine-power distribution. The symmetrized radar distribution is set identically equal to zero between 0° and 180°.

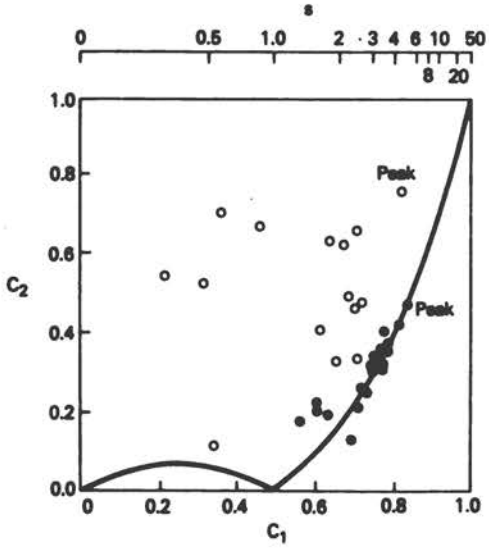

Figure 19 Radar (bullets) and buoy (open circles) first and second angular harmonic amplitudes compared with theoretical relationship of Cartwright.* The data, from radar file 89/3 and buoy record 2104 Z, are contained in the frequency range 0.078 Hz to 0.145 Hz.

*D. E. Cartwright (1963), "The Use of Directional Spectra in Studying the Output of a Wave Recorder on a Moving Ship," Ocean Wave Spectra (Englewood Cliffs, N.J.: Prentice-Hall), pp. 203-218.

Acknowledgments

Dr. J. E. Eckerman initiated the Goddard "Short Pulse Radar" program nearly a decade ago, and for many years he was the motivating force behind it. In 1974, he acquired the Geos-3 breadboard altimeter and hired one of us (W.T.W.) to make a working radar of it; subsequently, he hired another of us (F.C.J.) to figure out how and why it should be working. We can only hope that the accomplishment of the present work in some measure releases us from a nontrivial debt of gratitude.

The cooperation of the following individuals and institutions is gratefully acknowledged: P. Gloersen, NASA Goddard Space Flight Center; E. Peterson, NASA Ames Research Center, and the crew of the CV-990 aircraft, the Galileo II; S. Renwick, NOAA Data Buoy Office; S. Tryggstad, director, VHL River and Harbour Laboratory, Trondheim, Norway; and D. Ross and W. McLeish, NOAA Sea-Air Interaction Laboratory, Miami, Florida.

We thank T. Wilheit for a helpful suggestion; also, the contributions of J. McArthur, Applied Physics Laboratory, and C. Y. Peng, Science Systems and Applications, Inc., are acknowledged.

For the past three years this work has been supported by Supporting Research and Technology funding from the Oceanic Processes Branch of NASA Headquarters. We should like to thank W. S. Wilson and L. F. McGoldrick of the Oceanic Processes Branch for their support, and especially their patience in awaiting these results.

References

Alpers, W. and K. Hasselmann (1978), "The Two-Frequency Microwave Technique for Measuring Ocean Wave Spectra from an Airplane or Satellite," Boundary-Layer Meteorol., 13: 215-230.

Beal, R. C., P. S. DeLeonibus, and I. Katz, eds. (1981), Spaceborne Synthetic Aperture Radar for Oceanography (Baltimore: The Johns Hopkins University Press).

Blackmann, R. B. and J. W. Tukey (1958), The Measurement of Power Spectra (New York: Dover Publications, Inc.), p. 21.

Brown, G. S. (1978), "Backscattering from a Gaussian-Distributed Perfectly Conducting Rough Surface," IEEE Trans., AP-26: 472-482.

Cartwright, D. E. (1963), "The Use of Directional Spectra in Studying the Output of a Wave Recorder on a Moving Ship," Ocean Wave Spectra (Englewood Cliffs, N.J.: Prentice-Hall), pp. 203-218.

Cox, C. and W. Munk (1954), "Measurement of the Roughness of the Sea Surface from Photographs of the Sun's Glitter," J. Opt. Soc. Am., 44: 838-850.

Fedor, L. S., T. W. Godbey, J. F. R. Gower, R. Guptill, G. S. Hayne, C. L. Rufenach, and E. J. Walsh (1979), "Satellite Altimeter Measurements of Sea State--An Algorithm Comparison," J. Geophys. Res., 84: 3991-4002.

Hammond, D. L., R. A. Mennella, and E. J. Walsh (1977), "Short Pulse Radar Used to Measure Sea Surface Wind Speed and SWH," IEEE Trans., AP-25: 61-67.

Huang, N. E. and S. R. Long (1980), "An Experimental Study of the Surface Elevation Probability Distribution and Statistics of Wind-Generated Waves," J. Fluid Mech., 101: 179-200.

Jackson, F. C. (1981), "An Analysis of Short Pulse and Dual Frequency Radar Techniques for Measuring Ocean Wave Spectra from Satellites," Radio Science, 16: 1385-1400.

Jackson, F. C., W. T. Walton, and P. L. Baker (1981), "Directional Spectra from Air- and Spaceborne Radars," Directional Wave Spectra Applications, R. L. Wiegel, ed. (New York: American Society of Civil Engineers), pp. 299-314.

Johnson, J. W., W. L. Jones, and D. E. Weissman (1981), "Two-Frequency (Delta K) Microwave Scatterometer Measurements of Ocean Wave Spectra from Aircraft," Oceanography from Space, J. F. R. Gower, ed. (New York: Plenum Press), pp. 606-616.

Jones, W. L., L. C. Schroeder, and J. L. Mitchell (1977), "Aircraft Measurements of the Microwave Scattering Signature of the Ocean," IEEE J. Oceanic Eng., OE-2: 52-61.

LeVine, D. M., W. T. Walton, J. Eckerman, R. L. Kutz, M. Dombrowski, and J. E. Kalshoven, Jr. (1977), "GSFC Short Pulse Radar," JONSWAP-75, NASA TN D-8502.

Moore, R. K., L. J. Chastant, L. J. Porcello, J. L. Stevenson, and F. T. Ulaby (1975), "Microwave Remote Sensors," Manual of Remote Sensing, Vol. I, pp. 399-537, Am. Soc. Photogram., Falls Church, Virginia.

Tomiyasu, K. (1971), "Short Pulse Wide-Band Scatterometer Ocean Surface Signature," IEEE Trans., GE-9: 175-177.

Townsend, W. F. (1980), "An Initial Assessment of the Performance of the SEASAT-1 Radar Altimeter," IEEE J. Oceanic Eng., OE-5: 80-92.

Valenzuela, G. R. (1978), "Theories for the Interaction of Electromagnetic and Ocean Waves--A Review," Boundary-Layer Meteorol., 13: 61-85.

Walsh, E. J., D. W. Hancock, III, D. E. Hines, and J. E. Kenney (1981), "Surface Contour Radar Remote Sensing of Waves," Directional Wave Spectra Applications, R. L. Wiegel, ed. (New York: American Society of Civil Engineers), pp. 281-298.

Wentz, F. J. (1977), "A Two-Scale Scattering Model with Application to the JONSWAP '75 Aircraft Microwave Scatterometer Experiment," NASA Contractor Rpt. 2919, Contract NASI-14330, Dec. 1977.

Wilheit, T. T. (1979), "The Effect of Wind on the Microwave Emission from the Ocean Surface at 37 GHz," J. Geophys. Res., 84: 4921-4926.

REVIEW OF WAVE MEASUREMENT USING IN SITU SYSTEMS

Richard J. Seymour[1]

Introduction

The need to record wave climates, with data collected as frequently as several times a day for periods of years, has resulted in the development of a variety of wave-measuring instruments that can be mounted at a location and operated with little or no attention for very long periods. For reasons which will be noted, these instruments tend to be located either in rather deep water or very close to shore; few are placed at intermediate depths. In deep water, the instruments obtain wave data of greatest generality, particularly if the local depth is such that the wave-field intensity and direction have not been significantly altered by contact with the ocean bottom. These deep-water data, then, in theory, provide the input for predicting the wave field over a very broad area. The accuracy of the prediction, in practice, depends on the complexity of the intervening bathymetry and state-of-the-art techniques for estimating wave refraction, diffraction, and shoaling. Measurements made very close to shore--for example, just outside the surf zone--have very limited generality. Nevertheless, these data require little or no further projection, and thus minimize the errors in estimating what will happen to waves as they traverse the shelf. Measurements of waves at intermediate depths have the disadvantages of both deep and nearshore measurements and the advantages of neither. They are therefore seldom employed in the study of wave climates, although they may be of considerable interest to researchers studying wave transformations on the shelf.

Because of the obvious differences in the local environment, instruments to measure waves in shallow and deep regimes have taken divergent paths of development. Recently, however, the construction of fixed platforms in very deep water has allowed systems to be installed near the extremities of the shelf that were previously suitable only for nearshore use.

The details of the configuration and performance of in situ wave-measurement systems will be covered in three succeeding papers of these proceedings. Here, an overview is presented of the capabilities and limitations of in situ instruments as a group.

---

[1]Scripps Institution of Oceanography

In addition to categorization by the water depth at which they take wave measurements, a number of other natural groupings suggest themselves for classifying in situ instruments. Some configurations are capable of measuring only wave intensity (normally, by means of a time history of sea-surface elevation), without regard to the directional properties of the wave field. A second group is able to measure the directional distribution of wave intensity with varying degrees of resolution in frequency and direction space.

All the in situ instruments here mentioned that measure only intensity can be used more or less continuously, and are therefore suitable for wave-climate studies. Of those instruments that also measure direction, some are inherently unsuitable for continuous use, and some have not yet demonstrated this capability. The nearshore technique, for example, of using cinematography on a field of fixed wave poles, requires too much labor, and depends too much on visibility to be useful for any applications beyond occasional research. Directional buoys, now under development and demonstration, are not yet continuously operable. The in situ instruments here identified have been arranged by physical type within the functional framework set out in Table 1. Each general type will be discussed in succeeding sections.

Table 1 Classification of in situ wave instruments

	Wave Height Only	Wave Direction	
		Continuous	Short Term
Deep Water	Buoys Shipboard Recorders	??	Buoys
Near Shore	Bottom-Mounted	Arrays	Cinematography
	Surface-Piercing	Current Meters	

Wave-Measuring Buoys

Vertical Accelerometer Buoys

Vertical accelerometer buoys are a class of surface-following buoy, usually spherical in form, which are routinely moored in water depths

of 200 m and less. Typically, they return data by telemetry links to shore or to the GOES satellite. They measure wave intensity by double-integrating the output of an accelerometer held vertical by a pendulum to produce the required time history of buoy heave motion. The statistics of the buoy heave are then related to the wave statistics through a linear transfer function. There are two general methods to stabilize the accelerometer. In the first (Waverider), the pendulum is contained entirely within the spherical float so that the buoy need not be stabilized. In the second (Ahima, Wave-Track), the buoy itself is stabilized in the vertical by an external pendulum. Buoys of the first type are used for deep-water data in the national wave-climate-measurement programs of Canada, Australia, the United States, and several other countries.

Suspended Pressure Sensor

A variation of the accelerometer buoy measures buoy heave with a pressure sensor suspended at a considerable depth below the buoy. If the mean depth of the pressure gauge is such that the horizontal variations in pressure caused by waves are negligible, then the gauge's time history of pressure is proportional to that of buoy heave.

Directional Buoys

The first directional buoy was developed in Great Britain, and has been refined by researchers in Japan and the United States. Usually in the shape of a discus, it follows the tilt of the sea surface, and may or may not follow changes in its elevation as well. These buoys are unmoored, typically, because they tend to capsize in large waves if restrained.

Data are normally recorded on board: two components of tilt and heave and a compass heading. These data are sufficient to provide estimates of principal directions for each frequency interval. Because they are unmoored, directional buoys of this type can be used only for intermittent research activities, such as providing sea truth for remote sensing techniques.

A second class of direction-measuring buoys--moored, with telemetry systems, and with the promise of continuous operation--is being developed following the principles of the vertical accelerometer systems. As previously noted, they are not yet operational.

Shipboard Recorders

A shipboard recording system that employs an accelerometer to sense the ship's vertical motion and a pressure gauge to sense waterline changes has been installed as an *in situ* instrument in very deep water on

weather ships. It has been well intercalibrated with Waverider buoys and provides deep-sea data not normally attainable with single-purpose instruments.

Bottom-Mounted Height Sensors

The most commonly used bottom-mounted system is a pressure sensor that provides frequency-domain statistics which can be related to sea-surface-elevation statistics by linear theory. The use of the instrument is narrowly prescribed by depth. Higher frequencies are greatly attenuated with depth, but limited by the signal-to-noise ratio in shallow depths. In areas with great tidal extremes, the depth window can be quite small. Research programs demanding high resolution normally use differential gauges that remove all or part of the static head from the dynamic range. Cheaper and more reliable absolute gauges have been found acceptable in many wave-climate studies.

Upward-looking sonar has been used in Japan as the preferred bottom-mounted system. It eliminates the depth restrictions of the pressure sensor, but introduces calibration errors owing to temperature, salinity, and bubble content.

Surface-Piercing Wave Staffs

The first wave gauge was undoubtedly a pole with stripes on it, and these staffs are still used for certain applications in which visual observations are acceptable.

Automatic and remote recordings were made possible by the addition of electrical contacts at fixed locations to produce step gauges.

Modern wave staffs make continuous measurements of water elevation by determining changes in resistance, capacitance, or travel time.

Fixed-Orientation Directional Systems

Arrays

Directional arrays are groups of individual sensors, usually pressure gauges or wave staffs, arranged to extract directional information about the wave field from the phase correlations among the elements. The design of these arrays is somewhat artistic, attempting to balance those sacrifices in frequency and directional resolution necessitated by economics, and guided by the assumed characteristics of the wave climate. Arrays take the form of linear and polygonal configurations. In general, the more elements, the better the resolution; the scale is determined by the the longest wavelengths the configuration can resolve. Given enough elements, arranged with appropriate spacings, an array can produce a very creditable directional spectrum. A compact

four-element square array is used extensively in the United States, and has directional resolution that compares favorably with that of the tilt buoys. It also measures two components of sea-surface slope.

Two-Axis Current Meters

The current meter most commonly used to determine the directional properties of waves is the electromagnetic flow meter. This instrument produces directional information comparable to that of the square slope array, but is more difficult to maintain. It senses voltages induced by the flux of a conductor, seawater, through a magnetic field produced in the sensing head of the flow meter.

A second class of current meters measures two components of the drag force on a sensing head that ranges in configuration from a sphere to a nylon brush. Since drag is not linearly related to velocity, cross-spectral analysis is required to sort out the unbiased principal wave directions.

Cinematography

Particularly in Japan, a technique has been used consisting of a large number of striped poles arranged in a grid and photographed with a motion picture camera. The wave heights at each pole are measured frame by frame to provide a three-dimensional representation of the local sea surface. In addition to containing sufficient data, in theory, to construct a directional spectrum, the data set also provides a look at spatial inhomogeneity, a benefit that may offset the tremendous effort of digitizing the data.

Status of *In Situ* Systems

Papers following this brief summary address the capabilities and limitations of the more important *in situ* wave-measurement systems for various applications, and the analytic techniques used to enhance the capability of these systems or compensate for their limitations. The status of surface-mounted sensors is reviewed by Parker; Le Blanc and Middleton present the results of analyzing pitch-roll buoy data to yield directional spectra; and Forristall gives recent results for subsurface wave-measuring instruments.

WAVE MEASUREMENTS USING SURFACE-MOUNTED INSTRUMENTS

A. G. Parker[1]

Abstract

Described in this paper are some of the design considerations for obtaining wave measurements, and in brief, the techniques available for wave height and direction measurements using surface-mounted sensors.

Introduction

The reasons for needing to know wave-climate characteristics at a particular location are extremely varied. They range from the workboat captain's "There's waves higher than x meters out there and my contract says I don't have to go out!" to the requirements for operating offshore rigs implied by the limits on operating equipment and the need to know the loads imposed, to the needs for data of engineers designing structures for specific locations, and those of researchers who need accurate and diverse wave information--often from very remote sites--to understand oceanic processes.

With such a variety of requirements and users, it is hardly surprising that a diverse selection of instruments is available to provide wave information. The instruments present data from different sources, in many ways, and with different degrees of accuracy.

It is because of this diversity in requirements and solutions, and the confusion that often arises as a result, that this meeting has been called. I do not think that we will fully solve any of the problems before us. No simple answers are possible for what are very complex problems. Rather, I hope that by discussing the problems and the available options we will all leave with a better understanding of the advantages and disadvantages of various techniques, and the directions in which modern technology is advancing in the field of wave measurements. In the past decade or two, we have come a long way, but there is still a long way to go before we can say that we understand to our satisfaction any aspect of wave measurement.

In this paper, I concentrate on measurements using sensors mounted at the surface. The original request was for a paper on surface-piercing gauges, but sensors are now available that are mounted close to the surface yet do not pierce it. Since these are part of the same family as surface-piercing gauges, it is sensible that they should be included.

---

[1]Oceanographic Instruments Section, National Maritime Institute, England

It is not my intention to go into the technical details, problems, and advantages of every available sensor, or of all the kinds of sensors, but to discuss in general the problems and requirements of wave measurements made at the surface, and how these are met by various types of instruments.

Planning: What Measurements, When?

Long before any specific instrument is chosen, considerable thought must be given to answering the above questions. It is rare for marine data gathering trials to be simple. Most are complex operations involving considerable expertise, equipment, analysis, and finance. Time spent in planning is therefore well worthwhile.

First, one must ascertain what results are required, including their degree of accuracy, frequency range, sampling frequency, the periods for which data are required, and the total period during which data should be gathered. The workboat captain wants to know, in real time, the maximum (or significant or rms) wave height, requiring accuracy of about 10 percent, and often no permanent record.

At the other extreme, researchers need highly accurate long-term data, all recorded in a manner suitable for easy transfer to a computer. In the middle, the rig operator needs real-time data, perhaps already processed, on which to base engineering decisions. As critical as knowing the data is knowing the penalties that may be incurred by missing measurements, or by relying on those of decreasing accuracy.

Knowing the kind of results required, the methods of data analysis can be determined. The following questions about the physical aspects of analysis should be considered together with those of the mathematical aspects. Is a computer or microprocessor required for on-line analysis? Should raw data be recorded for later analysis? Is analysis needed, or will a digital/analog display suffice? If the data are on a paper chart, what is the intended use of the chart?

With the programs for data analysis established, it should be possible to determine the program necessary to acquire the data. Then, and only then, can the choice of sensors, and of conditioning and recording equipment be made.

Considerations in Choosing the Sensor

After these initial stages in planning, consideration turns to the site at which the wave data must be obtained, since the site will restrict the choice of sensors. Some of the questions that should be raised at this point include the following:

- Is a structure available at the site?
- If so, can a sensor be mounted on it?
- Will a sensor at that site be vulnerable to accidental damage or vandalism?

- What sort of power supply is available?
- How accessible is the structure?
- Is it manned?
- Is it of a size and shape that may alter the local wave pattern?
- If no structure is present, can one be installed?
- If not, is the site suitable for buoys?
- If so, what type of buoys?
- How far away is the nearest structure or the shore?
- What is the prevailing physical environment?
- What sort of wave climate characterizes the site?
- What is the water depth?
- What is the current?
- Is the area polluted?
- If so, by what type of pollution?
- What is the local topography, and will it affect the measurements?
- Is radio transmission necessary?
- If so, will there likely be transmission interference?

If the first two questions can be answered "yes," then it is almost certain that the method of measurement chosen will involve an instrument mounted at the surface. Even if they cannot, however, answers to the other questions might well indicate that surface-mounted instruments on custom-built structures or buoys are preferable to, say, satellite or seabed instruments.

Once the survey of the measurement site is complete, the most suitable sensor can be selected.

Choice of Sensor

Any sensor or measurement system must fulfill specific requirements, but in most cases, it should meet at least the following specifications. (Parker, 1978):

- It must be durable, surviving mechanical loads, corrosion, fouling, and other processes.

- It should selectively respond to the aspect of the environment it is designed to measure, remaining insensitive to all other aspects of the environment. If it does respond significantly to another environmental feature, this response should be well understood and monitored.

- Its response characteristics should not change significantly during the measurement period despite large changes in the environment.

- Its calibration should be simple, and calibration in laboratory conditions should also be valid at sea. Calibrations done at sea are very expensive and difficult to do with accuracy.

- It should be easy to check and service on location.
- It should measure the target parameter accurately.
- In some cases, it should consume little electrical power.
- It should be relatively inexpensive to replace, since by the end of the measurement period (and often before), it will be lost or useless. Initial cost is only one consideration, however, since the cost of sending a team to a remote location to replace an instrument that has failed, or whose calibration has drifted, is often many times greater than the instrument's initial cost.

Unless such specifications are established and met, it is all too easy to end up with instruments that are wholly unsuitable for the job. We probably all know of cases in which instruments have not been chosen because of their suitability for a particular task, but rather because, "We've already got one of these so we can use that," or "We can get one of those delivered within x weeks for only y dollars," or "I've always wanted to try one of these, let's see what it's like on this job." Almost invariably, choices made on these bases fail miserably.

Surface-mounted sensors (Driver, 1980; Ribe, 1979; Pitt, 1980) fall conveniently in six groups: visual, electrical, acoustic, float, optical, and radar.

Visual Observations

The use of visual observations is probably the most common, and at the same time most underrated way of obtaining wave data. Visual observations have been routinely obtained from several thousand ships since 1949, and a great amount of data is already available. For example, Figure 1 (Hogben, 1980) shows the number of visual observations in the North Sea, compared with the number of instrumented data stations. An indication of the accuracy of these data for determining significant wave height can be obtained from Figure 2 (Hogben and Lumb, 1967).

If data on significant wave height are required, then the use of a human observer might be seriously considered. Visual observations are a valid way of obtaining wave data and should be treated as such. A considerable amount of time and expense can often be saved by using an observer or previously obtained data of this type--if not for the main data collection program, at least to provide baseline data for the main program.

Electrical

Virtually all the truly surface-piercing instruments--that is, those that are always partly above and partly below the surface of the water--are electrical sensors. This type of sensor detects the location of the surface by using it to change the electrical

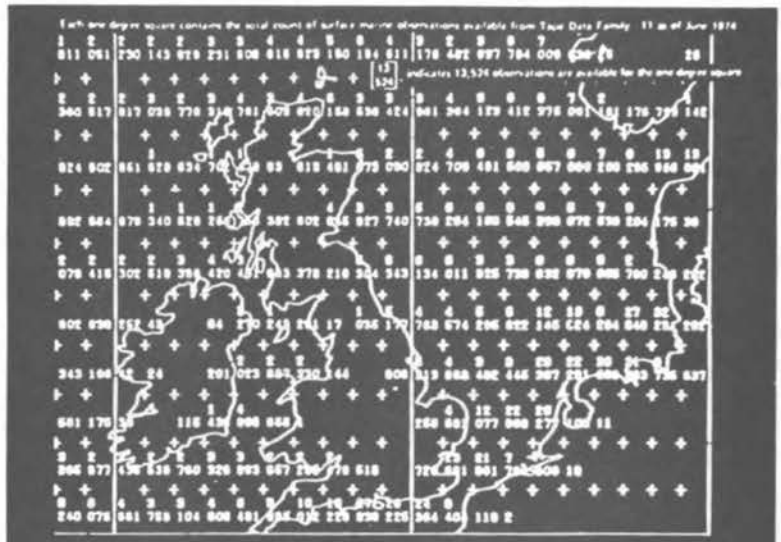

Visual Observation Count Chart for TDF11 Tapes:
(North West European Waters - Enlarged section from global charts available from the National Climatic Center, Asheville)

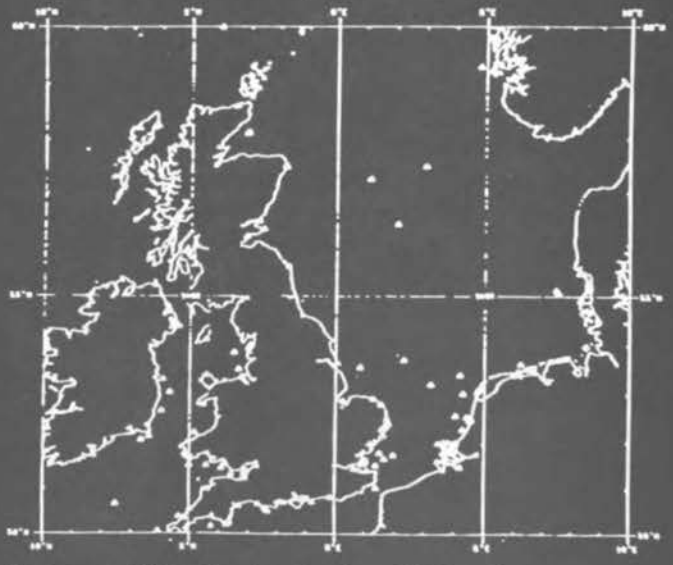

Instrumental Data Station Map from MIAS Catalogue:
(North West European Waters - The catalogue also contains a world map)

Figure 1 Visual observations versus instrument data

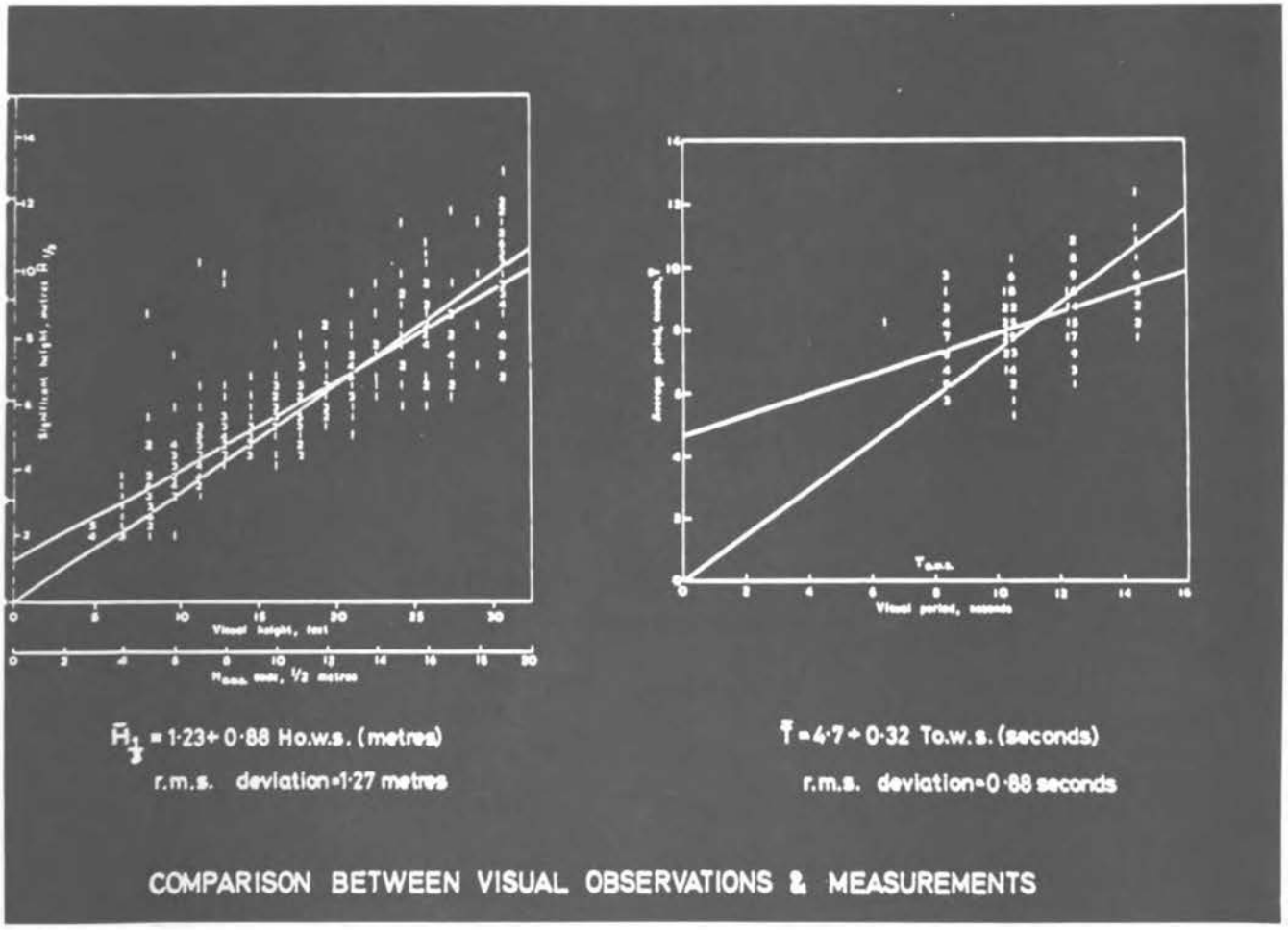
Visual height, feet
$\bar{H}_{\frac{1}{3}}$ = 1·23 + 0·88 Ho.w.s. (metres)
r.m.s. deviation = 1·27 metres
Visual period, seconds
$\bar{T}$ = 4·7 + 0·32 To.w.s. (seconds)
r.m.s. deviation = 0·88 seconds
COMPARISON BETWEEN VISUAL OBSERVATIONS & MEASUREMENTS

Figure 2

characteristics of a circuit normally either resistive, capacitive, or wave guide.

Resistive In its simplest form, a resistive staff consists of a single resistance wire vertically piercing the sea's surface so that the wire is neither totally immersed nor totally dry. AC voltage is supplied to the ends of the wire, and the resistance of the wire is measured by connecting it into, for example, a bridge circuit. Seawater wetting the wire shorts out the lower section of the wire; thus, the resistance of the wire varies linearly with the length of wire immersed. AC voltage is used to prevent polarization of the water. The frequency used is normally of the order of 1 kHz, which is rather surprising, since frequencies of 50-60 Hz, or even lower, are sufficient to prevent polarization and are more readily available.

Since the resistance of the wire is inversely proportional to its cross-sectional area, the resistance change per length immersed can be increased by using a smaller-diameter wire. However, the finer the wire, the more vulnerable it is to damage, so it is often mounted on an insulated straining member. Corrosion and fouling (either by pollution or by the growth of marine organisms) will change the resistance between the wire and the sea, and will therefore affect the calibration. The finer the wire used, the greater will be changes owing to contamination. To improve its sensitivity without making it too fine, the wire can be helically wound onto a straining member, greatly increasing the length of wire immersed per meter change in water level. An example is the Nova Scotia staff, shown from an unusual viewpoint in Figure 3, looking down from a research tower.

Because of their susceptibility to fouling, these types of staff should be used only when regular maintenance is possible. If regular cleaning is not possible, stepped resistance staffs can be used. These use a resistance ladder network, with the nodes of the ladder connected to the sea by closely spaced electrodes. Thus, standard precision resistors, chosen to give good signal levels, can be insulated from the sea and connected to it only by the electrodes. The resolution of this type of staff is dependent on the spacing between electrodes.

Another version, exemplified by the Etrometa BV, uses pressure switches activated by water pressure in place of the electrodes of the stepped gauge. A further refinement is the use of a resistance element and a contact strip encased within a flexible waterproof sheath. As the water level rises, pressure on the sheath forces the contact strip onto the resistance element, shorting out a part of it. The Seawave Recorders Metritape (Figure 4) is an example of this type of instrument.

Since resistive staffs depend solely on the length of wire immersed and not on any electrical field effect, the tension applied to the wire need not be very great, but the wire must be held taut enough to prevent wave-induced vibrations.

Figure 3 Nova Scotia wave staff

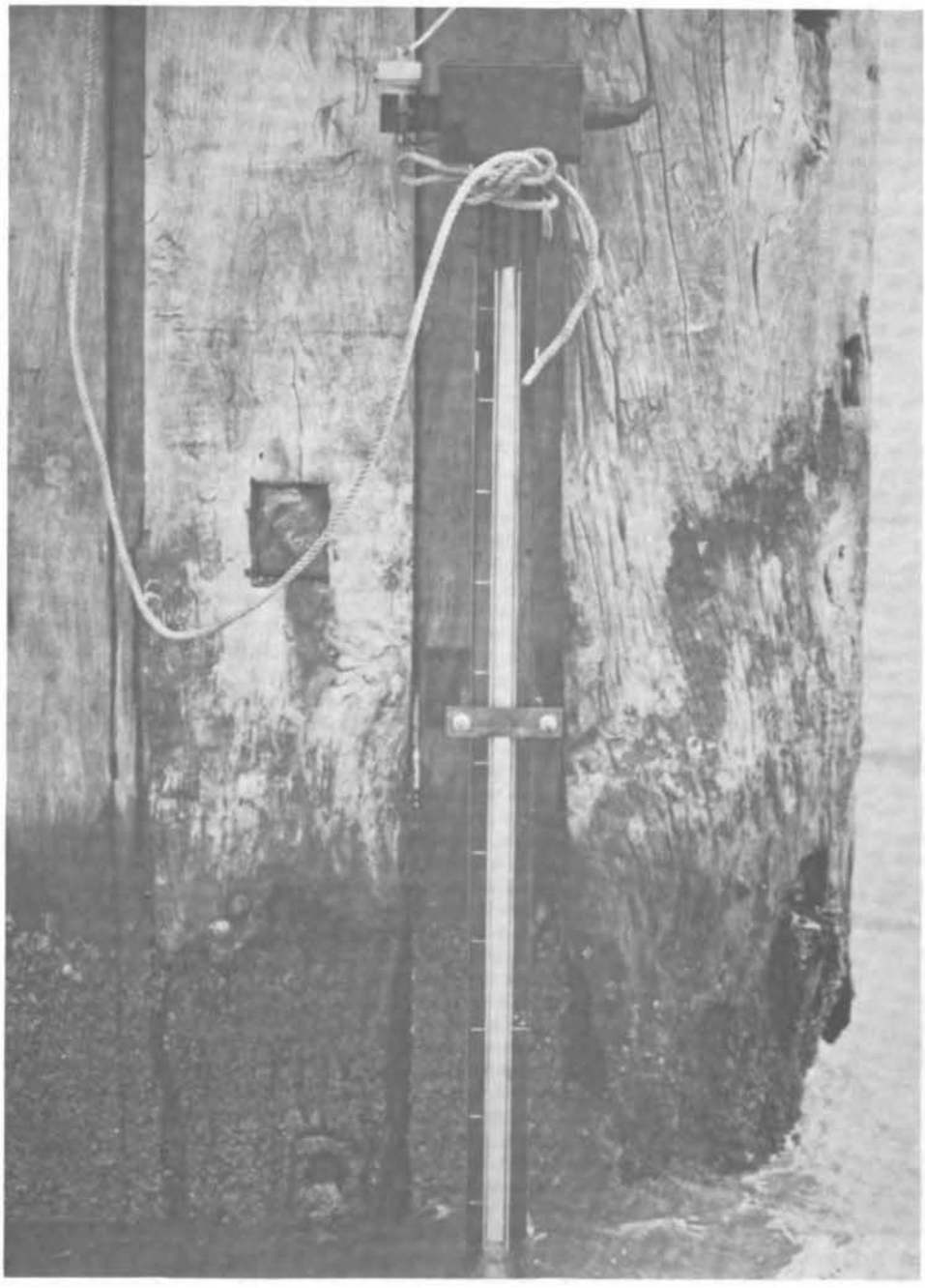

Figure 4 Seawave Recorders Metritape, a resistive wave staff

This type of gauge is very attractive, as the measurement of resistance is a straightforward technique, which, combined with the wire characteristics, makes a linear instrument that is accurate yet inexpensive. The type of instrument is not immune to fouling: Figure 5 shows the instrument pictured in Figure 4 after 2 months' use.

Capacitive The most common form of capacitive sensor (for example, the Comex, shown in Figure 6) uses a single insulated conductor mounted vertically and partially immersed. The conductor, powered by AC voltage, acts as one plate of a coaxial capacitor, with seawater forming the other plate. The insulation material is the dielectric. Thus, the capacitance of the staff is proportional to the water level around the staff. The thinner the insulating material, the greater the capacitance change of the instrument with depth, but also the more fragile it becomes, and the more susceptible to changes in the dielectric constant owing to an oil film or fouling.

The varying capacitance of the staff can be used as part of the tuning circuit of an oscillator. Thus, as the water level changes, the output frequency of the oscillator changes. Modern electronics enable very accurate measurement of small frequency changes; thus, a robust staff can be assembled with a thick layer of insulating dielectric material, since quite small changes in its capacitance can be converted into small but accurately measurable frequency changes.

Wave Guide Probably the most widely known and used of the wave-guide staffs is the Baylor Wave Gauge. This instrument uses two parallel, vertical cables of stainless steel wire piercing the surface, which are held under considerable tension to minimize their movement. An electromagnetic wave at 0.6 MHz is transmitted down the cables and reflected from the water surface. The standing wave ratio of the signal is measured; it is proportional to the length of the nonimmersed staff.

A coaxial transmission line staff has been developed by Zwarts in Canada. It uses a central conductor tube with a perforated tube (allowing the water level to rise and fall within) that is separated from the conductor tube by insulated spacers. Electromagnetic pulses travel down the annular space inside the wave guide and are reflected back by the water surface. The coaxial transmission line is used in the tuning circuit of a Gunn-diode oscillator, and the period of the output pulse is proportional to the nonimmersed length of the staff.

Obviously, wave-guide staffs are electrically more complex than resistive ones, and their selling price reflects this. However, they tend to be less prone to contamination and can be made much more robust.

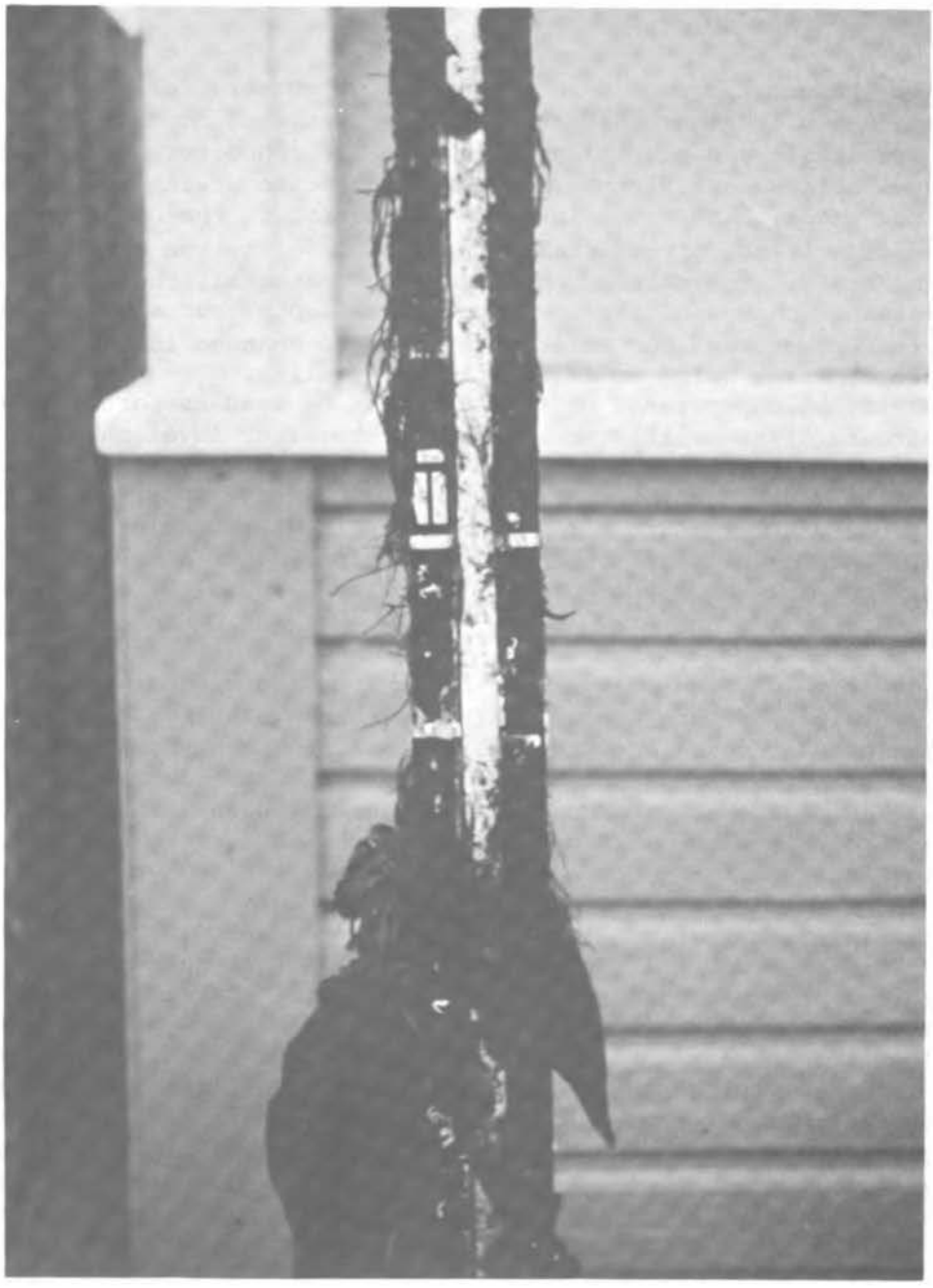

Figure 5 Biofouling of wave staff: two months' use

Except in extreme conditions, such as in the aeration produced by breaking waves or wetting of wires by blown spray that causes errors, electrical staffs have very good response characteristics. They can be used to measure a wide range of frequencies, including those of tides and surges, they are accurate, generally of good long-term stability, relatively easy to check, and usually inexpensive. However, because some portion of these instruments is always immersed, they suffer from corrosion and fouling, and are particularly vulnerable to damage from floating objects, such as debris or supply vessels. They must be regularly checked and cleaned. Divers are normally required for installation and maintenance procedures, leading to considerable delays and costs.

Acoustic

This type of instrument is essentially an echo sounder that works in air instead of water. A transmitter/receiver crystal mounted above the water surface transmits a pulse of acoustic energy in a narrow beam down to the surface and detects reflected echoes. The transit time for the pulse is proportional to the distance between the transducer and the surface, and to the speed of sound in air (VA). Since VA is only about 340 m/s, the transit times are relatively easy to measure. Moreover, VA for dry air depends only on the square root of absolute temperature, and over normal atmospheric ranges, the effects are small and easily corrected. Humidity causes very small alterations, and is almost invariably ignored.

This method would therefore appear very attractive. It has been used quite widely (with pulses in the ultrasonic band, at about 10 kHz) for measurement of levels in tanks and in tide gauges. However, the attenuation in air of acoustic pulses is high, and increases rapidly with frequency. At about 40 kHz, the maximum distance to a surface that can be measured with a simple low-power system is about 10 m. To extend the range, pulses of sonic frequency must be used, but this can lead to errors of up to 20 cps, depending on how many cycles of the returned echo are received before the trigger level of the electronics is reached. At this level, errors increase with decreasing frequency.

Because of problems in getting higher ranges and narrow beam widths, and because of loss of signal in extreme conditions, this type of instrument is not widely used for measurements of ocean waves.

Float

A widely applied method of measuring tides and levels in tanks relies on a float that rises and falls with the liquid level and that drives a mechanical recording system by a connecting cable. At least one version of this type of gauge (Van Essen BV) has been adapted for wave measurement by mounting the float in a perforated tube where its level rises and falls with the waves. Because of its large mechanical movements and the maintenance such a device requires, it is probably not suited to many wave-measurement needs.

Optical

Over the last few years, several wave-height instruments have appeared on the market that use laser-based sensors mounted above the surface. The lasers, which normally operate in the infrared or visible spectrum, project a very narrow beam of collimated light downward to the sea surface. Photo-detectors are used to pick up the reflections.

Two principal systems are used. In the first (e.g., EMI and Krupp Atlas), pulses of light are transmitted and the time until the reflection is received is measured (see Figure 7). In the second, a continuous beam is amplitude-modulated at a set frequency and transmitted. The transit time can be determined by measuring the phase change in the modulated signal between the transmitted and the reflected light.

Ideally, the measurement function of this type of instrument should not be affected by environmental conditions or time, as the speed of light is constant, and it should not require calibration or checking to preserve accuracy. Correct operation and alignment can be checked simply by introducing a reflective plate into the beam at a known distance from the head.

As the speed of light is approximately 3×10^8 m/s, the transit times are very short; thus, the electronic circuits must have extremely fast rise times. To obtain resolutions of the order of 0.1 m, timing must be accurate to at least 0.3 nanosecond. The use of lasers and very high-speed electronics for processing makes these devices much more expensive than their surface-piercing counterparts. However, the considerable advantage of having all of the sensor mounted well above the water, and in a position where it is readily accessible for maintenance or replacement in the event of malfunction, often outweighs the disadvantage of higher initial cost.

The pulsed type of instrument has proved very successful, progressing recently from the status of research tool to that of routinely installed monitoring equipment. It is not as likely as a continuous-beam instrument to pick up the stray reflections from the surface that introduce errors, although both types are probably subject to error in very calm conditions, in horizontally driven rain or fog, or when the tops of the waves are aerated.

Radar

In principle, radar or radio altimeter devices (e.g., Plessey or SAAB) are very similar to the laser devices, except that they reflect microwaves rather than light waves from the sea surface. Normally, either frequency-modulated or pulsed types of transmission are used. A prototype system has been developed by the National Maritime Institute and Plessey.

The advantages and disadvantages of these systems are similar to those of optical instruments, with the exception that a microwave transmitter may be less susceptible to contamination than an optical lens. Radar instruments are generally more expensive than optical instruments.

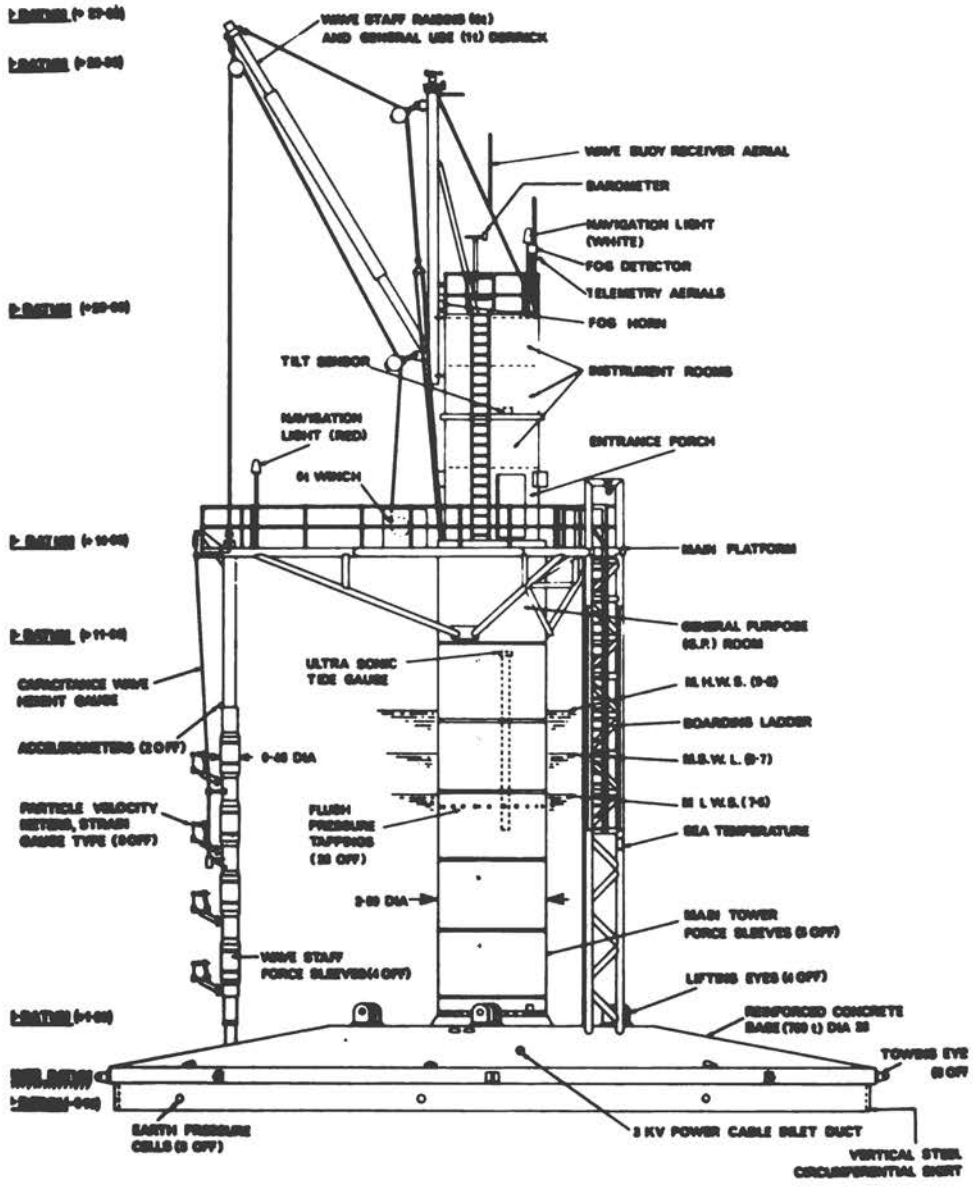

N.M.I. CHRISTCHURCH BAY TOWER

Figure 6 Capacitive wave gauge on instrumented platform

Figure 7 Laser-based system for wave-height measurement

Other Types

If a structure is not available on which to mount a wave sensor, there are two options: to install a structure or to use buoys. Close inshore, the former might well be feasible and could take the form of a fairly simple piled pole, on which any of the sensors described here could be used. Farther offshore, the use of buoys is probably indicated.

There are four types of buoys that might be selected:

- Small dedicated wave-height measuring buoys, such as Waverider, Wavecrest, or Wave Track, that use an accelerometer heave sensor.
- Much larger surface-contouring buoys, such as Marex or DBl, used to gather a range of oceanographic and meteorological data, including wave data, normally from an accelerometer heave sensor.
- Spar buoys designed to float vertically in the water and remain insensitive in heave to wave motions. Any of the previously described sensors can be mounted on these buoys.
- Shipborne wave recorders, such as that designed by the Institute of Oceanographic Sciences, consisting of accelerometers to measure longer waves and pressure units to measure the shorter ones, each of the two pressure transducers being mounted on either side of the ship 1-3 m below the water line.

Wave Direction

Considerable interest has been expressed for many years in directional wave measurements, but there are still no operational techniques that give satisfactory results. Part of the problem, I feel, is that many of the users who need directional information cannot really specify what they want. Do they merely want a measure of predominant wave direction (whatever that might be), or do they want directional wave spectra? If so, to what angular resolution? Until these questions are resolved, directional sensors are unlikely to move out of the arena of research into general production and use. However, it is worthwhile to review some of the techniques.

Predominant Direction

If the most basic of directional information is required, at least four methods are available to obtain it: visual observations, spar-on-its-side buoy, a two-buoy wave buoy, and a structure-mounted horizontally

scanning radar. As with wave-height measurements, the use of a good observer is often underrated. Quite accurate directional information can be obtained from visual records. Endeco has produced a spar buoy (the second method) that floats on its side and is moored at its center. This system, in the absence of current, aligns along the crests of the predominant waves for certain wave periods. The addition of an accelerometer sensor will yield wave height as well as direction. Third, one of the mooring options for the NBA Wavecrest buoy is for the active buoy to be moored to another surface buoy, which is conventionally moored to the seabed, as in Figure 8. In the absence of currents, this "dumbbell" arrangement will align normal to the crests of the predominant waves, so the addition of a compass will give the predominant wave direction. Fourth, much useful information can often be obtained with a standard centimetric, low-power, microwave radar unit with a slow scan rate, adjusted to emphasize the sea clutter, rather than to suppress it. With a little training, it is relatively easy to determine predominant directions from the display, or from Fourier analysis of the presented data.

Directional Spectra

To obtain spectral information, a minimum of three measurements must be taken and used to determine the first five coefficients in a finite Fourier series for directional wave energy. The way measurements are obtained is not critical. They may take any of the following forms, for example:

- Measurement of three heights from three staffs (any of the staffs described could be used) mounted in a triangular pattern, with the spacing between the staffs determining the wave frequency range for which the measurements will be effective.

- One height measurement from a staff and measurements of two horizontal components of particle velocity in the waves, or two horizontal components of force imposed on the structure.

- Full three-dimensional measurement of the particle velocities near the surface.

- One height measurement and two orthogonal measurements of local wave slope. It is this system, as in buoys outfitted with pitch, roll, and heave sensors, that has proved most successful (e.g., those manufactured by IOS, Marex, Datawell, Nereides, and Endeco). A prototype system is illustrated in Figure 9. However, one frequently forgotten feature of most of these buoys is that the signal from the accelerometer heave sensor normally used has phase lags of 300^{o}-360^{o} depending on frequency, but the pitch and roll signals do not. Data processing techniques should allow for these differences.

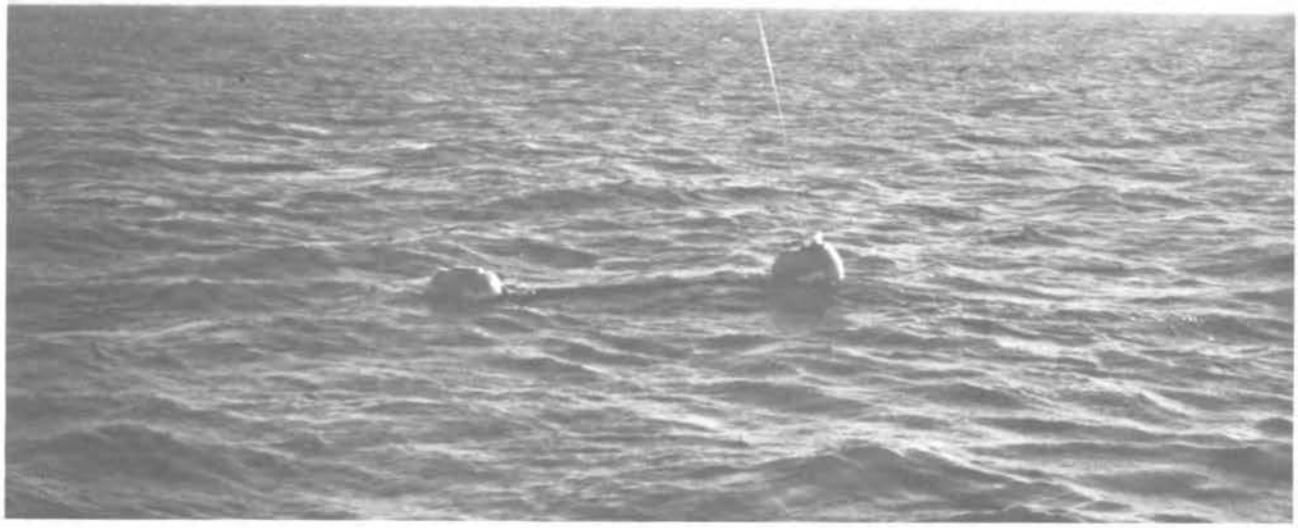

(a)

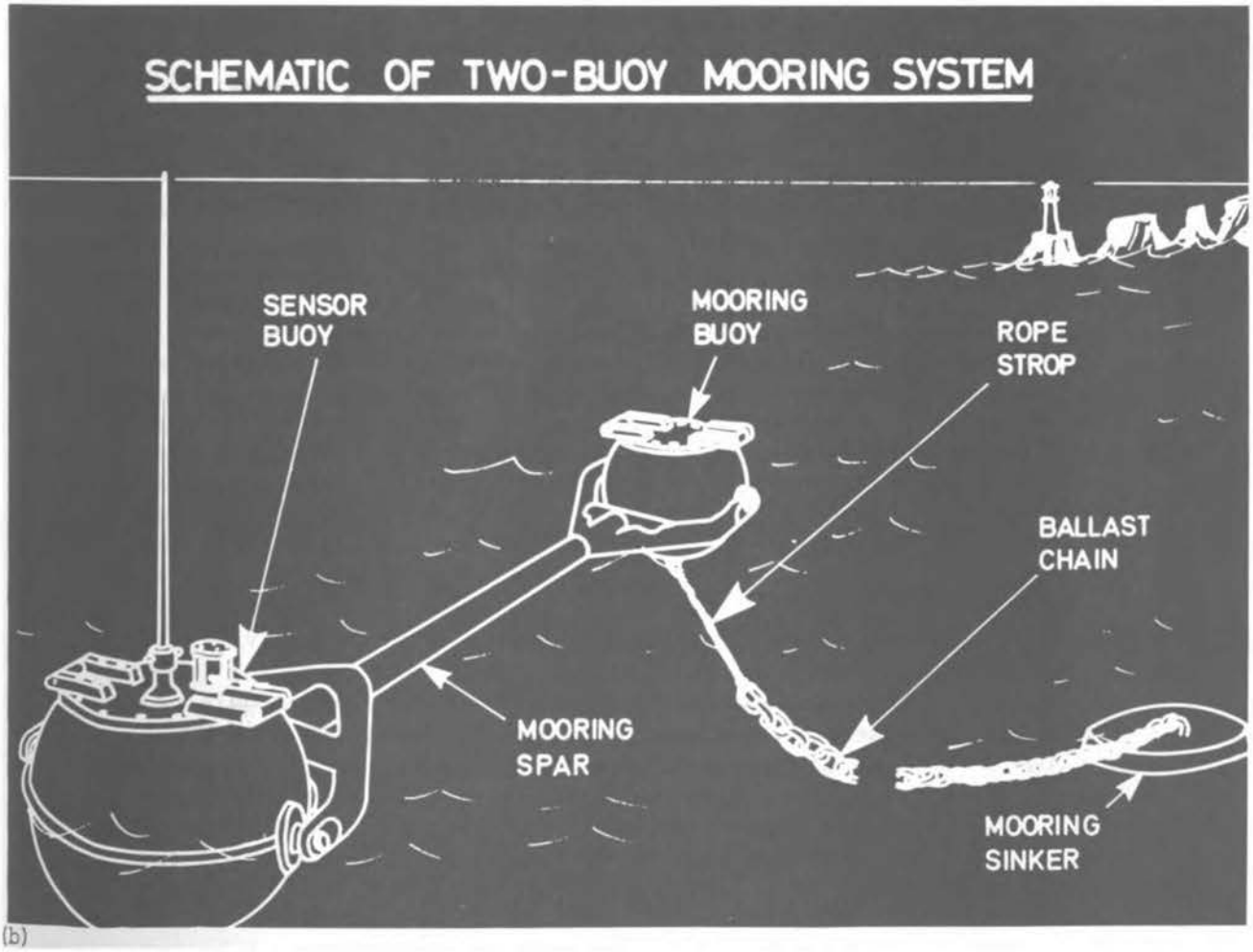

(b)

Figure 8 Two-buoy wave-measurement system: (a) as deployed; (b) schematic illustration of mooring arrangement

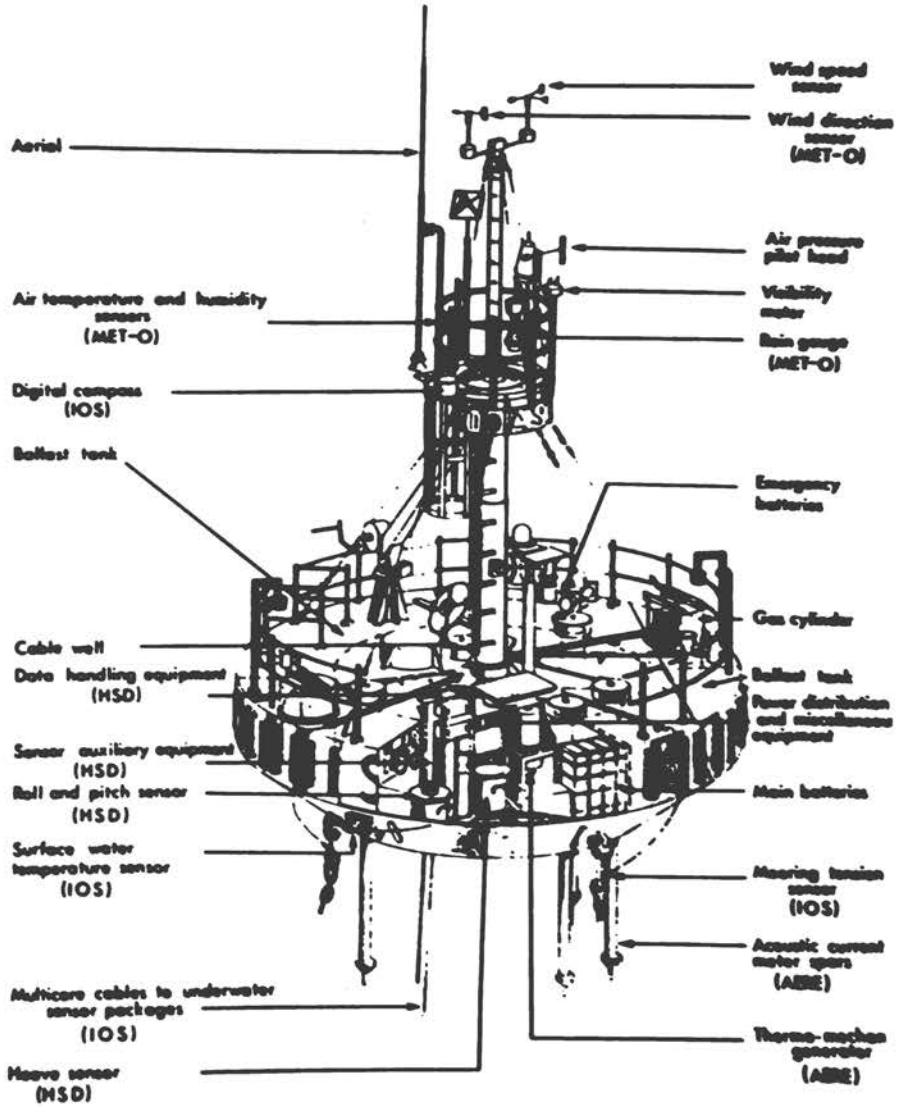

Figure 9 Ocean data buoy with heave, pitch, and roll sensors for wave measurements enabling derivation of directional wave spectra

If more accurate resolution of the directional spectrum is required, more than three measurements must be made. This can be done by using much larger arrays of staffs or more sophisticated buoys, such as the IOS cloverleaf buoy, which by measuring local wave curvature as well as slope enables the determination of up to nine coefficients in the Fourier series for directional wave energy. Both options involve complex and vulnerable installations, as well as considerable data handling and expert analysis. Therefore, while they are invaluable to researchers, they are not yet suitable for routine data gathering projects.

Another technique that has shown great promise for producing spectral information is the use of a horizontally scanning true Doppler microwave radar. Since this technique yields information on both the position and the speed of the target, height and directional data can be obtained together with information about surface currents. This type of system is still in the research stage.

Data Handling and Analysis

A complete account of recording and analysis techniques is much beyond the scope of this paper; it would necessitate a major work that would be out of date by the time it was published.

Present-day electronic techniques are so good that data can be recorded and manipulated in several ways with equivalent ease. The skill lies in selecting an economical solution--the minimum needed to produce the required results--and selecting the simplest system to achieve it. One of the most serious problems today is that it is easy to collect too many data. We all do collect too many, saying that the data might eventually prove useful, but they seldom do; more often, they become a nuisance.

The first major decision that should be made, then, concerns which data really need to be recorded. For many operational requirements, not much more than a very simple permanent record is really necessary, and the choices come down to whether a digital or analog display will be used, where the display will be placed, whether to use engineering units or not, and whether to include high/low alarms. If permanent records are required, then what type should they be? The answer depends almost entirely on the uses planned for the data and where and when the data will be reviewed and analyzed. Although still widely used for wave recording, paper charts are, quite rightly, rapidly giving way to modern magnetic tape cassette recorders or data loggers, for which the choice again comes down to digital versus analog displays.

For data manipulation in real time, the mighty micro is coming more and more into its own in wave measurement, particularly with the advent of the versions now available that consume very little power. Much can be done with these devices, and a wide range of input and output options can be exercised to record, display, transmit, or plot the data.

Data handling is no longer difficult, but great care must be taken in threading through the labyrinth of available options and selecting those most suited to the work at hand. Careful planning and detailed knowledge of the task and its applications are necessary to select any hardware.

Conclusions

In this paper, I have attempted to describe the prospects and problems of gathering ocean wave data with surface-mounted sensors, including some of the requisite planning considerations, brief accounts of some of the types of surface-mounted wave sensors available, and general comments on the options for data recording and analysis.

References

Driver, J. S. (1980), "A Guide to Sea Wave Recording," Institute of Oceanographic Sciences, U. K., Report No. 103 (with Appendix, "Wave Recording Instruments for Civil Engineering Use," by L. Draper and J. S. Driver).

Hogben, N. (1980), "Basic Data Requirements--A Review with Emphasis on Wave and Wind Data," Paper presented at the Workshop on Coastal Engineering, First Pan-American Conference on Oceanic Engineering, Mexico City, October 1980 (available from National Maritime Institute, U. K., Report No. R 92, November 1980).

Hogben, N. and F. E. Lumb (1967), "Ocean Wave Statistics," National Physical Laboratory, Ministry of Technology, U. K., H. M. Stationery Office, London.

Parker, A. G. (1978), "Instrumentation--All at Sea," IEEE J. Oceanic Eng., OE-3: 191-199.

Pitt, E. G. (1980), "The Measurement of Ocean Waves and Currents," J. Soc. Underwater Tech., Winter 1980, pp. 4-12.

Ribe, R. L. (1979), Wave Sensor Survey, Technical Report No. 78 (Washington, D.C.: National Oceanic and Atmospheric Administration, July 1979).

PITCH-ROLL BUOY
WAVE DIRECTIONAL SPECTRA ANALYSIS

L. R. LeBlanc*[1] and F. H. Middleton[1]

Introduction

In many different engineering operations offshore and in coastal regions, one of the most valuable in situ measurements for engineers is that of sea state. Until recently, operating engineers who design floating, semi-submersible, and bottom-mounted structures for use in hostile regions had to be content with rough power spectral density (PSD) information. In some cases, the sensor used to measure wave height was one of several types of wave staffs attached to a fixed platform or pier. In other cases, when no stationary reference frame was available, useful results were obtained by wave-following buoys of several types.

For offshore oil and gas operations, commercial fishing, pleasure boating, shipping, design of harbors and breakwaters, dredging, pipe laying, beach protection, and other activities, more information than simple PSD data is required. In many situations at sea, the direction of wave propagation is nearly as important as the sea state itself. This is particularly obvious in the dependence of vessel response to the angle of attack of waves on the bow. The damage from storm waves impinging on a beach also depends heavily on the angle of the waves' approach.

The deployment of multiple staffs and buoys in a spatial array has been successful in measuring wave spectra and direction of wave propagation, but the cost of deployment and retrieval is high, and the practice is limited to shallow water. Longuet-Higgins et al. (1963) discuss the directional wave spectrum observed by a single free-floating buoy that was designed to follow the surface of the sea in displacement and in slope. Directional wave spectra were extracted from data on the motion of the buoy. They are as accurate, then, as the buoy's ability to follow the motion of the water particles.

A somewhat different approach is described in this paper. A single small buoy, either free-floating or tethered to an anchor, is designed not to follow the slope of the water surface, but instead to pitch and roll according to the orbital particle-velocity gradient. The dynamics of this buoy system are such that the data obtained on heave, pitch, roll, and compass bearing can be transformed into complete directional wave spectra. The data processing technique is presented in this paper, and applied to an ocean storm experiment. The

---

*Presenter

[1]University of Rhode Island

buoy used to produce these data was an Endeco Model 956 Wave-Track buoy and the experiment was conducted as part of ARSLOE (Atlantic Remote Sensing Land-Ocean Experiment, fall 1980).

Buoy Comparison

Sensing the direction of propagation of storm waves with a single device or buoy is convenient. Two basic methods are available. Figure 1 illustrates the principal difference between the slope-following and orbital-following buoys. The slope buoy experiences zero pitch-roll at the crest and the trough of the wave, while the orbital buoy experiences maximum pitch-roll at the crest and the trough. Thus, for the slope buoy, the phase difference between the wave displacement and wave slope is 90° in the presence of an ideal sinusoidal wave, and in the same situation, the orbital buoy has a phase difference of 0° between the displacement signal and the pitch or roll signal. The difference between the phase behavior of the two buoys is quite insignificant in the analysis presented in a succeeding section.

The slope-following buoy is generally constructed in the form of a raft, or a toroid that is axially symmetric. The orbital-following buoy is usually tall and thin, and moored so that the vertical particle-velocity differential from top to bottom provides a tilting torque to the assembly. This technique for sensing the direction of wave propagation is quite similar to that of using various vector current-meter arrays, as reported in the literature (for example, Forristall et al., 1978).

Theory

The primary transducer in the buoy is a gimbaled accelerometer that maintains vertical orientation. The accelerometer output is double-integrated and filtered to produce a signal, ξ_1, that is proportional to the vertical displacement of the buoy assembly as it follows the motion of the waves. This signal can be represented in fast Fourier transform representation as shown in equation (1), wherein E_{1n} is the displacement Fourier coefficient:

$$\xi_1 = \frac{1}{T} \sum_{n=-\infty}^{\infty} E_{1n} e^{jn\omega_o t} \qquad (1)$$

$$\xi_2 = \frac{1}{T} \sum_{n=-\infty}^{\infty} E_{2n} e^{jn\omega_o t} \qquad (2)$$

$$\xi_3 = \frac{1}{T} \sum_{n=-\infty}^{\infty} E_{3n} e^{jn\omega_o t} \qquad (3)$$

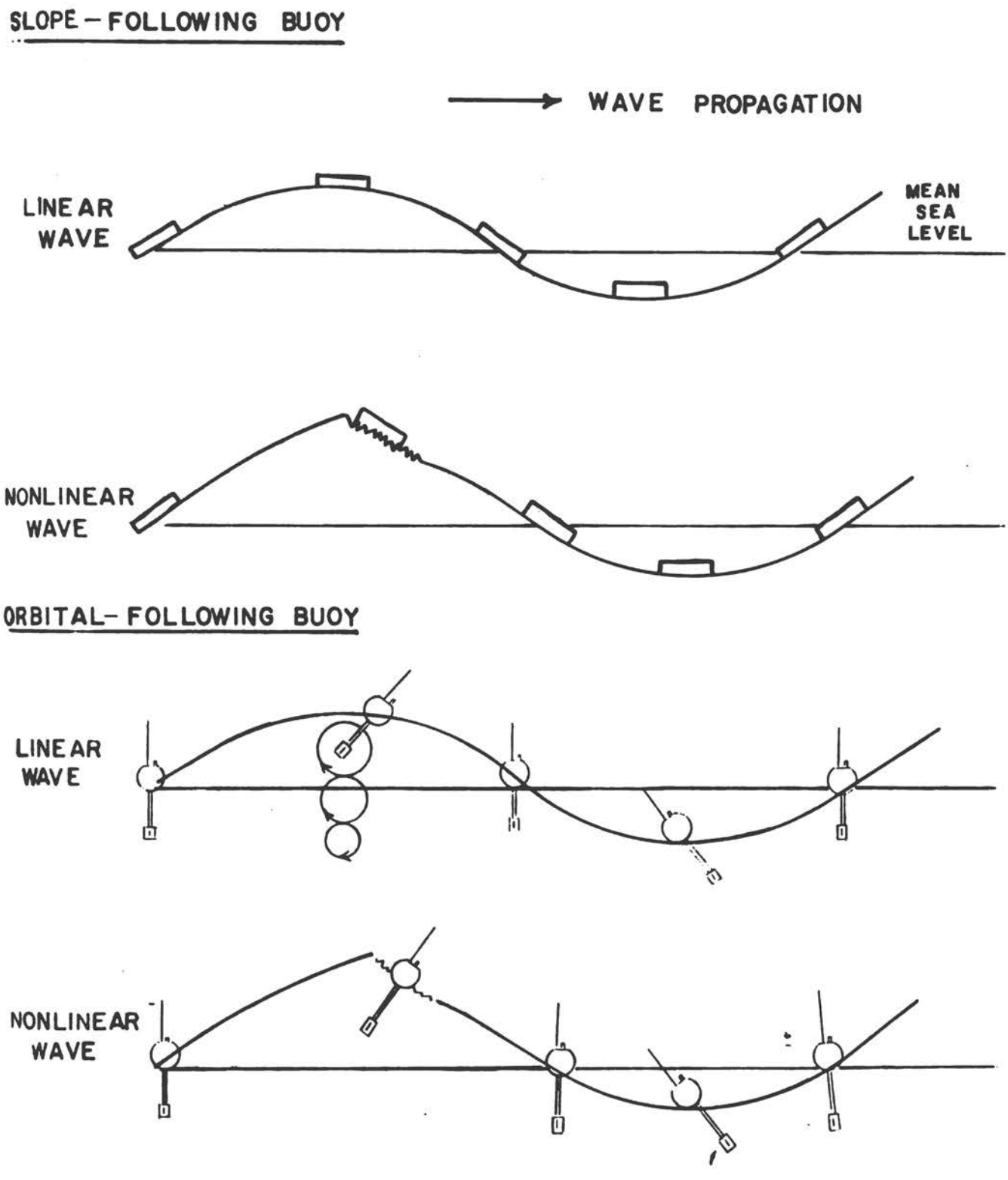

Figure 1 Principal pitch-roll buoy types

The buoy is equipped with a magnetic compass and a two-axis inclinometer of a special design. The compass output and the two inclinometer signals are combined to produce the north-south pitch-angle signal and the east-west roll-angle signal. These signals, ξ_2 and ξ_3, respectively, and their corresponding Fourier coefficients E_{2n} and E_{3n}, are identified in equations (2) and (3).

Equation (4) indicates how the heave Fourier coefficient E_{1n}, for frequency bin n, is produced by summing the plane-wave buoy heave response over all angles, ϕ, from 0^o (N) to 360^o (N):

$$E_{1n} = H_{1n} \int_0^{2\pi} D_n(\phi)\, e^{jK\cdot X}\, d\phi \qquad (4)$$

$$E_{2n} = H_{2n} \int_0^{2\pi} \cos\phi\, D_n(\phi)\, e^{jK\cdot X}\, d\phi \qquad (5)$$

$$E_{3n} = H_{3n} \int_0^{2\pi} \sin\phi\, D_n(\phi)\, e^{jK\cdot X}\, d\phi \qquad (6)$$

H_{1n} is the combined frequency transfer function of the heave response and electronic integrator of the buoy, which is, of course, independent of ϕ. $D_n(\phi)$ is the directional Fourier coefficient of the sea used to compute the directional spectrum, which is the final objective of the buoy system. H_{2n} and H_{3n} are the frequency transfer functions of the N-S and the E-W pitch and roll channels. Because of the axial symmetry of the buoy assembly, H_{2n} and H_{3n} are identical, each representing the dynamic roll in response to the propagating wave field. The amplitude and the phase of each of these frequency transfer functions are important in the analysis, as will be indicated later.

Once the Fourier coefficients E_{1n}, E_{2n}, and E_{3n} are determined from (4), (5), and (6), one can compute the real and imaginary parts of the cross-spectral density as shown in equations (7) and (8):

$$CO_{n,\,i,\,1} = \mathrm{Re}\left\{\frac{1}{T} \langle E_{in} E_{1n}^{*} \rangle\right\} \qquad (7)$$

$$QUO_{n,\,i,\,1} = \mathrm{Im}\left\{\frac{1}{T} \langle E_{in} E_{1n}^{*} \rangle\right\} \qquad (8)$$

In equations (7) and (8), the angle brackets denote ensemble averaging, and all possible combinations of (7) and (8) for i = 1, 2, and 3 can be displayed in the matrix form of equation (9). Note that only six terms in the matrix are unique.

$$\{CO_n + jQUO_n\} = \begin{bmatrix} CO_{n11} & CO_{n12} + jQUO_{n12} & CO_{n13} + jQUO_{n13} \\ CO_{n12} - jQUO_{n12} & CO_{n22} & CO_{n23} + jQUO_{n23} \\ CO_{n13} - jQUO_{n13} & CO_{n23} - jQUO_{n23} & CO_{n33} \end{bmatrix} \qquad (9)$$

The auto-spectral terms in (9) are the diagonal elements, CO_{n11}, CO_{n22}, and CO_{n33}, the heave CO spectrum, the N-S pitch CO spectrum, and E-W roll CO spectrum. Equation (10) shows that the first of these, CO_{n11}, is produced by combining equations (7) and (4), in which $\underline{K}$ is the vector wavenumber with components (k cos ϕ, k sin ϕ), and $\underline{X}$ means

f(x, y). Small k is the magnitude of the wavenumber for a plane wave propagating in the direction ϕ. The purpose of equation (10),

$$CO_{n11} = |H_{1n}|^2 \int_0^{2\pi} \frac{1}{T} \langle D_n(\phi) D_n^*(\phi) \rangle \, d\phi \qquad (10)$$

is to relate the heave CO spectrum, CO_{n11}, to the directional Fourier coefficient of the sea acting upon the buoy, $D_n(\phi)$.

In equations (10) and (11), $G_n(\phi)$ is the directional spectrum, which is related to the directional Fourier coefficients of the sea in the manner of equation (11). To get equation (10), one combines (7) and (4):

$$G_n(\phi) = \frac{1}{T} \langle D_n(\phi) D_n^*(\phi) \rangle \qquad (11)$$

There is the important matter now of determining the magnitude and the phase of each of the frequency transfer functions, H_{1n}, H_{2n}, and H_{3n}--all combined response operators. This must be done if one can hope to produce the directional spectrum from the available measured time-series channels. One could place a pitch-roll buoy in an ideal plane-wave field, or in a wave tank, and measure the required amplitude and phase characteristics of heave, pitch, and roll. This scaling could be done more efficiently, however, by operating in some way on the measured data. Fortunately, this can be done partially once the three CO spectra--CO_{n11}, CO_{n22}, and CO_{n33}--are computed from equation (7).

Inserting equations (7) and (8) into (5) and (6) yields equation (12), and after rearrangement, equation (13) for the calibration constants:

$$CO_{n22} + CO_{n33} = \frac{|H_{2n}|^2}{|H_{1n}|^2} CO_{n11} \qquad (12)$$

$$\alpha_n^2 = \frac{|H_{1n}|^2 (CO_{n22} + CO_{n33})}{CO_{n11}} = |H_{2n}|^2 = |H_{3n}|^2 \qquad (13)$$

This scale-factor result can be put into a useful form by equation (14), which includes amplitude estimates of the roll response operators and their measured phase characteristics. The matrix quantity $\{P_n\}$ can be called an instrument transfer function matrix.

$$\{P_n\} = \begin{bmatrix} \frac{e^{j\beta_1}}{|H_{1n}|} & 0 & 0 \\ 0 & \frac{e^{j\beta_2}}{\alpha_n} & 0 \\ 0 & 0 & \frac{e^{j\beta_3}}{\alpha_n} \end{bmatrix} \qquad (14)$$

Actually, the phase characteristics can be obtained in a wave tank or even in the field, where a undirectional sea condition might prevail. The heave channel response operator, H_{1n}, is measured in a sea test configuration.

When the instrument transfer function matrix is applied now to the cross-spectral density matrix (equation 15), a new compensated CO and QUO matrix, $\{\alpha_n\}$, results as shown in equations (16) through (21). This new cross-spectral density matrix is a valuable product of the data because it leads in a simple way to the desired directional spectrum, $G_n(\phi)$, of equation (22). The five Fourier coefficients, a_o, a_1, a_2, b_1, and b_2, are related easily to the $\{\alpha_n\}$ matrix elements by equations (23) and (24).

$$\{P_n\}\ \{CO_n + jQUO_n\}\ \{P_n^*\}^T = \{\gamma_n\} \tag{15}$$

where $\{\gamma_n\}$ = phase and amplitude corrected CO and QUO spectra.

$$\gamma_{n11} = \int_0^{2\pi} G_n(\phi)\ d\phi \tag{16}$$

$$\gamma_{n12} = \int_0^{2\pi} \cos\phi\ G_n(\phi)\ d\phi \tag{17}$$

$$\gamma_{n13} = \int_0^{2\pi} \sin\phi\ G_n(\phi)\ d\phi \tag{18}$$

$$\gamma_{n22} = \int_0^{2\pi} \cos^2\phi\ G_n(\phi)\ d\phi \tag{19}$$

$$\gamma_{n23} = \int_0^{2\pi} \cos\phi \sin\phi\ G_n(\phi)\ d\phi \tag{20}$$

$$\gamma_{n33} = \int_0^{2\pi} \sin^2\phi\ G_n(\phi)\ d\phi \tag{21}$$

$$G_n(\phi) = \frac{a_0}{2\pi} + \frac{1}{\pi}\sum_{i=1}^{2}\{a_i \cos(i\phi) + b_i \sin(i\phi)\} \tag{22}$$

$$a_0 = \gamma_{n11} \qquad a_1 = \gamma_{n12} \qquad b_1 = \gamma_{n13} \tag{23}$$

$$a_2 = (\gamma_{n22} - \gamma_{n33}) \qquad b_2 = 2\gamma_{n23} \tag{24}$$

Results

During October 1981, a most interesting large-scale ocean wave experiment was performed off the coast of North Carolina: the Atlantic Remote Sensing Land-Ocean Experiment, or ARSLOE. One of the orbital wave buoys that performed successfully through the life cycle of a storm was a Type-956 Endeco Wave-Track Buoy. Through the sponsor of this research program, Dr. Ledolph Baer of NOAA, the data tape was made available to the authors. The heave displacement, the N-S pitch, and the E-W roll signals were processed as outlined in the foregoing discussion. The buoy was programmed to transmit these three signals continuously through the life of the storm.

Figure 2 is a computer printout sample of the processed data for a 17-minute data segment. The wave band was divided into 20 frequency bins, and all of the five Fourier coefficients for each bin are indicated. Also, the energy density in each bin was computed and listed in the printout. The most interesting features of sea state during a storm are perhaps the direction of wave propagation and the period of the most energetic components of the wave field. Figures 3 through 10 are two-dimensional plots of contours of constant energy density from the quiet before the storm through the calm following. The plots are cartesian for simplicity of computer plotting and for ready identification of their main features. Wind direction and speed are indicated by the heavy horizontal line in each figure; significant wave height ($H_{1/3}$) in each instance is given in the figure caption.

Starting with Figure 3, $H_{1/3}$ was only 3 ft and the wind was just starting to build out of ENE direction. The wind observation was obtained from the NDBO buoy some 30 km farther offshore from the Endeco, which was about 12 km offshore. Here, the nine small contours surround regions where nonzero energy density was found.

Ten hours later, the wind had increased by 50 percent and moved slightly to the northeast. Figure 4 shows a fairly large energy peak at about a 6 s period, just a few degrees away from the wind direction.

Twelve hours later, as seen in Figure 5, the wind had dropped a bit and the energy had spread out in the direction-frequency plane, leaving one major peak still where the previous one existed. Note that a small contour means a undirectional and monochromatic wave field rather than small energy density. As would be expected here, $H_{1/3}$ had fallen slightly from the previous observation.

Figure 6 shows signs of the storm coming on some 10 hours later. The wave period of the main peak held at about 6 s, $H_{1/3}$ had risen to 10 feet, and the wind magnitude had also risen, by about one third, in a steady direction. The height of the energy density peak is very much increased.

Figure 7 illustrates the situation 12 hours later: $H_{1/3}$ had risen by 20 percent, the wind had decreased somewhat, and a new energy peak appeared in line with the wind, but now with a shorter period.

In Figure 8 the storm is near its peak--the wind is high and has moved to almost southerly rather than easterly direction. More important, the dominant wave period has perhaps doubled, and the peak has moved toward the new wind direction.

ENVIRONMENTAL DEVICES CORPORATION
TYPE 956 DIRECTIONAL WAVE-TRACK BUOY
ARSLOE TAPE - NORTH CAROLINA
INSTRUMENT 9560001
START: 23-OCT-80 AT 13:15:00
STATISTICS
FOURIER COEFFICIENTS

BAND	FREQ	A0	A1	B1	A2	B2
2	.037	31.68	0.12	-8.10	-10.24	-1.48
3	.062	3.49	-0.55	0.15	-0.09	-0.52
4	.086	0.78	-0.17	-0.09	-0.18	0.23
5	.110	0.58	-0.03	0.10	-0.18	0.10
6	.135	0.42	-0.04	0.01	-0.05	0.03
7	.159	8.70	4.04	1.83	0.72	3.89
8	.184	35.15	25.22	6.75	14.52	9.22
9	.208	19.18	9.82	8.42	-1.45	11.73
10	.232	9.72	4.30	3.08	-0.51	4.41
11	.257	4.39	1.06	0.82	1.13	-0.08
12	.281	3.51	1.32	1.00	0.10	1.47
13	.306	2.07	0.13	0.74	-0.62	0.15
14	.330	1.22	0.07	0.32	-0.46	0.12
15	.354	1.56	-0.04	0.53	-0.24	0.14
16	.379	1.52	0.26	0.45	-0.47	0.25
17	.403	0.29	0.04	0.05	0.03	-0.11
18	.428	0.48	0.05	-0.01	0.06	-0.11
19	.452	0.39	-0.01	0.06	0.18	-0.05
20	.477	0.32	0.12	-0.04	-0.09	-0.09

FREQUENCY BANDNUMBER	CENTER FREQUENCY	CENTER PERIOD	ENERGY DENSITY	BEST ANGLE 1	BEST ANGLE 2	SPREADING FACTOR
2	.037	26.9	31.68	291.	291.	0.7
3	.062	16.3	3.49	32.	231.	0.4
4	.086	11.6	0.78	156.	257.	0.7
5	.110	9.1	0.58	101.	101.	0.4
6	.135	7.4	0.42	154.	230.	0.2
7	.159	6.3	8.70	-29.	133.	2.1
8	.184	5.4	35.15	19.	96.	5.8
9	.208	4.8	19.18	-1.	83.	4.1
10	.232	4.3	9.72	-16.	97.	2.4
11	.257	3.9	4.39	58.	96.	0.9
12	.281	3.6	3.51	-31.	125.	1.8
13	.306	3.3	2.07	47.	47.	1.1
14	.330	3.0	1.22	37.	37.	0.7
15	.354	2.8	1.56	59.	59.	1.0
16	.379	2.6	1.52	29.	29.	1.0
17	.403	2.5	0.29	45.	305.	0.6
18	.428	2.3	0.48	198.	382.	0.2
19	.452	2.2	0.39	99.	99.	0.4
20	.477	2.1	0.32	297.	381.	1.3

SIGNIFICANT WAVE HEIGHT (H 1/3) = 7.0 ROOT-MEAN-SQUARE WAVE HEIGHT = 5.0

Figure 2 Sample wave-data printout

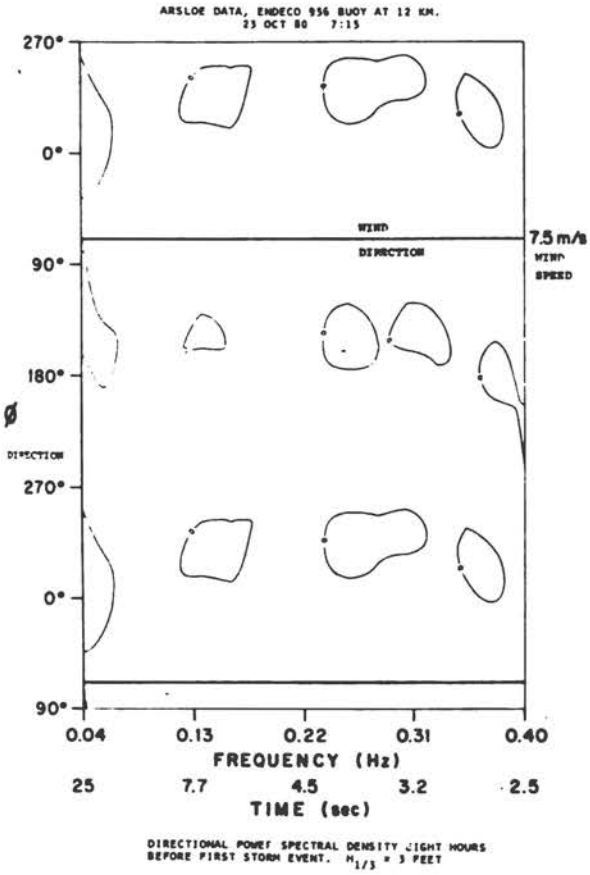

Figure 3

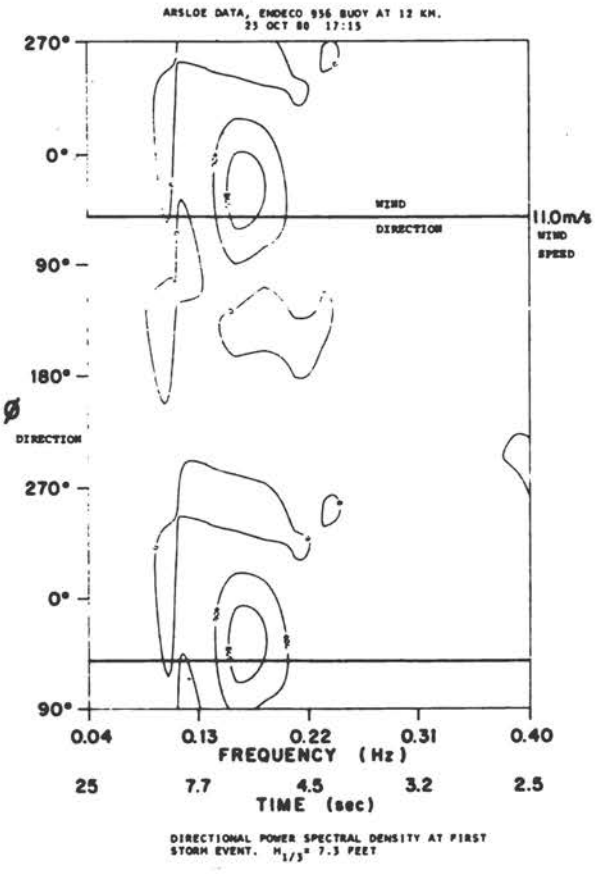

Figure 4

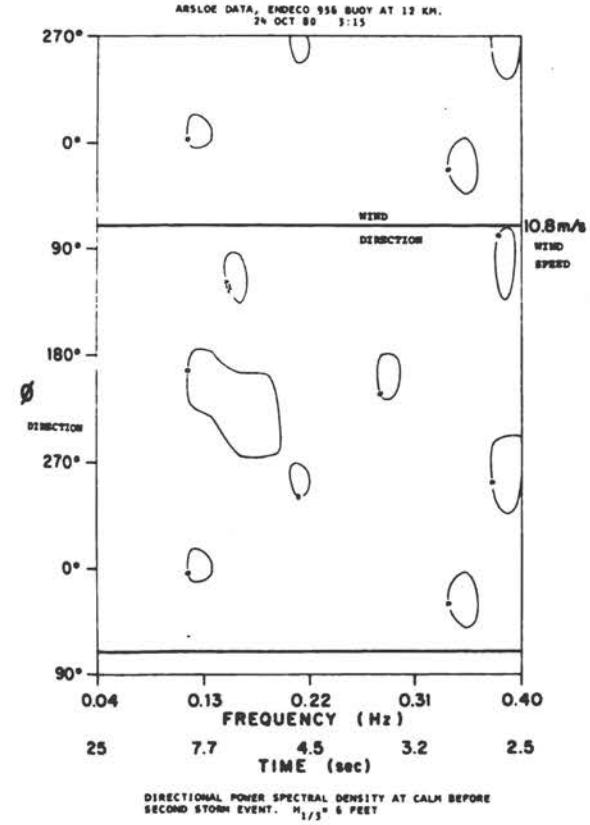

Figure 5

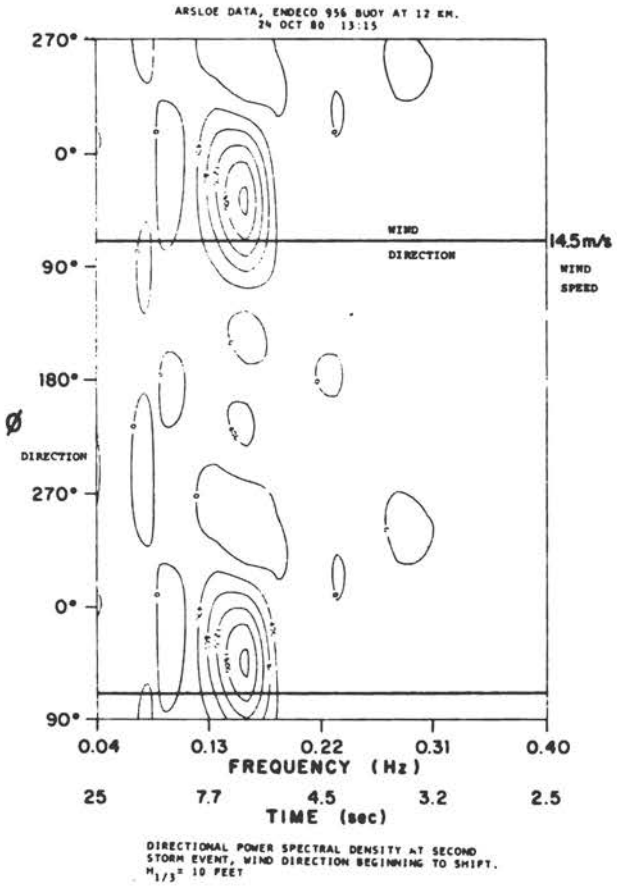

Figure 6

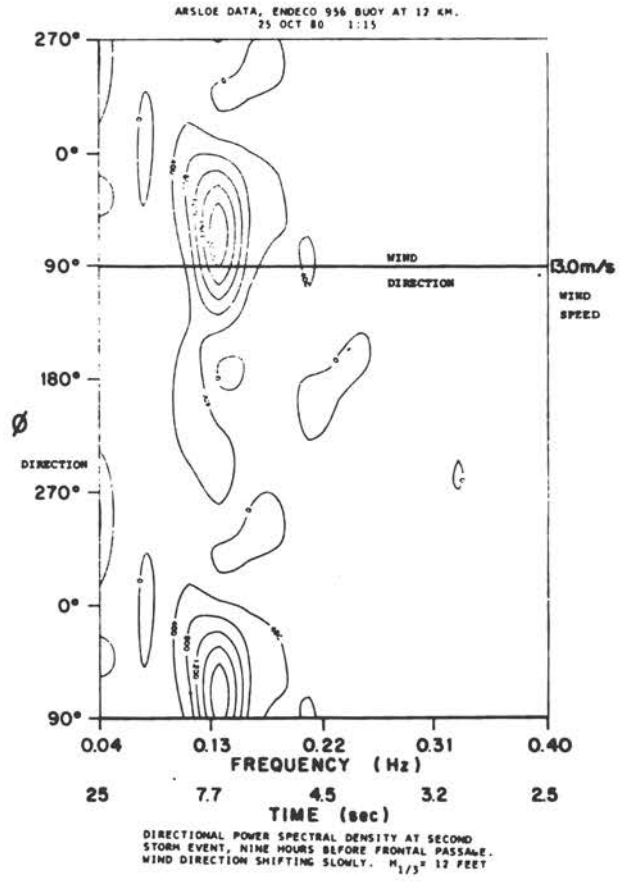

Figure 7

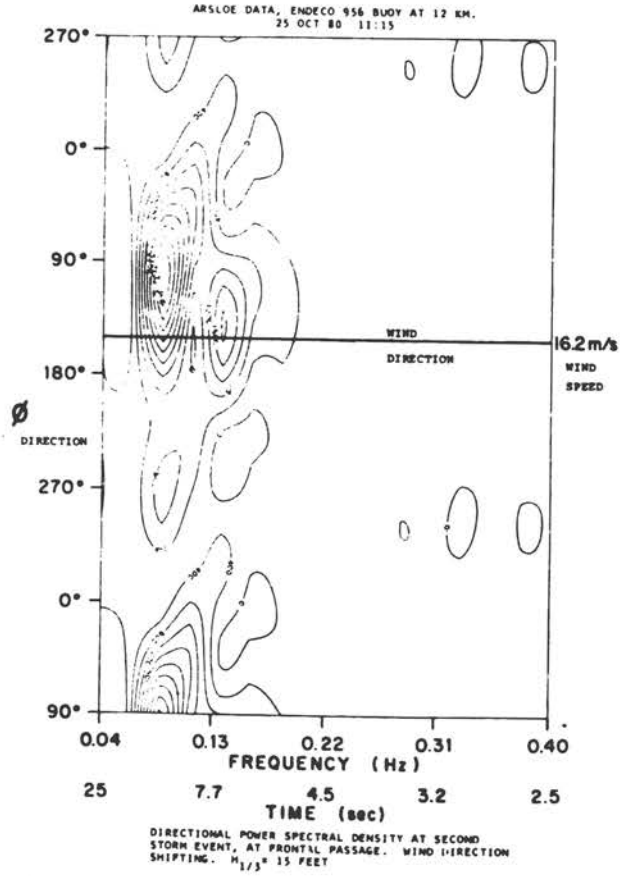

Figure 8

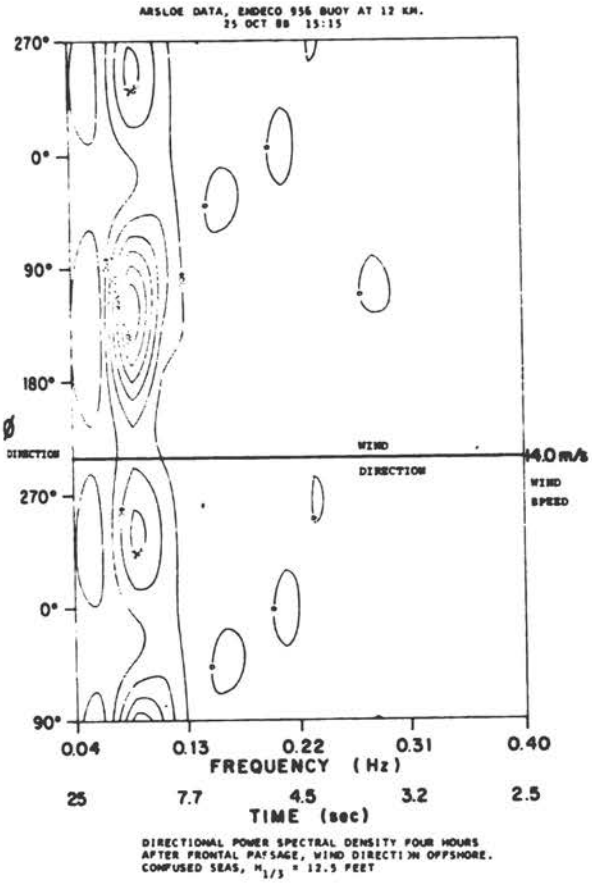

Figure 9

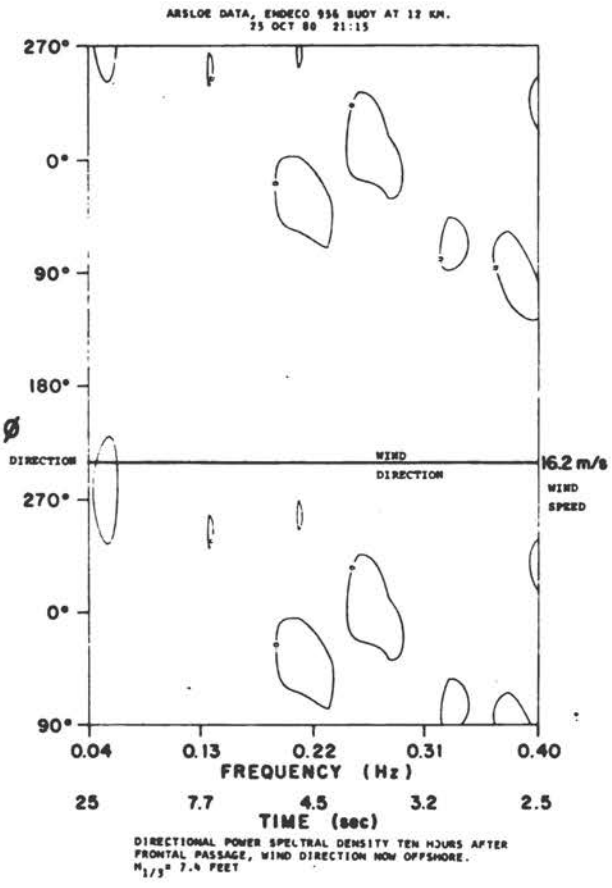

Figure 10

Figure 9 is just four hours later, past the peak of the storm; the wind has moved to southwest, nearly offshore, and is still blowing well. $H_{1/3}$ has dropped, and the dominant wave direction peak has not responded to the direction change in the wind. Ten hours later (Figure 10), the wind is still strong, but now is offshore, and the sea has greatly quieted.

Conclusions

To compare this analysis of orbital buoy data with that of Longuet-Higgins et al. (1963) of slope buoy data, reference is made to equations (25), (26), and (27)*:

$$G_n(\phi) \propto (1 + \cos \phi)^S \tag{25}$$

$$S = \frac{\sqrt{a_1^2 + b_1^2}}{a_0 - \sqrt{a_1^2 + b_1^2}} \tag{26}$$

$$\text{Best angles, } \phi_1, \phi_2 \tag{27}$$

The first of these equations represents a useful model of a directional wave spectrum. In this expression, S is the power of $(1 + \cos \phi)$, which is referred to as the "spreading coefficient." The size of S is actually a measure of the directivity of a wave band component--large S, high directivity, low "spread."

A word should be said about angular resolution, because this concept is important to the user of wave-buoy data. When one says that the directional resolution is 90°, it is important to remember that this refers specifically to a single frequency. That is, if two waves of the same frequency propagate at an angle between them of less than 90°, then the buoy cannot distinguish the two waves. Instead, the buoy will indicate a vector sum of the two waves. At first, this seems a serious limitation, but such an occurrence depends on wind direction, duration, fetch, water depth, and other factors being just right, and as these conditions cannot last, the effect is likely to be transitory.

For engineering purposes, the most important wave-direction measurements are reliable indications of the height and directions of the most energetic parts of the wave field. In considering the design and operation of a structure placed in the North Sea, for example, the most important data concern the direction from which a wave field may strike the structure, and the energy and wavelength of the wave spectrum. Similarly, the angle of attack of a sea upon a shore is as important as the significant wave height.

---

*To relate the results of this work to those referenced for a slope buoy, two best angles were defined by Longuet-Higgins et al. (1963). The reader is directed to that work for a definition of "best" angles.

In the results section of this paper, the point is made that wave data alone are sufficient to derive both the amplitude and the phase of the heave and the pitch-and-roll frequency transfer functions. This offers a neatly effective way to avoid complex and expensive tank calibrations for the hydrodynamics of an individual orbital buoy. The point is particularly important when physical changes are made in the buoy at the time of deployment. The installation of a larger battery pack to extend the period of the buoy's use, for example, will change the height of the seawater level on the buoy, and the added mass will clearly influence heave, pitch, and roll. The auto-calibration techniques set out in this paper obviate the need for recalibration each time changes are made.

References

Forristall, G. Z., E. G. Ward, V. F. Cardone, and L. E. Borgmann (1978), "The Directional Spectra and Kinematics of Surface Gravity Waves in Tropical Storm Delia," J. Phys. Oceanogr., 8: 888-909.

Longuet-Higgins, M. S., D. E. Cartwright, and W. D. Smith (1963), "Observations of the Directional Spectrum of Sea Waves Using the Motions of a Floating Buoy," Ocean Wave Spectra (Englewood Cliffs, N.J.: Prentice-Hall), pp. 111-136.

SUBSURFACE WAVE-MEASURING SYSTEMS

George Z. Forristall[1]

Abstract

Pressure transducers were one of the first means used to measure waves in coastal waters. Nevertheless, some stigma has been attached to their use, since the wave signal is attenuated by overlying water. In some investigations, the correction for this attenuation has not been done, or has been done improperly. Contemporary high-resolution instruments and digital data processing techniques can now be used to get accurate wave data in many situations. An intercomparison between a wave staff and a pressure transducer mounted 56 ft below mean water level was conducted at the Buccaneer platform in February 1980. The analysis showed that spectral methods could be used to convert the pressure record to wave height for attenuation factors up to about 10 to 1. Fast-response current meters can be used in conjunction with pressure transducers or wave staffs to estimate the directional wave spectrum. In the past few years, this technique has become more or less routine. Some recent examples include the Ocean Test Structure experiment to study wave forces on platforms, a fatigue-monitoring program at the Cognac platform, an experiment to study the attenuation of waves propagating over a soft muddy bottom, and a tripod used for study of the bottom boundary layer.

Introduction

In relatively shallow water, it is often convenient to use pressure transducers to measure surface waves. The transducers can be made quite accurate: subsurface placement eliminates the problems associated with mounting surface-piercing gauges and with buoys, which can be destroyed by fishing. Much good work has been done with pressure transducers; for example, the classic study of wave propagation across the Pacific Basin by Snodgrass et al. (1966). Yet Kinsman (1965, p. 144) enjoins us not to "go around making general statements about the sea surface on the strength of bottom pressure records," and many ocean engineers instinctively distrust results obtained from pressure records.

The difficulty with pressure records is that they do not exactly duplicate the wave heights above them, but present instead a highly filtered version of those heights. For a sinusoidal wave with frequency f and wavenumber k described by linear theory,

---

[1]Shell Development Company

$$P = \frac{H \cosh (kz)}{\cosh (kD)} \qquad (1)$$

where the pressure P and the wave height H are both expressed in units of length (head), D is the water depth, and z is the height of the pressure transducer above the bottom. If the depth is small compared to the wave length so that kD is small, the pressure and wave height will be nearly equal. However, if a gauge is installed on the bottom in 100 ft of water, the pressure from a wave with a period of 5 s will be attenuated by a factor of 67.

Even though the pressure record is not directly equal to the wave height, it should be possible to recover wave height from the record if the filter function is known. Equation (1) is often used for this purpose, but there are several possible problems with its use. The dynamic pressure due to the kinetic energy of wave orbital motions has been neglected in its formulation, and it is based on linear theory, which only approximates the solution of the boundary value problem for waves of finite steepness. Theoretical calculations can be used to show that errors resulting from these problems should be relatively small, but verification of equation (1) in field conditions is still highly desirable.

Real ocean waves are not sinusoidal, but complex and irregular. It is thus natural to use Fourier analysis to decompose the wave and pressure records into their component frequencies and verify that equation (1) describes the transfer function between the variables. It is also possible to select individual waves from the record and apply equation (1), using the wavenumbers appropriate to the periods of those individual waves. This wave-by-wave analysis ignores the fact that individual waves contain harmonics other than the frequency of the zero crossing period, but the technique is apparently still widely used.

Grace (1978) measured swell in 37 ft of water off Honolulu using a resistance wave staff and a Bendix wave pressure gauge. Defining

$$n = \frac{H \cosh (kz)}{P \cosh (kD)} \qquad (2)$$

he found from a wave-by-wave analysis that n was greater than 1 for long waves and decreased to less than 1 for shorter waves. There was much scatter in the observed values of n for this type of analysis.

Tubman and Suhayda (1976) found a similar decline in n with decreasing wavelength in their wave-by-wave analysis of measurements from East Bay off the Mississippi Delta. The water depth at the site was 65 ft and the waves were considerably shorter than those studied by Grace. Suhayda (1977) pointed out that pressures higher than those predicted by linear theory were consistent with an elastic response of a soft bottom.

Grace (1978) also performed a Fourier analysis of one of his records and found that n in equation (2) was very close to unity for

component waves to D/L = 0.3, where L is the computed length of the component wave. It is possible, however, to explain the discrepancy between the results of the two methods of analysis. If the zero crossing period for a wave is long, a small correction factor appropriate to a long wave is applied, even though short-wavelength components contribute to over-all wave height. The wave height calculated by correcting the pressure record is thus likely to be too small. The opposite effect may occur when the zero crossing wave period is short, since the correction factor chosen may be too large.

The problems of wave-by-wave analysis of pressure data can be illustrated using simulated wave-height and pressure data. We performed such simulations using specified wave spectra with phase angles given by a pseudo-random number generator. The wave time series was synthesized using the inverse Fourier transform and the pressure time-series was produced by applying equation (1) to each Fourier component of the wave spectrum. Thus, n = 1 exactly for all frequencies if a spectral analysis of the simulations is performed. In contrast, a wave-by-wave analysis leads to the large scatter shown in Figure 1. This particular simulation was for a Pierson-Moskowitz spectrum at a wind speed of 25 miles per hour and a water depth of 65 ft with the pressure transducer on the bottom. The scatter in the values of n and the decline of n with increasing D/L are similar to the features observed in the real data discussed above. Simulations with different spectral shapes gave somewhat different results, with broad spectra producing the most variation in n, as expected.

The simulations clearly show that pressure records should not be corrected with wave-by-wave analysis, and that equation (1) should be verified by spectral analysis. Simpson (1969) performed a spectral analysis of measurements made from the end of a pier at Blackpool. The water depth at high tide was 20 ft and the pressure transducer was mounted 8 ft from the bottom. The wave staff used was a capacitance type, the pressure transducer an LC oscillator tuned by a capacitor whose plates were moved by the pressure. Results of the analysis agreed very well with equation (1) up to (D - z)/L = 0.4.

Esteva and Harris (1970) made similar measurements from the Steel Pier in Atlantic City. Mean water depth was 15.5 ft, and the lowest pressure gauge was near the bottom. They found good agreement with equation (1) for D/L up to 0.3, noting that for higher waves, n in equation (2) was closer to 1 and showed less scatter.

Cavaleri et al. (1978) made measurements from a tower in the Adriatic Sea in 52 ft of water. A resistance wave staff was used, and the pressure transducers were set at various depths to 48 ft during the experiments. Their spectral analysis showed that n was neither constant nor close to unity, but decreased from 1.2 at low frequency to 0.8 at high frequency. They found no evidence of finite-amplitude effects.

The weight of the evidence suggests that equation (1) may be used to convert pressure measurements to wave heights, but in view of the careful work by Cavaleri et al. (1978), some doubt must remain. Additional data would be welcome, particularly those obtained from measurements in deeper water. We recently installed a pressure

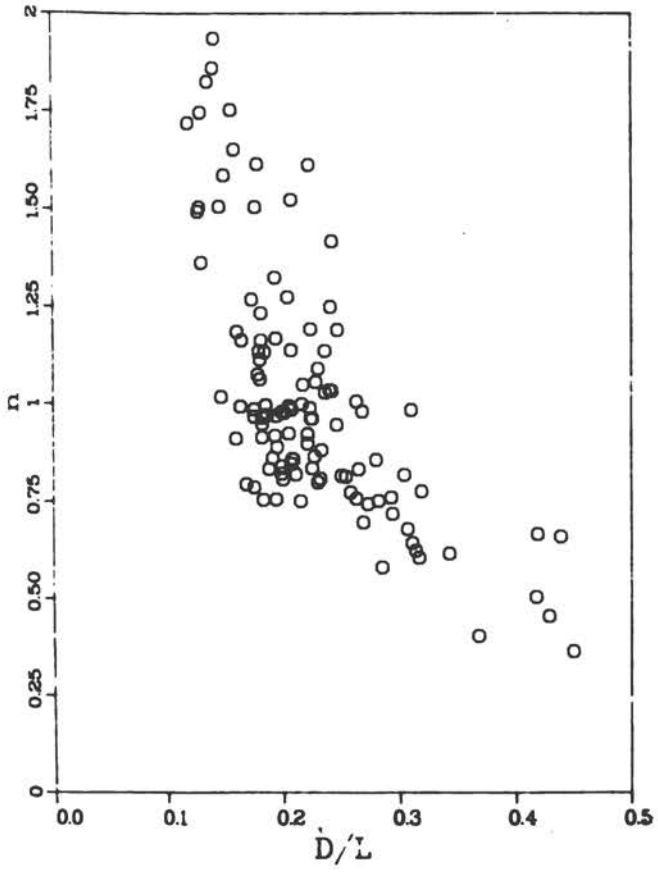

Figure 1 Wave-by-wave analysis of simulated wave staff and pressure records

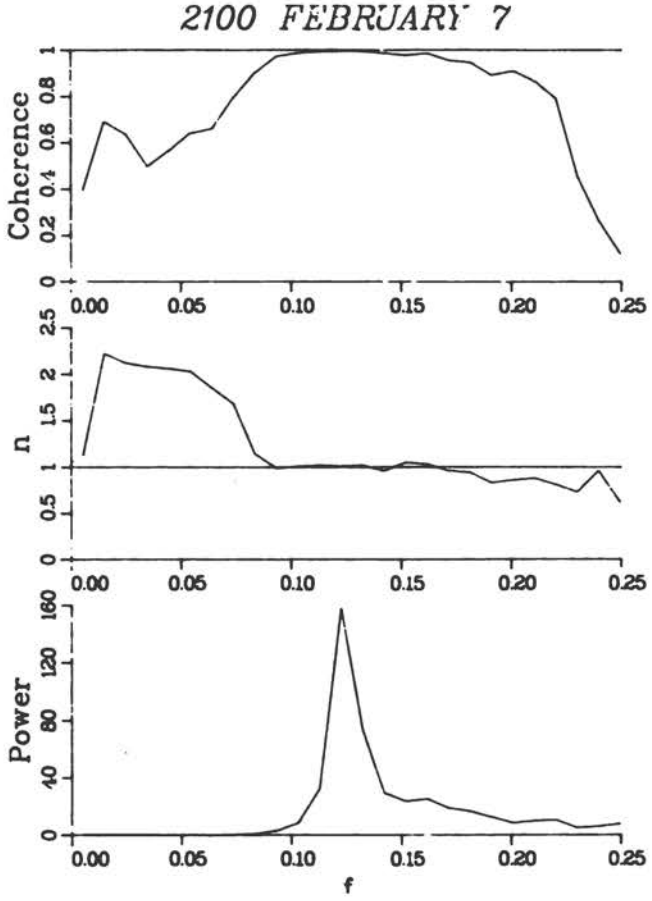

Figure 2 Cross-spectral analysis of the wave staff and pressure measurements made at Buccaneer at 2100 hours, February 7, 1980

transducer in a study of the attenuation of waves by a soft bottom, similar to the work of Suhayda (1977), and at his site. Thus, we were quite interested in learning the response of the transducer and conducted a short comparison experiment at the Buccaneer platform.

The Buccaneer Comparison Experiment

The Buccaneer production platform is located approximately 25 miles south of Galveston, Texas, in 68 ft of water. An oceanographic station was maintained at the platform for a number of years and collected some interesting information on storm waves (Forristall et al., 1978). The station is no longer operated continuously, but some of the hardware, including the wave staff, remains in place. The bottom in the area is stiff clay alternating with sand. The location was logistically convenient for the test.

The two structures comprising the platform are connected by a 200-ft bridge. A Baylor inductance wave staff was stretched between the center of the bridge and a 20,000-pound deadweight anchor on the seafloor. The wave staff was calibrated by shorting it at two points before and after the test. The pressure transducer used was a Digiquartz manufactured by Paroscientific, which functions by sensing the vibrational frequency of a piezoelectric crystal. The precision and accuracy of the instrument in static tests are quite remarkable. We checked the performance of the instrument prior to installation by comparing its output to a mercury barometer to within 0.01 inch of mercury.

The pressure transducer was installed by mounting it on a taut wire loop previously used to hold current meters and lowering it to 12 ft above the seafloor. Its frequency signal was converted to a voltage by a specially designed circuit, and both this signal and that of the wave staff were recorded on a low-speed Geotech recorder.

Continuous recordings were made by the system from February 6 to February 26, 1980. A moderately strong winter storm that arose soon after installation produced south to southeasterly winds up to 30 miles per hour. The weather for the rest of the recording period was rather mild, producing no large waves. After the analog tape was recovered, all of the data were digitized at two samples per second and subjected to cross-spectral analysis.

Figure 2 shows an example of the analysis for a period during the storm at 2100 CST, February 7. All three panels of the figure have a common frequency ordinate. The bottom curve shows the power spectrum from the wave staff in ft^2/Hz, which has a reasonably sharp peak at $f = 0.123$ Hz. The top panel of the figure shows the coherence squared between the wave staff and pressure transducer. It is very close to 1 for the range of frequencies over which the pressure signal is above the noise level. The value of n calculated from the transfer function and equation (2) is shown in the middle panel. For the frequency range over which the coherence is high, n is close to 1, showing that linear theory adequately describes the attenuation of pressure with depth, and that equation (1) can be used to convert pressure records to

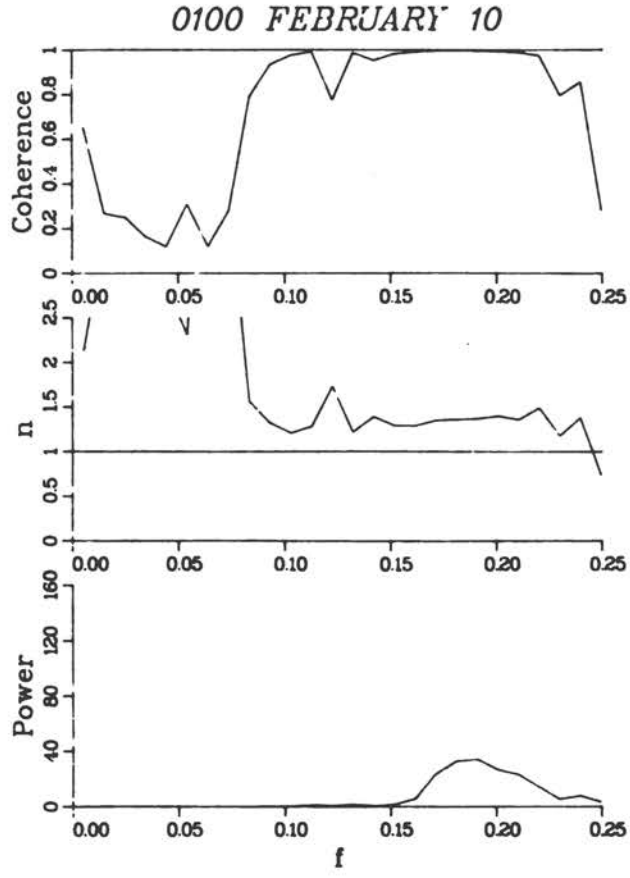

Figure 3 Cross-spectral analysis of the wave staff and pressure measurements made at Buccaneer at 0100 hours, February 10, 1980

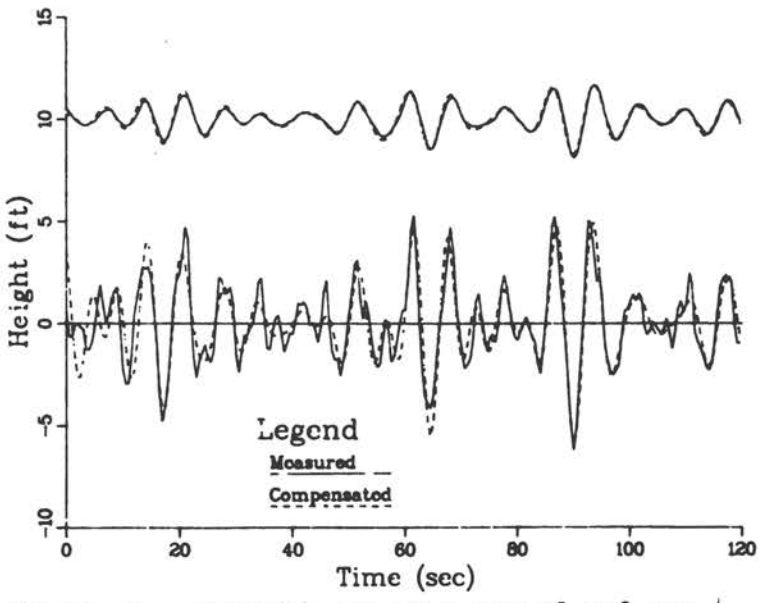

Figure 4 Comparisons of measured and reconstructed pressure and wave records from Buccaneer. The curves labeled "compensated" were constructed using data from the other sensors and linear theory.

wave-height records over a reasonably wide frequency range. For the example given in Figure 2, it seems that the compensation could be carried out reliably to about f = 0.22 or (D - z)/L = 0.5.

The results shown in Figure 2 are representative of all cases in which the significant pressure variation exceeded 1 ft. When the signal was smaller, the analysis showed much more scatter from unity in n. Figure 3 represents a record taken a little over 2 days after that of Figure 2. The wave spectrum has decreased considerably and components with frequencies less than 0.15 Hz have almost disappeared. The pressure signal is thus quite weak. The coherence between wave and pressure is still high over a wide range, but n is rather far from unity. Although n is relatively constant in the example plotted, it was not constant across all low wave-height records. Figure 3 illustrates the worst case. The reason is not known, but we suspect that it may be the poor response of our recording system at low signal levels.

No information on the phase between the wave and pressure signals is given in Figures 2 and 3, since the phase difference was always small when coherence was high. The pressure transducer was located about 6 ft north of the wave staff, and the phase lag of the pressure behind the wave for f = 0.123 on February 7 was about 5°, consistent with a wave propagating northward. There was also a tendency for the phase lag to increase with increasing frequency.

The high coherence between the wave and pressure records suggests that it should be possible to use equation (1) to construct one of the signals, given the other. Figure 4 shows the results of this compensation for a short section of the data that were analyzed in producing Figure 2. The top pair of traces in Figure 4 shows the measured pressure and the wave signal converted to pressure using equation (1). Both traces were shifted up arbitrarily by 10 ft for display. The bottom pair of traces shows the measured wave height and the pressure compensated for hydrodynamic attenuation through the inverse of equation (1). Both compensations were made in the frequency domain and converted to time series using the inverse fast Fourier transform. Since the coherence drops off rapidly for high frequencies, only frequencies below 0.215 Hz were used in the compensations.

The top two curves in Figure 4 are nearly identical, showing that a pressure time-series near the bottom can be accurately calculated from a wave-height time series. The bottom traces also agree, but there are some errors in the details of the compensated pressure. High-frequency components are missing, and the details of the peaks of the individual waves are not reproduced exactly.

The difference between the comparisons is due to the attenuation of the high-frequency components. For (D - z)/L greater than 0.5, the pressure signal drops off very rapidly; thus, the high-frequency components of the waves are irretrievably lost. We conclude that pressure can be accurately calculated from wave measurements and wave measurements from those of pressure, and that both calculations are good enough for many practical purposes, provided that data on the high-frequency components are not required. However, it would not be

sound to use pressure measurements to study wave features such as the skewness caused by nonlinearities.

Using contemporary instruments and methods of analysis, it is possible to convert pressure measurements to wave heights for frequencies such that $(D - z)/L$ is less than 0.5. The compensation for attenuation should be applied in the frequency domain to each individual Fourier component. For site surveys, the components above the high-frequency cutoff might be restored by fitting an equilibrium range to the measurements.

The Directional Spectrum from Current-Meter Measurements

Subsurface sensors can also be used to estimate the directional wave spectrum. One obvious method would be to set out an array of pressure transducers, and this has in fact been done with some success. However, the use of electromagnetic current meters has become much more popular in the past few years. The current meter measures the oscillations under the waves, giving directional information equivalent to a triangle of wave gauges or a tilt-and-roll buoy.

Electromagnetic current meters were used to measure the directional properties of waves 15 years ago by Bowden and White (1966). The instruments have now been made sufficiently stable and reliable to be used almost routinely. Several recent experiments using these instruments are described below.

The Ocean Test Structure

Much of the recent work with electromagnetic current meters has been done by the offshore oil industry. The design of offshore structures can be improved by knowing the directional spectrum, and the structures themselves are a good place to mount the instruments.

In November 1976, Exxon installed the Ocean Test Structure in 66 ft of water in the Gulf of Mexico. Although the structure was 20 x 40 x 120 ft, it was actually intended as a large-scale model of prototype platforms for exploration and production that are much larger. The program attracted the support of many other companies and drew on the talents of several consultants for instrumentation and analysis. Over-all descriptions of the program are given by Haring et al. (1978) and Geminder and Pomonik (1979).

The experiment was designed to produce an improved understanding of the forces caused by storm waves. The structure and instrumentation system were designed to enable calculation of the total lateral load and overturning moment from strain measurements made at the base level. In addition, local forces were measured at many locations and a detailed description of the waves was provided by 5 wave staffs and 11 electromagnetic current meters. The instrumentation layout is shown in Figure 5. The data acquisition system recorded 96 channels of information at 10 Hz during storms.

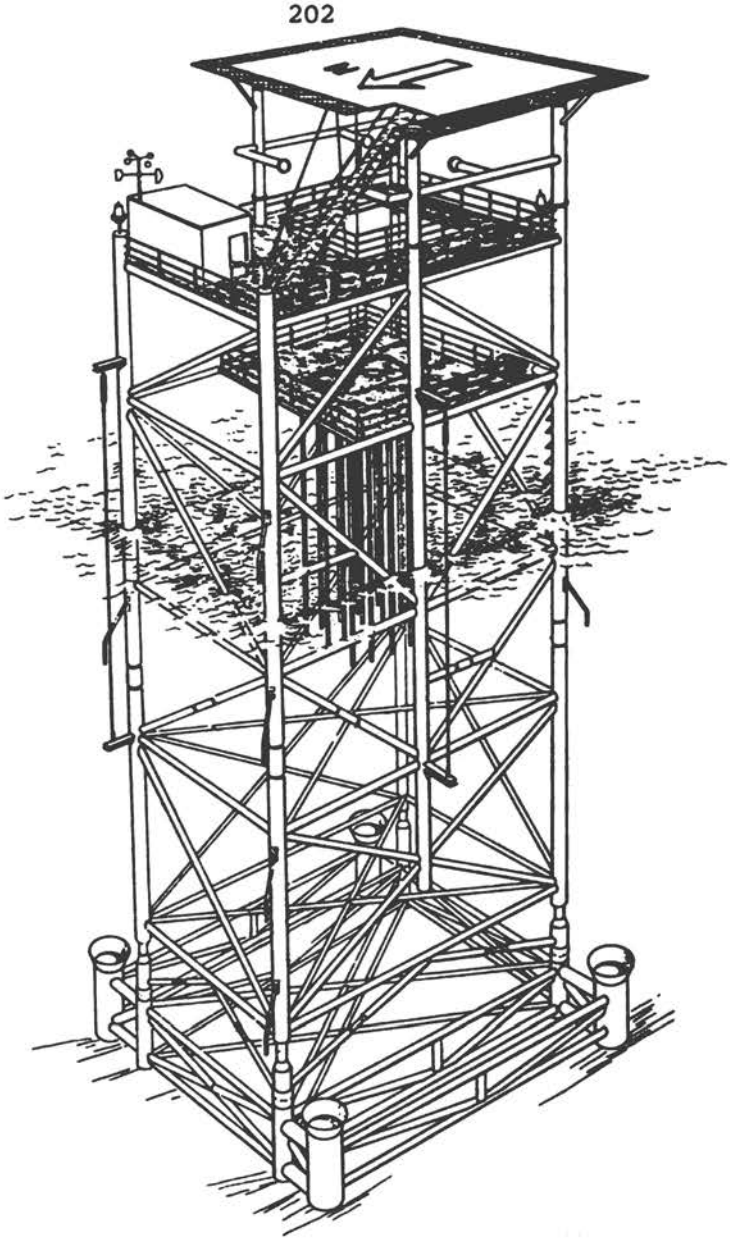

Figure 5 The Ocean Test Structure

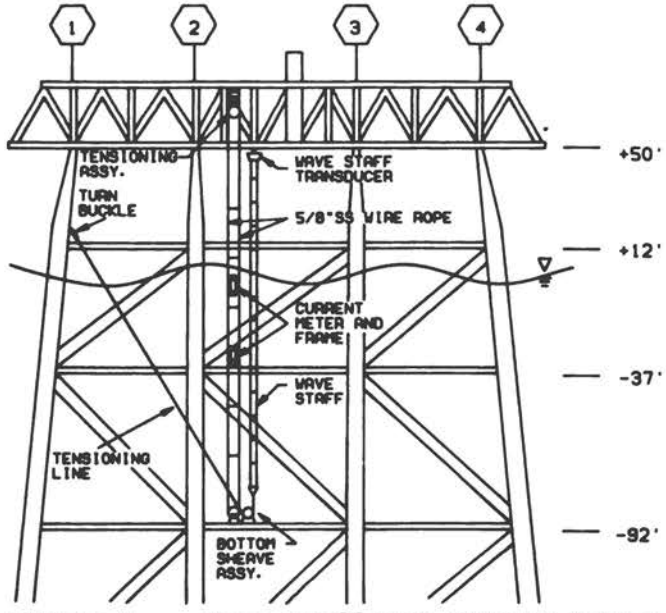

Figure 6 Wave-staff and current-meter locations at the Cognac platform

The large number of oceanographic sensors on the platform permitted an investigation of different methods of describing the directional spectrum. A single current meter and wave staff provide only limited information about directional spreading. This information seems best used in determining the parameters of a unimodal and symmetrical function. The parameters give the mean direction of travel and some measure of the spreading at each frequency. The method works well if the true spectrum is unimodal and symmetrical at each frequency, but poor results will be obtained if these conditions are not met. Previous experiments with high directional resolution have indicated that the directional form is usually simple, but the issue is far from resolved. The Ocean Test Structure results provide a valuable opportunity to determine the optimal number of sensors for obtaining directional spectra.

Borgman and Yfantis (1979) calculated the cross-spectrum between each pair of a set of sensors and formed a large system of equations for the Fourier coefficients of the spreading function. A method of weighted least squares was used for the solution of the system. They found that even though there were many sensors, only a few coefficients could be reliably calculated, since the spatial separation of the sensors was rather small compared to the wavelengths of interest. However, they were still able to test for bimodal spreading functions. They could not clearly identify any cases of bimodality in several hours of data from different storms. This negative result is quite useful, since it suggests that a single wave staff and current meter provide enough data for most purposes. It seems that different directions of wave travel are largely separated into different frequency ranges.

Cognac Platform

After structures are designed and installed, the need often remains to monitor the waves and the response of the structure, particularly when the structure or the site is new. The Cognac platform just south of the Mississippi delta is such a structure, constructed at sea from three huge prefabricated pieces to form the largest oil production platform. It stands in just over 1000 ft of water.

The design of the Cognac platform took into account results from a fatigue analysis (Kinra and Marshall, 1979), since the fundamental period was in the range where almost continuous wave action was expected. Millions of low-stress cycles could damage the structure through fatigue. The analysis showed, however, that directional spreading of the waves substantially reduced the stresses.

More platforms will certainly be built in similar environments and water depths, so it is valuable to monitor the Cognac platform's performance, and to compare actual performance to the design calculations. For this purpose, a rather complete system of instrumentation was designed and installed with the platform. A 32-channel microcomputer data acquisition system records such variables as strain in selected platform members and acceleration of the deck. Estimates of the

directional wave spectra are deduced from the measurements of a wave staff and two electromagnetic current meters. Figure 6 shows the arrangement of the wave staff and current meters.

The current meters are supported on a taut wire system of the type described by Forristall and Hamilton (1978). It consists of a single wire rope stretched over an upper and lower sheave and tensioned with an adjustable spring above the upper sheave. The current meters are clamped in frames which are supported by the taut wires. The meters may be raised or lowered by rotating the sheaves. The system has been proved in several installations. It provides a nearly rigid mount with minimal interference to the incident flow.

For the Cognac instrumentation project, the current meters were originally set at 7 and 27 ft below mean water level. The upper meter was set high to provide good directional information on short waves, which cause the bulk of fatigue loads; the bottom meter was placed low enough that it would only rarely come out of the water (in high storm waves, for example).

The monitoring program has been in constant operation since the spring of 1979, and many useful data have been collected, including measurements during Hurricanes Bob, Frederic, and Allen.

The Sea Wave Attenuation Measurement Program (SWAMP)

The Cognac wave measurements are also being used as data in a program focusing on the attenuation of waves as they propagate over a soft bottom. The Mississippi delta lies just north of the Cognac platform, and the soft sediments deposited there can attenuate water waves through frictional dissipation.

To obtain quantitative information on this mechanism, SWAMP was initiated the summer of 1979, using a Waverider buoy moored in 70 ft of water in East Bay. The Cognac system and the buoy obtained data during Hurricane Frederic. In December 1979, the shallow-water measurements were extended to include platform-based measurements using a wave staff and two electromagnetic current meters. This system has been described by Forristall et al. (1980). The wave staff and current meters are supported by a mast hung from a 200-ft bridge connecting two platforms. Figure 7 shows the current meters mounted on the mast just before the mast was rotated into the water. The mast is designed to be reasonably transparent to waves propagating through it. Guy wires stiffen it, keeping it almost motionless, even in storm waves.

The first step in the analysis of the SWAMP data is comparing the directional wave spectra measured at Cognac and those measured at the site in East Bay. In order to determine accurately the degree of attenuation owing to the deformable bottom, transformations due to the shape of the bottom contours must first be calculated. Thus, we performed a complete refraction analysis for each frequency and direction of travel at the shallow-water site.

Figure 8 shows the result of refracting the spectrum that was measured at 1200 CDT on September 12, 1979, during Hurricane Frederic. The directional spreading is described by the parametric form

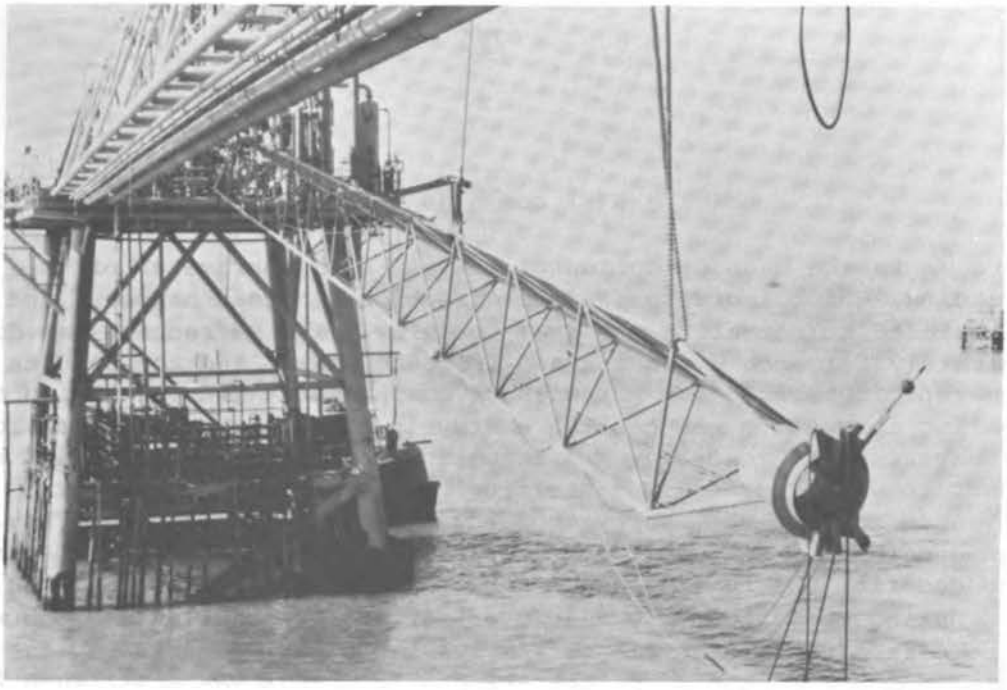

Figure 7 The SWAMP instrument mast being lowered into the ocean. One spherical current meter is visible at the end of the mast and the other is held by a frame above the mast.

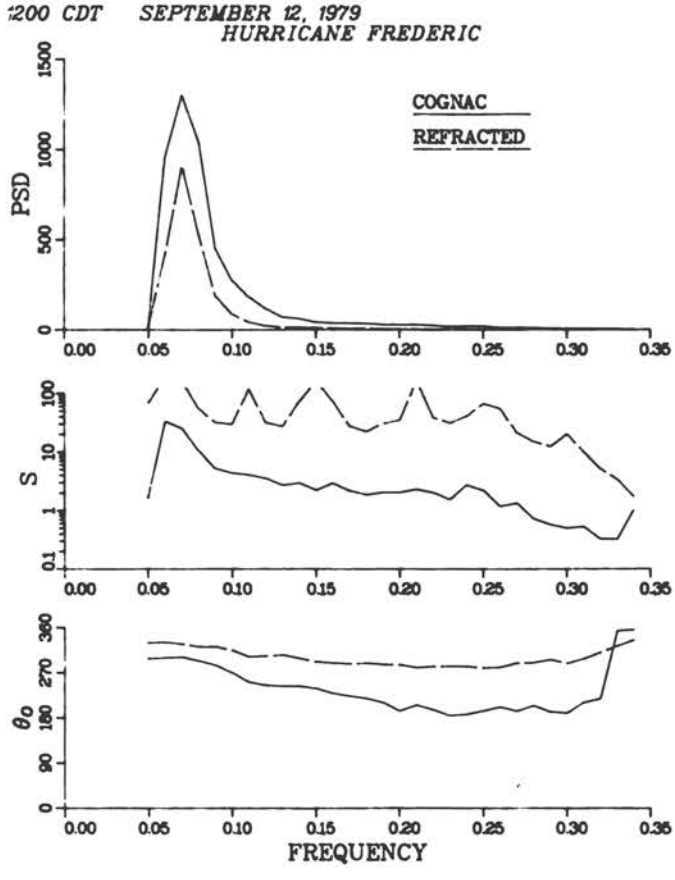

Figure 8 Parameters of a directional spectrum measured during Hurricane Frederic. The refracted spectrum was produced by applying gain factors to each frequency and direction in the measured Cognac spectrum.

$$H(\theta) = N(s) \cos^{2s} (\theta - \theta_o) \qquad (3)$$

where θ_o is the mean direction of travel, s the parameter of spreading, which increases as the directional spread narrows, and N(s) is included to normalize the area to unity. The refraction was done separately for each direction and frequency band, and the results were then reparameterized for purposes of comparison. The refraction and shoaling correction reduces the energy in the spectrum and also rotates the wave rays so that they are traveling closer to due north and are closer to unidirectional. Shielding by the passes of the delta prevented most of the energy above 0.10 Hz from entering East Bay. The values of θ_o and s above those frequencies in the refracted spectrum thus describe the few rays that curved around the passes.

During Frederic, only the Waverider was in place in shallow water, so no directional measurements are available for comparison. The measured power spectrum (Forristall et al., 1980) was still much less than the refracted spectrum, showing attenuation by a nonlinear process. Analysis of storm data, including directional measurements, is now in progress.

The Boundary-Layer Measurement System (BLMS)

Measurements of the directional spectrum using current meters do not necessarily need to be made from platforms. The same sort of system is also well suited to making measurements in the bottom boundary layer. The dynamics of this layer have been one traditional focus of sediment transport studies, but they are also important to the design of pipelines. The fluid velocity very near the bottom governs the stability of a pipeline laid on it. To prevent wasteful overdesign, the pipeline should not be buried when its weight on the bottom is sufficient to prevent its motion in storm waves.

The American Gas Association (AGA), a trade group that sponsors many research projects to better the industry, has funded work on the stability of pipelines for several years. The association's latest project was the design, construction, and deployment of a bottom-supported tripod holding a stack of five current meters and a pressure transducer, as well as related equipment (Dick and James, 1980).

The complete instrument package is shown in Figure 9. The current sensors are spaced at 9, 18, 37, 73, and 145 inches above the bottom, with roughly logarithmic spacing to provide maximum information about the wave and current boundary layers that are expected to have a logarithmic structure. The tripod is supported on the ocean floor by three disk-shaped pads: these provide stability in storm conditions and maintain a low pressure on the bottom. Data are stored on Sea Data cassette recorders in a burst mode, triggered by storm events that exceed preset thresholds.

Analysis of the data usually begins with determination of the directional spectrum, using data from the top current meter (which is least affected by boundary-layer effects) and the pressure transducer.

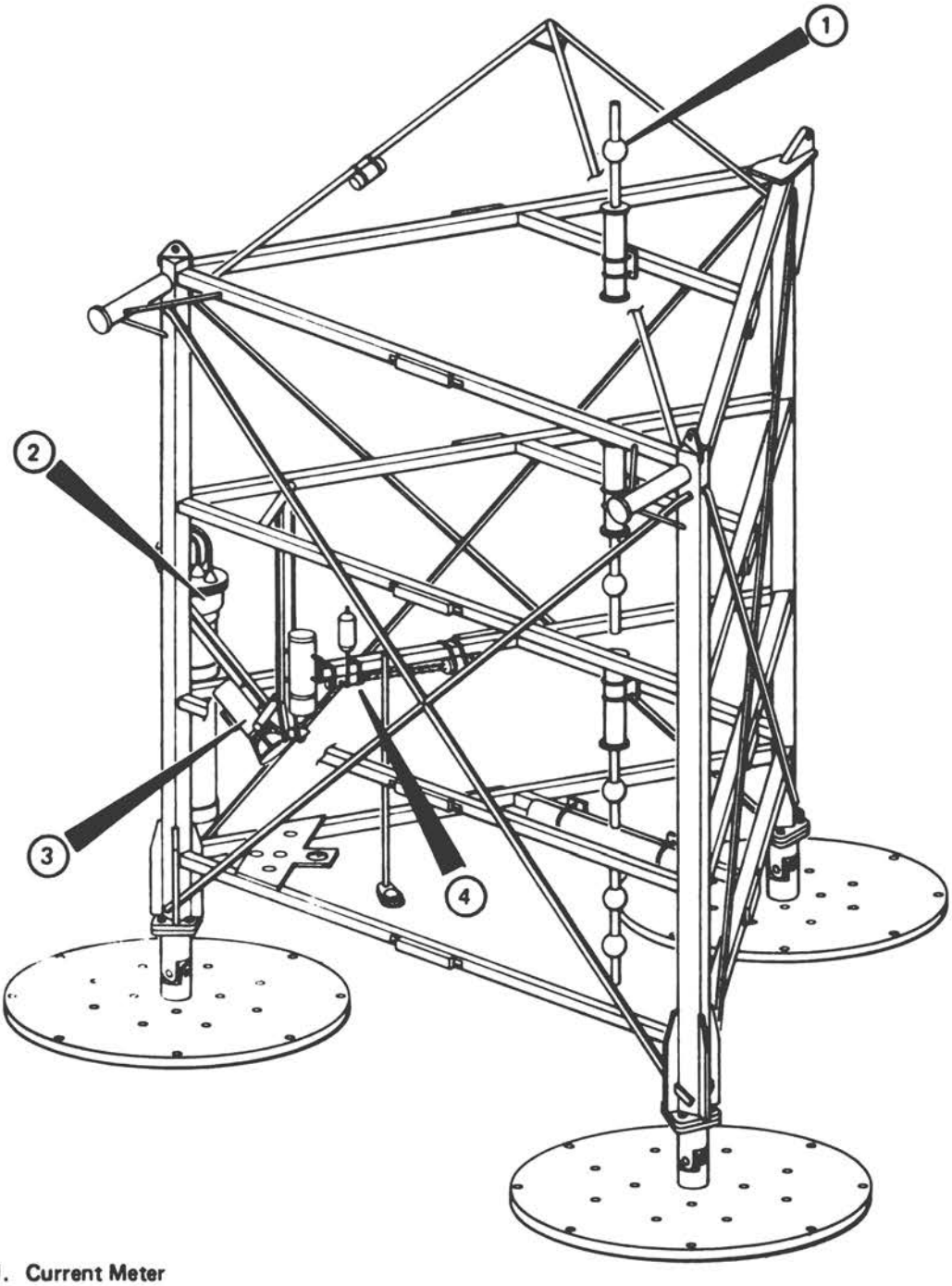

1. Current Meter
2. Recording and Control Module
3. Camera
4. Pressure Sensor

Figure 9 Arrangement of the boundary-layer measurement system tripod and instruments

In this case, attenuation of the high-frequency components of the spectrum is of little consequence, since the pressure transducer and current-meter signals are affected nearly equally. The signals that penetrate to the sensors are the only ones important in producing the boundary layers.

Conclusions

Subsurface sensors have an important role in wave measurement. Pressure transducers can be used to measure the wave spectrum for wavelengths greater than twice the water depth if spectral techniques are used in the data analysis. The use of current meters to estimate the directional spectrum has now become routine and is an excellent choice for this purpose whenever a stable location for the meters can be found.

References

Borgman, L. E. and E. Yfantis (1979), "Three-Dimensional Character of Waves and Forces," ASCE Civil Engineering in the Oceans IV (New York: American Society of Civil Engineers).

Bowden, K. F. and R. A. White (1966), "Measurements of the Orbital Velocities of Sea Waves and Their Use in Determining the Directional Spectrum," Geophys. J. Roy. Astron. Soc., 12: 33-54.

Cavaleri, L., J. A. Ewing, and N. D. Smith (1978), "Measurement of the Pressures and Velocity Field below Surface Waves," Turbulent Fluxes through the Sea Surface, Wave Dynamics, and Prediction, A. Favre and K. Hasselmann, eds. (New York: Plenum Press).

Dick, J. L. and A. L. James (1980), "Boundary Layer Measurement System," Oceans '80 (Washington, D.C.: Marine Technology Society).

Esteva, D. and D. L. Harris (1970), "Comparison of Pressure and Staff Wave Gage Records," Proceedings of the Twelfth Conference on Coastal Engineering (New York: American Society of Civil Engineers).

Forristall, G. Z. and R. C. Hamilton (1978), "Current Measurements in Support of Fixed Platform Design and Construction," Proceedings of a Working Conference on Current Measurement, Technical Report DEL-S9-3-78, W. Woodward, C. N. K. Mooers, and K. Jensen, eds. (Newark, Del.: College of Marine Studies).

Forristall, G. Z., A. M. Reece, M. E. Thro, E. G. Ward, E. H. Doyle, and R. C. Hamilton (1980), "Sea Wave Attenuation due to Deformable Bottoms," Paper presented at ASCE Convention and Exposition, Miami, Florida.

Forristall, G. Z., E. G. Ward, V. J. Cardone, and L. E. Borgman (1978), "The Directional Spectra and Kinematics of Surface Gravity Waves in Tropical Storm Delia," J. Phys. Oceanogr., 8: 888-909.

Geminder, R. and G. M. Pomonik (1979), "The Ocean Test Structure Measurement System," ASCE Civil Engineering in the Oceans IV (New York: American Society of Civil Engineers).

Grace, R. A. (1978), "Surface Wave Heights from Pressure Records," Coastal Engineering, 2: 55-67.

Haring, R. E., D. H. Shumway, L. P. Spencer, and B. K. Pearce (1978), "Operation of an Ocean Test Structure," Paper presented at European Offshore Petroleum Conference and Exhibition, London, England.

Kinra, R. K. and P. W. Marshall (1979), "Fatigue Analysis of the Cognac Platform," Offshore Technology Conference Paper 3378, Houston, Texas.

Kinsman, B. (1965), Wind Waves (Englewood Cliffs, N.J.: Prentice-Hall).

Simpson, J. H. (1969), "Observation of the Directional Characteristics of Waves," Geophys. J. Roy. Astron. Soc., 17: 93-120.

Snodgrass, F. E., G. W. Grover, K. F. Hasselmann, G. R. Miller, W. H. Munk, and W. M. Powers (1966), "Propagation of Ocean Swell Across the Pacific," Phil. Trans. Roy. Soc. Lond., A 259: 431-497.

Suhayda, J. N. (1977), "Surface Waves and Bottom Sediment Response," Marine Geotechnology, 2: 135-146.

Tubman, M. W. and J. N. Suhayda (1976), "Wave Action and Bottom Movements in Fine Sediments," Proceedings of the Fifteenth Conference on Coastal Engineering (New York: American Society of Civil Engineers).

WAVE-MEASUREMENT TECHNOLOGY IN THE 1980s

A. W. Green[1]

1. Introduction

In the preparation of this presentation, I reviewed the evolution of in situ wave-measuring systems since the early 1960s.[2] While this effort uncovered measurement systems that I had never heard of or had long forgotten, I was also struck by the number of wave detectors that had not changed. I was particularly impressed with the fundamental progress achieved in the early 1960s: many of the scientific and technical problems we face today were first defined then. Most of our gains since that time have been in refinements of measurement systems through adaptations of integrated circuit technologies, the most important of which are microprocessors. Such improvements in measuring systems, and the widespread availability of digital processing systems designed to sample numerous sensors at high rates, have provided the basis for recent improvements in our understanding of the physics of wave-train instabilities and wave-group phenomenology.

Thus, I begin the presentation of wave-measurement technology in the 1980s with a brief review of the advances critical to the development of in situ systems in the past two decades and attempt to project their further development (Section 2). In Section 3, I describe novel wave-sensing methods that might be used in systems of the near and mid-term future, and in Section 4, I synthesize some of these ideas to simulate futuristic in situ ocean wave-measurement systems.

2. Evolution of Wave-Measuring Systems

In the 1960s, a typical in situ wave-measurement system consisted of analog detectors, such as heave sensors, capacitive-, inductive-, or resistance-type wave staffs that were linked in some fashion to a data logging unit (Figure 1). The heart of the data logging subsystem was a multichannel, multispeed FM tape recorder, an analog (or hybrid

---

[1]Physical Oceanography Branch, Naval Ocean Research and Development Activity, U.S. Navy

[2]For general references on the evolution of wave-measurement technology, see National Academy of Sciences (1963) Ocean Wave Spectra (Englewood Cliffs, N.J.: Prentice-Hall); American Society of Civil Engineers (1974), Proc. Int. Symp. Ocean Wave Measurement and Analysis, Vol. 1, September 9-11, 1974, New Orleans, Louisiana; Farve, A. and K. Hasselmann (1977), Turbulent Fluxes through the Sea Surface (New York: Plenum Press).

A SIMPLIFIED BLOCK DIAGRAM OF A WAVE MEASUREMENT/DATA PROCESSING SYSTEM 1960-1970

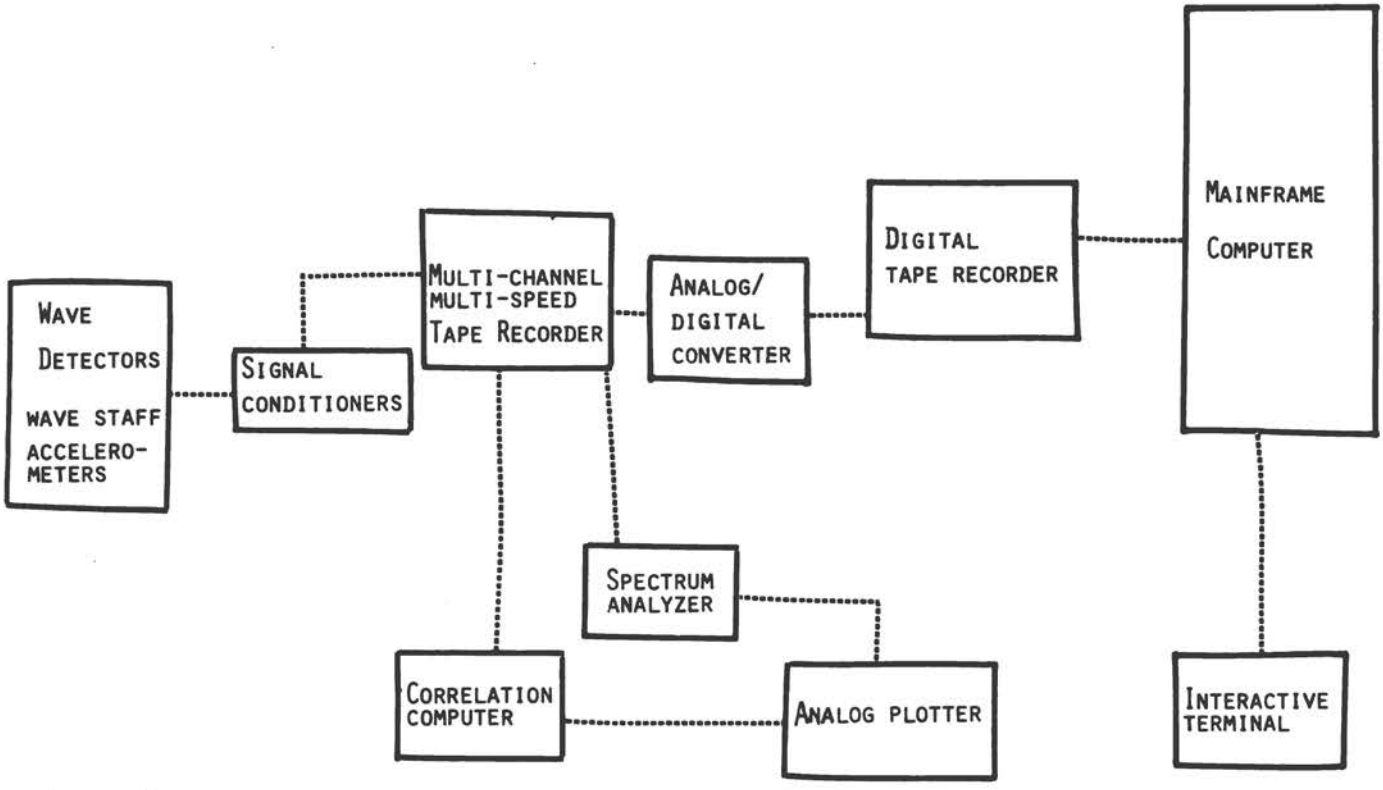

Figure 1

A SIMPLIFIED BLOCK DIAGRAM OF A WAVE MEASUREMENT/DATA PROCESSING SYSTEM 1970-1980

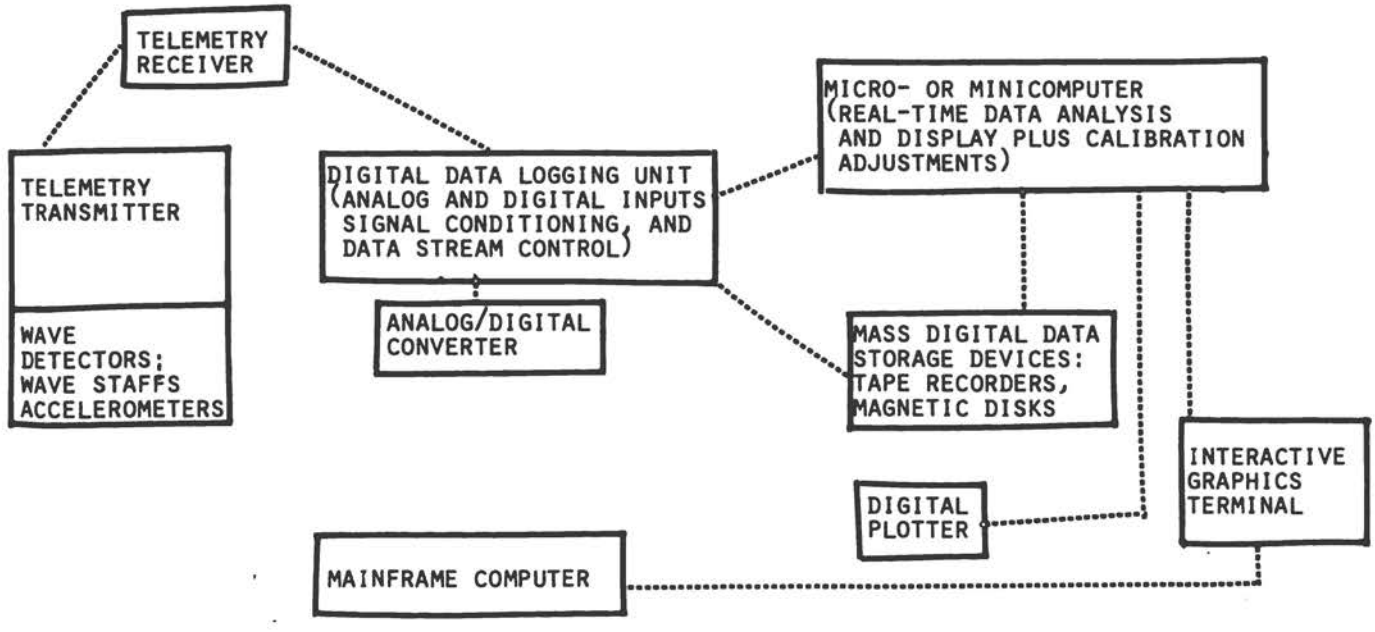

Figure 2

analog/digital) spectrum analyzer, and an analog plotter. More prosperous workers were eventually able to afford high-speed analog/digital converters (A/D) connected to digital tape recorders. The digital records were analyzed on mainframe computers that could be programmed to perform the appropriate analysis. Calibration data for the analog system could be incorporated at this stage. In a few instances, interactive graphic display was available from the mainframe computer.

By the mid- to late 1970s, the typical measurement systems included the same types of detectors, but were equipped with digital data logging systems made up of microprocessor-controlled A/Ds coupled with digital tape recorders (Figure 2). A local microprocessor-based minicomputer was often available for partial analyses of incoming data, controlled by interactive graphics terminals. Initial evaluations of data quality could also be performed routinely. More extensive analyses were made on the mainframe computer, which was able to convolve calibration data with the data stream and perform data quality checks. A large selection of library programs was available for time series analysis. Digital systems greatly improved the stability and accuracy of measurements; the earlier analog systems were subject to drifts of references and were difficult to calibrate.

In some cases, the wave detector was coupled to the data logging system by a telemetry link. If space and power were sufficient, the entire measuring system, including the wave detector, the microprocessor-controlled data logging unit, and the telemetry link could be packaged as a remote station. The addition of a fast Fourier transform module, appropriate filters, and data conditioners enabled the remote station to preprocess spectral data. This new feature considerably reduced the communication linkage requirements. A system of this description has been used by the National Data Buoy Office (NDBO) for its large wave-recording data buoys (Steele and Johnson, 1979).

Two notable trends in these developments are: conversion of data to a digital format immediately after collection, and an increasingly versatile data logging system. One or more microprocessors function as data stream managers or as onboard computers programmed to analyze selected sequences of the data streams. The microcomputers are also capable of deconvolving the data stream with the transfer function of the wave detector. The final data product is stored on a digital tape recorder for later retrieval, or on a low-power, random-access memory until transmitted via the telemetry link. Tasks delegated to the large computer are usually only those that require considerably greater capacity than that of the microcomputer at the measurement site. These jobs include consistency checks between data and models, multidimensional probability distributions of large data sets, or computations of spectral transfer among the components of the wave spectrum.

These advances have been made possible by the concurrent shrinking in size of integrated circuit components and the remarkable increase in computer power. This trend should continue over the next decade. More on-site data analysis will allow us to select data from the measurement stream so that particular events of interest can be analyzed without having to wait for access to a mainframe computer.

We should also note that there has been little evolution in wave-detector systems. There are numerous possible reasons for this; among the most important, perhaps, is that available detectors give the desired responses. The consistent use of the same types of detectors also gives a continuity to measurements from one system to the next, although it is quite clear that there are no well-defined standards for the detector. Consistent differences between wave-measuring detectors have been noted by a number of authors (see Hasselmann et al., 1973), but the reasons for these differences are now fairly well understood. One change that has occurred is the greatly increased number of wave detectors that can be serviced by a given data system. Wave-measurement systems in use today may have the capabilities to service arrays of 50 to 100 detectors. Using a greater number of detectors in a given experiment permits finer space-time resolution of particular events or processes in the wave field. Based on the observation that few changes have been made in wave detectors in the recent past, I surmise that few will be made in the next decade.

3. Sensors for the Future

In this section, I speculate freely about future adaptations of present and emerging technologies for wave detection. I also briefly discuss the implications of compressing wave detection and data logging systems.

A New Pitch-Roll Sensor

Vali and Shorthill (1976) showed that a fiber ring interferometer detects angular rotations owing to the Sagnac effect. The Sagnac effect (see Post, 1967, for details) occurs when the ring interferometer is rotated about an axis normal to the plane of the interferometer. The interferometer (Figure 3) is composed of a long segment of fiber-optic wave guide that is wound around a support, a beam splitter, a light source (laser, laser diode, or other line source of light), and a fringe detector. The light beam is split so that each portion propagates from opposite ends of the fiber. The light waves emerging from the ends of the wave guides form interference patterns (fringes) when they are superposed. When the interferometer is rotated at angular velocity Ω, there is a shift in the fringe pattern,

$$\Delta Z = 2\Omega LR/\lambda c$$

where L is the length of the fiber loop, R is the radius of the loop, λ is the free-space wavelength of the light, c is its free-space velocity, and Ω is the angular rotation rate. Variants of this device have a long and interesting history (Post, 1967). Lin and Giallorenzi (1979) showed that the fiber ring interferometer could detect Sagnac-effect rotations with sensitivities on the order of 1/1000 degree per

SAGNAC EFFECT

FIBER RING INTERFEROMETER

MULTI-TURN SINGLE-MODE

OPTICAL FIBER LOOP

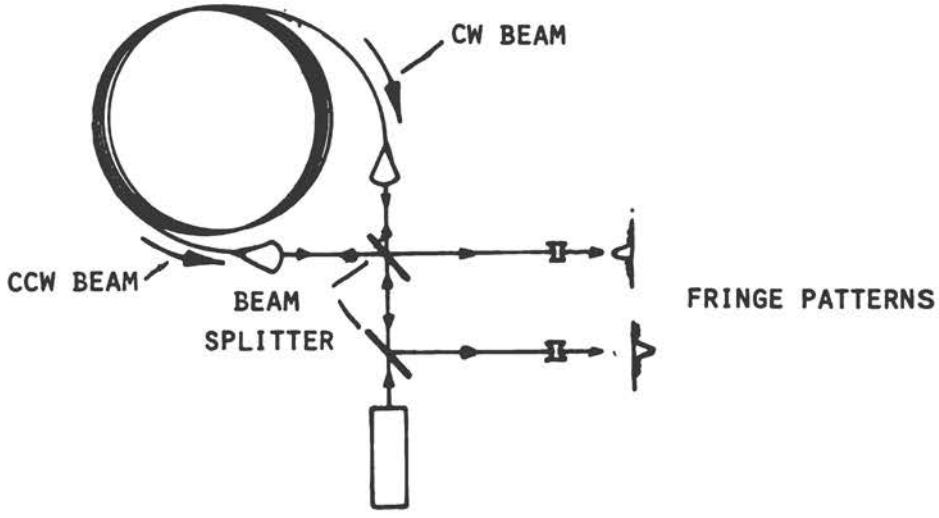

Figure 3

SCHEMATIC REPRESENTATION OF A 3-AXIS SAGNAC EFFECT "GYRO"

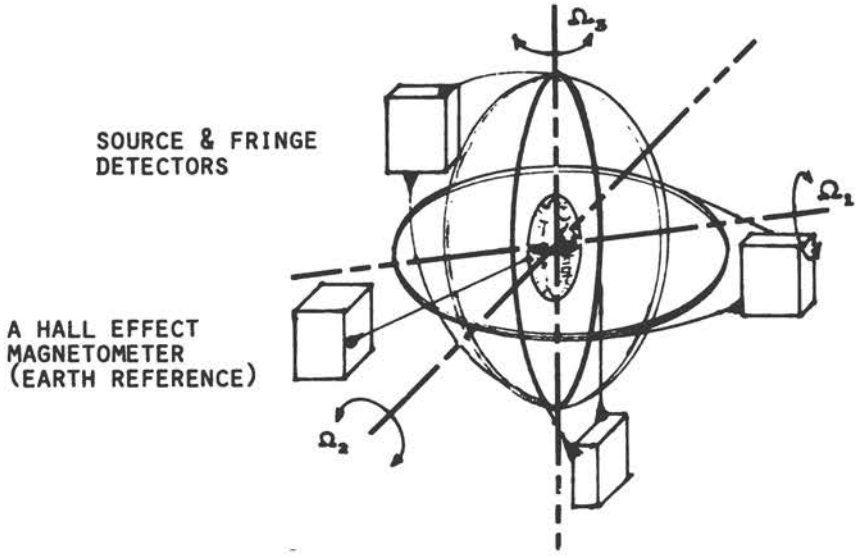

Figure 4

hour. This sensitivity is much greater than that required to detect pitch and roll on a wave-following buoy.

The device could be the "ultimate" pitch-roll detector. First, it has no moving parts. Second, it shows no inherent drift. Third, it can be constructed very inexpensively from easily obtainable components, and its configuration can be made robust. Nested interferometer rings (Figure 4) could be configured as a sensitive inertial navigation system, or as a Sagnac-effect pitch-roll detector, with much less stringent design requirements and at somewhat lower costs. These detectors would be linear in their response to pitch and roll, whereas those used today, operating on mechanical principles, are subject to resonances and liable to highly nonlinear response under some forcing conditions.

The absence of moving parts would also eliminate the mechanical failures of present-day pitch-roll sensors. A three-axis Hall-effect magnetometer could furnish an "earth reference" for the new sensors.

Subsurface Wave-Height Detectors

Bottom-mounted pressure transducers have been used successfully for at least a decade to measure pressure fluctuations due to surface waves. These detectors have a linear response when the waves are in the shallow-water regime, and when local, dynamically generated pressure fluctuations are removed. The limitations of these detectors are well known, and appropriate transfer functions can be used to compensate for some of the errors introduced by the sensors. Robert Dean (private communication) recently developed a variant of the pressure transducer array (Figure 5), that may replace the arrays now in use. This device detects differential pressures between elements of the array. The mean hydrostatic field over the array is subtracted as a background measurement, and the differential pressures across the array are measured directly. This method reduces random error in the estimates of pressure gradients caused by taking differences among total pressures--measurements that include a large hydrostatic term.

Direct measurements of water-height variations can also be made using sonar. Roderick (1979) demonstrated that arrays of ultra-high-frequency sonar transducers could be used to measure surface-height variations with a high degree of resolution (Figure 6). I believe this method of wave detection has not been more extensively used because it requires the coordinated application of techniques from two distinct disciplines, acoustics and hydrodynamics. In addition, the high data rate demands specialized processing methods.

Sonar wave detectors have one decisive advantage over pressure transducers; namely, their response to surface displacements is inherently linear. Instrument noise is mostly predictable, although problems can be caused by air bubbles.

Since the publication of Roderick's work, the costs of assembling sonar wave detectors may have decreased with large-scale integration of the circuits. For instance, the transducer, driver, amplifier,

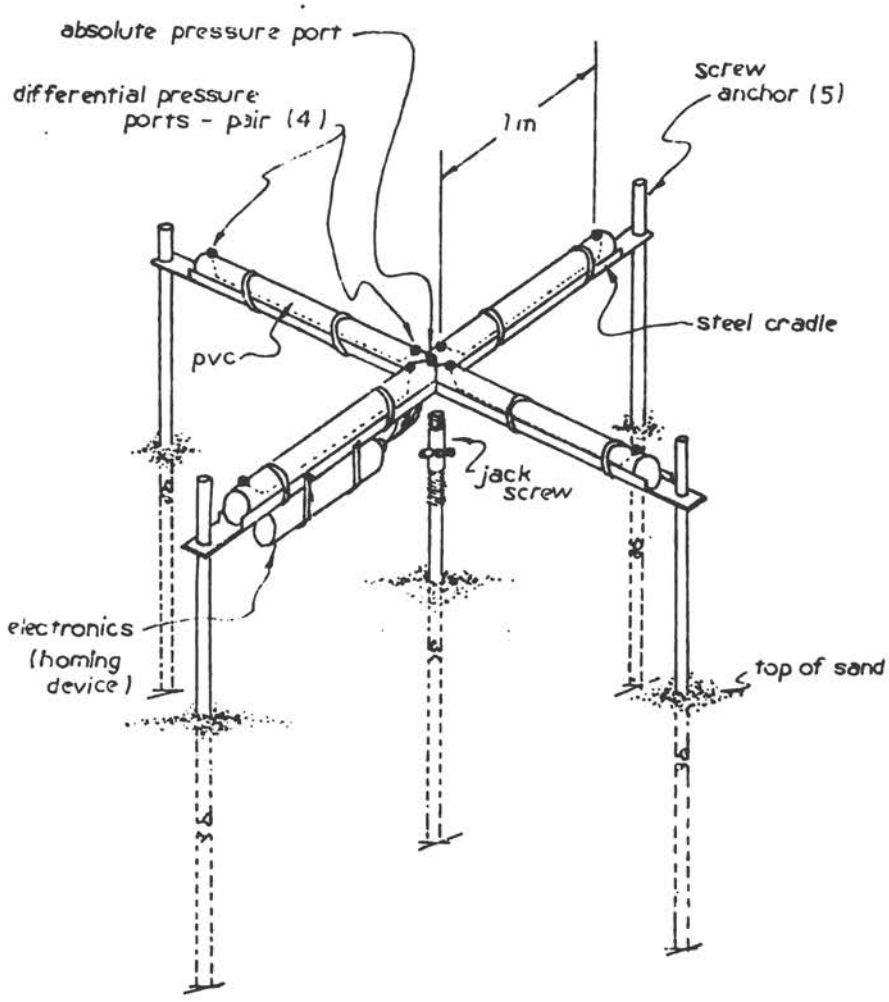

Figure 5 Pressure transducer array

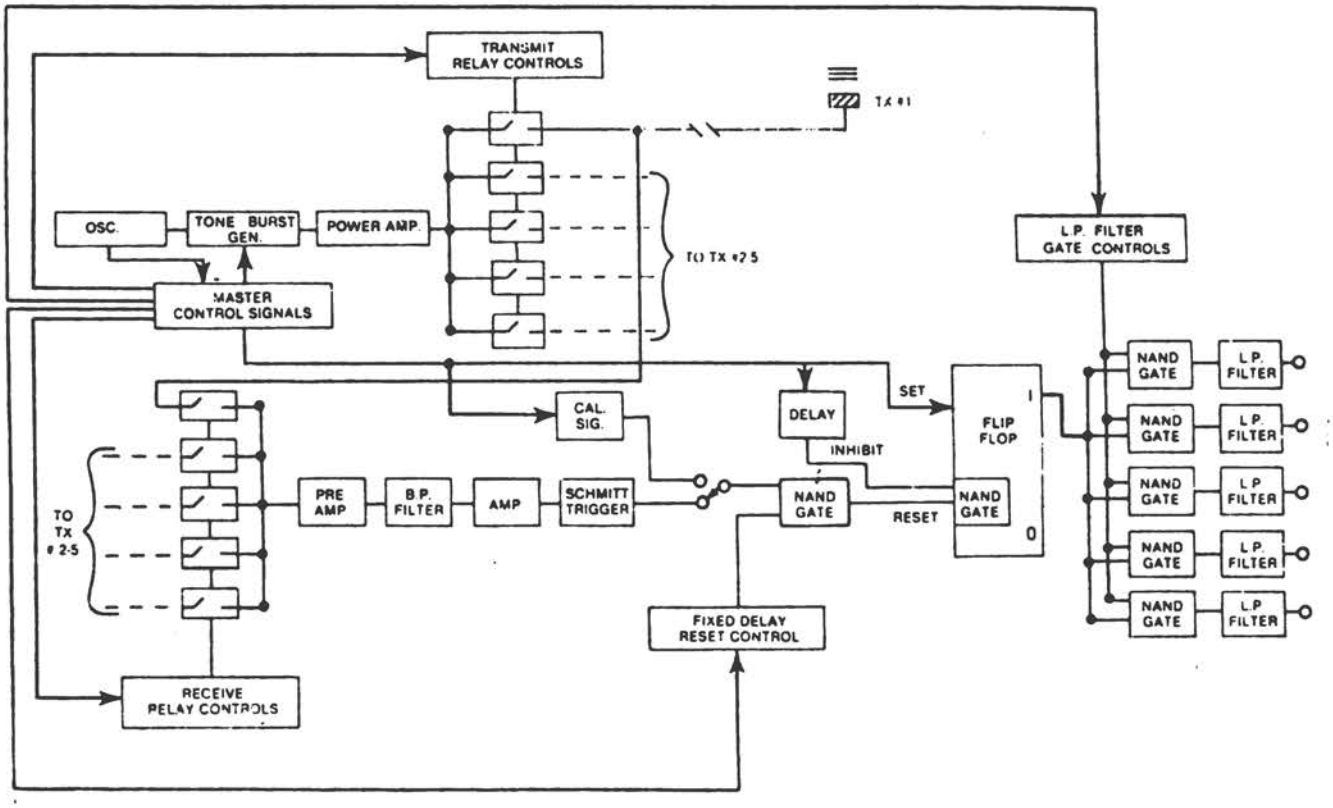

Figure 6 Simplified block diagram of five-sensor, acoustic wave-height measuring system*

*Adapted from W. I. Roderick (1979), "Doppler Spectra of Bistatic Reverberations from the Sea Surface," Naval Underseas Systems Command Technical Report No. 6031, New London, Connecticut.

detector, and timing circuitry required for a basic system are now available on a single LSI (large-scale, integrated) circuit, the cost of which is quite low. These circuits are commonly used in depth sounders and in fish detectors on recreational boats. Measures of wave steepness and directional spectra can be obtained from arrays of these sonar transducers. Advances in integrated circuit technology would also reduce the size of the data control network that was originally used in Roderick's demonstration of the concept.

Substitutes for Wave Staffs

Sea state is often continuously monitored on offshore structures by wave staffs that detect resistance or capacitance changes caused by water-surface displacement. Although these systems have proved quite reliable, they are subject to marine fouling and are sometimes expensive to maintain.

There are two interesting alternative detectors for wave measurements from stable platforms in shallow water. One is radar sounding of the water surface by a narrow-beam radar transmitter/receiver mounted on the platform. Such a system is now under development at Grundy Environmental Systems in San Diego, California. Ranging from the platform to the sea surface is also possible with ultra-high-frequency sonar. This method may have an advantage in that parametric beam-forming can produce a sufficiently small footprint at an acceptable power level. To the best of my knowledge, there is no development under way of a sonar system to measure wave direction.

As Dr. Allan Parker notes in these proceedings ("Wave Measurements Using Surface-Mounted Instruments"), laser wave-height systems are already in service. Arrays of radar, acoustic, or laser transducers could be used to make measurements of wave steepness and directional spectra with the appropriate processing equipment, but special data processing methods would have to be developed for the high data rates. In many cases, maintenance of these systems could be somewhat less costly than maintenance of existing wave-staff systems.

Compression and Standardization of Wave-Height Measurement Systems

With the large-scale integration of electronic circuitry available today, the reduction of an entire data-logging system, including data quality control, filtering, and spectral analysis modules, could conceivably be compressed to a volume less than 1000 cc. This could include mass-storage devices based on bubble memories, with capacities equivalent to the standard digital cassette. Compression of the data processing electronics, combined with standardization of circuitry, would lead to significant cost savings for users: the data computer would incorporate a standard computer communications interface. Reduction in costs would also allow system redundancy, further increasing system reliability.

I have mentioned some possibilities in this section for new types of sensors and modifications of data logging systems. In the succeeding section, I wish to show how these features can be synthesized into wave-measurement equipment with a broad range of applications.

Designs for Wave-Measuring Systems of the Future

The extensions and applications of technologies I have mentioned are conceptually possible. The principal constraint acting against their development is lack of an interested sponsor. No government agency appears willing and financially able to undertake the necessary developments, and the private sector may see the risks as high and the ultimate financial reward as relatively low, owing to the limited number of users. If the need for wave data is indeed great, we might anticipate that investments will be made in modernizing our wave-measurement systems. In the spirit of futurism, I propose some novel systems that might have important advantages.

Deep-Water Wave Monitors

Pitch-roll buoys of various forms have been used since the 1960s to measure wave steepness and the directional properties of wave fields. The response of pitch-roll buoys to wave forcing is fairly well known for most methods of deployment (see Blendermann, 1980, for a general review). Little attention has been given to standardizing these wave-following buoys, perhaps because there are few designs. Lack of diversity, however, stems from the limited number of users of these systems, not from optimization of design.

As noted in a previous section, the NDBO pitch-roll buoy is a prototype of future systems, with the exception that it does not follow the trend to compression of the electronics and wave-detection packages. Wave-monitoring systems could be reduced to a size that would allow deployment from small ships or from aircraft. Of course, the large data buoy system must also provide measurements of atmospheric pressure and wind speed, but these, too could be obtained by means of a much smaller integrated system.

The shrinking of a system's size, such as that of the NDBO buoy, would offer several economic advantages. The compression in size and standardization of the electronic package, wave detectors, and other sensors could potentially lower the unit cost. Costs associated with large seagoing vessels for deployment and maintenance could be appreciably reduced. The vessels required to deploy the large data buoy systems cost in excess of $10,000 a day to operate. A deployment sequence may require 2-10 days, and servicing is required in the event of equipment failures or accidents with fishing and cargo vessels. Total deployment and maintenance costs are high, perhaps from $50,000 to $100,000 a year. This cursory analysis suggests it would be beneficial, in terms of costs and resource allocations, to explore the development of much more compact and standardized systems.

Agencies other than NOAA have need of wave-climate measurements in remote areas. Units deployable by air would be of considerable use to the Navy, since they would afford access to regional wave climates, and would furnish ground-truth data for future wave-measuring satellite systems. An advanced deep-sea wave-measurement system of this type can be depicted as a block diagram (Figure 7) that includes the following elements: 1) data management and processing modules, which would be the heart of the system; 2) nonvolatile, low-power memory, providing mass data storage when the telemetry linkage cannot be used; 3) pitch-roll detectors in the form of a three-axis Sagnac-effect gyro; 4) local earth-fixed reference, furnished by a three-axis Hall-effect magnetometer; 5) subsurface current and temperature sensors attached to the bottom of the buoy; 6) a surface meteorology package consisting of a pressure transducer (barometer), and water-surface and air thermometers; 7) wind-speed measurements inferred from multispectral analysis of subsurface sound field (see Shaw et al., 1978, concerning this application); 8) the telemetry link, most likely through a satellite to a ground station. A satellite Doppler navigational system also would be included as a check against navigation data furnished by the gyro and compass system. The tethering system for the buoy would be determined by the particular application. In remote areas, where synoptic coverage for many months is needed, buoys could be deployed from ships of opportunity or possibly from the air. In remote locations, buoys could be considered expendable, if their unit cost is below that of their recovery.

Synchronized Arrays of Wave Buoys

The final glimpse into the future of *in situ* measurement systems might be regarded as an attempt to answer some fundamental scientific questions about the evolution of wave groups and the soliton-like behavior of wave packets in developing seas. Determining the physical processes of wave-group evolution requires a relatively dense array of sensitive measuring devices. Simultaneous measurements of deep-sea waves uninhibited by boundaries and water depth could be made by freely drifting arrays of buoys outfitted with synchronized timing and accurate position-finding systems and with a small response function programmed in the onboard data system so that the dynamical response of the buoy would be compensated in the recorded measurements.

Acoustic tracking from buoy to buoy can also enhance the spatial resolution of the array. Twenty years ago, systems of this complexity would have appeared to be far beyond the borders of the futuristic in the territory of the outlandish (and may still be); however, we should note that within the last 20 years, we have gained the capability to mount entire data systems, including recording for mass data storage, in containers of only a few thousand cubic centimeters, and it seems almost believable that we can develop systems for upper-ocean measurement on this scale. The primary factor inhibiting development of any of these new systems is lack of the necessary concerted and continuous efforts.

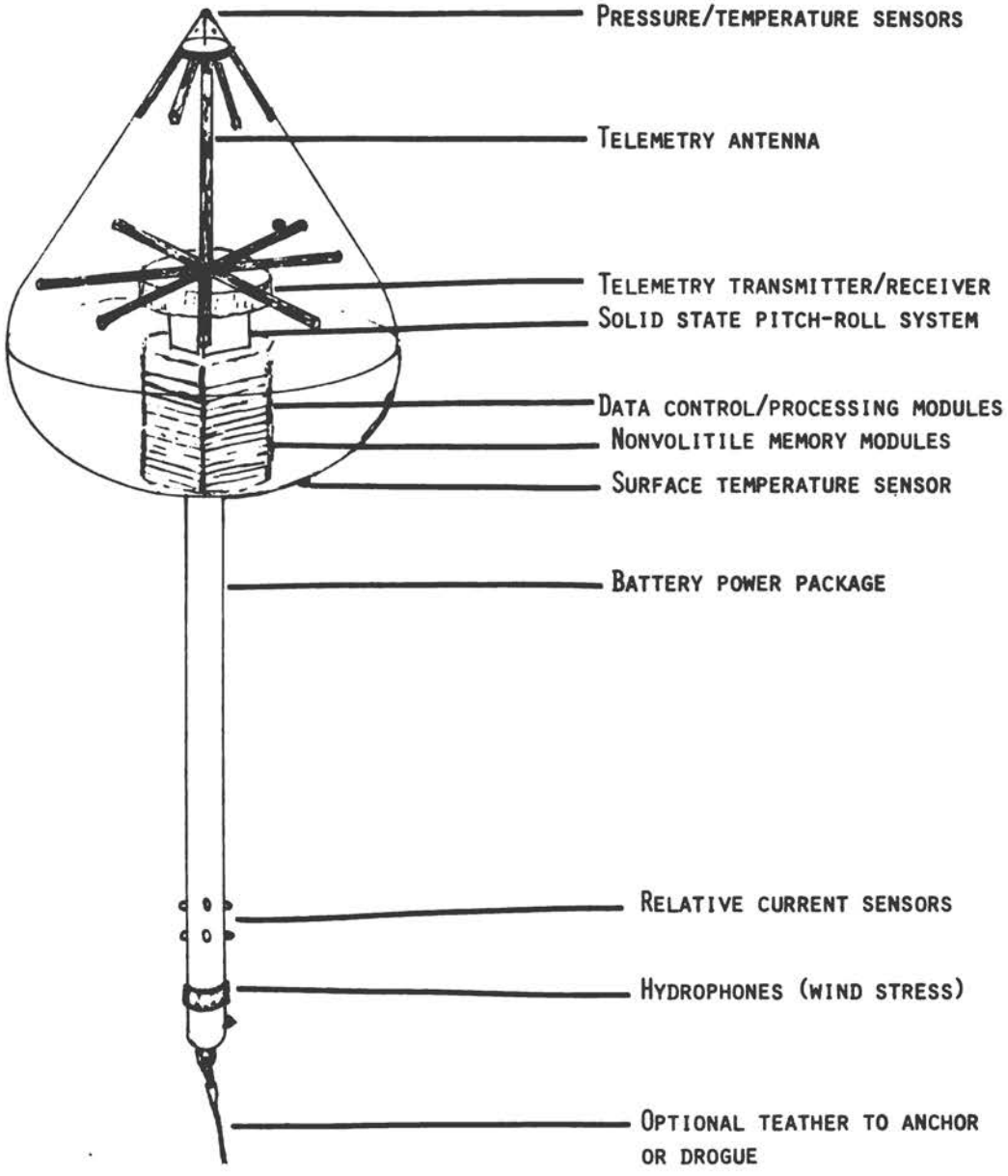

SKETCH OF A BUOY EQUIPPED TO COLLECT AND PROCESS WAVE AND MET. DATA

Figure 7

4. Discussion

Preceding sections give a brief summary of the obvious trends in wave-measurement technology. Continued compression of the data loggers will continue regardless whether the "wave-measuring community" adopts the advances. Incorporation of the more exotic devices, such as the Sagnac-effect pitch-roll detectors, is a more remote possibility, but the benefits could be great, since the instruments could furnish absolute orientation data. Freely drifting buoys equipped with flow velocimeters could provide accurate estimates of upper-ocean currents; these measurements are not reliable now, since undetermined platform motions cause signficant errors.

Standardization and Calibrations

No physical standards laboratory has been established for large-scale calibration of wave-measurement systems. The lack of physical standards or references for wave measurements creates problems in comparing results among systems using different wave-detector elements and data processing. All too often, problems that have arisen in the limited number of intercomparisons of wave-measurement systems have been ignored, or simplistic explanations of the differences have been given without sound justification in terms of data and theory. Adoption of standard references and tests for wave-measurement systems could eliminate these problems. The use of detectors without moving parts would greatly ease testing and maintaining the reference standards. Fortunately, most of our shallow-water wave detectors are solid state, but deep-water units depend on mechanical linkages or direct measurements of force; consequently, there are inherent problems of drift of the electronic references and the sensors. Adoption of a standard data logging module would help eliminate inconsistencies in the initial treatments of the data. If this workshop could start a long-term effort to develop wave-measurement references and standards for <u>in situ</u> instruments, it would be a notable result.

More Technical Challenges

I have restricted this discussion of wave measurement to the technology of sensors and ancillary electronics. There are other technological challenges that have defied us for years and will continue to do so in the future. First, marine fouling of detectors is an ever-present threat to wave detectors in deep and shallow waters, particularly when long-term measurements are required. In highly productive zones disabling fouling of instruments can occur within a few weeks if anti-foulants are not applied. Measurements that use undisturbed detectors for more than six months are subject to fouling, even with the application of anti-foulants. Although research has considerably

advanced understanding of biofouling processes, there is still no long-term anti-foulant treatment.

A second technical (and sociological) challenge is the loss or destruction of moored and bottom-implanted systems in ship collisions and fishing activities. The production of much smaller, less conspicuous buoys could reduce the hazards, and the reduction of costs (by standardizing parts and reducing sizes) could make buoys less expensive to lose.

References

Blendermann, W. (1980), "Buoys," Air-Sea Interaction (New York: Plenum Press), pp. 645-679.

Hasselmann, K. et al. (1973), "Measurement of Wind Wave Growth and Swell Decay During the Joint North Sea Wave Project (JONSWAP)," Dt. Hydrogr. Z., Supplement A.

Lin, S.-C. and T. G. Giallorenzi (1979), "Sensitivity Analysis of the Sagnac-Effect Optical-Fiber Ring Interferometer," Applied Optics, 18: 915-931.

Longuet-Higgins, M. S., D. E. Cartwright, and N. D. Smith (1963), "Observations of the Directional Spectrum of Sea Waves Using the Motions of a Floating Buoy," Ocean Wave Spectra (Englewood Cliffs, N.J.: Prentice-Hall), pp. 111-132.

Post, R. J. (1967), Reviews of Modern Physics, 39: 475-485.

Roderick W. I. (1979), "Doppler Spectra of Bistatic Reverberations from the Sea Surface," Naval Undersea Systems Command Technical Report No. 6031, New London, Connecticut.

Shaw, P. T., D. R. Watts, and H. T. Rossby (1978), "On the Estimation of Oceanic Wind Speed and Stress from Ambient Noise Measurements," Deep-Sea Res., 25: 1225-1233.

Steele, K. and A. Johnson, Jr. (1979), "Data Buoy Wave Measurements," Ocean Wave Climate (New York: Plenum Press).

Vali, V. and R. W. Shorthill (1976), "Fiber Ring Interferometer," Applied Optics, 15: 1099-1100.

RESULTS OF THE WORKSHOP

An important objective of the meeting that is the subject of these proceedings was to identify and describe the outstanding problems requiring solution in wave measurement. In the interest of this objective, the steering committee planned workshops structured to elicit as much of the expertise and informed opinion of the assembled participants as possible. From a full list of problems articulated by all participants, consensus would be sought on the ten most important or urgent, and their order of priority.

Nominal Groups

The structure selected by the panel for the workshops was that of nominal groups (Van de Ven and Delbecq, 1971). In nominal groups, the members work in one another's presence, but without interaction. It has been demonstrated that in the critical phase of program planning reserved for speculative consideration of all aspects of a problem, interacting groups tend to generate and pursue far fewer ideas than nominal groups (Delbecq and Van de Ven, 1971). The nominal group technique allows a period for the silent generation of ideas. Each member then presents an idea in turn, continuing until all ideas are recorded or the allotted time expires. The ideas are not discussed: questions may be asked for clarification of statements.

First Workshop

Participants were divided arbitrarily into six nominal groups to develop statements of the principal problems facing wave measurement. Close to 300 individually numbered statements, each recorded on a large wax-backed card, were brought to the committee at the conclusion of the first workshop. The committee grouped similar statements together and gave them a single number. The statements were then displayed, and each participant given a ballot to cast weighted votes, 10 for the first-ranked through 1 for the last-ranked, most important or urgent problems. Scores were tallied by the committee in preparation for the second workshop, and presented to the participants.

Second Workshop

A chairman was selected for each problem, and participants divided by interest to develop a clear description of the problem, and the outline of a program addressing the problem. These were recorded by each group on large flip-chart sheets.

In plenary session, the participants reviewed and refined each elaborated priority in turn until satisfaction was expressed by the assembly. The consensus statement of the meeting respecting the most important and urgent problems of wave measurement is set out in the succeeding section.

References

Delbecq, A. L. and A. H. Van de Ven (1971), "A Group Process Model for Problem Identification and Program Planning," J. Applied Behavioral Sci., 7: 466-492.

Van de Ven, A. H. and A. L. Delbecq (1971), "Nominal Versus Interacting Groups for Committee Decision-Making Effectiveness," Acad. of Mgmt. J., 14: 203-212.

THE TEN MOST IMPORTANT AND URGENT PROBLEMS FOR WAVE MEASUREMENT

1. WAVE DIRECTION Technology of directional wave-spectra measurement, analysis, and reporting

Problem Several significant problems limit wave-direction information for operational applications, ocean and coastal engineering, and scientific studies. These problems include:

- Lack of technology for use in high sea states and in deep water where there are no fixed platforms available.

- Lack of directional resolution systems at reasonable cost to provide directional resolution consistent with wave models (used for forecasting and hindcasting) and with resolution needed for such studies as wave refraction (and diffraction), sediment transport, wave-current interactions, and for calculation of wave forces.

- Need for well-accepted analysis procedures to improve directional resolution based on both spectral and nonspectral concepts. Most directional information is now provided by statistical techniques, but there is evidence that other methods of analysis, such as data-adaptive techniques, can significantly improve resolution.

- Existing directional measurement systems (and nondirectional systems) have uncertainties at both very low (less than 0.05 Hz) and very high (greater than 0.20 Hz) frequencies. Data at very low frequencies are needed for swell studies. Data at both high and low frequencies are needed for wave-generation studies.

- Better resolution in shallow water is complicated by nonhomogeneous spatial variations in wave conditions owing to local bottom effects.

- There is no consensus on how good existing systems are or on their limitations (including responses).

Over-all, there is a need for directional measurement systems that will work in shallow water, in deep water where there are no platforms, and in high seas. Ideally, these systems should operate reliably for long-term periods, be inexpensive enough to be used for applications rather than just short-term special studies, and provide directional data verifiable by calibration or intercomparison.

Program To define present capabilities, it would be most useful to conduct a series of intercomparison experiments. Actual needs of the

users of data and technical requirements should be defined first. Synthetic experiments using simulated data and available field or laboratory data will be very useful in the experimental design. Laboratory experiments can also improve understanding of the physical processes of various techniques.

Field experiments comparing in situ and remote instruments should be carefully designed so that all systems sample at the same time and place. Selecting a region of the ocean expected to be homogeneous would be best for the first experiments. High-resolution systems are needed as a basis for comparison.

Several possibilities for the development of new systems should be investigated. Low-frequency acoustic backscattering should work in a fashion analogous to radar backscattering. It would be desirable to mount sensors on the bottom in shallow water, if this is feasible. Angled arrays of electromagnetic ranging sensors mounted on platforms could give improved resolution.

Faster and less expensive methods for analyzing surface images should be developed. High-density data storage and in situ processing methods should be developed for in situ systems.

2. DEVELOPMENT OF DATA QUALITY ASSURANCE AND DATA DISPLAY TECHNIQUES

Problem Data quality assurance* is a fundamental problem to all data acquisition and analysis programs. Without this assurance, bounds cannot be set on the measurement results in terms of their relation to the actual phenomena being measured. Thus, the users of the data can have little faith in their application.

There are several components of the quality assurance problem for oceanographic measurement and data processing systems. First, the manufacturer or supplier of the sensor system (either in situ or remote) must ensure that the instrument responds in a repeatable and quantifiable manner to the measured quantity. Second, the data analysis software must be understood by the user(s). Third, reporting of the data must seek to minimize errors of interpretation, and maximize the communication and understanding of the data.

The goal is to establish a systematic and coordinated program for improving the data quality assurance in ocean measurement systems, techniques, and presentation.

Program Data quality assurance for ocean measurement systems encompasses three categories: the sensor-related aspects, the data processing aspects, and the data display and presentation aspects.

---

*Data quality assurance is defined as the use of systems or techniques that can be error-bounded, and that can serve as a reference for other systems.

For the data acquisition/sensor system, a useful course of action would be to develop a commonly understood and accepted reference system and apply it to "validate" other systems. The reference system used for a particular measurement technology may be dependent on the measurement goal, but it should be traceable to other reference systems. Similarly, the reference system may be intended for use in the laboratory or the ocean site, depending on the measurement need, but it should be a system accepted by all suppliers and users.

For the data processing portion of the system, data quality assurance would be greatly enhanced by requiring that all processed output be accompanied by a clear, quantitative statement of the processing techniques used. It is expected that these techniques will eventually become commonly accepted practices. Deviations from common practice should be accompanied by an explanation. Systems that combine sensing and data processing must, of course, observe both sets of accepted practice.

For data quality assurance in the display and presentation of data, standard practices and formats need to be promulgated. In those cases for which these practices and formats are not suitable, a clear quantitative description of the techniques used should accompany the display or presentation (or both).

3. PROGRAM FOR INTERCOMPARING VARIOUS MEASUREMENT SYSTEMS TO DETERMINE DIFFERENCES IN RESULTING DATA SETS

Problem Since there is no absolute standard, it is necessary to intercompare various measurement systems to determine the differences in resulting data sets. This is difficult; we do not have full knowledge of the transfer characteristics, the interactions of the systems with the environment, or the natural variability of the environment.

Some systems provide point data over a period of time. Others operate over space. A wide range of environmental conditions must be considered.

The Atlantic Remote Sensing Land-Ocean Experiment (ARSLOE) took much-needed initiative respecting the problem of intercomparison, but did not test all systems adequately. Methods are needed for establishing the equivalent of a homogeneous environment, but one that varies over time, to provide the whole dynamic range of environmental conditions. One unsolved problem is how to perform the intercomparisons taking appropriate account of the probabilities.

Program Evaluation of ARSLOE results needs to be expeditiously completed and reported to inform decisions about the next steps in the intercomparison program.

Statistical methods for intercomparing data from different types of measurement systems are needed.

A long-term international committee consisting of a broad range of scientists and engineers should be established to develop and promote experiments and methodologies for intercomparison of wave-measurement systems.

4. NEARSHORE WAVE FIELDS AND RELATED PROCESSES

Problem The nearshore wave field has severe measurement problems owing to very large gradients in both alongshore and cross-shore directions. Present measurement technology is capable of limited-resolution point values of the three-dimensional wave field. There is a need to develop measuring technology to improve resolution and broaden the area of coverage to allow definition of spatially inhomogeneous fields.

To understand the variability of these fields, measurement and analysis techniques need to be developed for sediment-boundary layer and air-sea interactions, long waves, surf beat, edge waves, and nearshore circulation and breaking waters.

Program

1. Create a remote sensing system applicable to defining inhomogeneous nearshore wave fields.
2. Develop in situ measurement capability within the surf zone for:

   - o run-up
   - o percolation, pore pressure
   - o breaking-wave characteristics
   - o velocity field, especially near bottom
   - o long waves.

3. Develop in situ capability for higher-resolution directional measurement outside the surf zone.
4. Improve understanding of:

   - o nonlinear effects of shoaling
   - o wind-wave interactions close to shore
   - o wave-current interactions
   - o wave-topography interactions.

5. Establish nearshore wave climatologies through extensive regional networks in a variety of coastal regimes.

5. NONLINEAR PHENOMENA

Problem Nonlinear phenomena have a significant influence on the interpretation of wave measurements and the dynamics of surface waves. Examples of specific problems for the interpretation of wave measurements include:

- o What is the influence of nonlinear wave shapes on buoy measurements?
- o What is the influence of wave nonlinearity on the interaction of electromagnetic (e.g., microwave radar) waves and ocean waves? How do standard perturbational and asymptotic

scattering theories break down as wave slopes and nonlinear wave motions increase? What is the effect on extraction of accurate radar measurements?

- o What is the role of short-wave interactions with longer waves in the interpretation of microwave radar measurements?

Examples of specific problems in understanding the dynamics of surface waves include:

- o What are the modulational or wave-grouping properties of ocean waves?
- o What are the relationships between short waves (capillaries, short gravity waves) and longer gravity waves in the ocean?
- o What measurements of breaking waves and whitecaps need to be made to identify the role of these waves, upper-layer mixing processes, surface energy balance, and extreme wave properties? For interpretation of electromagnetic measurements?
- o What part do nonlinear wave processes play in sediment transport in coastal environments?
- o How are surface waves altered (and how much) by interaction with spatially inhomogeneous currents?

Program

1. Develop a measurement system capable of resolving short-wave (capillary) properties along longer waves.
2. Initiate a research program to identify the relationship between properties of waves and electromagnetic backscattering as a function of increasing wave steepness.
3. Create a system to measure spatial wave-modulation properties.
4. Conduct research to identify and measure relationship between nonlinear wave properties and coastal transport processes.
5. Develop a measurement system for simultaneous, spatially distributed measurements of waves and surface currents.
6. Characterize and improve measurement capability of buoys for nonlinear wave shapes.
7. Measure the effects of wave-current interactions on waves.

6. DEVELOPMENT OF REMOTE SENSORS

Problem Microwave sensors now available should be optimized for accuracy, resolution, and calibration, and for coastal, tower, ship, aircraft, and satellite operation. New sensors need to be developed to measure other ocean parameters, such as rainfall, differences in air and sea temperatures, the directional wave spectrum, surface currents, and nearshore processes. Each of these parameters has an effect on waves and wave measurements. Maximum use should be made of radars able to measure both amplitude and velocity (HF through microwave Doppler radars).

Program

1. Develop improved understanding and models of the interaction of EM waves with the ocean surface.
2. Further improve single-frequency and multifrequency, pulsed and coherent radars (HF through microwave).
3. Test various sensors in Space Shuttle and aircraft for later routine use in satellites.
4. Develop efficient means for processing remotely sensed data and efficient means for distributing the data to users.
5. Consider applying inverse scattering techniques to infer ocean parameters.

7. IMPLEMENTATION OF GLOBAL WAVE-MEASUREMENT SYSTEM

Problem Global wave information in forecast, nowcast, and climatological data base forms is needed by numerous users, such as deep-sea mining concerns, shipping industry, and coastal communities, and for national defense. Remote sensing techniques are the only feasible means for providing continuous wave and wind information in real time, as well as for the global wave climatological data base.

Spaceborne and ground-based sensors are available in either operational or advanced developmental stages. A program should be undertaken to provide the needed data.

Research on nonlinear wave phenomena and development of new remote sensors should be carried out simultaneously to support the task of interpreting remotely sensed data.

Program

1. Significant wave height ($H_{1/3}$) and other wave statistics can be measured by altimeters, as demonstrated by previous satellites. An operational satellite should be launched as soon as possible, or an altimeter should be incorporated into one of the NOAA satellites.
2. HF radar systems, operating in both ground- and sky-wave modes can provide large-area measurements immediately, and should be routinely deployed for this purpose.

8. BUOY* DEVELOPMENT

Problem

Lack of adequate transfer functions	Transfer functions for wave-measuring buoys are needed to extract system errors so that data of consistently high resolution and accuracy can be produced

*Small wave-measuring buoy systems, their sensors and associated components, and transfer functions.

Lack of relative current data affecting transfer function	Wave-measuring buoys do not provide measurements of flow relative to the body. The relative flow measurements are critical for accurate representation of the wave-buoy transfer functions.
Lack of solid-state sensors	The sensors now used in wave-measuring buoys lack the robustness and reliability that could be obtained with solid-state sensors.
Lack of onboard signal processors and data quality control	Present wave-measuring buoys do not include data quality control, processing, or analysis hardware on board.
Lack of capability in extreme sea states	Available systems also lack the capability to make measurements in extreme wave conditions.
Lack of small, expendable wave-measuring buoys	There is a need for small, expendable wave-measuring buoys that provide basic wave measurements with modest accuracy and reliability.
Lack of adequate power systems	The power supplies for small wave-measuring buoys are not adequate for moderate- to long-term deployment.
	The mode of data communication and telemetering from wave buoys should be upgraded for transmission of digital data and data housekeeping functions.

Program

1. Transfer functions: studies should be instituted to determine transfer functions for existing wave-measuring buoy systems. The investigations should include flow measurements to determine the transfer functions of the transducer elements in the electronics, but they must also encompass:

- o The hydrodynamic response of the hull to wave motion and ambient currents
- o The effects of various mooring-system configurations on the over-all transfer function of wave-measuring buoys
- o Methods for determining errors derived from extrapolation of laboratory measurements of transfer functions to sea conditions.

2. Sensor reliability: a program should be undertaken for research and development of several types of solid-state motion sensors plus ancillary data processing hardware and software. This program should also include investigations of the physical phenomena that could be most reliably used to make motion-sensing elements. An important factor is that these motion-sensing elements be economical and easily tested for consistency of response. The program should progress to the stage that a "best" sensor could be integrated into a platform that possesses the optimum hydrodynamic response function for the particular sensor.

3. Onboard processing: it is generally considered feasible to develop specialized data processing equipment of sufficiently small size and power consumption that a significant amount of data processing could occur at the scene of wave measurement. Development of the electronics should be undertaken to formulate data processing requirements, including the degree of local programming of various types of data, and electronic systems that could be adapted to these requirements. It is also highly desirable to develop data systems that would be able to detect data errors, system errors, and data transmission errors. As the data transmission and processing problems are solved, parallel efforts need to be made to improve the telemetry ground stations.

4. Wave measurements in extreme sea-state conditions: the development program for these wave-measuring buoys should include a number of intermediate evaluations to assess performance in extremely high sea-state and sea-state/current conditions, which could be encountered in typical deployments. Research on methods for deployment of wave-measuring buoys in high sea-state conditions should be initiated at the outset. Several configurations should be evaluated in identical conditions. Special consideration should be given to recovery of a maximum amount of recorded data. This may include the development of special types of sensors, or motion-detection algorithms that are activated only in extreme conditions.

5. Expendable buoys: the developments necessary to improve the accuracy and reliability of buoys will lead to more sophisticated systems that will probably be more expensive. In parallel with these developments, work should be undertaken on much less sophisticated wave buoys with ostensibly shorter lifetimes and less sensitivity; however, these devices must be made robust enough to be deployed by air, ships, or boats of opportunity, with minimum cost in manpower or resources. This development would not be aimed at providing data to improve basic knowledge about surface wave fields, but would be accessible enough for use over large areas of the ocean. The data gathered by this type of device would also be of aid to industrial concerns that are strongly affected by ambient wave fields. The research or development program associated with this type of system

would have to draw elements from other programs, such as solid-state sensors. The requirements of compact size and durability may require that special electronic circuits be developed for this particular application.

6. Power supplies: at least three possibilities for improving the power supplies of wave-measuring buoys should be investigated:

- o Achieving high reliability and power density by adaptating available technology
- o Hybrid or mixed sources of power for use in specialized applications; for example, photovoltaic power supplies with standard batteries
- o Using the energy of the wave field to supply base-level power that could be augmented by other power supplies.

The three programs should be concurrent: the latter two possibilities could require significant engineering development work.

9. NEW SENSORS AND PROCESSING TECHNIQUES FOR INTEGRATION INTO WAVE-MEASUREMENT SYSTEMS

Problem As general problems of sensors and processing systems are inherent to other priorities for wave measurements, the specific subject of this priority is needed measurements for which techniques either do not exist or are totally inadequate for field measurement programs.

The technological gaps to be closed through the development of new sensors and signal/data processors are:

1. Routine measurement of high-frequency and capillary waves
2. Measurement of ocean surface curvature and higher-order descriptors (parameters) of ocean surface waves
3. Routine field measurements of wave-induced, large-amplitude motion of water particles
4. Concurrent measurement of surface wave parameters and bottom topography to obtain interaction data
5. Spatial/temporal views of wave patterns and amplitudes from fixed sensors not available from present single-point *in situ* sensors or remote sensors: while aircraft-mounted remote sensors can provide the resolution necessary for the patterns, lack of amplitude and expenses of platforms militate against their routine use
6. Techniques for the processing, storage, and presentation of the large amounts of data generated by wave-measuring systems, both *in situ* and remote.

Program The problems stated here have been addressed in the past by scientists and engineers, but supporting technologies have now been developed that can aid solution. Advances in acoustics and in electro-optics, as well as their transducers and the associated electronics and microprocessors, provide a wide range of new directions for sensor and processor development. Other phenomena, such as electromagnetics, also provide new bases for systems development.

Any program, even using new technology, can profit by reviewing prior attempts both in the same application and in somewhat different applications to the problems of other fields.

The six technological gaps can be grouped into three areas:

- o Individual wave characteristics (1, 2, and 3)
- o Wave-field characteristics (4 and 5)
- o Data handling and presentation (6).

The first five programs would have the same first phase:

Phase 1 The known and postulated spatial/temporal characteristics should be reviewed, and their parameters identified and quantified so far as possible or necessary. This review should take into account the effects of interactions between waves and other phenomena where applicable, and review experiments involving similar measurements, both in the laboratory and in the field, to determine the sensitivities and other characteristics of such interactions.

Phase 2 Experimental sensor-system concepts should be developed based on the results of Phase 1, as well as expected environmental conditions, human factors, and costs.

Phase 3 From the most promising concept developed in Phase 2, an experimental measuring system should be fabricated and evaluated both in the laboratory and in the field, taking into consideration the unique conditions of each.

Phase 4 Technical results and other factors, such as application to specific field measurement programs, alternatives, and economics, should be further explored to enable specifications to be made for prototype engineering models.

Phase 5 The further development of prototype instruments should be accompanied by further engineering tests directed to (among other questions) verification of the quality of the data obtained, and determination of the instruments' reliability and maintainability.

Specific Comments on Technology Gaps 1-5

Gap 1 Studies of high-frequency and capillary waves are most likely conducted in conjunction with the excitation phenomena. Thus, lower-frequency wave measurements and wind measurements may be desired simultaneously. The concurrent measurement techniques should be taken into account.

Gap 2 The data obtained of wave curvature and higher-order descriptors can be useful both for the development and verification of wave theory and as inputs to wave-buoy signal-processing circuitry. The sensor and programmatic approach for these two applications may be quite different, and perhaps conducted by different groups. The data and sensor concepts should be coordinated between the groups to provide greater visibility of the options.

Gap 3 The measurement of large-amplitude wave-particle motion is four-dimensional and very dependent on depth and wave spectra. The closing of this gap will probably have to be taken in small steps, and may require concepts totally different from those of prior attempts, such as a combination of suspended-sediment particle scattering with Doppler and holography techniques using either optics or acoustics.

Gap 4 The concurrent measurement of wave parameters and bottom topography very likely will involve the concurrent use of two separate sensor systems whose data would be merged and correlated in a separate shore-based computer.

Gaps 4 and 5 From the perspective of wave measurement, gaps 4 and 5 are related: the objectives of each entail obtaining from fields of waves a number of wavelengths wide and long. Gap 4 has the added complication of concurrent topographic measurements of the ocean floor.

Gaps 5 and 6 These also have related technologies; however, the overlap is in the processing, storage, and presentation of large quantities of multidimensional wave data, which is the topic of the technological program to close gap 6.

Proposed Program for Gap 6 Vast quantities of ocean wave data are being routinely collected using systems placed aboard ships and other manned offshore platforms, from moored buoys, and from other unattended systems such as shore-mounted seismic sensors. However, the quantities of these data are relatively miniscule compared to those of multidimensional data that may become available from remote sensing systems using shore, aircraft, and satellite platforms. Data from Seasat have given an initial view of data possibilities. The problems of processing, of displaying multidimensional parameters, and of storing and recalling data from these remote sensing systems are looming. Likewise, the data from *in situ* systems required to close gaps 4 and 5 will present similar processing, display, and data storage/recovery problems.

Many organizations will be concerned with the use of systems that may evolve from an attack on gap 6. Furthermore, data analysis and presentation from other fields may be applicable. These may include such diverse fields as internal medicine, petroleum exploration, and intelligence, as well as the closely related fields of meteorology and climatology.

The Phase 1 approach to gap 6 may well merit a multidisciplinary workshop on gigabyte data processing and display. Better understanding could be gained from many perspectives: the extent of the problem throughout the engineering and scientific communities, approaches that have been tried, advances made, failures, and promising directions for the future.

Tentative specifications could then be developed for application to wave data. These would have to be refined further through some working organization, together with further analysis of various technological approaches.

Since the specifications for analysis and presentation of various data uses may differ in the required degree of sophistication, several of the more promising technological approaches will need to be pursued. Detailed specifications and analysis will be required in order to understand the systems to be developed and their various interfaces. These proposed solutions will need circulation through the engineering and scientific communities for comments on approach as well as utility.

One or more of the more promising approaches to data analysis, presentation, storage, and recovery should be implemented on a trial basis to verify their utility. It would be desirable that the evaluation include use of the system for similar problems in other fields (as identified in the workshop). Some hardware subsections may well require development, but available display systems, computers, and storage media would be employed as much as possible.

Revision of specifications and full systems development would follow an evaluation of the trial phase.

10. WAVE-MEASUREMENT RESOLUTION* AND ACCURACY NEEDED AND ATTAINABLE, AND DEVELOPMENT OF PROCEDURES AND INSTRUMENTS TO IMPROVE RESOLUTION

A classification of wave-data users--engineers, scientists, government agencies, industry, marine fisheries, shipping, oil spill operations, defense, and others--needs to be developed, and the resolution needed for each application and data type determined. Then:

- o The areas where present resolution is insufficient should be identified.
- o Software procedures and new instrumentation to make measurements and perform data analyses for these areas should be developed.
- o Ways need to be studied and tried for combining information from all sources to enhance resolution of instrument data.

*Resolution is defined as ability to separate two "bumps" near one another; accuracy is defined as nearness to standard or "true."

NOTE: UNITS OF MEASUREMENT

The International System of Units (SI) has gradually been accepted and applied in many scientific and engineering activities of the United States, owing to the several advantages of the system and to the efforts of national organizations that develop voluntary consensus standards (for example, the Institute of Electrical and Electronics Engineers, IEEE; American National Standards Institute, ANSI; and American Society for Testing and Materials, ASTM). Nevertheless, many applications of wave data are in fields of activity that still routinely use English units, and the SI recognizes for practical purposes such units as temperature in degrees Celsius* and the nautical mile. Thus, the reader of these proceedings may notice that various units from different systems are used in reporting wave-measurement results. Some key SI units and conversions are presented here for the reader's convenience.

ACCEPTED SI UNITS

Quantity	SI Unit	SI Symbol	Formula	Conversion to Units of Other Systems
Length	meter	m		m ∿ 3.3 ft (cm ∿ 0.4 in)
	kilometer	km		km ∿ 0.6 mi
Time	second	s		
Plane Angle	radian	rad	plane angle between two radii of a circle that subtend on the circumference an arc equal in length to the radius	

DERIVED SI UNITS

Frequency	hertz	Hz	one per second
Velocity		m/s	meter per second
Acceleration		m/s^2	meter per second squared
Wavenumber		m^{-1}	one per meter

ACCEPTED FOR USE WITH SI

Temperature	degrees Celsius	^oC	$^oC \times 9/5 + 32 = {}^oF$
Plane Angle	degrees	^{o}	$1^o = (\pi/180)$ rad
	minutes	'	$1' = (\pi/10{,}800)$ rad
	seconds	"	$1'' = (\pi/648{,}000)$ rad

ACCEPTED FOR PRACTICAL REASONS, BUT NOT FOR COMBINATION WITH SI UNITS

Unit	Abbreviation	Formula	Conversion to SI Units
nautical mile	nm (or nmi)		1 nm = 1852 m
knot	kn	nautical miles per hour	1 kn = 0.5 m/s

*The intervals of temperature in kelvin and degrees Celsius are the same ($K = {}^oC + 273.15$); expression in kelvin is preferred for thermodynamic temperatures, in degrees Celsius for ordinary temperatures.

A participant* in the meeting that is the subject of these proceedings proposes that a uniform set of SI units be used for all wave observations:

Wave height	m, cm
Wavelength	m
Free-surface spectral density	m^2/Hz, cm^2/Hz (or cm^2/mHz)
Water depth	m
Altitude of aircraft or satellite	m, km
Wavelength of radar or microwave signals	cm
Temperature	°Celsius
Dimensions of wave-measuring systems	cm, m
Particle velocity	cm/s
Velocity spectra	$cm^2/s^2/Hz$ (or $cm^2/s^2/mHz$)
Group or phase speeds	cm/s, m/s (or km/hr)

Other participants noted in the course of the meeting and subsequent communications that a consistent definition of spectral density (ft^2/Hz, $ft^2/rad/s$, or m^2/Hz) would be a most useful convention for reporting wave-measurement results and for intercomparisons.

---

*David H. Shonting, Naval Underwater Systems Center

SPEAKERS

Dr. Ledolph Baer received a Ph.D. from New York University: his dissertation was on wave forecasting. His principal research interests have broadened to include wave statistics and measurements. He developed wave criteria for the Polaris missile and managed the Ocean Sciences Division of Lockheed Aircraft Corporation before joining the National Oceanic and Atmospheric Administration. He is now manager of the Coastal Waves Program.

Dr. Leon Borgman, who holds joint appointments in the departments of geology and statistics at the University of Wyoming, conducts research in mining geostatistics, and in the application of mathematics and statistics to problems of geology, physical oceanography, coastal engineering, hydrology, mining, and ocean waves.

Dr. Norden Huang received a Ph.D. from Johns Hopkins University in fluid mechanics and mathematics, and did postdoctoral research at the University of Washington in oceanography. He has worked at NASA's Wallops Flight Facility for the past seven years as a research oceanographer, and is adjunct professor of oceanography at the University of Delaware and North Carolina State University. His research has concentrated on statistical wave theory and remote sensing.

Dr. Edward Walsh has bachelor's and Ph.D. degrees in electrical engineering from Northeastern University. His research concentrates on the analysis of radar systems and their interaction with the sea. For the past 11 years, he has worked at NASA's Wallops Flight Facility. He is now working on assignment at the Applied Physics Laboratory of Johns Hopkins University.

Dr. Robert Shuchman joined the Radar and Optics Division of the Environmental Research Institute of Michigan in 1973, where he is now head of the Radar Science Laboratory. His principal interest has been analysis of the synthetic aperture radar (SAR) system and the quantification of SAR signatures of the ocean surface. He has spent the last three years validating Seasat SAR data collected over the oceans. His Ph.D. was granted by the University of Michigan: his dissertation topic was hydrodynamic/electromagnetic modeling of SAR data.

Dr. Donald Barrick received bachelor's and master's degrees in electrical engineering, and a Ph.D. in electromagnetic theory from Ohio State University. He worked for seven years at Battelle Memorial Institute in Columbus, Ohio, and is now chief of the Sea-State Studies Branch of NOAA's Wave Propagation Laboratory in Boulder, Colorado. His research centers on the application of radar techniques to oceanography, and understanding radar scatter from rough surfaces.

Dr. Frederick Jackson received a master's degree in physics from the Polytechnic Institute of Brooklyn, and a Ph.D. in oceanography from New York University. He worked for General Electric for four years on microwave remote sensing of the ocean, and for Columbia University for two years analyzing satellite altimeter data on ocean tides. He joined NASA's Goddard Space Flight Center in 1978, where he has concentrated on experimental and theoretical techniques for measuring wave spectra from satellites, and achieving high directional resolution.

Dr. Richard Seymour received a Ph.D. from the University of California at San Diego in oceanography. He was vice president of Wire Equipment Manufacturing Company, head of rocket development for Thiokol Chemical Corporation's Elkton Division, chief engineer of United Technologies, and staff oceanographer of the California Department of Navigation and Ocean Development. He is now research associate at Scripps Institution of Oceanography, where he pursues investigation of coastal processes and analysis of wave measurements.

Dr. Allan Parker has bachelor's and Ph.D. degrees from London University in aeronautical engineering. He spent five years in the aeronautical engineering department of Texas A&M University, and returned to England in 1975 as the senior science officer of the National Maritime Institute. He is now head of the Oceanographic Instruments Section. His principal research interests are ocean instrumentation, marine trials, and hydrodynamics.

Dr. Lester LeBlanc received a Ph.D. from the University of Rhode Island in electrical engineering, and spent five years with Raytheon Submarine Signals before returning to the University of Rhode Island, where he is now professor of ocean engineering. His research concentrates on underwater acoustic analysis, oceanographic data analysis, and ocean instrumentation.

Dr. George Forristall received bachelor's, master's, and Ph.D. degrees from Rice University in mechanical engineering. He spent two years at the Federal Institute of Technology in Switzerland before joining Shell Development Company. His research focuses on the measurement and prediction of storm waves and currents.

Dr. Albert Green has a bachelor's degree in physics from Vanderbilt University and a Ph.D. in physical oceanography from the Massachusetts Institute of Technology. He spent two years at the Institute for Geophysics as a fellow of the Royal Norwegian Council for Scientific and Industrial Research, and was assistant professor of atmospheric and ocean sciences at the University of Michigan. In 1977, he joined the Naval Ocean Research and Development Activity as head of the Physical Oceanography Branch. He conducts research in nonlinear ocean waves, mesoscale dynamics in the ocean, and high-frequency internal gravity waves.

PARTICIPANTS

Paul Aagaard
Chevron Oil Field Research Company
La Habra, California

Louis C. Adamo
Louis C. Adamo, Inc.
Solana Beach, California

Fadhil Al-Kazily
University of Rhode Island
Kingston, Rhode Island

Stanley Alper
National Oceanic and
Atmospheric Administration
Rockville, Maryland

Ledolph Baer
National Oceanic and Atmospheric
Administration
Rockville, Maryland

Don Barrick
National Oceanic and Atmospheric
Administration
Boulder, Colorado

Tom Bartholomew
National Oceanic and Atmospheric
Administration
Rockville, Maryland

Robert C. Beal
Johns Hopkins Applied
Physics Laboratory
Laurel, Maryland

Joe Bishop
Marine Environments Corporation
Rockville, Maryland

Carl Blahnik
SRI International
Menlo Park, California

Kevin Bodge
University of Delaware
Newark, Delaware

Leon Borgman
University of Wyoming
Laramie, Wyoming

Edward C. Brainard II
Environmental Devices Corporation
Marion, Massachusetts

Kay R. Burnett
Johns Hopkins University
Baltimore, Maryland

Jack Cawley
National Oceanic and Atmospheric
Administration
Rockville, Maryland

Davidson T. Chen
Naval Research Laboratory
Washington, D.C.

Robert G. Dean
University of Florida
Gainesville, Florida

George Domurat
U.S. Army Corps of Engineers
San Francisco, California

Dennis G. Douglas
SRI International
Menlo Park, California

Marshall D. Earle
Marine Environments Corporation
Rockville, Maryland

Edward C. Escowitz
U.S. Geological Survey
Reston, Virginia

Douglas Evans
Evans-Hamilton, Inc.
Houston, Texas

George Z. Forristall
Shell Development Company
Houston, Texas

Albert W. Green
Naval Ocean Research and
Development Activity
Bay St. Louis, Mississippi

Phil Hadsell
National Ocean Data Center
Washington, D.C.

Jean-Pierre Hainsselin
Nereides
Houston, Texas

Robert C. Hamilton
Evans-Hamilton, Inc.
Houston, Texas

Paul Heinmiller
University of Rhode Island
Kingston, Rhode Island

Gary Howell
Coastal and Oceanographic
Engineering Laboratory
Gainesville, Florida

Y. Phil Hsueh
National Science Foundation
Washington, D.C.

Norden E. Huang
NASA Wallops Flight Facility
Wallops Island, Virginia

Lloyd C. Huff
National Oceanic and
Atmospheric Administration
Riverdale, Maryland

William Iseley
National Oceanic and
Atmospheric Administration
Riverdale, Maryland

Frederick Jackson
NASA Goddard Space Flight
Center
Greenbelt, Maryland

Charles D. Kearse
National Oceanic and
Atmospheric Administration
Rockville, Maryland

William C. Keller
Naval Research Laboratory
Washington, D.C.

Bruce M. Lake
TRW
Redondo Beach, California

Lester LeBlanc
University of Rhode Island
Kingston, Rhode Island

Dave Lichy
Coastal Engineering Research Center
U.S. Army Corps of Engineers
Ft. Belvoir, Virginia

Belinda Lipa
CODAR Research
Woodside, California

Orville T. Magoon
U.S. Army Corps of Engineers
San Francisco, California

Lawrence B. Marsh
Marsh-McBirney, Inc.
Gaithersburg, Maryland

Michael G. Mattie
Coastal Engineering Research Center
U.S. Army Corps of Engineers
Fort Belvoir, Virginia

Foster H. Middleton
University of Rhode Island
Kingston, Rhode Island

G. Graham Murray
Dataware, Inc.
San Diego, California

Lawrence McGoldrick
National Aeronautics and
Space Administration
Washington, D.C.

Owen Oakley
Gulf Research and Development Company
Houston, Texas

Nan Panicker
Mobil Research and Development
Corporation, Offshore Engineering
Dallas, Texas

Allan Parker
National Maritime Institute
Hampshire, United Kingdom

Denzil C. Pauli
Marine Planning, Systems Analysis,
Instrumentation Consultant
Silver Spring, Maryland

Steven S. Pawka
Scripps Institution of Oceanography
La Jolla, California

Willard J. Pierson
City College of New York
New York, New York

Douglas M. Pirie
U.S. Army Corps of Engineers
San Francisco, California

William J. Plant
Naval Research Laboratory
Washington, D.C.

Richard L. Ribe
National Oceanic and
Atmospheric Administration
Rockville, Maryland

Edward Ridley
National Ocean Data Center
Washington, D.C.

Maurice E. Ringenbach
National Oceanic and
Atmospheric Administration
Rockville, Maryland

Robin Robertson
University of Rhode Island
Kingston, Rhode Island

Gene Russin
National Oceanic and
Atmospheric Administration
Rockville, Maryland

Richard J. Seymour
Scripps Institution of Oceanography
La Jolla, California

David Shonting
Naval Underwater Systems Center
Newport, Rhode Island

Robert A. Shuchman
Environmental Research Institute
of Michigan
Ann Arbor, Michigan

Kenneth E. Steele
National Oceanic and
Atmospheric Administration
NSTL Station, Mississippi

Mike Szabados
National Oceanic and
Atmospheric Administration
Rockville, Maryland

Paul Teleki
U.S. Geological Survey
Reston, Virginia

Edward Thompson
U.S. Army Corps of Engineers
Fort Belvoir, Virginia

Gaspar R. Valenzuela
Naval Research Laboratory
Washington, D.C.

John A. Vermersch, Jr.
Exxon Production Research Company
Houston, Texas

David A. Walden
U.S. Coast Guard
Washington, D.C.

Louise Wallendorf
University of Rhode Island
Kingston, Rhode Island

Edward Walsh
Johns Hopkins Applied Physics
Laboratory
Laurel, Maryland

Todd Walton
Coastal Engineering Research Center
Fort Belvoir, Virginia

Ed Winston
Ed Winston and Company, Inc.
Rockville, Maryland

Wyman Wong
National Oceanic and
Atmospheric Administration
Rockville, Maryland

William Woodward
National Oceanic and
Atmospheric Administration
Rockville, Maryland

David Zopf
Oregon State University
Corvallis, Oregon

Experiments	
ARSLOE	Atlantic Remote Sensing Land-Ocean Experiment for sensor intercomparison, sensor development tests, and data for wave-model verification, 6 October to 30 November 1980, offshore Duck, North Carolina. Organized by the U.S. Army Corps of Engineers Coastal Engineering Research Center and the National Ocean Survey of NOAA with participation of people from four nations and many federal agencies.
DUCKEX or DUCK-X	Duck, North Carolina, Experiment, 12 August to 9 October 1978, intensive collection of sea-truth data to verify ocean monitoring by Seasat.
GARP	Global Atmospheric Research Program of the World Meteorological Organization and the International Council of Scientific Unions, to study general circulation of the atmosphere, and entailing a series of experiments or subprograms of oceanographic interests.
GOASEX	Gulf of Alaska Seasat Experiment for the validation of Seasat data, conducted in September 1978, and involving research vessels, weather ships, data buoys, and instrumented aircraft.
JASIN	Joint Air-Sea Interaction Experiment, an independently organized multinational effort (officially associated with GARP) to collect in situ surface data concurrently with collection of Seasat data in an area of the North Atlantic between Scotland and Iceland, July-August 1978.
JONSWAP	Joint North Sea Wave Project, July-August 1969. An independently organized multinational experiment to provide data for study of wave growth and decay.
Marineland	Experiment conducted off Marineland, Florida, to validate airborne SAR measurements of the ocean surface.
MARSEN	Marine and Atmospheric Sensing Experiment, North Sea, September-October 1979. Experiment to validate remote sensing of wind waves, currents, and internal waves.
SWOP	Stereo Wave Observation Project, North Atlantic (39°N, 65°W), 25 October 1954. Simultaneous stereo photography of the ocean surface from two aircraft to determine the form of the directional wave spectrum.

INSTRUMENTS		PLATFORMS	
AOL	Airborne Oceanic Lidar	GOES	Geostationary Operational Environmental Satellites--a series launched by NOAA
CODAR	Coastal Ocean Dynamics Application Radar		
LARAR	Large Antenna Real Aperture Radar	Seasat	Satellite equipped to monitor ocean parameters, launched in 1978: about 100 days of operation
SAR	Synthetic Aperture Radar		
SCR	Surface Contour Radar		
SASS	Seasat-A Scatterometer		
SLAR	Side-Looking Airborne Radar		
SMMR	Scanning Multichannel Microwave Radar	XERB	Experimental Environmental Research Buoy
VIRR	Visible Infrared Radiometer		

ORGANIZATIONS, FEDERAL AGENCIES AND UNITS

CERC	Coastal Engineering Research Center, U.S. Army Corps of Engineers
ENDECO or Endeco	Environmental Devices Corporation
ERIM	Environmental Research Institute of Michigan
FNOC	Fleet Numerical Oceanographic Center, U.S. Navy
JPL	Jet Propulsion Laboratory
NASA	National Aeronautics and Space Administration
NDBO	NOAA Data Buoy Office
NMI	National Maritime Institute (United Kingdom)
NOAA	National Oceanic and Atmospheric Administration
NORDA	Naval Ocean Research and Development Activity
NOS	National Ocean Survey of NOAA
NRL	Naval Research Laboratory
ONR	Office of Naval Research

UNCLASSIFIED

SECURITY CLASSIFICATION OF THIS PAGE *(When Data Entered)*

REPORT DOCUMENTATION PAGE		READ INSTRUCTIONS BEFORE COMPLETING FORM
1. REPORT NUMBER	2. GOVT ACCESSION NO.	3. RECIPIENT'S CATALOG NUMBER
4. TITLE *(and Subtitle)* MEASURING OCEAN WAVES; Ocean Instrumentation to Serve Science and Engineering		5. TYPE OF REPORT & PERIOD COVERED Proceedings of a Symposium and Workshops 6. PERFORMING ORG. REPORT NUMBER ---
7. AUTHOR(s) Committee on Wave-Measurement Technology and authors of individual papers Robert G. Dean, chairman		8. CONTRACT OR GRANT NUMBER(s) N00014-82-G-0032
9. PERFORMING ORGANIZATION NAME AND ADDRESS Marine Board of the National Research Council National Research Council Washington, D. C. 20418		10. PROGRAM ELEMENT, PROJECT, TASK AREA & WORK UNIT NUMBERS ---
11. CONTROLLING OFFICE NAME AND ADDRESS Office of Naval Research Department of the Navy Arlington, Virginia 22217		12. REPORT DATE November 1982 13. NUMBER OF PAGES
14. MONITORING AGENCY NAME & ADDRESS*(if different from Controlling Office)* ---		15. SECURITY CLASS. *(of this report)* UNCLASSIFIED 15a. DECLASSIFICATION/DOWNGRADING SCHEDULE

16. DISTRIBUTION STATEMENT *(of this Report)*

Distribution of this report is unlimited.

17. DISTRIBUTION STATEMENT *(of the abstract entered in Block 20, if different from Report)*

---

18. SUPPLEMENTARY NOTES

Financial support provided by the Departments of Interior, Commerce, State and Energy, U. S. Coast Guard, Navy, Army Corps of Engineers, and National Science Foundation.

19. KEY WORDS *(Continue on reverse side if necessary and identify by block number)*

Wave-Measurement Technologies
Ocean Instrumentation
Remote Sensing
In Situ Sensing
Needs for Wave Data
Future Wave-Measurement Systems
Priorities for Research and Development

20. ABSTRACT *(Continue on reverse side if necessary and identify by block number)*

The proceedings encompass review of the state of the art of leading technologies for measuring ocean waves, preceded by two presentations setting out needs of users for wave data, and needs of scientific research. In a series of structured workshops, participants identified the following priorities for research and development in wave measurement, in order of urgency or importance: Wave direction; standards and calibrations, data quality assurance; systems intercomparison; nearshore wave fields and related processes, nonlinear pheno-

(continued)

DD FORM 1 JAN 73 1473 EDITION OF 1 NOV 65 IS OBSOLETE
S/N 0102-014-6601

UNCLASSIFIED

SECURITY CLASSIFICATION OF THIS PAGE *(When Data Entered)*

mena; development of remote sensing; global wave-measurement system; wave-measuring buoy systems; new sensors, and wave-measurement resolution and accuracy.